



Maria Catarina Lopes Dias

**Continuous Detection of Errors using  
Electroencephalography**

**DOCTORAL THESIS**

to achieve the university degree of  
Doktorin der technischen Wissenschaften  
submitted to the

**Graz University of Technology**

Supervisor

Univ.-Prof. Dipl.-Ing. Dr.techn. Gernot R. Müller-Putz

Institute of Neural Engineering  
Faculty of Computer Science and Biomedical Engineering

Graz, February 2021



# Affidavit

I declare that I have authored this thesis independently, that I have not used other than the declared sources/resources, and that I have explicitly indicated all material which has been quoted either literally or by content from the sources used. The text document uploaded to TUGRAZonline is identical to the present doctoral dissertation.

---

Date

---

Signature





# Acknowledgements

I would like to express my sincere appreciation to my supervisor, Prof. Gernot Müller-Putz. At an initial stage, for his belief that I could successfully complete this PhD and for giving me the opportunity to study brain-computer interfaces. But mostly, for his support, trust and continuous encouragement. I would also like to acknowledge the assistance of Dr. Daniela Wyss and Dr. Renate Wildburger, whose help enabled the realisation of the last study of this thesis.

Furthermore, I would like to thank everyone I have met at the Institute of Neural Engineering, for contributing to the great work environment and to make my PhD a very pleasant journey. In particular, I am extremely grateful to all the members of Feel Your Reach: Andreea, Joana, Lea, Reinmar and Valeria. I learnt so much from all of them, professionally and personally. Thank you for the interesting discussions, helpful suggestions and all the fun trips and events.

I would also like to thank my parents, who are my greatest admirers, and my grandmother, for teaching me that formal education and academic titles do not contribute to a person's integrity. Most importantly, I would like to express my profound gratitude to Thomas. Thank you for always being there for me and for giving me the stability that I so many times lacked. I am sorry for all the days in which I came home in a bad mood and for all the jibber-jabber about classifiers, chance level and true positives. My deepest thanks for your unshakable support during this journey. I am now looking forward to the most exciting adventure of our lives!



# Abstract

Brain-computer interfaces (BCIs) can be an important tool to restore some independence in persons with severe motor disabilities. However, their use is not widespread. BCIs typically require a long offline calibration period before each single-use, which dissuades a regular use. Furthermore, BCIs are still prone to errors, by misinterpreting a user's intentions. The detection of the user's awareness of such errors can be used to improve his/her interaction with a BCI.

In this thesis, I investigated error-related potentials (ErrPs), which are the neural signature of error processing. More precisely, I used electroencephalography (EEG) to study the detection of ErrPs occurring during the continuous control of a cursor and of a robotic arm. The undertaken studies showed that the continuous detection of ErrPs was reliable, not only offline but also in online scenarios, in which users receive real-time feedback regarding the ErrP detections.

Furthermore, I developed a generic ErrP classifier, using the EEG signals from several non-disabled participants and showed that such a classifier can be directly used with new participants, if combined with a participant-specific threshold. These findings hint at the possibility of providing immediate feedback of the ErrP detections from the start of the BCI use, skipping offline calibration.

Finally, I tested this generic classifier for the continuous detection of ErrPs in an online experiment with no offline calibration. In this experiment two groups of participants continuously controlled a robotic arm: participants with a spinal cord injury (SCI) and non-disabled control participants. Participants with SCI displayed a heterogeneous ErrP morphology. Still, this classifier could be reliably used with all participants that displayed clear ErrP signals, independently of the SCI.

This thesis contributes to the investigation of the continuous detection of ErrPs and further expands it towards realistic online scenarios. Furthermore, it explores the transfer of an ErrP classifier across different populations and addresses its online use for the continuous detection of ErrPs in a population with SCI.



# Kurzfassung

Gehirn-Computer-Schnittstellen (brain-computer interface, BCI) können ein wichtiges Hilfsmittel sein, um Personen mit schweren motorischen Behinderungen eine gewisse Selbständigkeit zu verleihen. Die Verwendung von BCIs ist jedoch immer noch nicht sehr verbreitet. Eine Einschränkung ist, dass sie üblicherweise eine aufwendige Offline-Kalibrierung benötigen. Darüber hinaus sind BCIs immer noch fehleranfällig, weil sie häufig die Absichten eines Benutzers falsch interpretieren. Die Fehlererkennung des Benutzers kann hierbei berücksichtigt werden, um die Leistungsfähigkeit des BCIs zu verbessern.

In der vorliegenden Dissertation habe ich Fehlerpotentiale (error-related potential, ErrP) untersucht. Diese stellen ein neuronales Merkmal der Fehlerverarbeitung dar, mit dessen Hilfe die von einem Benutzer wahrgenommenen BCI-Fehler erkannt werden können. An Hand von Elektroenzephalographie (EEG) wurden ErrPs untersucht, die während der kontinuierlichen Kontrolle eines Cursors und eines Roboterarms auftreten. Die Ergebnisse dieser Untersuchungen zeigten, dass die kontinuierliche Erfassung von ErrPs sowohl offline als auch in Online-Szenarien, in denen eine Fehlerrückmeldung in Echtzeit gegeben wird, zuverlässig funktioniert.

Darüber hinaus entwickelte ich einen generischen ErrP-Klassifikator basierend auf den EEG-Signalen von nicht-beeinträchtigten Teilnehmenden, der mit Hilfe eines personenspezifischen Schwellwerts direkt auf neue Personen angewandt werden kann. Diese Erkenntnis zeigt die Möglichkeit auf, ErrP-Erkennung beim Beginn der Verwendung eines BCIs einzusetzen, ohne dabei auf eine Phase der Offline-Kalibrierung zurückgreifen zu müssen.

Abschließend testete ich diesen generischen Klassifikator für die kontinuierliche ErrP-Erkennung in einem Online-Experiment ohne Offline-Kalibrierung. In diesem Experiment wurde ein Roboterarm fortlaufend von Teilnehmenden aus zwei Gruppen kontrolliert: nicht-beeinträchtigte Personen und Personen mit einer Rückenmarksverletzung (spinal cord injury, SCI). Die Teilnehmenden der SCI-Gruppe zeigten hierbei eine inhomogene ErrP-Morphologie. Dennoch konnte der Klassifikator für alle Teilnehmenden,

die ein deutliches ErrP-Signal aufzeigten, zuverlässig eingesetzt werden, unabhängig von ihrer Gruppenzugehörigkeit.

Diese Dissertation trägt zur Untersuchung der kontinuierlichen Erkennung von ErrPs bei und erweitert diese auf ihre Anwendbarkeit in Online-Szenarien. Schließlich wird die Übertragung des generischen ErrP-Klassifikators auf verschiedene Populationen aufgezeigt und die Verwendbarkeit für die fortlaufende ErrP-Erkennung in Online-Szenarien für Teilnehmer und Teilnehmerinnen mit SCI dargestellt.

# Contents

<b>1. Introduction</b>	<b>3</b>
1.1. Neural basis of EEG . . . . .	3
1.2. Neural signature of error processing . . . . .	5
1.3. Brain-computer interfaces . . . . .	7
1.4. Error-related potentials in BCIs . . . . .	9
1.5. Generic ErrP classifiers . . . . .	11
1.6. Asynchronous detection of ErrPs . . . . .	12
1.7. ErrPs in potential end-users of BCIs . . . . .	14
1.8. ErrPs' applications for non-disabled users . . . . .	15
<b>2. Motivation and Aims</b>	<b>17</b>
2.1. Motivation . . . . .	17
2.2. Aim of the thesis . . . . .	18
<b>3. Methods and Results</b>	<b>19</b>
3.1. Offline asynchronous detection of ErrPs . . . . .	19
3.2. Online asynchronous detection of ErrPs . . . . .	25
3.3. Asynchronous detection of ErrPs with a generic classifier . . . . .	29
3.4. Online asynchronous detection of ErrPs in participants with SCI . . . . .	32
<b>4. Discussion and Conclusion</b>	<b>37</b>
4.1. Asynchronous detection of ErrPs . . . . .	37
4.2. Generic ErrP classifiers . . . . .	39
4.3. ErrPs in BCI end-users . . . . .	41
4.4. Limitations and recommendations . . . . .	42
4.5. Summary and conclusion . . . . .	43
4.6. Future perspectives . . . . .	44
<b>Bibliography</b>	<b>45</b>
<b>Acronyms</b>	<b>73</b>

*Contents*

<b>A. Authors Contributions</b>	<b>75</b>
<b>B. Selected Scientific Contributions</b>	<b>77</b>
<b>C. Core Publications</b>	<b>79</b>



# Structure of the thesis

This thesis is divided into 4 chapters.

Chapter 1 **Introduction** consists of an overview of the topics covered by this thesis. It describes the neural basis of EEG and its use to study error processing. Furthermore, it introduces brain-computer interfaces, error-related potentials and their asynchronous detection.

Chapter 2 **Motivation and Aims** describes the motivation of the thesis and frames it in relation to the state-of-the-art literature on the asynchronous detection of error-related potentials, which serves as background for the thesis. Furthermore, the main aims of this thesis are defined.

Chapter 3 **Methods and Results** summarises the scientific publications in the scope of the thesis and highlights their contribution to it.

Chapter 4 **Discussion and Conclusion** provides a discussion regarding the achievements of the presented scientific publications and emphasizes their contribution to the state-of-the-art literature. Furthermore, it proposes future applications and possible advancements of the developed work.



# 1. Introduction

## 1.1. Neural basis of EEG

Neurons are the fundamental units of the brain. They connect with each other at synapses and communicate by means of action potentials. These are short electric pulses with amplitude of about 100 mV and a typical duration of 1 to 2 milliseconds. A neuron sending an action potential through a synapse is called presynaptic neuron, while the neuron receiving it is called postsynaptic neuron. The action potential triggers a voltage change in the membrane of the postsynaptic neuron, which is known as postsynaptic potential (PSP). PSPs last tens to hundreds of milliseconds and are caused by ions flowing in or out of the postsynaptic neuron [1, 2]. This flow of current creates a small dipole, i.e., a pair of positive and negative charges separated by a small distance. When the dipoles of thousands or millions of neurons are spatial and temporally aligned, they can be summated and their sum approximated by a single equivalent current dipole [3]. A dipole located in a conductive medium, such as the cerebral cortex, generates a current that flows through the medium, in a process known as volume conduction. When this electric current reaches the scalp, it induces a voltage difference that can be measured by electrodes [4].

This technique of measuring the brain's electric activity with electrodes placed on the scalp, is known as electroencephalography (EEG) and was introduced by Berger in 1924, who succeeded in recording the first human EEG [5]. As the skull has low electric conductivity and attenuates the electric current, EEG can be seen as an attenuated measure of the extracellular current flow from the summated activity of a large population of neurons with similar spatial orientation. Pyramidal neurons of the cortex are thought to be responsible for most of the EEG signal, because they are spatially aligned and oriented perpendicular to the cortical surface [1, 6]. EEG is a non-invasive technique that offers a temporal resolution in the order of milliseconds and a spatial resolution in the order of centimetres. Despite offering a good temporal resolution, its spatial resolution is lower than the one offered by other measuring techniques, such as electrocorticography (ECoG) and magnetoencephalography (MEG).

## 1. Introduction

ECoG is a similar technique to EEG, with the difference of measuring the brain's electric activity through electrodes placed on the cortical surface, either outside or beneath the dura mater [7]. It offers a temporal resolution comparable to EEG but a much better spatial resolution, in the order of millimetres, because it does not suffer from the attenuation caused by the skull [8]. Nevertheless, ECoG presents major limitations and risks: the placement of electrodes can only be done in clinical settings and, due to its inherent risks, is only performed in persons suffering from a pathological condition, such as intractable epilepsy [9].

MEG is a non-invasive technique that captures the magnetic fields produced by the electrical currents occurring in the brain. Since the magnetic field of electric dipoles is perpendicular to their orientation, MEG mainly captures the activity of dipoles oriented parallel to the scalp. It offers a temporal resolution comparable to EEG but a spatial resolution in the order of millimetres, because magnetic fields suffer almost no distortion by the skull. Nevertheless, MEG requires large equipment, making it non-portable and expensive [10, 11].

An alternative approach to study the brain is offered by functional near-infrared spectroscopy (fNIRS) and functional magnetic resonance imaging (fMRI): they detect changes in the cerebral haemodynamic responses and rely on the close link between such changes and neuronal activation. Since firing neurons have a high need of energy, they are supplied with oxygen at a greater rate than inactive neurons. This causes a localised change in the relative levels of oxygenated and deoxygenated haemoglobin in the blood. fMRI and fNIRS exploit the fact that these two forms of haemoglobin have different magnetic and spectral absorption properties. fNIRS uses near-infrared light and measures the changes in its absorption by haemoglobin [12, 13]. It offers a temporal resolution in the order of a second and the spatial resolution in the order of a centimetre [14]. fMRI relies on blood-oxygen-level-dependent (BOLD) contrast and measures the changes in the magnetic susceptibility of blood. It provides a spatial resolution in the order of millimetres and a temporal resolution in the order of a second [15–18].

EEG is a non-invasive, portable and relatively inexpensive technique that offers a good compromise between temporal and spatial resolution. Hence, it is nowadays a common tool in research and clinical settings, where it is used to characterise and diagnose neurological disorders [19, 20]. EEG signals are often divided into two broad categories: ongoing oscillations and event-related potentials (ERPs).

Oscillations are produced by sustained synchronised electrophysiological activity in larger groups of neurons. They are, in general, not driven by events but can be strongly modulated by internal or externally triggered motor or cognitive tasks, such as motor execution, motor imagery or mental subtraction [21–23]. Such triggers can cause a short lasting increase or decrease of the ongoing oscillations' amplitude, which

is localised and specific to certain frequency bands [24]. These changes are known as event-related synchronisation (ERS) and event-related desynchronisation (ERD), respectively. They are time- but not phase-locked to the triggers [21, 25]. Hence, they cannot be extracted by a linear method, such as averaging, but can be detected by frequency analysis. Oscillations are conventionally categorized and named based on their frequency, despite the lack of agreement regarding the range of the main frequencies bands. The most common frequency bands are delta, theta, alpha, beta and gamma, which correspond, approximately, to the intervals [0.5, 4] Hz, [4, 8] Hz, [8, 12] Hz, [12, 30] Hz and [30, 140] Hz, respectively [4, 22].

ERPs are transient neural responses that are time- and phase-locked to discrete events, such as the onset of a stimulus or the execution of a motor response [4, 26]. Stimuli can be sensory: auditory, visual, tactile or olfactory stimuli; or cognitive, such as the awareness of an error. Although large ERPs can be visible as voltage fluctuations in the ongoing EEG, most ERPs are rather small and become visible only when multiple EEG epochs are combined together to form an average ERP waveform [26].

## 1.2. Neural signature of error processing

The study of error processing was first introduced by Rabbit, who described the occurrence of a slowing as a behavioural adjustment after the commitment of an error [27, 28]. This phenomenon is generally referred to as post-error slowing.

The study of the neural mechanisms associated with error processing was initiated in the 1990s by Falkenstein and Gehring, using EEG recordings. The neural signature of error processing was identified as an ERP with two distinct components, called error negativity (Ne or ERN) and error positivity (Pe) [4, 26, 29–31].

The error negativity (Ne) component is characterised by a negative potential with peak amplitude over the fronto-central channels, occurring 0 to 200 ms after the error. The Pe component is characterised by a positive potential with peak amplitude over centro-parietal channels occurring 200 to 500 ms after the error. Nevertheless, the latency of these components is dependent on the experimental paradigm [32]. In the frequency domain, the Ne component has also been associated with a power increase in the theta band over the medial frontal cortex [33–37].

EEG and fMRI studies suggest that the Ne is generated in the caudal part of the anterior cingulate cortex (ACC) [38–42]. The Pe is not so well studied, but it is believed to be generated in the rostral part of the ACC [43, 44]. Figure 1.1 depicts the location of the ACC within the human cortex.

Initially, it was believed that the Ne component represented the error recognition, as

## 1. Introduction

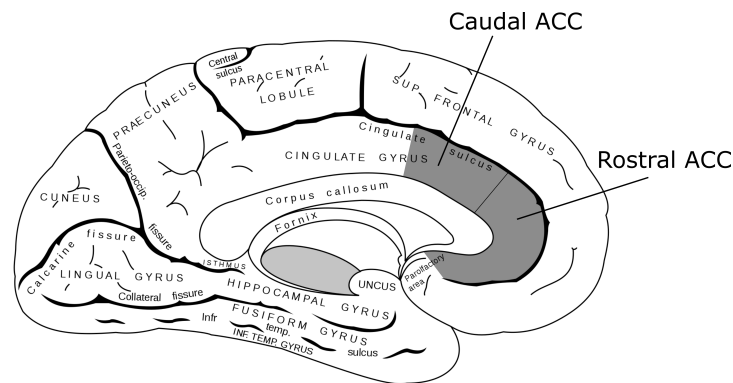


**Figure 1.1.:** Graphical representation of a sagittal section of the human cortex. The anterior cingulate cortex is highlighted in grey. Image modified from [45].

the outcome from the comparison between the expected and the verified responses [29–31]. However, later studies identified that the Ne component can also be present after correct responses [46–48]. These findings support the hypothesis that the Ne reflects the comparison process itself and not the outcome of the comparison. The significance of the Pe component is not so well understood, since it shows high variance across participants and tasks. It is believed to be associated either with the error awareness or with a subjective error assessment process, modulated by the individual significance of an error [49].

The Ne and Pe components can be modulated by several factors [32]. For instance, making the errors more meaningful, and thus increasing the participants' engagement not to commit them, leads to an increase in the Ne amplitude [50, 51]. Furthermore, older participants show a reduction of the Ne and Pe amplitudes [32, 52]. The Ne has been observed when participants commit errors in a wide variety of tasks, leading to the belief that it is associated with the existence of a generic error-processing system [53].

There is still no definite theory regarding the neural basis of error processing. The main theories are the comparator theory, the conflict monitoring theory and the reinforcement learning theory. The comparator theory, popular in the 1990s, proposed that the Ne results from the outcome of the comparison between the internal representations of a correct action and of the actual action [46]. Nevertheless, this theory assumes that the brain would have access to the correct action, which could have been executed. The conflict monitoring theory addresses this issue. It proposes that the ACC detects a conflict between simultaneously active, competing representations of an action. For instance, it proposes that when a person commits an error, there is a simultaneous activation of the representations of the actual erroneous action and of the intended

correct action. The ACC detects such conflict and engages the frontal cortex to resolve it [54–56]. The reinforcement learning theory proposes that the Ne is associated with the occurrence of an outcome that is worse than expected. For instance, it proposes that when a person commits an error, there is a drop in dopaminergic activity, which activates the ACC and transmits a negative reinforcement learning signal to the frontal cortex [39, 53]. Both conflict monitoring and reinforcement learning theories are backed up by strong evidence and neither theory seems capable of disproving the other. Alternatively, Botvinick proposes an integrative approach that combines both theories, in which the conflict acts as a teaching signal driving the negative reinforcement learning [57–59].

## 1.3. Brain-computer interfaces

In 1973, Vidal proposed a strategy, based on EEG, for brain-computer communication, coining the term brain-computer interface (BCI) [60, 61].

A BCI was initially defined as a system that converts consciously modulated brain signals into the control signal for an external device, without using the activity of any muscles or peripheral nerves [62, 63]. This definition was later expanded to include BCIs that are controlled with non-intentionally modulated brain activity or that combine different input signals [64–67]. BCIs controlled with intentionally modulated brain activity are nowadays known as active BCIs [68]. BCIs controlled with non-intentionally modulated brain activity can be divided into reactive BCIs and into passive BCIs [66, 69]. Reactive BCIs are controlled with brain activity that arises in reaction to external stimulation [70–73], and thus users can indirectly modulate their brain activity to control an application [66]. Passive BCIs are controlled by non-intentionally modulated brain activity, which does not have the purpose of voluntary control. Passive BCIs can be used to monitor the ongoing cognitive state of the user and, e.g., detect changes in attention and workload or identify error processing [74–79]. BCIs that simultaneously process different types of brain signals [80–88] or that combine brain signals with other types of inputs, such as eye gaze [89, 90] or heart beat [91], are known as hybrid BCIs [65, 67, 92–95].

As depicted in Figure 1.2, the first step of a BCI system is the acquisition of a user's brain signals, which can be done with EEG or other techniques that measure brain signals. Afterwards, the brain signals are processed, using approaches such as spatial and temporal filtering, in order to extract meaningful features. These features are then evaluated by a classifier that decodes the user's brain signals. Finally, the output of the classifier is translated into the control signal of an external device, which the user sees as feedback of the BCI's assessment of his/her brain signals.

## 1. Introduction

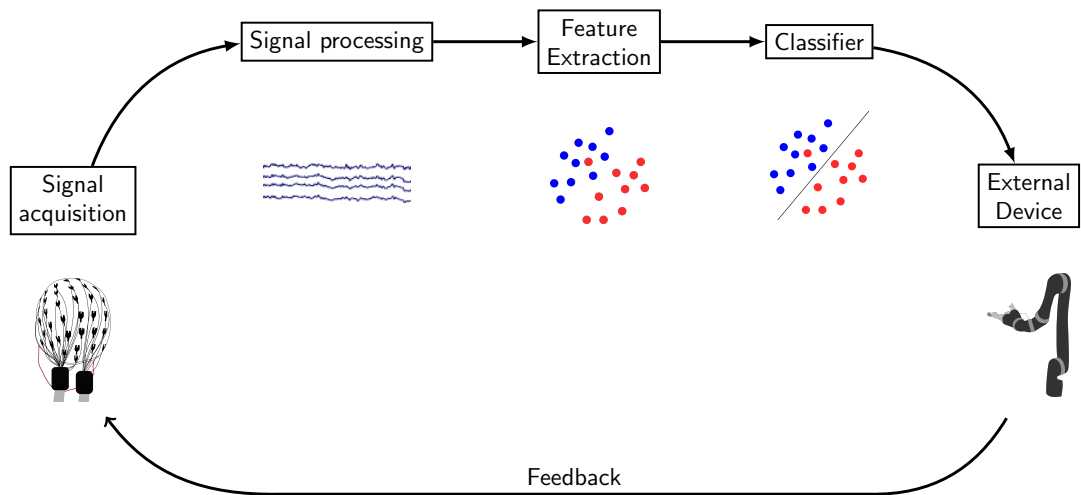


**Figure 1.2.:** Main components of a BCI. First, the brain signals of a user are recorded and processed in order to extract meaningful features. These features are used to classify the user's brain activity. The output of the classifier is converted into the control an external device. Finally, the user perceives the behaviour of the external device as feedback resulting from his/her own brain signals.

By definition, a BCI is a closed-loop system, which is able to process a user's brain signals and provide meaningful feedback in real-time. Due to this, BCIs are said to operate in an online manner. For the real-time processing to be possible, it is first necessary to build a classifier. Nowadays, the classifiers used in BCIs are typically machine learning models constructed from pre-recorded brain signals, which are capable of making predictions or decisions regarding previously unseen brains signals [96]. The construction of a classifier is also known as training a classifier, the pre-recorded brain signals are known as training data and the unseen signals are known as testing data. In order to acquire training data, a user is typically asked to perform several repetitions, also known as trials, of specific mental or motor tasks in order to generate brain signals that are distinguishable by the classifier. The acquisition of training data is known as calibration and it is often done without the user receiving any feedback of the BCI, i.e., in an offline manner.

The main aim of BCI research is to assist and support people with disabilities [64, 97, 98]. This target population is commonly referred to as BCI end-users [98, 99] and includes, e.g., persons with a spinal cord injury (SCI) or with amyotrophic lateral sclerosis (ALS) [98, 100–102]. BCIs can be used to replace communication [72, 103, 104] or movement [105, 106] through, e.g., the use of a spelling system or the control



#### 1.4. Error-related potentials in BCIs

of a wheelchair. Additionally, BCIs can also be used to restore movement through, e.g., the use of functional electrical stimulation of muscles in paralysed persons [107–109], and to improve brain function in the context of stroke rehabilitation [110]. Differently, BCI research can also target non-disabled users [66]. In this context, BCIs can be used to monitor the users' brain activity during prolonged tasks and provide information regarding changes in the user's cognitive state by, e.g., detecting lapses of attention [75, 77, 79, 111].

EEG is the most commonly used technique to record neural signals for BCI applications [64] and many different types of EEG signals can be used in BCIs [112, 113]. For instance, BCIs can rely on brain oscillations, which can be intentionally modulated by execution and imagination of movements as well as by certain mental tasks [23, 25, 114–116, 116–119]. Furthermore, several types of evoked potentials and event-related potentials can be used in BCIs [70, 73, 120–122]. For example, the P300 potential is the most commonly used signal for communication purposes, in applications known as P300 spellers [71, 123–125]. Recently, an effort has been made to develop BCIs based on more intuitive control signals [126–128]. Examples of such efforts are the use of movement-related cortical potentials (MRCPs) to detect movement intention or to identify different grasp types [129–133], or the use of error-related potentials (ErrPs) to detect a user's subjective awareness of errors [134–136].

### 1.4. Error-related potentials in BCIs

BCIs are a promising technology but are still prone to errors in the recognition of a user's intents. In 2000, Schalk and colleagues described, for the first time, the occurrence of an ErrP following errors of a BCI [134]. In this experiment, participants controlled a cursor along a vertical line towards a target at one of the line's extremities, using intentionally modulated brain oscillations. The EEG signals after the cursor reached any of the line's extremities were analysed. It was considered a correct outcome when the cursor reached the target and an incorrect outcome when the cursor reached the opposite line extremity. An ErrP was defined as the difference between the signal following incorrect outcomes and the signal following correct outcomes. The ErrP signal closely relates with the neural signature of error processing, characterised by the Ne and the Pe components, which was described before. Nevertheless, the subtraction of the correct signal from the error signal can lead to dissimilarities between the ErrP and the neural signature of error processing, since the correct signal can also present an Ne component in some experimental paradigms [47, 48].

Schalk's discovery led to the understanding that EEG signals could be used not only to control a BCI but also to identify and correct its errors, leading to an improvement

## 1. Introduction

of the BCI's performance [135]. To this end, it was necessary to establish a reliable single trial detection of error signals, which was first explored by Parra and Blankertz, in the context of incorrect motor actions of participants [137–139].

In the BCI field, single trial detection of ErrPs actually refers to the detection of the neural signature of error processing. This nomenclature is not very accurate, since in a single trial situation either the error signal or the non-error signal is detected, rather than the difference between the two signals. Nevertheless, from here onwards, we will adhere to the conventionally used nomenclature: single trial detection of error-related potentials.

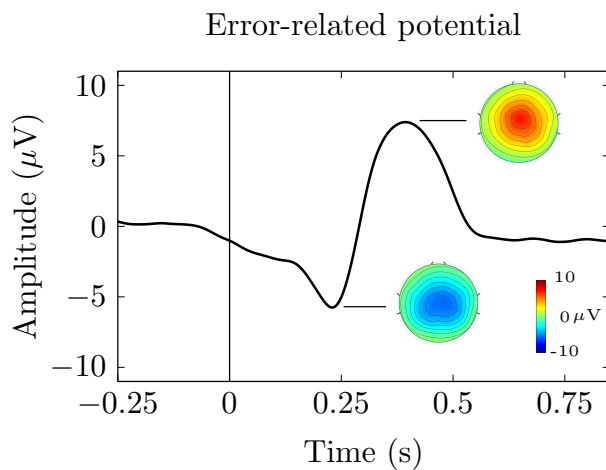


**Figure 1.3.:** Error-related potential at channel FCz. Figure generated with data from [140].

Ferrez and colleagues proposed the following categorization of ErrPs, based on the situations in which the errors occur and based on who committed them [136]. Response ErrPs arise following a participant's incorrect motor action. Feedback ErrPs arise following the presentation of a stimulus that indicates an incorrect performance of the participant. Observation ErrPs arise following the observation of errors made by an external agent. In the context of BCIs, interaction ErrPs arise following unintended responses of the interface. Furthermore, Ferrez and colleagues also analysed the occurrence and the single trial detection of interaction ErrPs at individual steps of a task rather than at the end of a longer task, as done by Schalk [85, 136, 141, 142]. Moreover, they clarified that ErrPs were not simply a consequence of errors being rare events [136, 143, 144] and showed that ErrPs' morphology was stable during long periods of time and across participants [143]. Iturrate and colleagues further investigated the single trial recognition of ErrPs during the observation of a robot that moved in discrete steps [145, 146]. More recently, ErrPs were investigated in tasks in which

continuous movement was coupled with an additional discrete feedback [79, 147–149]. Figure 1.3 illustrates an ErrP. When filtered with a non-causal filter, ErrPs display a negative peak at approximately 200 ms after the error onset followed by a positive peak at approximately 300 ms after the error onset. The peaks of the ErrP are more pronounced over the fronto-central electrodes. Nevertheless, the timing of the ErrP peaks are dependent on the task [150–152].

ErrPs-based BCIs can be used either in a corrective manner or in an adaptive manner [135]. The corrective approach is mainly used in the context of hybrid BCIs that combine ErrPs' detection with an intentionally modulated control signal, e.g., motor imagery [85, 148, 153]. The intentionally modulated signal is used to decode the user's intentions from the EEG and a misclassification of these intentions results in an erroneous feedback action by the BCI. The detection of ErrPs aims to identify the user's perception of such errors and, in case ErrPs are successfully detected, the BCI can take corrective actions. The BCI can, e.g., prevent an erroneous action from being fully executed or revert its outcome [85, 87, 139, 154–156]. The adaptive use of ErrP-based BCIs can be applied either in the context of the hybrid BCIs or in the context of passive BCIs, in which the ErrP is the only signal analysed. In hybrid BCIs, the ErrP signal can be used to modify or adapt the classifier corresponding to the active control signal, in order to prevent future errors of the respective classifier [88, 153, 157–163]. When the ErrP is the only controlling signal of a BCI, it can be used a penalty signal in reinforcement learning tasks [143, 164–166].

## 1.5. Generic ErrP classifiers

A main challenge when developing BCIs is the construction of meaningful classifiers, that accurately translate the brain signals of a user into his/her intended actions. Since EEG signals can be highly subject specific [167], BCI classifiers are usually trained with each participant's own brain signals [168]. These classifiers are known as personalised classifiers. Classifiers that are not trained with a user's own brain signals are also known as generic classifiers [169–171]. Additionally, due to the non-stationarity of EEG signals, i.e., due to the change of the signal's characteristics with time, the brain patterns extracted for classification can differ across sessions, leading to a poor BCI's performance [168, 172]. As a consequence, calibration is often repeated before each BCI use in order to retrain the classifier. Several works attempted to address these constraints and investigated strategies to reduce calibration and to adaptively retrain classifiers [158, 172–176]. Nevertheless, these approaches are not regularly applied in online scenarios [177].

ErrPs are still not commonly incorporated in BCIs. The limited use of ErrPs in BCIs

## 1. Introduction

can be possibly linked with most BCIs relying on session-specific personalised classifiers that require a long calibration period. This is particularly critical when combining ErrPs with other EEG-based controlling signals, in a hybrid BCI, as it would lead to a further increase of the calibration duration. Therefore, the use of ErrPs classifiers that require little or no calibration with the user could encourage the construction of BCIs that combine ErrPs with other control modalities, by avoiding a significant extension of the calibration period.

Grizou, Iturrate and colleagues investigated the construction of ErrP classifiers that do not require offline calibration [178–181]. The ErrP signal is particularly good candidate for the study of a classifier’s transfer, due to its stability over long periods of time and across participants [143]. The transferability of ErrP classifiers, across participants and across tasks, has been investigated in the context of discrete tasks. Iturrate and colleagues investigated the transfer of an ErrP classifier across different participants and also proposed a latency correction method for transferring an ErrP classifier across different time-locked tasks [150, 182]. Spüler and colleagues studied the transferability of ErrPs across non-disabled participants and across participants with ALS and showed that the transfer of ErrPs across non-disabled participants was successful [84]. Nevertheless, this was not the case for participants with ALS and the authors suggested that, for motor impaired participants, personalised classifiers should be used. Kim and colleagues investigated the transfer of an ErrP classifier across participants and also from an observation task to an interaction task [183, 184] and concluded that the transfer across tasks outperformed the transfer across participants. These studies show promising results regarding the transferability of ErrPs in offline scenarios. Hence, they can be seen as a strong foundation for the study of ErrPs’ transfer in online scenarios.

### 1.6. Asynchronous detection of ErrPs

One important application of BCIs is to provide an alternative control mechanism to persons with motor disabilities. BCI research is evolving in the direction of finding strategies to offer BCI users a more natural control of an external device [126–128, 130–132, 185, 186]. One strategy to achieve such a natural control is to allow users to continuously control the BCI through intuitive strategies [187–192].

In the context of continuous actions, the user can realise at any moment that an error occurred. Hence, such situations require a continuous detection of ErrPs. This strategy of continuously analysing brain signals in order to detect ErrPs is also known as asynchronous detection of ErrPs [193–195] and contrasts the more commonly used technique, known as synchronous, in which only epochs of brain signals, time-locked to events, are evaluated [142, 146, 148, 153].

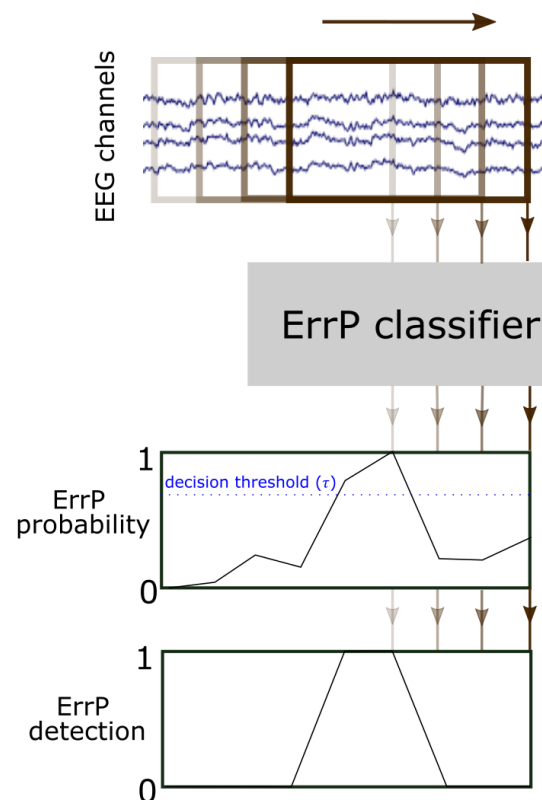


**Figure 1.4.:** Representation of the offline asynchronous detection of ErrPs using a sliding window approach. At a predefined rate, a time-window of brain signals is evaluated by the classifier. The output of the classifier is then translated into the detection of ErrPs, through a decision threshold.

Figure 1.4 depicts a schematic representation of the asynchronous detection of ErrPs using a sliding window, in an offline scenario. In this approach, brain signals are analysed by sliding a window at a fixed rate through the pre-recorded EEG. Each EEG window is evaluated by the classifier and leads to a classifier output, which is transformed into the probability of the window belonging or not to the error class. This probability can then be used for the detection of ErrPs by means of a decision threshold  $\tau$ , which serves as a boundary between the two classes, and affects the bias of the classifier towards one of them. This approach is directly transferable to an online scenario, in which the ongoing EEG signals are analysed in real-time and the participants can receive real-time feedback resulting from their brain signals.

The asynchronous detection of ErrPs was first proposed by Milekovic and colleagues

## 1. Introduction

in 2013. They used ECoG signals to evaluate the asynchronous detection of ErrPs during a computer game [196, 197]. Afterwards, Omedes and colleagues showed the feasibility of asynchronously detecting ErrPs from EEG signals, during the monitoring of continuous tasks on a computer screen [193–195]. Spüler and colleagues expanded the asynchronous detection of ErrPs with EEG to a situation in which participants continuously controlled a cursor, in a computer game similar to the one used by Milekovic and colleagues [197, 198]. So far, the study of the asynchronous detection of ErrPs during continuous actions has only been investigated in offline scenarios, in which the participants received no feedback of their ErrPs.

### 1.7. ErrPs in potential end-users of BCIs

Despite the developments in the BCI field in the last 20 years, few BCIs have been actually tested with potential BCI end-users [100, 101, 108, 109, 116, 199–203]. Furthermore, such studies typically include very few participants. A brain signal of interest in a population of potential BCI end-users can differ from the corresponding signal in a non-disabled population [204–207]. Hence, a crucial step for the development of BCIs for end-users is the characterisation of the brain signals of interest in the target populations.

The study of ErrPs in potential end-users of BCIs is still in its early stages and the application of online ErrPs-based BCIs in end-users is very still scare [84, 208–210]. In 2012, Spüler and colleagues studied ErrPs in six participants with ALS, in an online experiment in which participants used a P300 speller [84]. In 2017, Seer and colleagues studied ErrPs in persons with ALS and verified an attenuated amplitude of the negativity of the ErrP in participants with poorer executive functioning [208]. In 2019, Keyl and colleagues compared the electrophysiology of ErrPs in participants with SCI and in control participants. They concluded that although the ErrP morphology was comparable among the groups, participants with SCI displayed reduced peak amplitudes [211]. Kumar and colleagues studied ErrPs during post-stroke rehabilitation movements but did not obtain clear ErrP signals [209].

### 1.8. ErrPs' applications for non-disabled users

Most BCIs attempt to offer strategies for communication or control for daily live activities of persons with disabilities. Nevertheless, some BCIs also target recreational activities of these persons, by addressing activities such as gaming, painting, music composition and internet browsing [212–215]. In recent years, the development of

### *1.8. ErrPs' applications for non-disabled users*

BCIs for non-disabled persons has also attracted considerable interest [66, 74, 216–220].

Passive BCIs, which do not require an intentional modulation of brain signals, are particularly suited for non-disabled users. They can be used simultaneously with standard control strategies relying on motor control in order to provide an additional source of information regarding what the user is experiencing [66, 221]. For example, passive BCIs can be used to monitor the brain activity during prolonged tasks and detect changes in attention, workload, or identify error awareness [75–78].

The ErrP signal is particularly suited for BCI applications targeting non-disabled users. Recently, ErrPs have been investigated in real world situations of such users, such as driving a car [79, 147, 222, 223] and virtual environments [144, 224–227]. For instance, Zhang, Chavarriaga and colleagues investigated ErrPs occurring during simulated and real driving tasks and classified ErrPs, offline and online, in a time-locked manner [79, 147, 222, 223]. The detection of errors occurring in virtual reality (VR) environments can be used to improve users' immersive experience. Still, the studies on ErrPs occurring in VR environments mainly focus on the electrophysiological characterisation of ErrPs and, to the best of our knowledge, have not attempted classification [144, 224–227].





## 2. Motivation and Aims

### 2.1. Motivation

BCIs are a promising technology to restore some independence in persons with severe motor disabilities but are still prone to errors. Hence, BCIs would benefit from the incorporation of an error detection system, either to correct actions of a BCI or to improve its performance [135].

Former BCIs relied on mental strategies that were not necessarily intuitive [80, 82]. More recently, research on BCIs is evolving in the direction of establishing more intuitive and natural approaches [126]. A particular example of such approaches is the study of decoding strategies that would provide BCI users with an intuitive continuous control of an end effector, such as a robotic arm [187]. In the context of continuous actions, a user can realise at any moment that an error occurred. To address this aspect, research on ErrPs evolved in the direction of establishing strategies for detecting ErrPs during continuous movement.

A first approach to address the detection of errors in continuous actions was proposed by Kreilinger and consisted in coupling predefined discrete events to the continuous trajectory, to which the error signals could be time-locked [148, 149]. Nevertheless, such approach did not take into account the possibility of the users realising the occurrence the errors at any moment. More recently, the need of coupling discrete events to continuous tasks was overcome and ErrP research focused on establishing reliable strategies for the continuous detection of ErrPs. In particular, this was addressed by the works of Omedes on the detection of ErrPs during the observation of continuous actions [193–195] as well as by the works of Spüler and Milekovic on the detection of ErrPs during the control of a cursor [196–198].

The works mentioned in this section investigated strategies for the continuous detection of ErrPs. Nevertheless, they are theoretical investigations that were conducted in offline conditions. In my opinion, a limitation of the current state-of-the-art literature on ErrPs is the lack of a demonstration of the use of continuous ErrP detection in

## *2. Motivation and Aims*

online conditions as well as the establishment of its pertinence in applications targeting potential end-users of BCIs.

### **2.2. Aim of the thesis**

The central aim of this thesis is to explore ErrPs occurring during continuous control, by developing a strategy for their asynchronous detection in online scenarios that could be applicable to potential end-users of BCIs. Specifically, this thesis aims to shift the study of the asynchronous detection of ErrPs from theoretical investigations done in offline conditions to online applications closer to real-world conditions, in which participants can receive real-time feedback of their own ErrPs. Additionally, this thesis aims to characterise ErrPs in a population with SCI. Finally, it aims to investigate the transferability of an ErrP classifier for online asynchronous ErrP detection, across different populations of participants, with and without SCI.

## 3. Methods and Results

### 3.1. Offline asynchronous detection of ErrPs

[228] C. Lopes-Dias, A. I. Sburlea, and G. R. Müller-Putz. Masked and unmasked error-related potentials during continuous control and feedback. *Journal of Neural Engineering*, 15(3):036031, 2018.

The aim of the first study of the thesis was to investigate the occurrence of ErrPs during the execution of a continuous task. For that, we developed an experiment in which participants controlled a cursor towards one of four targets on a computer screen using a joystick. We recorded the EEG signals of 15 non-disabled participants and analysed the signals offline.

The experiment consisted of 12 experimental blocks with 30 trials each. In 30 % of the trials of each block, the participants lost control of the cursor at a random moment during its trajectory towards the targets. When this happened, the cursor followed a trajectory perpendicular to the previous ongoing movement, as depicted in Figure 3.1. These losses of control were defined as errors and the respective trials were considered error trials. The trials in which no error occurred were considered correct trials. The cursor's position on the screen was presented in two different feedback conditions: jittered feedback (masked) and normal feedback (unmasked). The masked feedback aimed to introduce some uncertainty on the moment in which errors were detected by the participants. The errors occurring in trials with masked feedback were labelled masked errors and the errors occurring in trials with normal feedback were labelled unmasked errors. Half of the blocks displayed masked feedback.

In this work, we first investigated the electrophysiological signature of correct and error trials, irrespectively of the feedback modality. Figure 3.2 displays the grand average correct and error signals at channel FCz. Correct trials were not associated with any event and thus the electrophysiological trace of their average presented no noticeable

### 3. Methods and Results



**Figure 3.1.:** Experimental protocol. Left: A possible cursor's trajectory in an unmasked error trial. Right: A possible cursor's trajectory in a masked correct trial.

potential. The average error trace was consistent with descriptions of ErrPs from state-of-the-art literature.

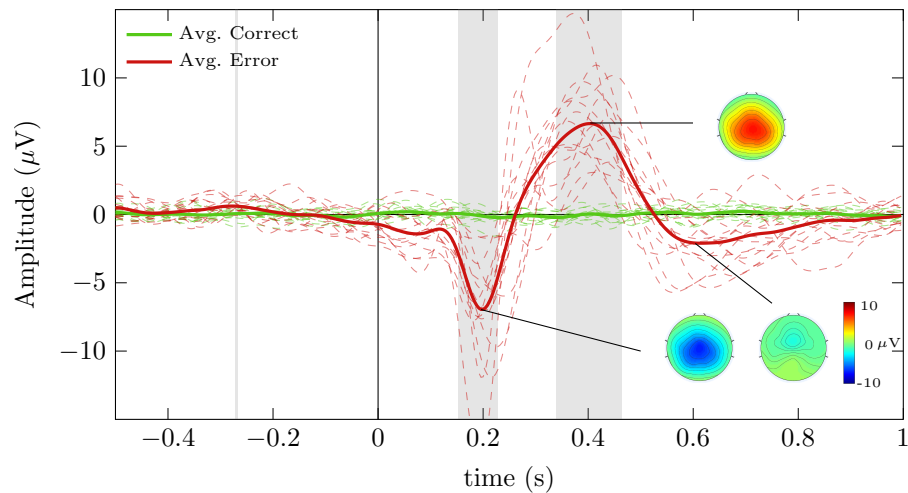


**Figure 3.2.:** Grand average correct and error signals at channel FCz (in green and red, respectively). The grey areas denote the intervals in which correct and error signals are significantly different (Wilcoxon signed-rank tests, Bonferroni corrected, with  $p < 0.05$ ). The dashed lines represent the average error and correct signals of each participant. The scalp distribution of the grand average error signal is displayed at the peaks of the error signal.

When comparing the error signals obtained in the two feedback modalities, the grand average masked error signal presented a delay of 28 ms in relation to the grand average unmasked error signal. The delay in the masked condition could have resulted from

### 3.1. Offline asynchronous detection of ErrPs

a higher task complexity. Surprisingly, the time-locked classification of masked errors against unmasked errors yielded results not significantly above chance level. Hence, masked and unmasked conditions were combined for the asynchronous ErrP detection. The asynchronous strategy is particularly suited for the detection of ErrPs during continuous tasks, in which the moment of the occurrence of the errors cannot be predetermined.

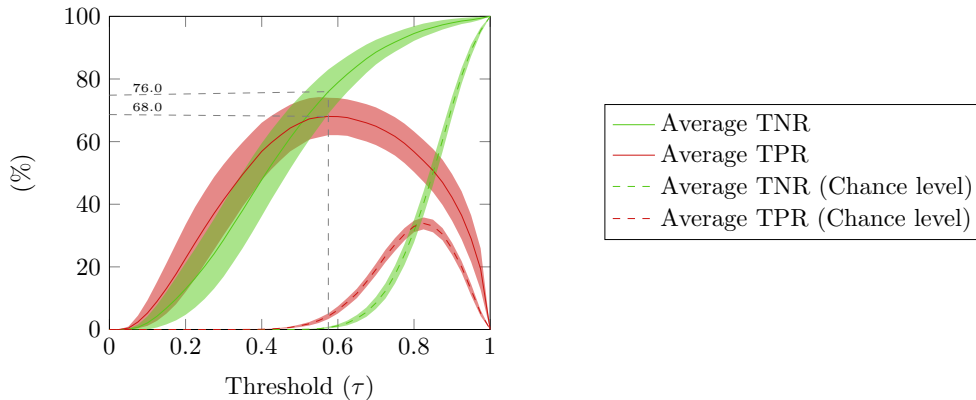


**Figure 3.3.:** Asynchronous detection – cross-validation in the first 80 % of the data: Grand average true negative rate (TNR) and true positive rate (TPR) (green and red solid lines, respectively) in function of the threshold  $\tau$ . The chance level of the TNR and TPR are represented in green and red dashed lines, respectively. The shaded areas represent the 95 % confidence interval of the average curves. The grey dashed lines indicate the threshold that maximises the grand average TPR ( $\tau = 0.575$ ) as well as the corresponding TPR and TNR results (68.0 % and 76.0 %, respectively).

Our approach for the asynchronous ErrP detection was based on the use of a shrinkage linear discriminant analysis (sLDA) classifier [229] with two classes, correct and error. The classifier relied on time domain features whose dimensionality had been reduced, by using principal component analysis (PCA) and only keeping the components that explained 99 % of the data’s variance. We defined an ErrP detection as the occurrence of two consecutive EEG windows with an error probability above a predefined decision threshold  $\tau$ . This strategy aimed to minimise false positive ErrP detections. Furthermore, we defined trial-based metrics to evaluate the asynchronous ErrP detection. Error trials were considered positive and correct trials were considered negative. Hence, a true positive trial was defined as an error trial with no ErrP detections before the error onset and at least one ErrP detection after the error onset. A true negative trial was defined as a correct trial with no ErrP detections. The evaluation of the asynchronous ErrP detection was done in terms of TPR and TNR. TPR was defined

### 3. Methods and Results

as the fraction of error trials that were true positive trials and TNR was defined as the fraction of correct trials that were true negative trials.

Moreover, we used a  $10 \times 5$ -fold cross-validation in the first 80 % of the data to evaluate offline the asynchronous ErrP detection and the effect of varying the classifier's decision threshold  $\tau$ . Figure 3.3 displays the results obtained for all the tested  $\tau$ . The chance level curves were obtained by repeating the cross-validation procedure with permuted training labels. The decision threshold that maximised the grand average TPR was  $\tau = 0.575$ .

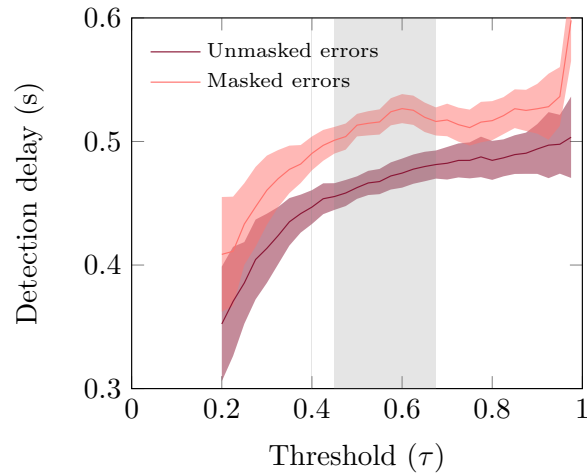


**Figure 3.4.:** Asynchronous ErrP detection – cross-validation in the first 80 % of the data: Average delay of the ErrPs detection in masked and unmasked error trials successfully classified (pink and dark red lines, respectively). The corresponding shaded areas indicate the 95 % confidence intervals. The shaded grey areas indicate the regions in which the delay in masked and unmasked trials was significantly different (Wilcoxon signed-rank test, Bonferroni corrected, with  $p < 0.05$ ).

Despite having combined masked and unmasked errors for the asynchronous detection of ErrPs, we still evaluated the effect of the two feedback modalities on the moment in time in which the ErrPs were detected. Figure 3.4 depicts the average ErrP detection delay, i.e., the period between the error onset and the ErrP detection, in the masked and unmasked error trials successfully classified (TP trials). In this evaluation, we only considered the decision thresholds  $\tau$  with which all participants had at least one error trial successfully classified.

Finally, we evaluated the asynchronous detection of ErrPs in a pseudo-online scenario, in which the first 80 % of the data was used to train the ErrP classifier and the last 20 % of the data was used to test it. Figure 3.5 presents the results obtained with the decision

### 3.1. Offline asynchronous detection of ErrPs

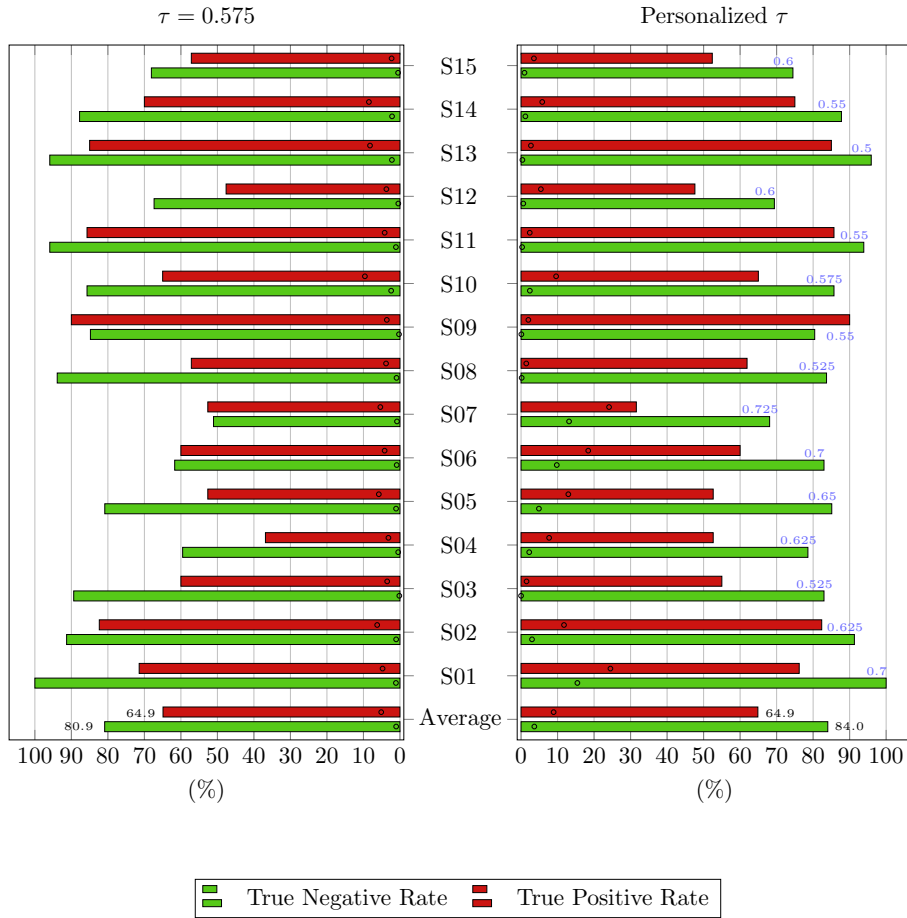


**Figure 3.5.:** Asynchronous ErrP detection – Chronological split (80% - 20%): The percentage of correct trials successfully classified (TNR) are depicted with green bars and the percentage of error trials successfully classified (TPR) are depicted with red bars. The chance level results are represented with small circles. Left: Asynchronous ErrP detection using the threshold  $\tau = 0.575$ . Right: Asynchronous ErrP detection using individual thresholds. The blue numbers indicate the threshold of each participant.

threshold  $\tau = 0.575$  (left), which maximised the grand average TPR, as well as with the threshold  $\tau$  that maximised the individual TPR (right). To prevent overfitting, the thresholds used in the pseudo-online scenario were obtained from the cross-validation in the first 80% of the data. This figure also illustrates that some participants benefit from an individualised decision threshold when using a personalised ErrP classifier.

### *3. Methods and Results*

**Contribution to the thesis:** In this work, we developed the core methodology for the asynchronous detection of ErrPs, which we used in the subsequent studies. We showed the feasibility of asynchronously detecting ErrPs using a classifier based on time-domain features. Furthermore, we investigated the use of a personalised ErrP classifier in combination with a personalised decision threshold, in a pseudo-online scenario.



## 3.2. Online asynchronous detection of ErrPs

[140] C. Lopes-Dias, A. I. Sburlea, and G. R. Müller-Putz. Online asynchronous decoding of error-related potentials during the continuous control of a robot. *Scientific Reports*, 9(1):17596, 2019.

The main aim of the second study of this thesis was to asynchronously detect ErrPs in an online experiment. Furthermore, we introduced an experimental setup that resembled a possible use of a BCI by an end-user.

In this study, we measured the EEG signals of 15 non-disabled participants while they used their right hand to continuously control a robotic arm towards one of two targets placed on a wooden structure, as depicted in Figure 3.6. The participants' hand movement on the tabletop was tracked and translated into the robot's movement on a horizontal plane. Each trial corresponded to a movement towards one of the targets. In 30% of the trials, the paradigm triggered an error at a random moment during the robot's trajectory. The error consisted in interrupting the participants' control of the robot and adding an upwards displacement to the robot's hand. Participants perceived the error by noticing the robot stopping and lifting. These trials were called error trials and the remaining ones were called correct trials.

The experiment was divided into two parts, the calibration and the online parts, which took place consecutively. The calibration part consisted of 8 blocks and the online part consisted of 4 blocks, with 30 trials each: 21 correct and 9 error trials. The calibration part was used to collect the participants' EEG data, with which we trained a personalised ErrP classifier, based on PCA and sLDA. The calibration data were also used to determine a personalised decision threshold for every participant, using cross-validation. The chosen threshold was the one that maximised the product of TPR and TNR. Finally, the personalised ErrP classifier was combined with the personalised decision threshold.

In the online part of the experiment, the classifier was tested asynchronously and participants had the possibility of correcting the robot's errors. If a true positive ErrP detection occurred, i.e., if an ErrP was detected after an error, the robot's hand lowered and the participants regained its control. The downward movement informed the participants of the ErrP detection. Participants were instructed to move the robot's hand to the selected target when regaining control. For a matter of fluidity of the experiment, we decided not to give participants feedback of the false positive ErrP detections, i.e., of the ErrP detections occurring before the error onset or during correct trials.

### 3. Methods and Results

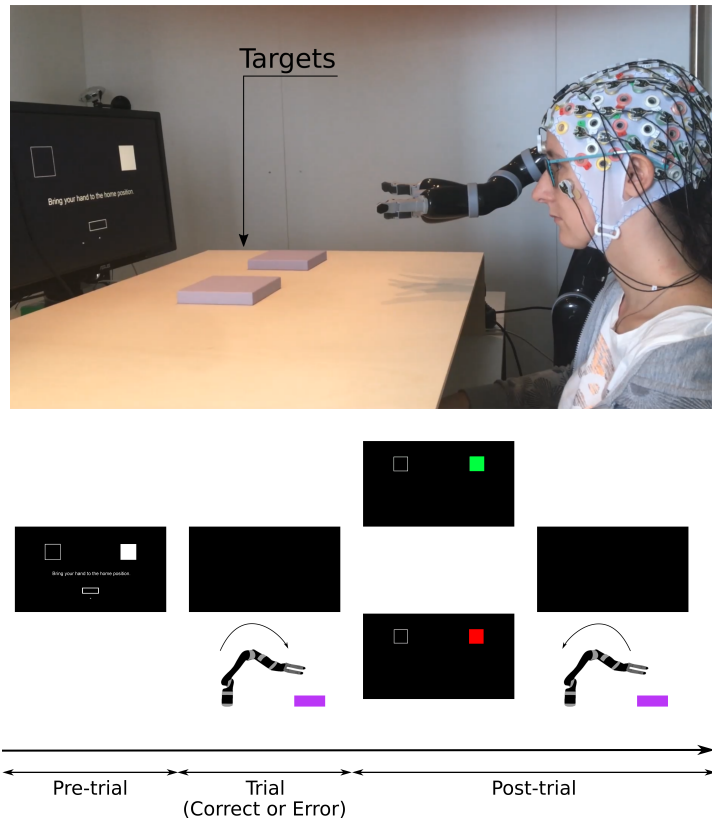


**Figure 3.6.:** Experimental setup and protocol. **Top:** Experimental setup. **Bottom:** Experimental protocol. During the pre-trial period, the white square on the screen indicated the physical target of the coming trial. During the trials, the participants moved the robot to the target on the wooden structure. In the post-trial period, the white square on the screen changed colour to either green or red, indicating whether or not the robot reached the physical target, and the robot automatically returned to its home position.

The electrophysiological signatures of the grand average correct and error signals at channel FCz are depicted in Figure 3.7. The presented signals were filtered with a causal filter in order to illustrate their electrophysiological signature in an online scenario. The use of a causal filter led to a change in the error signal's morphology in comparison to the use of a non-causal filter, which is more commonly applied to depict ErrPs. In particular, it caused a shift of the negative component of the ErrP to after its positive component.

The results regarding the asynchronous ErrP detection in the online part of the exper-

### 3.2. Online asynchronous detection of ErrPs

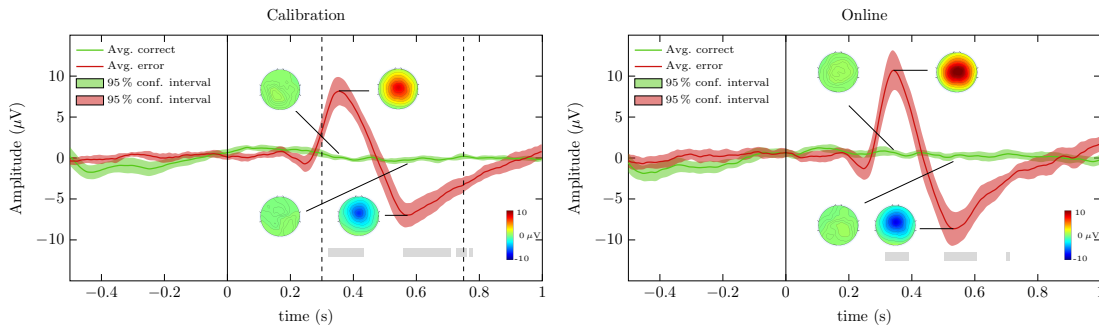


**Figure 3.7.:** Grand average correct and error signals at channel FCz and the corresponding 95% confidence intervals, in green and red, respectively. The grey areas represent the time-points in which the signals were significantly different (Wilcoxon rank-sum tests, Bonferroni corrected,  $p < 0.01$ ). The scalp distribution of the signals are displayed at the time-points corresponding to the peaks of the error signal.

iment are summarised in Figures 3.8 and 3.9. Figure 3.8 depicts the TNR and TPR obtained for each participant and their average. Figure 3.9 depicts the time-points of the ErrP detections during the error trials, in relation to the error onset ( $t = 0$ s). These results indicate that most ErrP detections occurred within one second after the error onset.

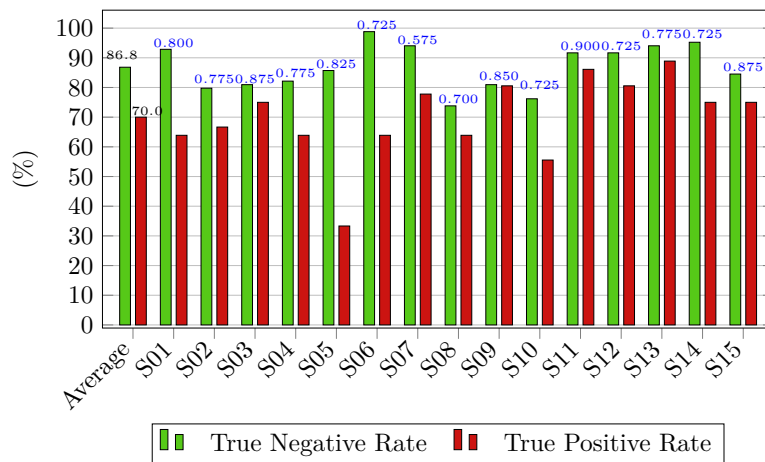


**Figure 3.8.:** Online asynchronous ErrP detection. The green and red bars represent the TNR and TPR, respectively, of every participant and their average. The average TPR was 70.0% and the average TNR was 86.8%. The blue numbers indicate the decision threshold  $\tau$  of each participant.

### 3. Methods and Results

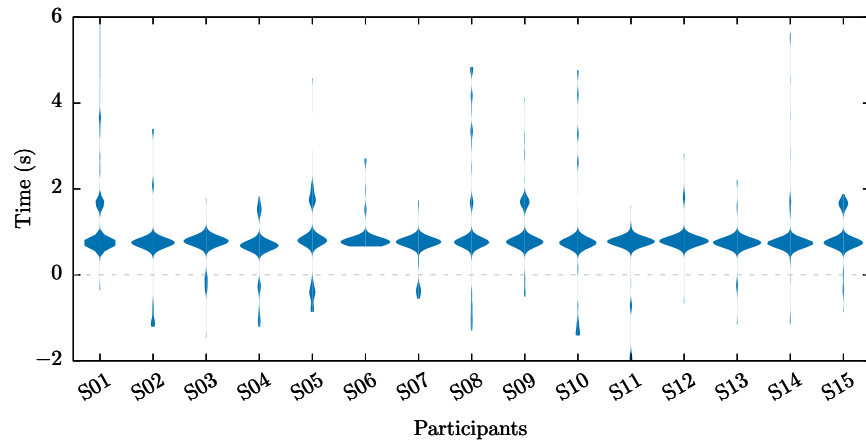


**Figure 3.9.:** ErrP detections' delay in the online scenario. Violin plots, for every participant, of the time-points of all ErrPs detections during the error trials of the online part of the experiment, in relation to the error onset ( $t = 0$  s).

**Contribution to the thesis:** This work is the first demonstration of the asynchronous detection of ErrPs in an online scenario. The experimental setup resembled a possible use of a BCI by end-users, due to the continuous control of the robotic arm and to its use as feedback of the BCI output. This is a first step in the direction of applying the asynchronous detection of ErrPs to potential BCI end-users.

### 3.3. Asynchronous detection of ErrPs with a generic classifier

[230] C. Lopes-Dias, A. I. Sburlea, and G. R. Müller-Putz. Asynchronous detection of error-related potentials using a generic classifier. In *8th Graz Brain-Computer Interface Conference 2019*, pages 54–58, 2019.

[231] C. Lopes-Dias, A. I. Sburlea, and G. R. Müller-Putz. A generic error-related potential classifier offers a comparable performance to a personalized classifier. In *2020 42nd Annual International Conference of the IEEE Engineering in Medicine Biology Society (EMBC)*, pages 2995–2998, 2020.

After asynchronously detecting ErrPs in an online experiment with non-disabled participants, we decided that the next step would be the translation of the developed methods to potential end-users of BCIs. However, from the knowledge gained with the previous experiment, it was clear that it would not be viable to perform such a long experiment, consisting of a lengthy calibration and, additionally, of a testing online part. Therefore, we decided to investigate a strategy to reduce the experiment's duration.

In the two works presented in this section, we developed a generic classifier for the asynchronous detection of ErrPs and showed that such classifier offers a classification performance comparable to a personalised ErrP classifier.

In the first article of this section [230], we used the EEG data of the 15 participants of the previous study to develop a generic ErrP classifier. For each participant, we trained a classifier with the calibration data of the remaining 14 participants and tested it asynchronously on the calibration data of the participant not used for the training. Figure 3.10 (top) shows the grand average classification results obtained and the results of a chance level classifier, which was constructed using a random permutation of the training labels. The vertical grey dashed line represents the optimal threshold at a group level ( $\tau = 0.7$ ), i.e., the threshold that maximises the product of the grand average TPR and the grand average TNR. Figure 3.10 (bottom) depicts the individual results of every participant. The blue dashed line depicts the optimal individual threshold and the grey dashed line depicts the optimal threshold at a group level.

In the second article of this section [231], we used the generic classifier trained in calibration data of 14 participants, just as before, but now we tested it, asynchronously, in the online part of the experiment of the participant not used in the training. Testing the generic ErrP classifier in the online part of the participants' data allowed us to

### 3. Methods and Results

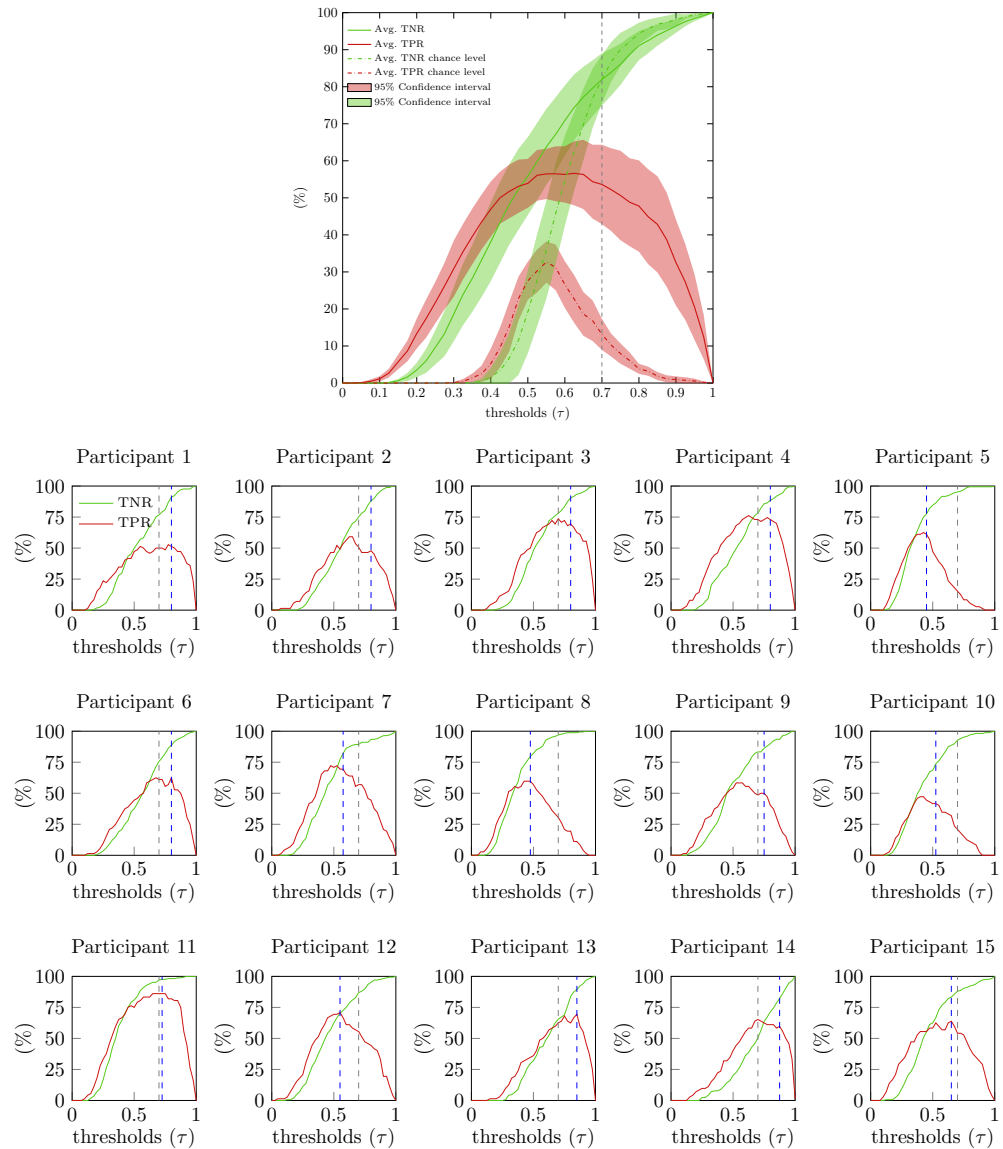


**Figure 3.10.:** **Top:** Grand average TNR and TPR (green and red solid lines, respectively) for the asynchronous ErrP detection with a generic classifier. The chance level results are depicted with green and red dashed lines. The shadowed areas represent the 95% confidence intervals of the curves. The optimal threshold at a group level ( $\tau = 0.7$ ) is represented with a grey vertical dashed line. **Bottom:** Average TNR and TPR obtained for every participant. The optimal individual threshold is represented with a blue dashed line and the optimal threshold at a group level is represented with a grey dashed line.

### 3.3. Asynchronous detection of ErrPs with a generic classifier

directly compare the generic classifier with the personalised classifier of the previous study, since both classifiers were evaluated in the same dataset. The classification results obtained with both classifiers are depicted in Figure 3.11. The classifiers' performances, in terms of TNR and TPR, were not significantly different (Wilcoxon signed ranksum test,  $p = 0.63$  for TNR and  $p = 0.72$  for TPR).

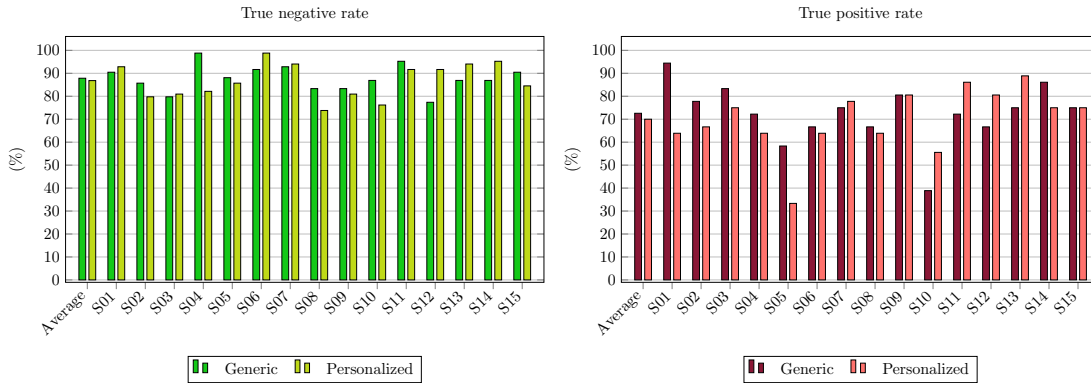


**Figure 3.11.:** Comparison of the asynchronous ErrP detection results obtained with a generic and a personalised ErrP classifiers. Left: TNR using the generic and the personalised classifiers (dark green and light green, respectively). Right: TPR using the generic and the personalised classifiers (dark red and pink, respectively).

**Contribution to the thesis:** These works propose a generic classifier for the asynchronous detection of ErrPs and show that such classifier offers a comparable performance to a personalised ErrP classifier. Moreover, our results reveal that some participants benefit from a personalised threshold when using a generic ErrP classifier. These works allowed the development of an online experiment that did not require offline calibration, leading to a reduction of the experimental duration.

### 3.4. Online asynchronous detection of ErrPs in participants with SCI

[232] C. Lopes-Dias, A. I. Sburlea, K. Breitegger, D. Wyss, H. Drescher, R. Wildburger, and G. R. Müller-Putz. Online asynchronous detection of error-related potentials in participants with a spinal cord injury by adapting a pre-trained generic classifier. *Journal of Neural Engineering*, 2020, accepted.

The aim of the final study of this thesis was to test the asynchronous detection of ErrPs with a generic classifier, in an online scenario and with potential end-users of BCIs. We chose to conduct the experiment with participants with a spinal-cord injury due to the convenience of recruiting them through the Rehabilitation Clinic Tobelbad, Austria.

The experiment consisted of 8 online blocks, each with 30 trials. We kept the experimental setup and protocol of this study very similar to our previous one, as depicted in Figure 3.12. The main difference between the experimental setups was the replacement of the physical targets by targets on a screen. The errors were identical to the previous experiment. Therefore, we could use the EEG data of the previous experiment to train a generic ErrP classifier. This classifier was tested asynchronously in an online experiment, in which 8 participants with SCI and 8 non-disabled control participants took part. Each participant in the SCI group was matched with a control participant of the same gender and a maximum age difference of 5 years.

The experiment required no previous offline calibration with the participants and they received feedback of the ErrP detections during its entire duration. Similarly to the previous study, we decided not to give participants feedback of the false positive detections, i.e., of the ErrP detections occurring before the error onset or during correct trials. The generic classifier was initiated with a generic decision threshold  $\tau = 0.7$  since, in our previous investigation, this was considered to be the optimal threshold at a group level, as depicted in Figure 3.10 of the previous section.

Despite giving participants feedback during the entire duration of the experiment, we still used the first three blocks to tailor the decision threshold to each participant. Hence, after each of these blocks, we evaluated offline the asynchronous ErrP detection with the generic classifier, on all the available EEG data of each participant at that moment. We used the optimal threshold resulting from this evaluation as the personalised decision threshold in the coming block. From block 4 onwards, we kept the decision threshold of every participant fixed. Therefore, we only used the remaining blocks, i.e., blocks 4 to 8, for the evaluation of the classifier, since no parameter was



### 3.4. Online asynchronous detection of ErrPs in participants with SCI

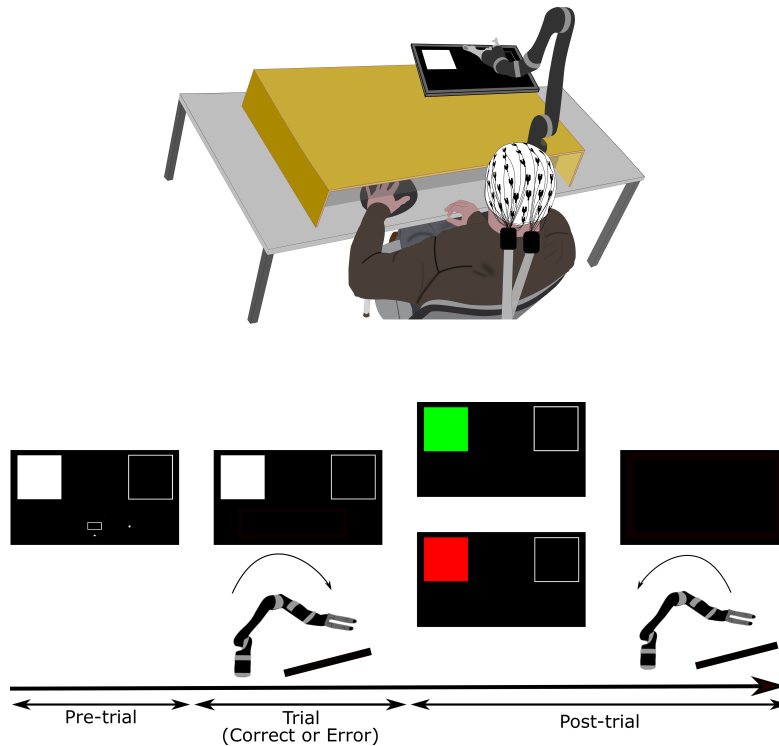


**Figure 3.12.:** **Top:** Experimental setup. **Bottom:** Experimental protocol. During the pre-trial period, two squares were displayed on the top part of the screen. The white square was the target of the coming trial. The participants were instructed to move the robot to the target square during the trials. Afterwards (post-trial period), the target changed colour to either green or red, indicating whether the robot reached or not the target and the robot automatically returned to its home position.

changed in these blocks.

In this work, we also presented the electrophysiology of ErrPs in participants with SCI and in non-disabled control participants, at a group level and for the individual participants, as depicted in Figure 3.13.

Moreover, we tested asynchronously and online, the transfer of a generic ErrP classifier from non-disabled participants to two distinct populations: participants with SCI and a different group of non-disabled control participants. The classification results obtained, in terms of TNR and TPR, are depicted in Figure 3.14. Figure 3.15 illustrates the online asynchronous detection of ErrPs and the trials' offline evaluation for participant C1.

### 3. Methods and Results

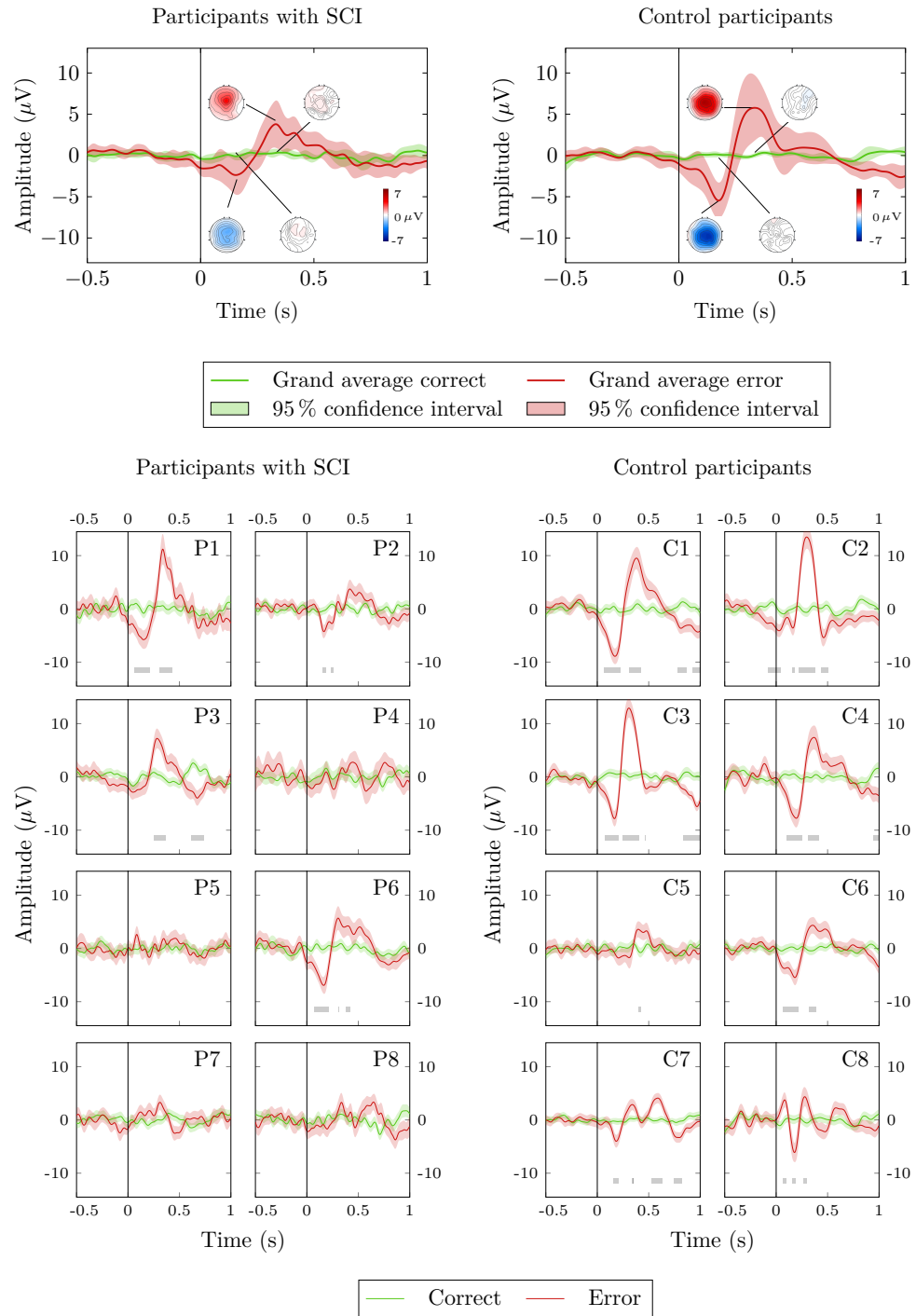


**Figure 3.13.:** Grand average (top) and individual average (bottom) correct and error signals at channel FCz (green and red solid lines, respectively) for participants with SCI and control participants. The shaded areas represent the 95 % confidence interval of the grand average curves. The grey regions indicate the time-points in which correct and error signals were statistically different (Wilcoxon ranksum tests, Bonferroni corrected,  $\alpha = 0.01$ )

### 3.4. Online asynchronous detection of ErrPs in participants with SCI

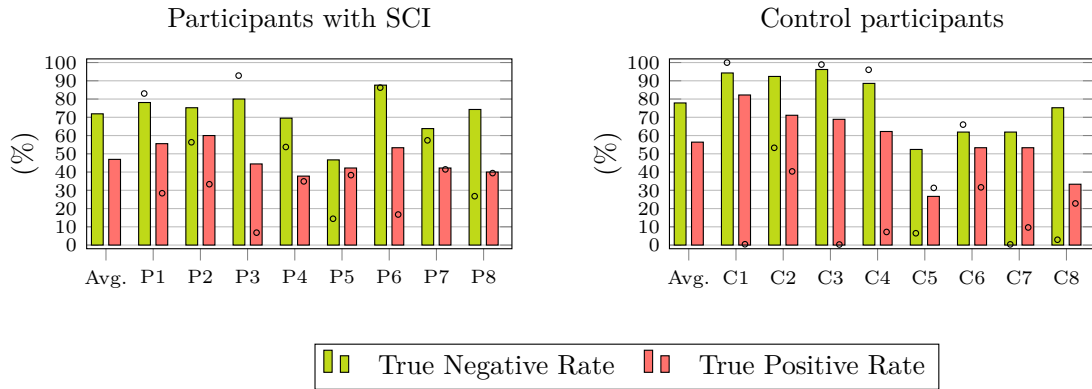


**Figure 3.14.:** Generic classifier: ErrP detection results, in terms of true TPR and TNR, using the generic classifier online. The circles on the individual bars represent the chance level of the corresponding metric for every participant.

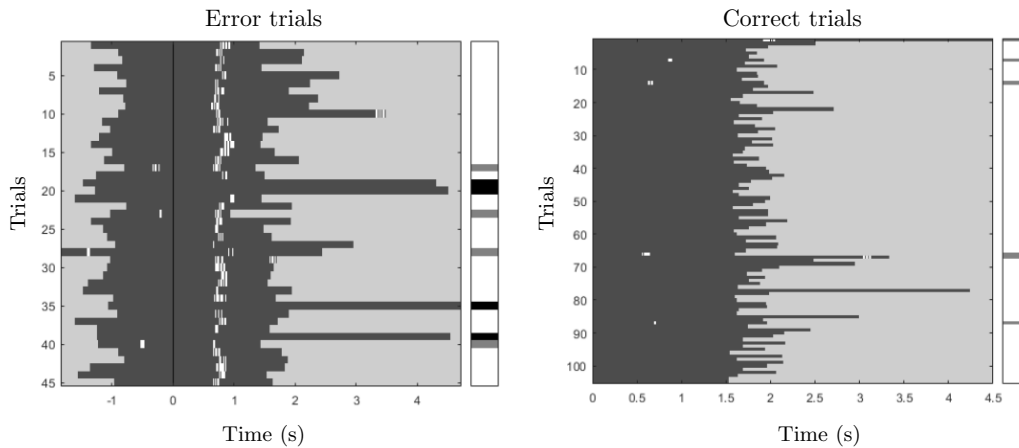


**Figure 3.15.:** Online detection of ErrPs with the generic classifier and trials' offline evaluation for participant C1. Left: Error trials, aligned to the error onset (black vertical line). Right: Correct trials, aligned to the start of the trial. The dark grey areas represent the trials and the white marks within them represent the ErrP detections. The narrow rectangles colour code the trials' offline evaluation. In these rectangles, trials successfully classified (true positive trials and true negative trials) are coded in white and trials with false positive ErrP detections are coded in light grey. Error trials with no ErrP detections are coded in black.

Finally, we evaluated the asynchronous detection of ErrPs with a personalised classifier,

### 3. Methods and Results

offline, using a  $10 \times 5$ -fold cross-validation. Figure 3.16 depicts the classification results obtained with a personalised classifier and a personalised decision threshold.

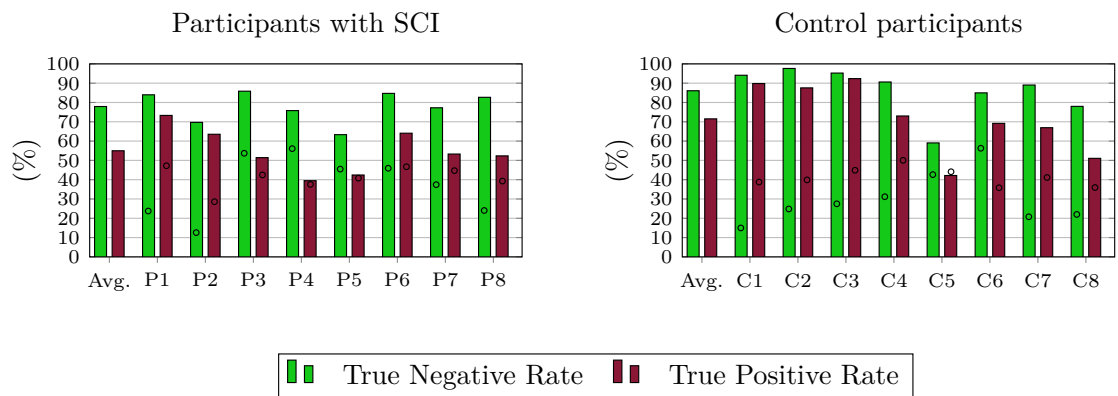


**Figure 3.16.:** Personalised classifier: Average TNR and TPR resulting from the offline cross-validation procedure with the personalised classifier. The circles on the individual bars represent the chance level of the corresponding metric for every participant.

In this study, we concluded that participants who did not present clear ErrP signals obtained a chance level performance with the generic classifier. Despite half of the participants with SCI not presenting clear ErrP signals, we hypothesise that such effect can be associated with psychological factors rather than with the SCI itself.

**Contribution to the thesis:** This study shows the feasibility of asynchronously detecting ErrPs online in participants with SCI. Moreover, it shows that it is possible to transfer a classifier for the asynchronous detection of ErrPs across non-disabled participants and also from non-disabled participants to participants with SCI, in case the latter present clear ErrP signals. These results suggest that the use of a generic ErrP classifier is a viable approach to give participants feedback of the ErrP detections from the start of an experiment, avoiding the offline calibration of ErrPs.

## 4. Discussion and Conclusion

The main aims of this thesis were the study of the asynchronous detection of ErrPs during continuous control and the investigation of its applicability to online scenarios. To this end, we started by focusing on the asynchronous detection of ErrPs using a personalised classifier, both in offline and in online scenarios. Furthermore, we developed a generic classifier for the asynchronous detection of ErrPs. This classifier was tested in an online scenario, both with participants with SCI and with non-disabled control participants. In the following sections, we summarise the achievements of this thesis and discuss them in relation to the current state of the art.

### 4.1. Asynchronous detection of ErrPs

In recent years, BCI research is rapidly evolving in the direction of establishing intuitive and natural approaches to control a BCI [126–128, 130–132, 185, 186, 233, 234]. In particular, there was a strong emphasis on the investigation of strategies that would offer BCI users an intuitive and continuous control of an end effector, such as a cursor or a robotic [187, 188, 190–192]. In the context of continuous control, the user's perception that an error occurred can happen at any moment. Hence, the identification of errors in such situations requires an asynchronous detection of ErrPs. This is a relatively recent research topic, yet it has a great potential for exploration and applicability.

As mentioned in the Introduction, the asynchronous detection of ErrPs has been investigated by Milekovic, Omedes and Spüler. Milekovic showed the feasibility of detecting ErrPs from ECoG signals [196, 197]. Omedes then established the asynchronous detection of ErrPs from EEG signals in an observation task [193–195]. Spüler and colleagues further pursued this line of research, by using EEG signals to asynchronously detect ErrPs in a task involving the continuous control of a cursor [198]. All these studies were performed in offline conditions, i.e., the asynchronous ErrP detection was conducted after the end of the experiment. Thus, the participants received no feedback of their

#### 4. Discussion and Conclusion

ErrPs.

In the study described in section 3.1 [228], we also investigated, offline, the asynchronous detection of ErrPs in a task involving continuous control of a cursor. We proposed an ErrP classifier based on time domain features. This classifier offered a classification performance comparable to the results presented in [193, 198], which were based either on frequency domain features or on a combination of time and frequency domain features.

In [228], we introduced two modalities of continuous feedback: masked and unmasked. The unmasked feedback referred to the normal feedback. The masked feedback combined the normal feedback with a jitter component. The masked feedback aimed to create some uncertainty regarding the moment in which users perceived the errors. In [228], we showed that, on average, the ErrP detections occurred later in the masked condition than in the unmasked condition. This results possibly reflect that participants took longer to realise the occurrence of the errors in the masked condition.

The asynchronous detection of ErrPs is, by design, a very unbalanced problem. Errors are isolated events that occur unexpectedly and are separated by longer periods of time with no errors. We considered two main strategies to approach the asynchronous detection of ErrPs. First, we defined an ErrP detection as the occurrence of two consecutive EEG windows with an error probability above the decision threshold  $\tau$ . This strategy helped to reduce the false positive ErrP detections. Furthermore, in [228], we showed that the use of a personalised decision threshold in combination with the ErrP classifier can improve the classification performance in an asynchronous scenario, by biasing the classifier towards one of the classes. Thus, we applied these strategies in our subsequent studies.

Offline experiments are important because they allow researchers to investigate strategies to improve BCIs' performance. However, the ultimate goal of BCI research should be the development of solutions that are applicable to real-world scenarios, in an online manner. So far, the online detection of ErrPs has been only investigated in a time-locked manner, using either discrete tasks [87, 153, 155] or a combination of continuous tasks with additional discrete feedback moments [146, 148, 149].

To the best of our knowledge, we present in this thesis the first demonstration of the online detection of ErrPs in an asynchronous manner. In the study described in section 3.2 [140], non-disabled participants controlled a robotic arm towards two targets. This experimental setup aimed to resemble a possible use of a BCI by an end-user. The errors occurred during the robot's movement towards the targets and were automatically generated by the paradigm. This strategy assured that all participants experienced the same number of errors and aimed to elicit comparable motivation and engagement across participants.

This study was composed of two distinct parts: an offline calibration and an online part, in which the classifier was tested. When constructing the ErrP classifier, we incorporated our previous findings, by combining the personalised classifier with a personalised decision threshold. In the online part, participants could correct the errors triggered by the paradigm, in case an ErrP was detected by the classifier. We decided not to give participants feedback of the false positive detections of ErrPs. This aimed to preserve the experimental conditions as much as possible, from calibration to online parts and across participants. Moreover, it avoided that the possible occurrence of many false positive ErrP detections would disturb the fluidity of the experiment. In any case, giving participants feedback, even if only partially as in our study, will always influence them. For instance, in this study, we observed that the peak amplitudes of the ErrPs were, on average, more pronounced during the online part of the experiment than during the calibration [140]. We hypothesise that this is a consequence of an increase in participants' engagement caused by the feedback [26, 32].

The online asynchronous detection of ErrPs is an important step towards the applicability of ErrPs in real-world scenarios. However, in online experiments, all the methodological decisions are made before the experiment. Thus, online experiments will probably not lead to the best possible classification results. Instead, they offer a glimpse of what is an expectable performance in real-word scenarios.

## 4.2. Generic ErrP classifiers

The big majority of BCIs rely on personalised classifiers, which are trained with the participants own brain signals. These classifiers typically use brain signals recorded during an offline calibration task, taking place right before each BCI use.

An alternative to personalised classifiers are generic classifiers. These are trained with brain signals acquired either during a different task or from other participants. The construction and use of a generic classifier is also known as classifier transfer, either across different tasks or across different participants. Generic classifiers require minimal or no offline calibration and thus have the potential of making the use of BCIs more straightforward and less time consuming. However, the study of generic classifiers is still scarce [170, 171, 173, 179–181, 235], possibly due to the belief that they offer a worse performance than personalised classifiers.

The ErrP signal is a particularly good candidate for the construction of a generic classifier because its morphology is stable across participants and over long periods of time [143]. In recent years, the study of generic ErrP classifiers has received a renewed interest [236–238]. However, so far, the transfer of ErrP classifiers has only

#### 4. Discussion and Conclusion

been studied in tasks in which the ErrP detection is done in a time-locked manner and in offline scenarios. Iturrate and colleagues [150, 182] studied the transfer of an ErrP classifier across different participants and different tasks, proposing a latency correction method. Furthermore, Kim and colleagues extended the transfer of ErrP classifiers not only across different participants but also across tasks involving different types of ErrPs: interaction and observation ErrPs [183, 184]. Kim and colleagues concluded that the transfer across tasks outperformed the transfer across participants. However, transferring ErrP classifier across very different tasks, in particular from 2D tasks on a computer screen to a real-world 3D tasks ErrPs, is not always successful and poses additional challenges that remain to be addressed [150, 239].

In this thesis, we present, to the best of our knowledge, the first demonstration of the use of a generic classifier for the asynchronous detection of ErrPs, offline and online. In section 3.3 [230, 231], we present a generic ErrP classifier which was tested asynchronously, by transferring the classifier across different participants [230]. For each of the 15 participants of our first online experiment [140], we trained an ErrP classifier with data from the 14 remaining participants and tested it asynchronously in the participant not used for training. In [230], we also show that although the proposed classifier does not necessarily require calibration, participants benefit from a personalised decision threshold when using the generic classifier, similarly to what we had verified with the personalised ErrP classifier. Moreover, we show that the performance of the generic ErrP classifier is comparable to the performance of a personalised ErrP classifier [231]. These results challenge the common belief that a personalised classifier always yields a better classification performance than a generic classifier. Moreover, these findings can encourage the incorporation of ErrP classifiers when constructing BCIs, since the proposed classifier does not require offline calibration.

Furthermore, in this thesis we present the first demonstration of the asynchronous detection of ErrPs with a generic classifier in an online scenario. In section 3.4 [232], we describe an online experiment in which we asynchronously detected ErrPs using a generic classifier with personalised decision thresholds. This experiment is, in its structure, similar to our first online experiment [140]. The main methodological differences are the use of a generic ErrP classifier, the elimination of the offline calibration and the incorporation of two distinct groups of participants: 8 non-disabled participants and 8 participants with SCI.

In this study, we evaluate the performance of the generic classifier during an online experiment, and also the performance of a personalised classifier, offline through cross-validation [232]. These different approaches do not allow us to directly compare the performance of the two classifiers since they are not tested with the exact same dataset. Still, the different performances of the two classifiers in non-disabled participants suggests that these participants would have benefited from a personalised classifier. Hence,



interestingly, these results do not support our previous findings, which indicated that a generic ErrP classifier offers a comparable performance to a personalised ErrP classifier [231]. The main difference between the non-disabled populations that participated in the experiments [140] and [232] is their age range. Participants in [140] were mostly recruited from a population of university students while the non-disabled participants in [232] were age-matched with the participants with SCI and, thus, were of a much broader age range. Hence, in [232], the generic ErrP classifier was transferred across populations with a very different age range. Several studies report a decrease of the ErrP peak amplitudes with age [32, 52]. The electrophysiological results of this study also support such decrease in amplitudes [232]. We hypothesise that the average drop in performance with the generic ErrP classifier verified in the non-disabled participants, can be related with the transfer of the classifier, trained with ErrPs from a relatively homogenous population, to a population with a broader age range. Interestingly, we observed that older participants were more likely to benefit from lower personalised decision thresholds, possibly to compensate the lower amplitudes of their ErrPs.

### 4.3. ErrPs in BCI end-users

A substantial challenge in the BCI field is to test BCIs with potential end-users. A first reason for the limited literature on BCIs with end-users is the logistical difficulties in recruiting such participants, which often results in studies with very few participants [98, 100–102, 127, 128, 203, 240, 241]. The comprehensible desire of thoroughly testing the BCIs in non-disabled participants before using them with potential BCI end-users, can delay its application. In addition, the brain signals of interest in non-disabled participants are not necessarily representative of the corresponding signals in end-users. Moreover, it is important to focus on end-user needs, through user-centred approaches, which take into account the users' subjective preferences [242].

Recently, efforts have been made in the direction of characterizing ErrPs in potential BCI end-users [208, 209, 211]. Our work complements the existing state-of-the-art literature, by providing a characterization of ErrPs in 8 participants with SCI [232]. We show that the ErrP morphology is not homogenous across participants with SCI. However, further studies are necessary to unveil the reasons behind the dissimilarities. In [232] we hypothesise that age variation and psychological reasons can influence such dissimilarities [243–247].

In this thesis, we also present, to the best of our knowledge, the first demonstration of the asynchronous detection of ErrPs in potential BCI end-users. In [232], we constructed a generic ErrP classifier, trained with data from non-disabled participants, and tested the classifier online for the asynchronous detection of ErrPs not only with

#### 4. Discussion and Conclusion

a different group of non-disabled participants but also with participants with SCI. All the participants, with or without SCI, that displayed clear ErrP signals obtained classification performances above chance level with the generic classifier. Moreover, we show that most participants without clear ErrP signals would also not have benefited from personalised classifiers. Hence, our work also shows that it is possible to transfer a generic ErrP classifier from non-disabled users to participants with SCI, when the latter display clear ErrP signals.

In 2012, Spüler and colleagues investigated the transfer of an ErrP classifier across participants with ALS and also across non-disabled participants [84] and hypothesised that, for motor impaired participants, personalised ErrP classifiers were necessary. Spüler did not investigate the ErrP transfer from non-disabled participants to participants with ALS. The participants with ALS in [84] displayed a heterogeneous ErrP morphology. This possibly explains the lack of success when transferring an ErrP classifier across them. In our study [232], participants with SCI also displayed a heterogeneous ErrP morphology. Hence, we hypothesise that transferring an ErrP classifier from non-disabled participants to potential BCI end-users is a better strategy than transferring an ErrP classifier across potential BCI end-users.

#### 4.4. Limitations and recommendations

The pursuit of a feasible implementation of our studies, compelled us to undertake some compromises. In this section, we present the main limitations of our work and discuss possible future strategies to overcome them.

A limitation of this thesis regards our choice of not giving participants feedback of the false positive ErrP detections during the online experiments. This was not a technical limitation but rather an experimental design choice. ErrPs are modulated by factors such as motivation and engagement. Hence, we wanted to avoid that the possible occurrence of many false positive ErrP detections would lead to a loss of the participants' motivation. Any type of feedback, even if only partial as in our experiments, will influence the participants. Giving them, in addition, feedback of the false positive ErrP detections would lead to an even more unequal scenario across participants. Giving participants full feedback regarding the asynchronous detection of ErrPs is a straightforward step, since no methodological changes are needed in relation to the work presented in this thesis. Nevertheless, the results of such an experiment have to be interpreted with caution, since participants will not necessarily be in comparable conditions.

Other limitation of our online experiments is the fact that, although we aimed to mimic

an intuitive use of a BCI, the manner in which the errors were triggered was not very natural. A more intuitive strategy would have been the introduction of a sideways deviation, instead of the stopping and lifting of the robotic arm. Nevertheless, the incorporation of the vertical dimension conferred practical benefits. The subsequent lowering of the robotic arm was integrated as a cue regarding the ErrP detections, eliminating the need of extra feedback modalities.

Moreover, in all our experiments, the errors were externally triggered, what does not happen in the real use of a BCI. In such context, only the user knows about the occurrence of errors, since they result from his/her subjective evaluation of a situation. The use of artificially triggered errors is a common practice in ErrP research. It allows researchers to establish a ground truth, which can be used as a reference to evaluate the performance of ErrP classifiers. Alternatively, if the errors are not known, one could use an approach in which the user reports the perception of errors, such as described in [248], to test the asynchronous detection of ErrPs.

Finally, an obvious limitation of our work is the use of the participants' own movement to achieve continuous control of the cursor and the robot, and not their brain signals. This choice was a consequence of our belief that intuitive mental strategies for continuous trajectory decoding using EEG are still unable to provide reliable control, despite major progresses in recent years [190–192]. Alternatively, we could have used less intuitive strategies to achieve continuous control, such as the modulation of sensory motor rhythms [148, 249]. However, we considered that such alternatives would have led us to deviate from the intended natural control of the robot. In any case, the methods developed in this thesis can be directly applicable to a situation where the continuous control is decoded from brain signals.

## 4.5. Summary and conclusion

In this thesis, we investigated the asynchronous detection of ErrPs, in offline and online experiments. Additionally, we developed a generic ErrP classifier that does not require previous offline calibration with the user. We showed that such classifier offers a performance comparable to a personalised ErrP classifier. Moreover, we asynchronously tested the generic ErrP classifier in an online experiment, in which participants with SCI and also non-disabled participants took part. Our results showed that the generic ErrP classifier is transferable across non-disabled participants and also from non-disabled participants to participants with SCI, as long as these display ErrPs.

The generic ErrP classifier developed requires no previous offline calibration and can be used asynchronously and online, by different populations of BCI users. Hence, our

#### 4. Discussion and Conclusion

findings have the potential to encourage the widespread incorporation of ErrP detection in BCIs. In my opinion, this thesis presents a significant contribution to the research on ErrPs in the BCI field, bringing the state of the art closer to the applicability of the asynchronous detection of ErrPs to real life situations.

### 4.6. Future perspectives

Many interesting research questions remain to be investigated. Since the asynchronous detection of ErrPs is a relatively recent research topic, the investigation of methodological aspects to improve it should, in my opinion, be further pursued. For instance, it is worth to further investigate and evaluate the benefit of using frequency features, time features or a combination of both, for the asynchronous detection of ErrPs with personalised and generic classifiers.

Furthermore, deeper investigations on the asynchronous use of generic ErrP classifiers can lead to an expansion of the applicability of ErrPs. In this thesis, we asynchronously tested the transfer of a generic ErrP classifier across participants who took part in two very similar experiments. It remains to be investigated, e.g., if such transfer is also generalisable across very different tasks or across distinct sessions with the same participant.

Finally, the most promising future extension of the work presented here is, in my opinion, the application of the online asynchronous detection of ErrPs to realistic daily life activities of non-disabled users. In such activities, ErrPs can be used to provide information regarding the user's subjective experience without requiring explicit communication. There are three main aspects that support this view.

First, given the current state of the art in BCIs, non-disabled users certainly find motor-based control more intuitive and reliable than BCI-based control. Hence, the asynchronous decoding of EEG signals that do not require an intentional modulation, such as the ErrP, could be easily integrated with motor tasks. Such strategy would probably be accepted by the users as long as it would be combined with a portable EEG headset that would not require a long preparation time.

Second, non-disabled users in realistic daily life activities would not be willing to calibrate a classifier often [219]. Hence, the use of a generic ErrP classifier, or the transfer of the classifier across different sessions, would be an asset when targeting ErrP detection in non-disabled users.

Lastly, most daily life activities of non-disabled users are continuous and not discrete. Therefore, the asynchronous detection of ErrPs is specially suited to such tasks. Examples of activities that could benefit from real-time ErrPs' detection are, e.g., driving

a car [79, 147], gaming [197, 198], and VR environments [144, 220, 250, 251]. During the completion of this thesis, we also studied ErrPs in a realistic environment: we investigated the time-locked single trial detection of ErrPs in a VR environment, in which participants performed a self-paced pick-and-place task, and attempted to differentiate distinct system errors that can occur [250]. Nevertheless, this and the previously mentioned studies are still, to some extent, artificial. In my opinion, the extension of such studies to even more realistic scenarios and the application of the asynchronous ErrP detection to daily life activities of non-disable persons can contribute to the development of reliable strategies to detect ErrPs which, in turn, would be applicable to BCIs targeting potentials end-users. In particular, the online use of a generic classifier to asynchronously detect ErrPs in daily life activities remains to be investigated in future.



# Bibliography

- [1] E. R. Kandel, J. H. Schwartz, and T. M. Jessell. *Principles of neural science*. McGraw-Hill, Health Professions Division, 4 edition, 2000. ISBN 0838577016,9780838577011.
- [2] W. Gerstner, W. M. Kistler, R. Naud, and L. Paninski. *Neuronal Dynamics: From Single Neurons to Networks and Models of Cognition*. Cambridge University Press, USA, 2014. ISBN 1107635195.
- [3] T. Kirschstein and R. Köhling. What is the source of the EEG? *Clinical EEG and Neuroscience*, 40(3):146–149, 2009.
- [4] S. J. Luck. *An introduction to the event-related potential technique*. The MIT Press, 2014.
- [5] H. Berger. Über das Elektrenkephalogramm des Menschen. *Archiv für Psychiatrie und Nervenkrankheiten*, 87(1):527–570, Dec 1929.
- [6] E. Niedermeyer, D. L. Schomer, and F. H. Lopes da Silva. *Niedermeyer's electroencephalography: Basic principles, clinical applications, and related fields*. Wolters Kluwer Health/Lippincott Williams & Wilkins, 2011. ISBN 9780781789424.
- [7] D. T. Bundy, E. Zellmer, C. M. Gaona, M. Sharma, N. Szrama, C. Hacker, Z. V. Freudenburg, A. Daitch, D. W. Moran, and E. C. Leuthardt. Characterization of the effects of the human dura on macro- and micro-electrocorticographic recordings. *Journal of Neural Engineering*, 11(1):016006, Jan 2014.
- [8] N. Hill, D. Gupta, P. Brunner, A. Gunduz, M. Adamo, and G. Schalk. Recording human electrocorticographic (ECoG) signals for neuroscientific research and real-time functional cortical mapping. *JoVE*, 64:e3993, Jun 2012.
- [9] M. Simon. Intraoperative electrocorticography (ECOG) for seizure focus localization. *Clinical Neurophysiology*, 127(9):e306, 2016.

## Bibliography

- [10] D. Cohen. Magnetoencephalography: Detection of the brain's electrical activity with a superconducting magnetometer. *Science*, 175(4022):664–666, 1972.
- [11] F. H. Lopes da Silva. EEG and MEG: Relevance to neuroscience. *Neuron*, 80(5):1112 – 1128, 2013.
- [12] F. Jobsis. Noninvasive, infrared monitoring of cerebral and myocardial oxygen sufficiency and circulatory parameters. *Science*, 198(4323):1264–1267, 1977.
- [13] A. Villringer, J. Planck, C. Hock, L. Schleinkofer, and U. Dirnagl. Near infrared spectroscopy (nirs): A new tool to study hemodynamic changes during activation of brain function in human adults. *Neuroscience Letters*, 154(1):101 – 104, 1993.
- [14] Y. Hoshi. Functional near-infrared spectroscopy: current status and future prospects. *Journal of Biomedical Optics*, 12(6):1 – 9, 2007.
- [15] S. Ogawa, T. M. Lee, A. S. Nayak, and P. Glynn. Oxygenation-sensitive contrast in magnetic resonance image of rodent brain at high magnetic fields. *Magnetic Resonance in Medicine*, 14(1):68–78, 1990.
- [16] S. Ogawa, T. M. Lee, A. R. Kay, and D. W. Tank. Brain magnetic resonance imaging with contrast dependent on blood oxygenation. *Proceedings of the National Academy of Sciences*, 87(24):9868–9872, 1990.
- [17] G. H. Glover. Overview of functional magnetic resonance imaging. *Neurosurgery Clinics of North America*, 22(2):133 – 139, 2011.
- [18] R. S. Menon, J. S. Gati, B. G. Goodyear, D. C. Luknowsky, and C. G. Thomas. Spatial and temporal resolution of functional magnetic resonance imaging. *Biochemistry and Cell Biology*, 76(2-3):560–571, 1998.
- [19] W. Tatum, G. Rubboli, P. Kaplan, S. Mirsatari, K. Radhakrishnan, D. Gloss, L. Caboclo, F. Drislane, M. Koutroumanidis, D. Schomer, D. Kasteleijn-Nolst Trenite, M. Cook, and S. Beniczky. Clinical utility of EEG in diagnosing and monitoring epilepsy in adults. *Clinical Neurophysiology*, 129(5):1056 – 1082, 2018.
- [20] P. Miranda, C. Cox, M. Alexander, S. Danev, and J. Lakey. Overview of current diagnostic, prognostic, and therapeutic use of EEG and EEG-based markers of cognition, mental, and brain health. *Integrative Molecular Medicine*, 6, Jan 2019.
- [21] G. Pfurtscheller and F. H. Lopes da Silva. Event-related EEG/MEG synchronization and desynchronization: basic principles. *Clinical Neurophysiology*, 110(11):1842 – 1857, 1999.



- [22] O. Jensen, E. Spaak, and J. M. Zumer. *Human Brain Oscillations: From Physiological Mechanisms to Analysis and Cognition*, pages 1–46. Springer International Publishing, Cham, 2014. ISBN 978-3-319-62657-4.
- [23] E. Friedrich, R. Scherer, and C. Neuper. The effect of distinct mental strategies on classification performance for brain–computer interfaces. *International journal of psychophysiology*, 84:86–94, 2012.
- [24] G. Pfurtscheller. Functional brain imaging based on ERD/ERS. *Vision Research*, 41(10):1257 – 1260, 2001.
- [25] G. Pfurtscheller and A. Aranibar. Event-related cortical desynchronization detected by power measurements of scalp EEG. *Electroencephalography and Clinical Neurophysiology*, 42(6):817 – 826, 1977.
- [26] S. Luck and E. Kappenman. *The Oxford Handbook of Event-Related Potential Components*. Oxford Library of Psychology. Oxford University Press, 2011. ISBN 9780199705870.
- [27] P. Rabbitt. Error correction time without external error signals. *Nature*, 212 (5060):438–438, Oct 1966.
- [28] P. Rabbitt and B. Rodgers. What does a man do after he makes an error? an analysis of response programming. *Quarterly Journal of Experimental Psychology*, 29(4):727–743, 1977.
- [29] M. Falkenstein, J. Hohnsbein, J. Hoormann, and L. Blanke. Effects of errors in choice reaction tasks on the ERP under focused and divided attention. *Psychophysiological Brain Research*, pages 192–195, 1990.
- [30] M. Falkenstein, J. Hohnsbein, J. Hoormann, and L. Blanke. Effects of crossmodal divided attention on late ERP components. ii. error processing in choice reaction tasks. *Electroencephalography and Clinical Neuro-physiology*, 78:447–455, 1991.
- [31] W. J. Gehring, B. Goss, M. G. Coles, D. E. Meyer, and E. Donchin. A neural system for error detection and compensation. *Psychological Science*, 4(6):385–390, 1993.
- [32] M. Falkenstein, J. Hoormann, S. Christ, and J. Hohnsbein. ERP components on reaction errors and their functional significance: a tutorial. *Biological Psychology*, 51(2):87 – 107, Feb 2000.
- [33] P. Luu and D. M. Tucker. Regulating action: alternating activation of midline frontal and motor cortical networks. *Clinical Neurophysiology*, 112(7):1295 – 1306, 2001.

## Bibliography

- [34] P. Luu, D. Tucker, and S. Makeig. Frontal midline theta and the error-related negativity: neurophysiological mechanisms of action regulation. *Clinical Neurophysiology*, 115:1821–1835, 2004.
- [35] J. F. Cavanagh, M. X. Cohen, and J. J. B. Allen. Prelude to and resolution of an error: EEG phase synchrony reveals cognitive control dynamics during action monitoring. *Journal of Neuroscience*, 29(1):98–105, 2009.
- [36] J. F. Cavanagh, L. Zambrano-Vazquez, and J. J. B. Allen. Theta lingua franca: A common mid-frontal substrate for action monitoring processes. *Psychophysiology*, 49(2):220–238, 2012.
- [37] J. F. Cavanagh and M. J. Frank. Frontal theta as a mechanism for cognitive control. *Trends in Cognitive Sciences*, 18(8):414 – 421, 2014.
- [38] S. Dehaene, M. I. Posner, and D. M. Tucker. Localization of a neural system for error detection and compensation. *Psychological Science*, 5(5):303–305, 1994.
- [39] W. H. R. Miltner, C. H. Braun, and M. G. H. Coles. Event-related brain potentials following incorrect feedback in a time-estimation task: Evidence for a “generic” neural system for error detection. *J. Cognitive Neuroscience*, 9(6):788–798, Nov 1997.
- [40] C. S. Carter, T. S. Braver, D. M. Barch, M. M. Botvinick, D. Noll, and J. D. Cohen. Anterior cingulate cortex, error detection, and the online monitoring of performance. *Science*, 280(5364):747–749, 1998.
- [41] K. Kiehl, P. Liddle, and J. Hopfinger. Error processing and the rostral anterior cingulate: an event-related fMRI study. *Psychophysiology*, 37(2):216—223, March 2000.
- [42] K. R. Ridderinkhof, M. Ullsperger, E. A. Crone, and S. Nieuwenhuis. The role of the medial frontal cortex in cognitive control. *Science*, 306(5695):443–447, 2004.
- [43] V. v. Veen and C. S. Carter. The timing of action-monitoring processes in the anterior cingulate cortex. *Journal of Cognitive Neuroscience*, 14(4):593–602, 2002.
- [44] M. J. Herrmann, J. Römmler, A.-C. Ehlis, A. Heidrich, and A. J. Fallgatter. Source localization (LORETA) of the error-related-negativity (ERN/Ne) and positivity (Pe). *Cognitive Brain Research*, 20(2):294 – 299, 2004.
- [45] H. Gray and W. Lewis. *Anatomy of the Human Body*. Lea & Febiger, 1918.

- [46] M. G. Coles, M. K. Scheffers, and C. B. Holroyd. Why is there an ERN/Ne on correct trials? response representations, stimulus-related components, and the theory of error-processing. *Biological Psychology*, 56(3):173 – 189, 2001.
- [47] F. Vidal, T. Hasbroucq, J. Grapperon, and M. Bonnet. Is the 'error negativity' specific to errors? *Biological psychology*, 51(2-3):109—128, January 2000.
- [48] F. Vidal, B. Burle, M. Bonnet, J. Grapperon, and T. Hasbroucq. Error negativity on correct trials: a reexamination of available data. *Biological Psychology*, 64 (3):265 – 282, 2003.
- [49] T. J. Overbeek, S. Nieuwenhuis, and K. R. Ridderinkhof. Dissociable components of error processing. *Journal of Psychophysiology*, 19(4):319–329, 2005.
- [50] W. J. Gehring, B. Goss, M. G. H. Coles, D. E. Meyer, and E. Donchin. The error-related negativity. *Perspectives on Psychological Science*, 13(2):200–204, 2018.
- [51] G. Hajcak, J. S. Moser, N. Yeung, and R. F. Simons. On the ERN and the significance of errors. *Psychophysiology*, 42(2):151–160, 2005.
- [52] G. P. Band and A. Kok. Age effects on response monitoring in a mental-rotation task. *Biological Psychology*, 51(2):201 – 221, 2000.
- [53] C. B. Holroyd and M. Coles. The neural basis of human error processing: Reinforcement learning, dopamine, and the error-related negativity. *Psychological Review*, 109:679–709, Oct 2002.
- [54] M. M. Botvinick, T. S. Braver, D. M. Barch, C. S. Carter, and J. D. Cohen. Conflict monitoring and cognitive control. *Psychological Review*, 108(3):624–652, 2001.
- [55] N. Yeung, M. Botvinick, and J. D. Cohen. The neural basis of error detection: Conflict monitoring and the error-related negativity. *Psychological review*, 111: 931–59, Nov 2004.
- [56] C. S. Carter and V. van Veen. Anterior cingulate cortex and conflict detection: An update of theory and data. *Cognitive, Affective, & Behavioral Neuroscience*, 7(4):367–379, Dec 2007.
- [57] M. M. Botvinick, J. D. Cohen, and C. S. Carter. Conflict monitoring and anterior cingulate cortex: An update. *Trends in Cognitive Sciences*, 8(12):539 – 546, 2004.

## Bibliography

- [58] M. M. Botvinick. Conflict monitoring and decision making: Reconciling two perspectives on anterior cingulate function. *Cognitive, Affective, & Behavioral Neuroscience*, 7(4):356–366, Dec 2007.
- [59] M. J. Frank, B. S. Worocho, and T. Curran. Error-related negativity predicts reinforcement learning and conflict biases. *Neuron*, 47(4):495 – 501, 2005.
- [60] J. J. Vidal. Toward direct brain-computer communication. *Annual Review of Biophysics and Bioengineering*, 2(1):157–180, 1973.
- [61] J. J. Vidal. Real-time detection of brain events in EEG. *Proceedings of the IEEE*, 65(5):633–641, 1977.
- [62] J. R. Wolpaw, N. Birbaumer, D. J. McFarland, G. Pfurtscheller, and T. M. Vaughan. Brain-computer interfaces for communication and control. *Clinical Neurophysiology*, 113(6):767 – 791, 2002.
- [63] G. Pfurtscheller. Brain-computer interface - state of the art and future prospects. In *2004 12th European Signal Processing Conference*, pages 509–510, 2004.
- [64] J. Wolpaw and E. W. Wolpaw. *Brain-Computer Interfaces: Something New under the Sun*, pages 1–424. Oxford Scholarship, Jan 2012.
- [65] G. Pfurtscheller, B. Allison, G. Bauernfeind, C. Brunner, T. Solis Escalante, R. Scherer, T. O. Zander, G. R. Müller-Putz, C. Neuper, and N. Birbaumer. The hybrid BCI. *Frontiers in Neuroscience*, 4:3, 2010.
- [66] T. O. Zander and C. Kothe. Towards passive brain-computer interfaces: applying brain-computer interface technology to human-machine systems in general. *Journal of Neural Engineering*, 8(2):025005, Mar 2011.
- [67] G. R. Müller-Putz, C. Breitwieser, F. Cincotti, R. Leeb, M. Schreuder, F. Leotta, M. Tavella, L. Bianchi, A. Kreiling, A. Ramsay, M. Rohm, M. Sagebaum, L. Tonin, C. Neuper, and J. d. R. Millán. Tools for brain-computer interaction: A general concept for a hybrid BCI. *Frontiers in Neuroinformatics*, 5:30, 2011.
- [68] T. O. Zander, C. Kothe, S. Jatzev, and M. Gaertner. *Enhancing Human-Computer Interaction with Input from Active and Passive Brain-Computer Interfaces*, pages 181–199. Springer London, London, 2010. ISBN 978-1-84996-272-8.
- [69] F. Cabestaing and P. Derambure. *Physiological Markers for Controlling Active and Reactive BCIs*, chapter 4, pages 67–84. John Wiley and Sons, Ltd, 2016. ISBN 9781119144977.

- [70] R. Fazel-Rezai, B. Allison, C. Guger, E. Sellers, S. Kleih, and A. Kübler. P300 brain computer interface: current challenges and emerging trends. *Frontiers in Neuroengineering*, 5:14, 2012.
- [71] A. Kübler, A. Furdea, S. Halder, E. M. Hammer, F. Nijboer, and B. Kotchoubey. A brain–computer interface controlled auditory event-related potential (P300) spelling system for locked-in patients. *Annals of the New York Academy of Sciences*, 1157(1):90–100, 2009.
- [72] C. Pokorny, D. S. Klobassa, G. Pichler, H. Erlbeck, R. G. Real, A. Kübler, D. Lesenfants, D. Habbal, Q. Noirhomme, M. Riseti, D. Mattia, and G. R. Müller-Putz. The auditory P300-based single-switch brain–computer interface: Paradigm transition from healthy subjects to minimally conscious patients. *Artificial Intelligence in Medicine*, 59(2):81 – 90, 2013.
- [73] G. R. Müller-Putz and G. Pfurtscheller. Control of an electrical prosthesis with an SSVEP-based BCI. *IEEE Transactions on Biomedical Engineering*, 55(1): 361–364, 2008.
- [74] M. Rötting, T. O. Zander, S. Trösterer, and J. Dzaack. Implicit interaction in multimodal human-machine systems. In C. M. Schlick, editor, *Industrial Engineering and Ergonomics*, pages 523–536, Berlin, Heidelberg, 2009. Springer Berlin Heidelberg.
- [75] J. Kohlmorgen, G. Dornhege, M. Braun, B. Blankertz, K.-R. Müller, G. Curio, K. Hagemann, A. Bruns, M. Schrauf, and W. Kincses. Improving Human Performance in a Real Operating Environment through Real-Time Mental Workload Detection. In *Toward Brain-Computer Interfacing*. The MIT Press, Jul 2007. ISBN 9780262256049.
- [76] B. Venthur, B. Blankertz, M. F. Gugler, and G. Curio. Novel applications of BCI technology: Psychophysiological optimization of working conditions in industry. In *2010 IEEE International Conference on Systems, Man and Cybernetics*, pages 417–421, 2010.
- [77] K.-R. Müller, M. Tangermann, G. Dornhege, M. Krauledat, G. Curio, and B. Blankertz. Machine learning for real-time single-trial EEG-analysis: From brain–computer interfacing to mental state monitoring. *Journal of Neuroscience Methods*, 167(1):82 – 90, 2008.
- [78] R. Schubert, M. Tangermann, S. Haufe, C. Sannelli, M. Simon, E. Schmidt, W. Kincses, and G. Curio. Parieto-occipital alpha power indexes distraction during simulated car driving. *International Journal of Psychophysiology*, 69(3):

## Bibliography

- 214, 2008. Abstracts of the 14th World Congress of Psychophysiology - The Olympics of the Brain - of the International Organization of Psychophysiology (I.O.P) Associated with the United Nations.
- [79] H. Zhang, R. Chavarriaga, Z. Khaliliardali, L. Gheorghe, I. Iturrate, and J. d. R. Millán. EEG-based decoding of error-related brain activity in a real-world driving task. *Journal of Neural Engineering*, 12(6):066028, Nov 2015.
- [80] B. Z. Allison, C. Brunner, C. Altstätter, I. C. Wagner, S. Grissmann, and C. Neuper. A hybrid ERD/SSVEP BCI for continuous simultaneous two dimensional cursor control. *Journal of Neuroscience Methods*, 209(2):299 – 307, 2012.
- [81] B. Z. Allison, C. Brunner, V. Kaiser, G. R. Müller-Putz, C. Neuper, and G. Pfurtscheller. Toward a hybrid brain–computer interface based on imagined movement and visual attention. *Journal of Neural Engineering*, 7(2):026007, Mar 2010.
- [82] G. Pfurtscheller, T. Solis-Escalante, R. Ortner, P. Linortner, and G. R. Müller-Putz. Self-paced operation of an SSVEP-based orthosis with and without an imagery-based “brain switch:” a feasibility study towards a hybrid BCI. *IEEE transactions on neural systems and rehabilitation engineering : a publication of the IEEE Engineering in Medicine and Biology Society*, 18 (4):409–14, Feb 2010.
- [83] S. Perdikis, R. Leeb, J. Williamson, A. Ramsay, M. Tavella, L. Desideri, E.-J. Hoogerwerf, A. Al-Khodairy, R. Murray-Smith, and J. d. R. Millán. Clinical evaluation of BrainTree, a motor imagery hybrid BCI speller. *Journal of Neural Engineering*, 11(3):036003, Apr 2014.
- [84] M. Spüler, M. Bensch, S. Kleih, W. Rosenstiel, M. Bogdan, and A. Kübler. On-line use of error-related potentials in healthy users and people with severe motor impairment increases performance of a P300-BCI. *Clinical Neurophysiology*, 123 (7):1328 – 1337, 2012.
- [85] P. W. Ferrez and J. d. R. Millán. Simultaneous real-time detection of motor imagery and error-related potentials for improved BCI accuracy. In *Proceedings of the 4th International Brain–Computer Interface Workshop and Training Course, Graz, Austria*, pages 197–202, 2008.
- [86] J. Omedes, A. Schwarz, G. R. Müller-Putz, and L. Montesano. Factors that affect error potentials during a grasping task: toward a hybrid natural movement decoding BCI. *Journal of Neural Engineering*, 15(4):046023, Jun 2018.

- [87] R. Yousefi, A. R. Sereshkeh, and T. Chau. Online detection of error-related potentials in multi-class cognitive task-based BCIs. *Brain-Computer Interfaces*, 6(1-2):1–12, 2019.
- [88] R. Yousefi, A. R. Sereshkeh, and T. Chau. Development of a robust asynchronous brain-switch using ErrP-based error correction. *Journal of Neural Engineering*, 16(6):066042, Nov 2019.
- [89] R. Vilimek and T. O. Zander. BC(eye): combining eye-gaze input with brain-computer interaction. In *Proceedings of the 5th International Conference on Universal Access in Human-Computer Interaction. Part II: Intelligent and Ubiquitous Interaction Environments*, UAHCI '09, pages 593–602, Berlin, Heidelberg, Jul 2009. Springer Berlin Heidelberg.
- [90] T. O. Zander, M. Gaertner, C. Kothe, and R. Vilimek. Combining eye gaze input with a brain-computer interface for touchless human-computer interaction. *International Journal of Human-Computer Interaction*, 27(1):38–51, 2010.
- [91] R. Scherer, G. R. Müller-Putz, and G. Pfurtscheller. Self-initiation of EEG-based brain-computer communication using the heart rate response. *Journal of Neural Engineering*, 4(4):L23–L29, Nov 2007.
- [92] G. R. Müller-Putz, R. Leeb, M. Tangermann, J. Höhne, A. Kübler, F. Cincotti, D. Mattia, R. Rupp, K.-R. Müller, and J. d. R. Millán. Towards noninvasive hybrid brain-computer interfaces: Framework, practice, clinical application, and beyond. *Proceedings of the IEEE*, 103(6):926–943, Jun 2015.
- [93] S. Amiri, R. Fazel-Rezai, and V. Asadpour. A review of hybrid brain-computer interface systems. *Advances in Human-Computer Interaction*, 2013:187024, Feb 2013.
- [94] R. Leeb, H. Sagha, R. Chavarriaga, and J. d. R. Millán. A hybrid brain-computer interface based on the fusion of electroencephalographic and electromyographic activities. *Journal of Neural Engineering*, 8(2):025011, Mar 2011.
- [95] C. Brunner, B. Z. Allison, D. J. Krusienski, V. Kaiser, G. R. Müller-Putz, G. Pfurtscheller, and C. Neuper. Improved signal processing approaches in an offline simulation of a hybrid brain-computer interface. *Journal of Neuroscience Methods*, 188(1):165 – 173, 2010.
- [96] L. C. Parra, C. D. Spence, A. D. Gerson, and P. Sajda. Recipes for the linear analysis of EEG. *NeuroImage*, 28(2):326 – 341, 2005.

## Bibliography

- [97] C. Brunner, N. Birbaumer, B. Blankertz, C. Guger, A. Kübler, D. Mattia, J. d. R. Millán, F. Miralles, A. Nijholt, E. Opisso, N. Ramsey, P. Salomon, and G. R. Müller-Putz. BNCI Horizon 2020: towards a roadmap for the BCI community. *Brain-Computer Interfaces*, 2(1):1–10, 2015.
- [98] A. Kübler, E. Holz, T. Kaufmann, and C. Zickler. A user centred approach for bringing BCI controlled applications to end-users. In R. Fazel-Rezai, editor, *Brain-Computer Interface Systems*, chapter 1. IntechOpen, Rijeka, 2013.
- [99] D. Coyle, editor. *Brain-Computer Interfaces: Lab Experiments to Real-World Applications*, volume 228. Elsevier, Netherlands, Aug 2016. ISBN 978-0-12-804216-8.
- [100] A. Kreilinger, V. Kaiser, M. Rohm, R. Rupp, and G. R. Müller-Putz. BCI and FES training of a spinal cord injured end-user to control a neuroprosthesis. *Biomedical Engineering / Biomedizinische Technik*, 58(SI-1-Track-S):00010151520134443, 2013.
- [101] J. Faller, R. Scherer, U. Costa, E. Opisso, J. Medina, and G. R. Müller-Putz. A co-adaptive brain-computer interface for end users with severe motor impairment. *PLOS ONE*, 9(7):1–10, Jul 2014.
- [102] E. M. Holz, L. Botrel, T. Kaufmann, and A. Kübler. Long-term independent brain-computer interface home use improves quality of life of a patient in the locked-in state: A case study. *Archives of Physical Medicine and Rehabilitation*, 96(3, Supplement):S16 – S26, 2015. The Fifth International Brain-Computer Interface Meeting Presents Clinical and Translational Developments in Brain-Computer Interface Research.
- [103] N. Birbaumer, N. Ghanayim, T. Hinterberger, I. Iversen, B. Kotchoubey, A. Kübler, J. Perelmouter, E. Taub, and H. Flor. A spelling device for the paralysed. *Nature*, 398(6725):297–298, Mar 1999.
- [104] F. Nijboer, E. Sellers, J. Mellinger, M. Jordan, T. Matuz, A. Furdea, S. Halder, U. Mochty, D. Krusienski, T. Vaughan, J. Wolpaw, N. Birbaumer, and A. Kübler. A P300-based brain-computer interface for people with amyotrophic lateral sclerosis. *Clinical Neurophysiology*, 119(8):1909 – 1916, 2008.
- [105] F. Galán, M. Nuttin, E. Lew, P. W. Ferrez, G. Vanacker, J. Philips, and J. d. R. Millán. A brain-actuated wheelchair: Asynchronous and non-invasive brain-computer interfaces for continuous control of robots. *Clinical Neurophysiology*, 119(9):2159 – 2169, 2008.



- [106] J. d. R. Millán, F. Galán, D. Vanhooydonck, E. Lew, J. Philips, and M. Nuttin. Asynchronous non-invasive brain-actuated control of an intelligent wheelchair. In *2009 Annual International Conference of the IEEE Engineering in Medicine and Biology Society*, pages 3361–3364, 2009.
- [107] G. Pfurtscheller, G. R. Müller, J. Pfurtscheller, H. J. Gerner, and R. Rupp. ‘Thought’ – control of functional electrical stimulation to restore hand grasp in a patient with tetraplegia. *Neuroscience Letters*, 351(1):33 – 36, 2003.
- [108] G. Pfurtscheller, G. R. Müller-Putz, J. Pfurtscheller, and R. Rupp. EEG-based asynchronous BCI controls functional electrical stimulation in a tetraplegic patient. *EURASIP Journal on Advances in Signal Processing*, 2005(19):628453, Nov 2005.
- [109] G. R. Müller-Putz, R. Scherer, G. Pfurtscheller, and R. Rupp. EEG-based neuroprosthesis control: A step towards clinical practice. *Neuroscience Letters*, 382(1):169 – 174, 2005.
- [110] S. Silvoni, A. Ramos-Murguialday, M. Cavinato, C. Volpato, G. Cisotto, A. Turolla, F. Piccione, and N. Birbaumer. Brain-computer interface in stroke: A review of progress. *Clinical EEG and Neuroscience*, 42(4):245–252, 2011.
- [111] A. Martel, S. Dähne, and B. Blankertz. EEG predictors of covert vigilant attention. *Journal of Neural Engineering*, 11(3):035009, May 2014.
- [112] J. d. R. Millán, R. Rupp, G. R. Müller-Putz, R. Murray-Smith, C. Giugliemma, M. Tangermann, C. Vidaurre, F. Cincotti, A. Kübler, R. Leeb, C. Neuper, K. Müller, and D. Mattia. Combining brain–computer interfaces and assistive technologies: State-of-the-art and challenges. *Frontiers in Neuroscience*, 4:161, 2010.
- [113] B. Graimann, B. Z. Allison, and G. Pfurtscheller. *Brain-Computer Interfaces: Revolutionizing Human-Computer Interaction*. Springer Publishing Company, Incorporated, 2013. ISBN 3642266355.
- [114] G. Pfurtscheller and C. Neuper. Motor imagery activates primary sensorimotor area in humans. *Neuroscience Letters*, 239(2):65 – 68, 1997.
- [115] G. Pfurtscheller and F. H. Lopes da Silva. Event-related EEG/MEG synchronization and desynchronization: basic principles. *Clinical Neurophysiology*, 110(11):1842 – 1857, 1999.
- [116] G. Pfurtscheller, C. Guger, G. R. Müller, G. Krausz, and C. Neuper. Brain oscillations control hand orthosis in a tetraplegic. *Neuroscience Letters*, 292(3): 211 – 214, 2000.

## Bibliography

- [117] J. Wolpaw, D. McFarland, G. Neat, and C. Forneris. An EEG-based brain-computer interface for cursor control. *Electroencephalography and clinical neurophysiology*, 78(3):252—259, March 1991.
- [118] D. J. McFarland and J. R. Wolpaw. Sensorimotor rhythm-based brain-computer interface (BCI): feature selection by regression improves performance. *IEEE Transactions on Neural Systems and Rehabilitation Engineering*, 13(3):372–379, 2005.
- [119] E. V. C. Friedrich, C. Neuper, and R. Scherer. Whatever works: A systematic user-centered training protocol to optimize brain-computer interfacing individually. *PLOS ONE*, 8(9), Sep 2013.
- [120] G. R. Müller-Putz, R. Scherer, C. Neuper, and G. Pfurtscheller. Steady-state somatosensory evoked potentials: suitable brain signals for brain-computer interfaces? *IEEE Transactions on Neural Systems and Rehabilitation Engineering*, 14(1):30–37, 2006.
- [121] B. Z. Allison, D. J. McFarland, G. Schalk, S. D. Zheng, M. M. Jackson, and J. R. Wolpaw. Towards an independent brain–computer interface using steady state visual evoked potentials. *Clinical Neurophysiology*, 119(2):399 – 408, 2008.
- [122] L. Farwell and E. Donchin. Talking off the top of your head: toward a mental prosthesis utilizing event-related brain potentials. *Electroencephalography and Clinical Neurophysiology*, 70(6):510 – 523, 1988.
- [123] E. Donchin, K. M. Spencer, and R. Wijesinghe. The mental prosthesis: assessing the speed of a P300-based brain-computer interface. *IEEE Transactions on Rehabilitation Engineering*, 8(2):174–179, 2000.
- [124] A.-M. Brouwer and J. Van Erp. A tactile P300 brain-computer interface. *Frontiers in Neuroscience*, 4:19, 2010.
- [125] A. Pinegger, J. Faller, S. Halder, S. C. Wriessnegger, and G. R. Müller-Putz. Control or non-control state: that is the question! an asynchronous visual P300-based BCI approach. *Journal of Neural Engineering*, 12(1):014001, Jan 2015.
- [126] G. R. Müller-Putz, A. Schwarz, J. Pereira, and P. Ofner. Chapter 2 - from classic motor imagery to complex movement intention decoding: The noninvasive Graz-BCI approach. In D. Coyle, editor, *Brain-Computer Interfaces: Lab Experiments to Real-World Applications*, volume 228 of *Progress in Brain Research*, pages 39 – 70. Elsevier, 2016.

- [127] G. R. Müller-Putz, P. Ofner, A. Schwarz, J. Pereira, G. Luzhnica, C. di Sciascio, E. Veas, S. Stein, J. Williamson, R. Murray-Smith, C. Escolano, L. Montesano, B. Hensing, M. Schneiders, and R. Rupp. MoreGrasp: restoration of upper limb function in individuals with high spinal cord injury by multimodal neuroprostheses for interaction in daily activities. In *7th Graz Brain-Computer Interface Conference 2019*, 2017.
- [128] G. R. Müller-Putz, P. Ofner, J. Pereira, A. Pinegger, A. Schwarz, M. Zube, U. Eck, B. Hensing, M. Schneiders, and R. Rupp. Applying intuitive EEG-controlled grasp neuroprostheses in individuals with spinal cord injury: Preliminary results from the MoreGrasp clinical feasibility study. In *41st Annual International Conference of the IEEE Engineering in Medicine and Biology Society (EMBC)*, pages 5949–5955, 2019.
- [129] A. I. Sburlea, L. Montesano, R. Cano de la Cuerda, I. M. Alguacil Diego, J. C. Miangolarra-Page, and J. Minguez. Detecting intention to walk in stroke patients from pre-movement EEG correlates. *Journal of NeuroEngineering and Rehabilitation*, 12:113–113, Dec 2015.
- [130] J. Pereira, A. I. Sburlea, and G. R. Müller-Putz. EEG patterns of self-paced movement imaginations towards externally-cued and internally-selected targets. *Scientific Reports*, 8(1):13394, Sep 2018.
- [131] A. Schwarz, P. Ofner, J. Pereira, A. I. Sburlea, and G. R. Müller-Putz. Decoding natural reach-and-grasp actions from human EEG. *Journal of Neural Engineering*, 15(1):016005, Dec 2017.
- [132] P. Ofner, A. Schwarz, J. Pereira, D. Wyss, R. Wildburger, and G. R. Müller-Putz. Attempted arm and hand movements can be decoded from low-frequency EEG from persons with spinal cord injury. *Scientific Reports*, 9(1):7134, May 2019.
- [133] D. Liu, W. Chen, K. Lee, R. Chavarriaga, F. Iwane, M. Bouri, Z. Pei, and J. d. R. Millán. EEG-based lower-limb movement onset decoding: Continuous classification and asynchronous detection. *IEEE Transactions on Neural Systems and Rehabilitation Engineering*, 26(8):1626–1635, 2018.
- [134] G. Schalk, J. R. Wolpaw, D. J. McFarland, and G. Pfurtscheller. EEG-based communication: presence of an error potential. *Clinical Neurophysiology*, 111(12):2138 – 2144, 2000.
- [135] R. Chavarriaga, A. Sobolewski, and J. d. R. Millán. Errare machinale est: the use of error-related potentials in brain-machine interfaces. *Frontiers in Neuroscience*, 8:208, 2014.

## Bibliography

- [136] P. W. Ferrez and J. d. R. Millán. Error-related EEG potentials generated during simulated brain–computer interaction. *IEEE Transactions on Biomedical Engineering*, 55(3):923–929, 2008.
- [137] B. Blankertz, G. Dornhege, C. Schäfer, R. Krepki, J. Kohlmorgen, K.-R. Müller, V. Kunzmann, F. Losch, and G. Curio. Boosting bit rates and error detection for the classification of fast-paced motor commands based on single-trial EEG analysis. *IEEE Transactions on Neural Systems and Rehabilitation Engineering*, 11(2):127–131, Jun 2003.
- [138] L. C. Parra, C. Alvino, A. Tang, B. Pearlmutter, N. Yeung, A. Osman, and P. Sajda. Linear spatial integration for single-trial detection in encephalography. *NeuroImage*, 17(1):223 – 230, 2002.
- [139] L. C. Parra, C. D. Spence, A. D. Gerson, and P. Sajda. Response error correction - a demonstration of improved human-machine performance using real-time EEG monitoring. *IEEE Transactions on Neural Systems and Rehabilitation Engineering*, 11(2):173–177, Jun 2003.
- [140] C. Lopes-Dias, A. I. Sburlea, and G. R. Müller-Putz. Online asynchronous decoding of error-related potentials during the continuous control of a robot. *Scientific Reports*, 9(1):17596, 2019.
- [141] P. W. Ferrez and J. d. R. Millán. You are wrong!: Automatic detection of interaction errors from brain waves. In *Proceedings of the 19th International Joint Conference on Artificial Intelligence, IJCAI'05*, pages 1413–1418, 2005.
- [142] P. W. Ferrez and J. d. R. Millán. EEG-based brain–computer interaction: Improved accuracy by automatic single-trial error detection. In J. C. Platt, D. Koller, Y. Singer, and S. T. Roweis, editors, *Advances in Neural Information Processing Systems 20*, pages 441–448. Curran Associates, Inc., 2007.
- [143] R. Chavarriaga and J. d. R. Millán. Learning from EEG error-related potentials in noninvasive brain–computer interfaces. *IEEE Transactions on Neural Systems and Rehabilitation Engineering*, 18(4):381–388, Aug 2010.
- [144] R. Pezzetta, V. Nicolardi, E. Tidoni, and S. M. Aglioti. Error, rather than its probability, elicits specific electrocortical signatures: a combined EEG-immersive virtual reality study of action observation. *Journal of neurophysiology*, 120(3): 1107—1118, September 2018.
- [145] I. Iturrate, L. Montesano, and J. Minguez. Single trial recognition of error-related potentials during observation of robot operation. In *2010 Annual International*

- Conference of the IEEE Engineering in Medicine and Biology Society*, pages 4181–4184, Aug 2010.
- [146] A. F. Salazar-Gomez, J. DelPreto, S. Gil, F. H. Guenther, and D. Rus. Correcting robot mistakes in real time using EEG signals. *2017 IEEE International Conference on Robotics and Automation (ICRA)*, pages 6570–6577, May 2017.
- [147] H. Zhang, R. Chavarriaga, L. Gheorghe, and J. d. R. Millán. Inferring driver's turning direction through detection of error related brain activity. In *2013 35th Annual International Conference of the IEEE Engineering in Medicine and Biology Society (EMBC)*, pages 2196–2199, 2013.
- [148] A. Kreilinger, C. Neuper, and G. R. Müller-Putz. Error potential detection during continuous movement of an artificial arm controlled by brain–computer interface. *Medical & Biological Engineering & Computing*, 50(3):223–230, 2012.
- [149] A. Kreilinger, H. Hiebel, and G. R. Müller-Putz. Single versus multiple events error potential detection in a BCI-controlled car game with continuous and discrete feedback. *IEEE Transactions on Biomedical Engineering*, 63(3):519–529, 2016.
- [150] I. Iturrate, R. Chavarriaga, L. Montesano, J. Minguez, and J. d. R. Millán. Latency correction of error potentials between different experiments reduces calibration time for single-trial classification. In *2012 Annual International Conference of the IEEE Engineering in Medicine and Biology Society*, pages 3288–3291, Aug 2012.
- [151] I. Iturrate, L. Montesano, and J. Minguez. Task-dependent signal variations in EEG error-related potentials for brain–computer interfaces. *Journal of Neural Engineering*, 10(2):026024, Mar 2013.
- [152] I. Iturrate, R. Chavarriaga, L. Montesano, J. Minguez, and J. d. R. Millán. Latency correction of event-related potentials between different experimental protocols. *Journal of Neural Engineering*, 11(3):036005, Apr 2014.
- [153] M. Mousavi, A. S. Koerner, Q. Zhang, E. Noh, and V. R. de Sa. Improving motor imagery BCI with user response to feedback. *Brain-Computer Interfaces*, 4(1-2):74–86, 2017.
- [154] B. Dal Seno, M. Matteucci, and L. Mainardi. Online detection of P300 and error potentials in a BCI speller. *Computational Intelligence and Neuroscience*, 2010: 307254, Feb 2010.

## Bibliography

- [155] N. M. Schmidt, B. Blankertz, and M. S. Treder. Online detection of error-related potentials boosts the performance of mental typewriters. *BMC Neuroscience*, 13(1):19, Feb 2012.
- [156] G. Visconti, B. Dal Seno, M. Matteucci, and L. Mainardi. Automatic recognition of error potentials in a P300-based brain-computer interface. In *in Proceedings of the 4th International Brain-Computer Interface Workshop and Training Course, Graz, Austria, 2008*.
- [157] D. Rotermund, U. A. Ernst, and K. R. Pawelzik. Towards on-line adaptation of neuro-prostheses with neuronal evaluation signals. *Biological Cybernetics*, 95(3):243–257, Sep 2006.
- [158] J. Blumberg, J. Rickert, S. Waldert, A. Schulze-Bonhage, A. Aertsen, and C. Mehring. Adaptive classification for brain computer interfaces. In *2007 29th Annual International Conference of the IEEE Engineering in Medicine and Biology Society*, pages 2536–2539, 2007.
- [159] A. Llera, M. A. van Gerven, V. Gómez, O. Jensen, and H. J. Kappen. On the use of interaction error potentials for adaptive brain computer interfaces. *Neural Networks*, 24(10):1120–1127, 2011.
- [160] A. Llera, V. Gómez, and H. J. Kappen. Adaptive classification on brain-computer interfaces using reinforcement signals. *Neural Computation*, 24(11):2900–2923, 2012.
- [161] X. Artusi, I. K. Niazi, M. Lucas, and D. Farina. Performance of a simulated adaptive BCI based on experimental classification of movement-related and error potentials. *IEEE Journal on Emerging and Selected Topics in Circuits and Systems*, 1(4):480–488, 2011.
- [162] R. Chavarriaga, A. Biasucci, K. Förster, D. Roggen, G. Tröster, and J. d. R. Millán. Adaptation of hybrid human-computer interaction systems using EEG error-related potentials. In *2010 Annual International Conference of the IEEE Engineering in Medicine and Biology*, pages 4226–4229, 2010.
- [163] S.-K. Kim, E. A. Kirchner, A. Stefes, and F. Kirchner. Intrinsic interactive reinforcement learning - using error-related potentials for real world human-robot interaction. *Scientific Reports (Sci Rep)*, 7: 17562, Dec 2017.
- [164] I. Iturrate, L. Montesano, and J. Minguez. Robot reinforcement learning using EEG-based reward signals. In *2010 IEEE International Conference on Robotics and Automation*, pages 4822–4829, 2010.

- [165] I. Iturrate, R. Chavarriaga, L. Montesano, J. Minguez, and J. d. R. Millán. Teaching brain-machine interfaces as an alternative paradigm to neuroprosthetics control. *Scientific Reports*, 13893, Sep 2015.
- [166] T. Zander, L. Krol, N. Birbaumer, and K. Gramann. Neuroadaptive technology enables implicit cursor control based on medial prefrontal cortex activity. In *Proceedings of the National Academy of Sciences of the United States of America*, volume 113(12), pages 14898–14903, Dez 2016.
- [167] J. Polich. On the relationship between EEG and P300: individual differences, aging, and ultradian rhythms. *International Journal of Psychophysiology*, 26(1): 299 – 317, 1997.
- [168] M. Krauledat, M. Tangermann, B. Blankertz, and K.-R. Müller. Towards zero training for brain-computer interfacing. *PLOS ONE*, 3(8):1–12, Aug 2008.
- [169] J. Jin, E. W. Sellers, Y. Zhang, I. Daly, X. Wang, and A. Cichocki. Whether generic model works for rapid ERP-based BCI calibration. *Journal of Neuroscience Methods*, 212(1):94 – 99, 2013.
- [170] A. Pinegger and G. R. Müller-Putz. No training, same performance!? – A generic P300 classifier approach. In *7th Graz Brain-Computer Interface Conference 2017*, pages 236–241. Verlag der Technischen Universität Graz, Sep 2017.
- [171] S. Lu, C. Guan, and H. Zhang. Unsupervised brain computer interface based on intersubject information and online adaptation. *IEEE Transactions on Neural Systems and Rehabilitation Engineering*, 17(2):135–145, Apr 2009.
- [172] P. Shenoy, M. Krauledat, B. Blankertz, R. P. N. Rao, and K.-R. Müller. Towards adaptive classification for BCI. *Journal of Neural Engineering*, 3(1):R13–R23, Mar 2006.
- [173] P.-J. Kindermans, M. Schreuder, B. Schrauwen, K.-R. Müller, and M. Tangermann. True zero-training brain-computer interfacing – an online study. *PLOS ONE*, 9(7):1–13, Jul 2014.
- [174] P.-J. Kindermans, D. Verstraeten, and B. Schrauwen. A bayesian model for exploiting application constraints to enable unsupervised training of a P300-based BCI. *PLOS ONE*, 7(4):1–12, Apr 2012.
- [175] A. Buttfeld, P. W. Ferrez, and J. d. R. Millán. Towards a robust BCI: error potentials and online learning. *IEEE Transactions on Neural Systems and Rehabilitation Engineering*, 14(2):164–168, Jun 2006.

## Bibliography

- [176] C. Vidaurre and B. Blankertz. Towards a cure for BCI illiteracy. *Brain Topography*, 23(2):194–198, Jun 2010.
- [177] F. Lotte, L. Bougrain, A. Cichocki, M. Clerc, M. Congedo, A. Rakotomamonjy, and F. Yger. A review of classification algorithms for EEG-based brain–computer interfaces: a 10 year update. *Journal of Neural Engineering*, 15(3):031005, Apr 2018.
- [178] J. Grizou, I. Iturrate, L. Montesano, M. Lopes, and P.-Y. Oudeyer. Zero-calibration bmis for sequential tasks using error-related potentials. *Workshop on Neuroscience and Robotics*, Nov 2013.
- [179] J. Grizou, I. Iturrate, L. Montesano, P.-Y. Oudeyer, and M. Lopes. Calibration-free BCI based control. In *Proceedings of the National Conference on Artificial Intelligence*, volume 2, Jul 2014.
- [180] J. Grizou, I. n. Iturrate, L. Montesano, P.-Y. Oudeyer, and M. Lopes. Interactive learning from unlabeled instructions. In *Proceedings of the Thirtieth Conference on Uncertainty in Artificial Intelligence, UAI'14*, page 290–299, Arlington, Virginia, USA, 2014. AUAI Press.
- [181] I. Iturrate, J. Grizou, J. Omedes, P.-Y. Oudeyer, M. Lopes, and L. Montesano. Exploiting task constraints for self-calibrated brain-machine interface control using error-related potentials. *PLOS ONE*, 10(7):1–15, Jul 2015.
- [182] I. Iturrate, L. Montesano, R. Chavarriaga, J. d. R. Millán, and J. Minguez. Minimizing calibration time using inter-subject information of single-trial recognition of error potentials in brain-computer interfaces. In *2011 Annual International Conference of the IEEE Engineering in Medicine and Biology Society*, pages 6369–6372, 2011.
- [183] S. K. Kim and E. A. Kirchner. Classifier transferability in the detection of error related potentials from observation to interaction. In *2013 IEEE International Conference on Systems, Man, and Cybernetics*, pages 3360–3365, Oct 2013.
- [184] S. K. Kim and E. A. Kirchner. Handling few training data: Classifier transfer between different types of error-related potentials. *IEEE Transactions on Neural Systems and Rehabilitation Engineering*, 24(3):320–332, Mar 2016.
- [185] A. Schwarz, M. K. Höller, J. Pereira, P. Ofner, and G. R. Müller-Putz. Decoding hand movements from human EEG to control a robotic arm in a simulation environment. *Journal of Neural Engineering*, 17(3):036010, May 2020.



- [186] P. Ofner, J. Pereira, A. Schwarz, and G. R. Müller-Putz. Online detection of hand open vs palmar grasp attempts in a person with spinal cord injury. In *8th Graz Brain-Computer Interface Conference 2019*, Sep 2019.
- [187] P. Ofner and G. R. Müller-Putz. Decoding of velocities and positions of 3D arm movement from EEG. In *2012 Annual International Conference of the IEEE Engineering in Medicine and Biology Society*, pages 6406–6409, Aug 2012.
- [188] R. J. Kobler, A. I. Sburlea, and G. R. Müller-Putz. Tuning characteristics of low-frequency EEG to positions and velocities in visuomotor and oculomotor tracking tasks. *Scientific Reports*, 8(1):17713, 2018.
- [189] Y. Inoue, H. Mao, S. B. Suway, J. Orellana, and A. B. Schwartz. Decoding arm speed during reaching. *Nature Communications*, 9(1):5243, 2018.
- [190] R. J. Kobler, A. I. Sburlea, V. Mondini, M. Hirata, and G. R. Müller-Putz. Distance- and speed-informed kinematics decoding improves M/EEG based upper-limb movement decoder accuracy. *Journal of Neural Engineering*, 2020.
- [191] V. Mondini, R. J. Kobler, A. I. Sburlea, and G. R. Müller-Putz. Continuous low-frequency EEG decoding of arm movement for closed-loop, natural control of a robotic arm. *Journal of Neural Engineering*, 17(4):046031, Aug 2020.
- [192] V. Martínez-Cagigal, R. J. Kobler, V. Mondini, R. Hornero, and G. R. Müller-Putz. Non-linear online low-frequency EEG decoding of arm movements during a pursuit tracking task. In *2020 42nd Annual International Conference of the IEEE Engineering in Medicine Biology Society (EMBC)*, pages 2981–2985, 2020.
- [193] J. Omedes, I. Iturrate, J. Minguez, and L. Montesano. Analysis and asynchronous detection of gradually unfolding errors during monitoring tasks. *Journal of Neural Engineering*, 12(5):056001, 2015.
- [194] J. Omedes, I. Iturrate, R. Chavarriaga, and L. Montesano. Asynchronous decoding of error potentials during the monitoring of a reaching task. In *2015 IEEE International Conference on Systems, Man, and Cybernetics (SMC2015)*, pages 3116–3121, Oct 2015.
- [195] J. Omedes, I. Iturrate, and L. Montesano. Asynchronous detection of error potentials. In *Proceedings of the 6th Brain-Computer Interface Conference 2014*, 2014.
- [196] T. Milekovic, T. Ball, A. Schulze-Bonhage, A. Aertsen, and C. Mehring. Error-related electrocorticographic activity in humans during continuous movements. *Journal of Neural Engineering*, 9(2):026007, 2012.

## Bibliography

- [197] T. Milekovic, T. Ball, A. Schulze-Bonhage, A. Aertsen, and C. Mehring. Detection of error related neuronal responses recorded by electrocorticography in humans during continuous movements. *PLOS ONE*, 8(2):1–20, Feb 2013.
- [198] M. Spüler and C. Niethammer. Error-related potentials during continuous feedback: using EEG to detect errors of different type and severity. *Frontiers in Human Neuroscience*, 9:155, 2015.
- [199] G. R. Müller-Putz. *Design of an electrical hand-grasp orthosis for direct control with the brain to restore the hand-grasp function of a tetraplegic*. Diplomarbeit. Graz: 2000. PhD thesis, Technische Universität Graz, 2000.
- [200] G. R. Müller-Putz, I. Daly, and V. Kaiser. Motor imagery-induced EEG patterns in individuals with spinal cord injury and their impact on brain–computer interface accuracy. *Journal of Neural Engineering*, 11(3):035011, May 2014.
- [201] G. R. Müller-Putz and R. Rupp. Achievements and challenges of translational research in non-invasive SMR-BCI-controlled upper extremity neuroprosthesis in spinal cord injury. In *2015 7th International IEEE/EMBS Conference on Neural Engineering (NER)*, pages 158–161, 2015.
- [202] R. Rupp, M. Rohm, M. Schneiders, A. Kreiling, and G. R. Müller-Putz. Functional rehabilitation of the paralyzed upper extremity after spinal cord injury by noninvasive hybrid neuroprostheses. *Proceedings of the IEEE*, 103(6):954–968, 2015.
- [203] R. Scherer, J. Faller, E. V. C. Friedrich, E. Opisso, U. Costa, A. Kübler, and G. R. Müller-Putz. Individually adapted imagery improves brain-computer interface performance in end-users with disability. *PLOS ONE*, 10(5):1–14, May 2015.
- [204] Y. Gu, D. Farina, A. R. Murguialday, K. Dremstrup, and N. Birbaumer. Comparison of movement related cortical potential in healthy people and amyotrophic lateral sclerosis patients. *Frontiers in Neuroscience*, 7:65, 2013.
- [205] R. Xu, N. Jiang, A. Vuckovic, M. Hasan, N. Mrachacz-Kersting, D. Allan, M. Fraser, B. Nasserolsami, B. Conway, K. Dremstrup, and D. Farina. Movement-related cortical potentials in paraplegic patients: abnormal patterns and considerations for BCI-rehabilitation. *Frontiers in Neuroengineering*, 7:35, 2014.
- [206] P. M. Iyer, K. Mohr, M. Broderick, B. Gavin, T. Burke, P. Bede, M. Pinto-Grau, N. P. Pender, R. McLaughlin, A. Vajda, M. Heverin, E. C. Lalor, O. Hardiman,

- and B. Nasseroleslami. Mismatch negativity as an indicator of cognitive sub-domain dysfunction in amyotrophic lateral sclerosis. *Frontiers in Neurology*, 8: 395, 2017.
- [207] E. Lopez-Larraz, L. Montesano, a. Gil-Agudo, J. Minguez, and A. Oliviero. Evolution of EEG motor rhythms after spinal cord injury: A longitudinal study. *PLOS ONE*, 10(7):1–15, Jul 2015.
- [208] C. Seer, M. Joop, F. Lange, C. Lange, R. Dengler, S. Petri, and B. Kopp. Attenuated error-related potentials in amyotrophic lateral sclerosis with executive dysfunctions. *Clinical Neurophysiology*, 128(8):1496 – 1503, 2017.
- [209] A. Kumar, Q. Fang, J. Fu, E. Pirogova, and X. Gu. Error-related neural responses recorded by electroencephalography during post-stroke rehabilitation movements. *Frontiers in Neurobotics*, 13:107, 2019.
- [210] A. Kumar, L. Gao, E. Pirogova, and Q. Fang. A review of error-related potential-based brain–computer interfaces for motor impaired people. *IEEE Access*, 7: 142451–142466, 2019.
- [211] P. Keyl, M. Schneiders, C. Schuld, S. Franz, M. Hommelsen, N. Weidner, and R. Rupp. Differences in characteristics of error-related potentials between individuals with spinal cord injury and age- and sex-matched able-bodied controls. *Frontiers in Neurology*, 9:1192, 2019.
- [212] A. Andreev, A. Barachant, F. Lotte, and M. Congedo. *Recreational Applications of OpenViBE: Brain Invaders and Use-the-Force*, chapter 14, pages 241–258. John Wiley and Sons, Ltd, 2016. ISBN 9781119332428.
- [213] J. I. Muenssinger, S. Halder, S. Kleih, A. Furdea, V. Raco, A. Hoesle, and A. Kübler. Brain painting: First evaluation of a new brain–computer interface application with ALS-patients and healthy volunteers. *Frontiers in Neuroscience*, 4:182, 2010.
- [214] A. Finke, A. Lenhardt, and H. Ritter. The mindgame: A P300-based brain–computer interface game. *Neural Networks*, 22(9):1329 – 1333, 2009.
- [215] A. Pinegger, H. Hiebel, S. C. Wriessnegger, and G. R. Müller-Putz. Composing only by thought: Novel application of the P300 brain–computer interface. *PLOS ONE*, 12(9):1–19, Sep 2017.
- [216] B. Z. Allison, S. Dunne, R. Leeb, J. d. R. Millán, and A. Nijholt. *Towards practical brain-computer interfaces: bridging the gap from research to real-world applications*. Springer Science & Business Media, 2012.

## Bibliography

- [217] M. Ahn, M. Lee, J. Choi, and S. Jun. A review of brain-computer interface games and an opinion survey from researchers, developers and users. *Sensors*, 14(8):14601–14633, Aug 2014.
- [218] B. Blankertz, M. Tangermann, C. Vidaurre, S. Fazli, C. Sannelli, S. Haufe, C. Maeder, L. Ramsey, I. Sturm, G. Curio, and K.-R. Müller. The berlin brain-computer interface: Non-medical uses of BCI technology. *Frontiers in neuroscience*, 4:198–198, Dec 2010.
- [219] J. van Erp, F. Lotte, and M. Tangermann. Brain-computer interfaces: Beyond medical applications. *Computer*, 45(4):26–34, 2012.
- [220] P. Aricò, G. Borghini, G. Di Flumeri, N. Sciaraffa, and F. Babiloni. Passive BCI beyond the lab: current trends and future directions. *Physiological measurement*, 39(8):08TR02, Aug 2018.
- [221] T. O. Zander, K. Shetty, R. Lorenz, D. R. Leff, L. R. Krol, A. W. Darzi, K. Gramann, and G.-Z. Yang. Automated task load detection with electroencephalography: Towards passive brain-computer interfacing in robotic surgery. *Journal of Medical Robotics Research*, 02(01):1750003, 2017.
- [222] R. Chavarriaga, X. Perrin, R. Siegwart, and J. d. R. Millán. Anticipation- and error-related EEG signals during realistic human-machine interaction: A study on visual and tactile feedback. In *2012 Annual International Conference of the IEEE Engineering in Medicine and Biology Society*, pages 6723–6726, 2012.
- [223] R. Chavarriaga, M. Ušćumlić, H. Zhang, Z. Khaliliardali, R. Aydarkhanov, S. Saeedi, L. Gheorghe, and J. d. R. Millán. Decoding neural correlates of cognitive states to enhance driving experience. *IEEE Transactions on Emerging Topics in Computational Intelligence*, 2(4):288–297, 2018.
- [224] G. Padrao, M. Gonzalez-Franco, M. V. Sanchez-Vives, M. Slater, and A. Rodriguez-Fornells. Violating body movement semantics: Neural signatures of self-generated and external-generated errors. *NeuroImage*, 124:147 – 156, 2016.
- [225] E. F. Pavone, G. Tieri, G. Rizza, E. Tidoni, L. Grisoni, and S. M. Aglioti. Embodying others in immersive virtual reality: Electro-cortical signatures of monitoring the errors in the actions of an avatar seen from a first-person perspective. *Journal of Neuroscience*, 36(2):268–279, 2016.
- [226] G. Spinelli, G. Tieri, E. Pavone, and S. Aglioti. Wronger than wrong: Graded mapping of the errors of an avatar in the performance monitoring system of the onlooker. *NeuroImage*, 167:1 – 10, 2018.

- [227] L. Gehrke, S. Akman, P. Lopes, A. Chen, A. K. Singh, H.-T. Chen, C.-T. Lin, and K. Gramann. Detecting visuo-haptic mismatches in virtual reality using the prediction error negativity of event-related brain potentials. In *Proceedings of the 2019 CHI Conference on Human Factors in Computing Systems*, CHI '19, page 1–11, New York, NY, USA, 2019. Association for Computing Machinery.
- [228] C. Lopes-Dias, A. I. Sburlea, and G. R. Müller-Putz. Masked and unmasked error-related potentials during continuous control and feedback. *Journal of Neural Engineering*, 15(3):036031, 2018.
- [229] B. Blankertz, S. Lemm, M. Treder, S. Haufe, and K.-R. Müller. Single-trial analysis and classification of ERP components - a tutorial. *NeuroImage*, 56(2): 814 – 825, 2011.
- [230] C. Lopes-Dias, A. I. Sburlea, and G. R. Müller-Putz. Asynchronous detection of error-related potentials using a generic classifier. In *8th Graz Brain-Computer Interface Conference 2019*, pages 54–58, 2019.
- [231] C. Lopes-Dias, A. I. Sburlea, and G. R. Müller-Putz. A generic error-related potential classifier offers a comparable performance to a personalized classifier. In *2020 42nd Annual International Conference of the IEEE Engineering in Medicine Biology Society (EMBC)*, pages 2995–2998, 2020.
- [232] C. Lopes-Dias, A. I. Sburlea, K. Breitegger, D. Wyss, H. Drescher, R. Wildburger, and G. R. Müller-Putz. Online asynchronous detection of error-related potentials in participants with a spinal cord injury by adapting a pre-trained generic classifier. *Journal of Neural Engineering*, 2020, accepted.
- [233] P. Ofner, A. Schwarz, J. Pereira, and G. R. Müller-Putz. Upper limb movements can be decoded from the time-domain of low-frequency EEG. *PLOS ONE*, 12(8):1–24, Aug 2017.
- [234] I. Iturrate, R. Chavarriaga, M. Pereira, H. Zhang, T. Corbet, R. Leeb, and J. d. R. Millán. EEG reveals distinct neural correlates of power and precision grasping types. *NeuroImage*, 181:635 – 644, 2018.
- [235] D. Hübner, T. Verhoeven, K. Müller, P. Kindermans, and M. Tangermann. Unsupervised learning for brain-computer interfaces based on event-related potentials: Review and online comparison. *IEEE Computational Intelligence Magazine*, 13(2):66–77, 2018.
- [236] S. Bhattacharyya, A. Konar, D. N. Tibarewala, and M. Hayashibe. A generic transferable EEG decoder for online detection of error potential in target selection. *Frontiers in Neuroscience*, 11:226, 2017.

## Bibliography

- [237] F. M. Schönleitner, L. Otter, S. K. Ehrlich, and G. Cheng. A comparative study on adaptive subject-independent classification models for zero-calibration error-potential decoding. In *2019 IEEE International Conference on Cyborg and Bionic Systems (CBS)*, pages 85–90, 2019.
- [238] F. M. Schönleitner, L. Otter, S. K. Ehrlich, and G. Cheng. Calibration-free error-related potential decoding with adaptive subject-independent models: A comparative study. *IEEE Transactions on Medical Robotics and Bionics*, 2(3): 399–409, 2020.
- [239] S. K. Ehrlich and G. Cheng. A feasibility study for validating robot actions using EEG-based error-related potentials. *International Journal of Social Robotics*, 11(2):271–283, Apr 2019.
- [240] S. Halder, A. Pinegger, I. Käthner, S. C. Wriessnegger, J. Faller, J. B. Pires Antunes, G. R. Müller-Putz, and A. Kübler. Brain-controlled applications using dynamic P300 speller matrices. *Artificial Intelligence in Medicine*, 63(1):7 – 17, 2015.
- [241] V. Martínez-Cagigal, J. Gomez-Pilar, D. Álvarez, and R. Hornero. An asynchronous P300-based brain-computer interface web browser for severely disabled people. *IEEE Transactions on Neural Systems and Rehabilitation Engineering*, 25(8):1332–1342, 2017.
- [242] A. Kübler, E. M. Holz, A. Riccio, C. Zickler, T. Kaufmann, S. C. Kleih, P. Staiger-Sälzer, L. Desideri, E.-J. Hoogerwerf, and D. Mattia. The user-centered design as novel perspective for evaluating the usability of BCI-controlled applications. *PLOS ONE*, 9(12):1–22, Dec 2014.
- [243] M. Ruchow, B. Herrnberger, P. Beschoner, G. Grön, M. Spitzer, and M. Kiefer. Error processing in major depressive disorder: Evidence from event-related potentials. *Journal of Psychiatric Research*, 40(1):37 – 46, 2006.
- [244] D. M. Olvet, D. N. Klein, and G. Hajcak. Depression symptom severity and error-related brain activity. *Psychiatry Research*, 179(1):30 – 37, 2010.
- [245] Z. Khazaeipour, S.-M. Taheri-Otaghsara, and M. Naghdi. Depression following spinal cord injury: Its relationship to demographic and socioeconomic indicators. *Topics in spinal cord injury rehabilitation*, 21(2):149–155, 2015.
- [246] C. Migliorini, B. Tonge, and G. Taleporos. Spinal cord injury and mental health. *Australian & New Zealand Journal of Psychiatry*, 42(4):309–314, 2008.

- [247] M. W. M. Post and C. M. C. van Leeuwen. Psychosocial issues in spinal cord injury: a review. *Spinal Cord*, 50(5):382–389, 2012.
- [248] F. Iwane, M. S. Halvagal, I. Iturrate, I. Batzianoulis, R. Chavarriaga, A. Billard, and J. d. R. Millán. Inferring subjective preferences on robot trajectories using EEG signals. In *2019 9th International IEEE/EMBS Conference on Neural Engineering (NER)*, pages 255–258, 2019.
- [249] A. J. Doud, J. P. Lucas, M. T. Pisansky, and B. He. Continuous three-dimensional control of a virtual helicopter using a motor imagery based brain-computer interface. *PLOS ONE*, 6(10):1–10, Oct 2011.
- [250] H. Si-Mohammed, C. Lopes-Dias, M. Duarte, F. Argelaguet, C. Jeunet, G. Casiez, G. R. Müller-Putz, A. Lécuyer, and R. Scherer. Detecting system errors in virtual reality using EEG through error-related potentials. In *2020 IEEE Conference on Virtual Reality and 3D User Interfaces (VR)*, pages 653–661, 2020.
- [251] Q. Zhao, L. Zhang, and A. Cichocki. EEG-based asynchronous BCI control of a car in 3D virtual reality environments. *Chinese Science Bulletin*, 54(1):78–87, Jan 2009.





# Acronyms

- ACC** anterior cingulate cortex 5
- ALS** amyotrophic lateral sclerosis 8
- BCI** brain-computer interface 7
- BOLD** blood-oxygen-level-dependent 4
- ECoG** electrocorticography 3
- EEG** electroencephalography 3
- ERD** event-related desynchronisation 5
- ERP** event-related potential 4
- ErrP** error-related potential 9
- ERS** event-related synchronisation 5
- fMRI** functional magnetic resonance imaging 4
- fNIRS** functional near-infrared spectroscopy 4
- MEG** magnetoencephalography 3
- MRCP** movement-related cortical potential 9
- Ne** error negativity 5
- PCA** principal component analysis 21
- Pe** error positivity 5
- PSP** postsynaptic potential 3
- SCI** spinal cord injury 8
- sLDA** shrinkage linear discriminant analysis 21

*Acronyms*

**TNR** true negative rate 21

**TPR** true positive rate 21

**VR** virtual reality 15

## A. Authors Contributions

C. Lopes-Dias, A. I. Sburlea, and G. R. Müller-Putz. Masked and unmasked error-related potentials during continuous control and feedback. *Journal of Neural Engineering*, 15(3):036031, 2018.

Author	Contribution	Description
CLD	70 %	conceptual idea, recording, analysis, writing
AIS	20 %	advice, analysis, proofreading
GRMP	10 %	conceptual idea, advice, proofreading

C. Lopes-Dias, A. I. Sburlea, and G. R. Müller-Putz. Online asynchronous decoding of error-related potentials during the continuous control of a robot. *Scientific Reports*, 9(1):17596, 2019.

Author	Contribution	Description
CLD	80 %	conceptual idea, study design, recording, analysis, writing
AIS	10 %	advice, proofreading
GRMP	10 %	conceptual idea, advice, proofreading

C. Lopes-Dias, A. I. Sburlea, and G. R. Müller-Putz. Asynchronous detection of error-related potentials using a generic classifier. In *8th Graz Brain-Computer Interface Conference 2019*, pages 54–58, 2019.

Author	Contribution	Description
CLD	90 %	conceptual idea, analysis, writing
AIS	5 %	advice, proofreading
GRMP	5 %	advice, proofreading

## A. Authors Contributions

C. Lopes-Dias, A. I. Sburlea, and G. R. Müller-Putz. A generic error-related potential classifier offers a comparable performance to a personalized classifier. In *2020 42nd Annual International Conference of the IEEE Engineering in Medicine Biology Society (EMBC)*, pages 2995–2998, 2020.

Author	Contribution	Description
CLD	90 %	conceptual idea, analysis, writing
AIS	5 %	advice, proofreading
GRMP	5 %	advice, proofreading

C. Lopes-Dias, A. I. Sburlea, K. Breitegger, D. Wyss, H. Drescher, R. Wildburger, and G. R. Müller-Putz. Online asynchronous detection of error-related potentials in participants with a spinal cord injury by adapting a pre-trained generic classifier. *Journal of Neural Engineering*, 2020, accepted.

Author	Contribution	Description
CLD	80 %	conceptual idea, study design, analysis, recording, writing
AIS	8 %	advice, proofreading
KB	1 %	recruitment of participants, clinical support
DW	1.5 %	participants' clinical evaluation, proofreading
HD	0.5 %	clinical support
RW	1 %	clinical supervision
GRMP	8 %	conceptual idea, advice, proofreading

## B. Selected Scientific Contributions

### Journal articles

C. Lopes-Dias, A. I. Sburlea, K. Breitegger, D. Wyss, H. Drescher, R. Wildburger, and G. R. Müller-Putz. Online asynchronous detection of error-related potentials in participants with a spinal cord injury by adapting a pre-trained generic classifier. *Journal of Neural Engineering*, 2020, accepted.

C. Lopes-Dias, A. I. Sburlea, and G. R. Müller-Putz. Online asynchronous decoding of error-related potentials during the continuous control of a robot. *Scientific Reports*, 9 (1):17596, 2019.

C. Lopes-Dias, A. I. Sburlea, and G. R. Müller-Putz. Masked and unmasked error-related potentials during continuous control and feedback. *Journal of Neural Engineering*, 15(3):036031, 2018.

### Conference papers

C. Lopes-Dias, A. I. Sburlea, and G. R. Müller-Putz. A generic error-related potential classifier offers a comparable performance to a personalized classifier. In *2020 42nd Annual International Conference of the IEEE Engineering in Medicine Biology Society (EMBC)*, pages 2995–2998, 2020.

H. Si-Mohammed\*, C. Lopes-Dias\*, M. Duarte, F. Argelaguet, V. Jeunet, G. Casiez, G. R. Müller-Putz, A. Lécuyer and R. Scherer. Detecting system errors in virtual reality using EEG through error-related potentials. In *2020 IEEE Conference on Virtual Reality and 3D User Interfaces (VR)*, pages 653-661, 2020.

## B. Selected Scientific Contributions

C. Lopes-Dias, A. I. Sburlea, and G. R. Müller-Putz. Asynchronous detection of error-related potentials using a generic classifier. In *8th Graz Brain-Computer Interface Conference 2019*, pages 54–58, 2019.

M. Bevilacqua, C. Lopes-Dias, A. I. Sburlea, and G. R. Müller-Putz. Expectation mismatch during a tracking task: an EEG study. In *8th Graz Brain-Computer Interface Conference 2019*, pages 65-70, 2019.

C. Lopes-Dias, A. I. Sburlea, and G. R. Müller-Putz. Error-related potentials with masked and unmasked onset during continuous control and feedback. In *7th Graz Brain-Computer Interface Conference 2017*, pages 320-332, 2017.

\* these authors contributed equally to this manuscript

## Posters

C. Lopes-Dias, A. I. Sburlea, G. R. Müller-Putz. Using ErrPs to improve continuous BCIs. Annual Meeting of the Society for Neuroscience 2019, Chicago, United States.

C. Lopes-Dias, A. I. Sburlea, G. R. Müller-Putz. Asynchronous detection of interaction errors. CuttingEEG 2017, Glasgow, United Kingdom.

## Talks

C. Lopes-Dias. Asynchronous detection of error-related potentials using a generic classifier. In *8th Graz Brain-Computer Interface Conference 2019*.

C. Lopes-Dias. Error-related potentials with masked and unmasked onset during continuous control and feedback. In *7th Graz Brain-Computer Interface Conference 2017*.

## **C. Core Publications**





# Masked and unmasked error-related potentials during continuous control and feedback

Catarina Lopes Dias<sup>✉</sup>, Andreea I Sburlea<sup>✉</sup> and Gernot R Müller-Putz<sup>✉</sup>

Institute of Neural Engineering, Graz University of Technology, Graz, Austria

E-mail: [gernot.mueller@tugraz.at](mailto:gernot.mueller@tugraz.at)

Received 29 November 2017, revised 26 February 2018

Accepted for publication 20 March 2018


Published 27 April 2018



## Abstract

The detection of error-related potentials (ErrPs) in tasks with discrete feedback is well established in the brain–computer interface (BCI) field. However, the decoding of ErrPs in tasks with continuous feedback is still in its early stages. *Objective.* We developed a task in which subjects have continuous control of a cursor's position by means of a joystick. The cursor's position was shown to the participants in two different modalities of continuous feedback: normal and jittered. The jittered feedback was created to mimic the instability that could exist if participants controlled the trajectory directly with brain signals. *Approach.* This paper studies the electroencephalographic (EEG)—measurable signatures caused by a loss of control over the cursor's trajectory, causing a target miss. *Main results.* In both feedback modalities, time-locked potentials revealed the typical frontal-central components of error-related potentials. Errors occurring during the jittered feedback (masked errors) were delayed in comparison to errors occurring during normal feedback (unmasked errors). Masked errors displayed lower peak amplitudes than unmasked errors. Time-locked classification analysis allowed a good distinction between correct and error classes (average Cohen- $\kappa$  = 0.803, average TPR = 81.8% and average TNR = 96.4%). Time-locked classification analysis between masked error and unmasked error classes revealed results at chance level (average Cohen- $\kappa$  = 0.189, average TPR = 60.9% and average TNR = 58.3%). Afterwards, we performed asynchronous detection of ErrPs, combining both masked and unmasked trials. The asynchronous detection of ErrPs in a simulated online scenario resulted in an average TNR of 84.0% and in an average TPR of 64.9%. *Significance.* The time-locked classification results suggest that the masked and unmasked errors were indistinguishable in terms of classification. The asynchronous classification results suggest that the feedback modality did not hinder the asynchronous detection of ErrPs.

Keywords: interaction error-related potential, asynchronous classification, continuous control, continuous feedback, brain–computer interface, EEG, jittered feedback

 Supplementary material for this article is available [online](#)

(Some figures may appear in colour only in the online journal)



Original content from this work may be used under the terms of the [Creative Commons Attribution 3.0 licence](#). Any further distribution of this work must maintain attribution to the author(s) and the title of the work, journal citation and DOI.

## 1. Introduction

Brain–computer interfaces (BCIs) convert mentally modulated brain activity into actions of an external device, constituting a resource that offers more independence to people with severe motor disabilities [1, 2].

In the context of BCIs, the brain activity is often measured non-invasively at the scalp level, using electroencephalography (EEG). The conversion of EEG signals into a device's actions is not flawless and hence BCIs sometimes misinterpret their users' intentions. These misinterpretations prompt increased frustration and lack of motivation among BCI users [3]. Therefore, BCIs can benefit from the incorporation of an error detection system in order to provide a smoother and robust interaction between user and external device. Such system can be used either to correct an action perceived as erroneous by the user (corrective approach) or to decrease the chance of future misclassifications (by adapting the classifier responsible for the action generation–adaptive approach) [4].

The development of an error detection system is possible because the recognition of an error elicits a neuronal response, which can be measured using EEG and is associated with a coarse differentiation between favorable and unfavorable outcomes [5]. The electrophysiological signature of error detection is named error-related potential (ErrP). Different types of ErrPs have been described in literature [4]. Response ErrPs occur in speeded response time tasks in which subjects are asked to respond as quickly as possible to a stimulus [6–9]. Observation ErrPs occur when subjects observe an error being committed by an external agent [10–12]. Feedback ErrPs occur when subjects receive the information that the action they performed was not correct [13]. Finally, interaction ErrPs occur in the context of BCIs, when users believe that the command they issued was misinterpreted by the interface [14, 15].

The inclusion of error detection systems in BCIs that control devices whose actions occur in a discrete way (discrete BCIs) is well established, both in the corrective and adaptive approaches [16–21]. However, BCIs controlling devices whose actions occur in a continuous manner (continuous BCIs) offer a more intuitive interaction with their users and have already been developed [22–24].

The study of error detection during continuous actions requires an asynchronous detection of errors and it is still in the early stages. Kreilinger *et al* studied interaction errors in a BCI that combined continuous and discrete feedback [22, 25]. Iturrate *et al* showed that errors can be detected during the observation of a continuous task [26], and Omedes *et al* detected them in an asynchronous manner [27]. Omedes *et al* also studied sudden and gradually unfolding errors in an observation task [28]. Milekovic *et al* showed that interaction errors can be detected during a task with continuous control and feedback using electrocorticographic recordings [29] and Spüler *et al* showed that it was also possible to do it using EEG [30].

One potential breakthrough of continuous BCIs would be to provide the users with full trajectory control of a cursor or a robotic arm. Nevertheless, existing studies on trajectory decoding from brain signals showed some instability in the

decoded trajectory [31, 32]. We aim to investigate the effect of feedback's instability in error-related potentials during a task with continuous control and feedback. For that, we developed a task in which participants used a joystick to continuously control a cursor towards a target. The continuous feedback of the cursor position was either normal or jittered. The jittered feedback intended to mask the cursor's position. In some of the trials (error trials), the participants lost the control of the cursor during the trial, therefore not reaching the target (giving rise to masked and unmasked errors). We created this protocol with three main goals in mind. First, we want to investigate if the jittered feedback would affect the electrophysiological signature of the error signals. Second, we intend to perform time-locked classification of correct trials against error trials, and of masked errors against unmasked errors. Finally, we aim to detect error-related potentials in an asynchronous manner.

## 2. Materials and methods

### 2.1. Hardware and data acquisition

EEG data were recorded at a sampling rate of 1000 Hz using BrainAmp amplifiers and an actiCap system (Brain Products, Munich, Germany) with 61 active electrodes and three EOG electrodes. The amplifiers used have a 0.016 Hz hardware high-pass filter of first-order. The EEG electrodes were placed at positions Fp1, Fp2, AF3, AF4, F7, F5, F3, F1, Fz, F2, F4, F6, F8, FT7, FC5, FC3, FC1, FCz, FC2, FC4, FC6, FT8, T7, C5, C3, C1, Cz, C2, C4, C6, T8, TP9, TP7, CP5, CP3, CP1, CPz, CP2, CP4, CP6, TP8, TP10, P7, P5, P3, P1, Pz, P2, P4, P6, P8, PO9, PO7, PO3, POz, PO4, PO8, PO10, O1, Oz, and O2. The ground electrode was placed at position AFz and the reference electrode was placed on the right mastoid. The EOG electrodes were placed above the nasion and below the outer canthi of the eyes.

### 2.2. Participants and experimental environment

Fifteen volunteers (aged between 19 and 27 years old, nine male) participated in the experiment, which took place in a shielded room. The participants sat in a comfortable armchair, in front of a screen that displayed the experimental protocol. The refresh sampling rate of the screen was 60 Hz. The right armrest of the chair was removed and in its location was placed a table with a joystick on it. The joystick position was adjusted for each participant in order to allow its comfortable manipulation by the participants, whilst keeping their elbow on the table. After the experimental protocol was explained to the participants, they signed an informed consent form that had been previously approved by the local ethics committee.

### 2.3. Experiment overview

The experiment consisted of 12 blocks of 30 trials each. The trial duration was variable, lasting on average  $4.6 \pm 0.7$  s (mean  $\pm$  SD). Between each trial, there was a 2.5 s break. Between each block, the participants could rest for as long as they needed. Half of the blocks consisted of *masked trials*.

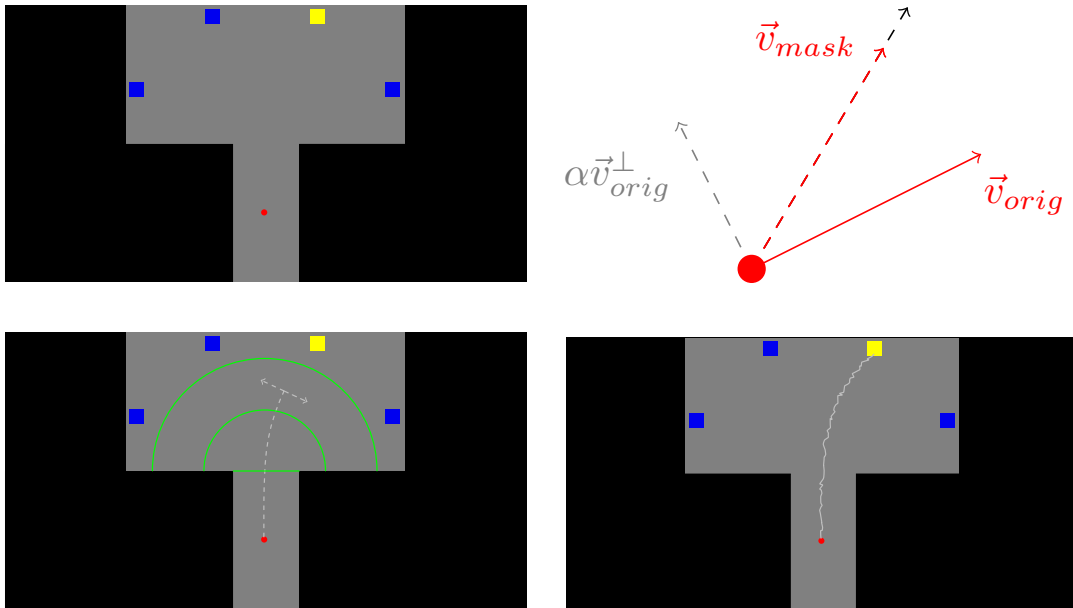


**Figure 1.** Top left: One of the four possible setups of the experimental protocol at the beginning of a trial. Top right: Schematic calculation of the cursor's velocity in the masked trials. The modified velocity vector is depicted with a dashed red arrow. Bottom left: Illustration of a possible cursor's trajectory and error onset in an unmasked error trial. All the green elements (semicircles and midline) were invisible to the participants. Bottom right: Illustration of a possible cursor's trajectory in a masked correct trial.

30% of trials of each block were *error trials*, leading to the same number of masked and unmasked error trials.

**2.3.1. Trial and task description.** At the beginning of a trial, four equally spaced squares were displayed on the upper part of a computer screen, at the same distance from its centre. On the lower part of the screen there was a red circle that represented the cursor. The squares and the circle were displayed on a gray area, inside which the cursor could move (see figure 1, top left image). In each trial, one of the squares was randomly selected by the paradigm as the target and therefore colored yellow, whilst the others were blue. All squares had the same probability of being selected. The cursor was controlled by the participants through a joystick. The displacement of the joystick corresponded to the direction of the movement of the cursor, which moved at a constant velocity. The task consisted in moving the cursor from its initial position to the target. A trial ended when the cursor reached the target or when it hit the boundary of the gray region (see supplementary video, available at [stacks.iop.org/JNE/15/036031](https://stacks.iop.org/JNE/15/036031)). The participants were instructed to shift their gaze to the target at the beginning of each trial and to keep it fixed on the target during the entire trial, to minimize the eye movements during the cursor movement.

**2.3.2. Masked trials.** In these trials, the cursor jittered perpendicularly to the direction of its movement. To achieve this effect, at each time-point was created a new velocity vector ( $v_{mask}$ ), by combining the original velocity vector ( $v_{orig}$ ) and its orthogonal vector ( $v_{orig}^\perp$ ):  $v_{mask} = v_{orig} + \alpha v_{orig}^\perp$ , with  $\alpha \in \text{unif}(-0.75, 0.75)$ .  $v_{mask}$  was then scaled to keep the velocity constant (see figure 1, top right and bottom right

images). Masked trials can be either correct or error trials (as well as the unmasked ones).

**2.3.3. Correct trials.** We considered as correct trials all the trials in which the participants successfully guided the cursor to the target (see figure 1, bottom right image). Participants completed on average  $20.2 \pm 0.5$  correct trials per block.

**2.3.4. Error trials.** In these trials, the participants lost control over the cursor (error onset). The error onset occurred when the cursor was located within the green semicircles depicted in the bottom left image of figure 1 (at a uniformly random distance from the centre of the screen). At the error onset, the cursor moved perpendicularly to its last direction, until the trial ended. The side of the cursor's deviation was randomly assigned and each side had the same probability of being chosen. The participants were instructed to keep their gaze fixed on the target and to bring the joystick to its resting position when realizing that the control over the cursor was lost. The joystick automatically returns to the resting position when no pressure is applied.

## 2.4. Preprocessing

The EEG signal was resampled to 250 Hz and band-pass filtered between 1 and 10 Hz with a zero-phase Butterworth filter of order 4. To remove outlier channels, we calculated the variance of the amplitude of each channel during correct and error trials. The first and third quartiles ( $Q1$  and  $Q3$ ) of the channels' variance were used to calculate the IQR interval ( $IQR = Q3 - Q1$ ). Channels whose variance lied outside  $[Q1 - 3 \times IQR, Q3 + 3 \times IQR]$  were excluded,

due to being considered extreme outliers [33]. Artifactual trials were rejected by visual inspection of the EEG channels. Additionally, error trials contaminated with eye movements around the error onset were removed. For that, error trials were epoched in the interval  $[-0.5, 1.0]$  s, time-locked to the error onset ( $t = 0$  s) and the variance of the horizontal and vertical derivatives of the EOG channels during this period was calculated. Error trials whose variance would be higher than  $Q3 + 3 \times IQR$  were removed. The maximum number of removed channels per subject was 3 ( $0.4 \pm 0.9$  (mean  $\pm$  SD)). On average,  $8.6 \pm 5.6\%$  of the error trials and  $1.9 \pm 2.5\%$  of the correct trials were excluded (mean  $\pm$  SD).

## 2.5. Electrophysiological analysis

After the preprocessing, correct and error trials were epoched, retaining a 1.5-s window interval per trial. In the correct trials, we chose the interval  $[-0.5, 1.0]$  s, time-locked to the cursor crossing the horizontal midline of the screen ( $t = -0.5$  s). The horizontal midline of the screen is depicted in the bottom left image of figure 1. In the error trials, we chose the interval  $[-0.5, 1.0]$  s, time-locked to the error onset ( $t = 0$  s).

## 2.6. Time-locked classification

After the preprocessing, the EEG signal was low-pass filtered and resampled to 50 Hz. For the time-locked classification of correct trials against error trials, we used a shrinkage-LDA classifier with two classes (correct and error), which was tested using a ten times five-fold cross-validation [34]. The features used to train the classifier for the correct class consisted of the amplitudes of all EEG channels during the correct trials (masked and unmasked) in the  $[0.1, 0.5]$  s, time-locked to the cursor crossing the horizontal midline of the screen ( $t = -0.5$  s). The features used to train the classifier for the error class consisted of the amplitudes of all the EEG channels during the error trials (masked and unmasked) in the interval  $[0.1, 0.5]$  s, time-locked to the error onset ( $t = 0$  s).

We also performed a time-locked classification of masked error trials against unmasked error trials. In this case, we used the same classification procedure described above but now with two other classes: unmasked errors and masked errors. The features used to train the classifier were the same as the ones described for the error class, but taking into consideration the type of trial (masked or unmasked).

In order to assess the performance of the time-locked classification, we used the true positive rate (TPR), the true negative rate (TNR) and the Cohen- $\kappa$  coefficient as performance measures [35]. The chance-level results were calculated at a subject level by using a classifier with randomly shuffled training labels. Additionally, we also calculated the 95% confidence interval for the performance measures of a theoretical chance-level classifier.

## 2.7. Asynchronous classification

After the preprocessing, the EEG signal was, again, low-pass filtered and resampled to 50 Hz. Correct and error trials were

epoched from the time-point in which the cursor crossed the horizontal midline of the screen until the trial ended, avoiding the period of the trials in which eye movements could have happened. Epoched this way, the correct trials lasted on average  $2.37 \pm 0.25$  s and the error trials lasted on average  $3.20 \pm 0.62$  s (mean  $\pm$  SD).

We used a shrinkage-LDA classifier with two classes: correct and error. As features to train the classifier for the correct class, we considered the amplitudes of all EEG channels during the correct trials (both masked and unmasked), in the interval  $[0.1, 0.5]$  s, time-locked to the cursor crossing the horizontal midline of the screen ( $t = -0.5$  s). As features to train the classifier for the error class, we considered the amplitudes of all EEG channels during the error trials (both masked and unmasked), in the interval  $[0.1, 0.5]$  s time-locked to the error onset ( $t = 0$  s). The number of features was then reduced using principal component analysis (PCA), conserving the components that explained 99% of the signal's variance. These components were used as features to train the classifier in a time-locked manner. The classifier was then tested asynchronously, by sliding a 400 ms window over the trials, what resulted in a classifier's output every 20 ms.

For each fixed threshold ( $\tau$ , such that  $\tau \in [0, 1]$  with steps of 0.025) for the error class probability ( $p_e$ ), we considered an *error event* when  $p_e \geq \tau$  in at least two consecutive windows. The evaluation metric that we used to assess the asynchronous classification defines a correct trial as successfully classified if no error event was detected during the entire trial duration (true negative trial). An error trial was considered to be successfully classified if no error event was detected before the error onset and at least one error event was detected after the error onset (true positive trial). The average duration between the error onset and the end of the trial was  $1.48 \pm 0.64$  s (mean  $\pm$  SD).

Two methods were used to evaluate the classifier asynchronously. The first method consisted in performing a ten times five-fold asynchronous cross-validation in the first 80% of the data (the first 80% of the correct trials and of the error trials). To assess the performance of the asynchronous cross-validation classification, we used TPR and TNR as performance measures. The chance level results were calculated at a subject level, by using a classifier with randomly shuffled training labels. The second method consisted in using a chronological split (80%–20%) of the data to perform asynchronous classification (the first 80% of the trials were used to train the classifier in a time-locked way and the last 20% of the trials were used to test it asynchronously). To assess the performance of the asynchronous classification on the chronological split, we used TPR and TNR as performance measures. The chance level results were calculated at a subject level, by averaging 50 repetitions of the classification done with randomly shuffled training labels.

The asynchronous cross-validation and the search of the optimal thresholds were performed only on the first 80% of the data. On the remaining 20% of the data, we evaluated the asynchronous classification using all thresholds. The results for optimal thresholds at group- and subject-level were compared. The TPR was chosen as the optimization measure



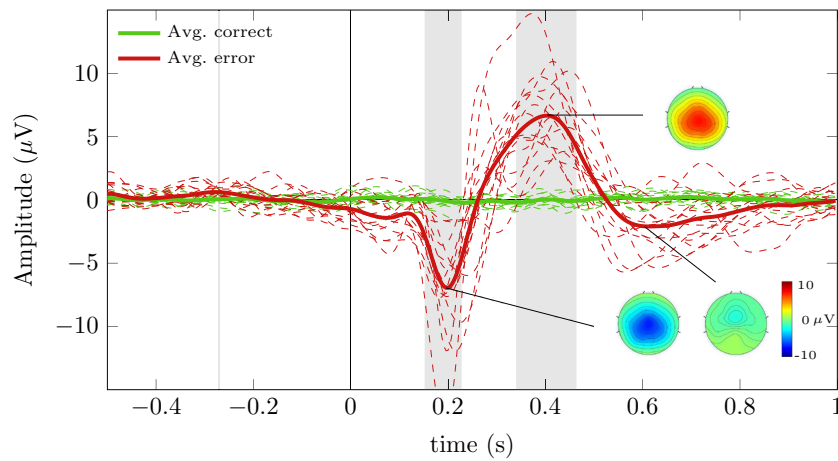


**Figure 2.** Grand average correct and error signals at channel FCz (in green and red, respectively). Both masked and unmasked trials were considered to obtain the presented the grand averages. The gray areas denote the intervals in which correct and error signals are significantly different (Wilcoxon signed-rank tests, Bonferroni corrected, with  $p < 0.05$ ). The dashed lines represent the average error and correct signals of each participant. The scalp distributions of the grand average error signal are displayed at  $t = 196$  ms,  $t = 404$  ms and  $t = 616$  ms.

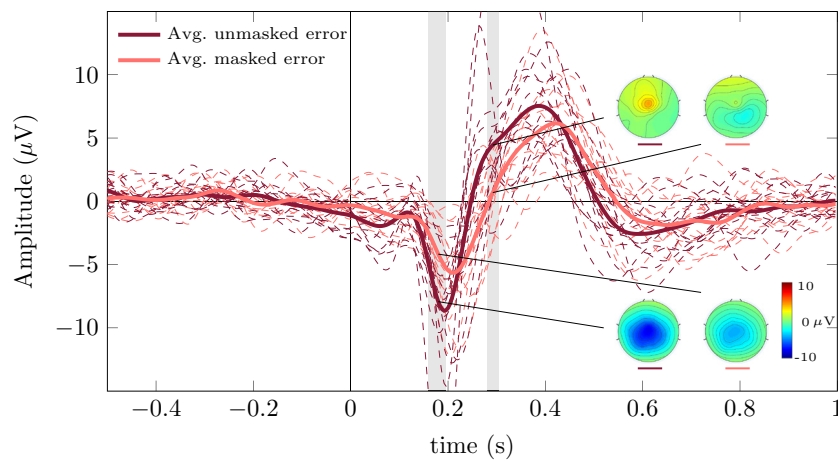


**Figure 3.** Grand average masked and unmasked error signals at channel FCz (in pink and dark red, respectively). The gray areas denote the intervals in which masked and unmasked error signals are significantly different (Wilcoxon signed-rank tests, Bonferroni corrected, with  $p < 0.05$ ). The dashed lines represent the averaged masked and unmasked error signals of each participant. The scalp distributions of the grand average masked and unmasked error signals are displayed for  $t = 180$  ms and  $t = 292$  ms.

to select the optimal thresholds because true positive trials contain two distinct periods (one in which no error happens and no error event is detected by the classifier, and another that starts with the error onset, and in which an error event is detected). This choice prevents the classifier from being too biased towards any of the classes.

### 3. Results

#### 3.1. Electrophysiological results

**3.1.1. Correct and error signals.** The grand average correct and error signals at channel FCz are displayed in figure 2 (in green and red color, respectively). Defining the error onset at  $t = 0$  s, the grand average error signal presents a first negative peak at 196 ms, followed by a positive peak at 404 ms, and a later negative peak at 616 ms. The error-related potential (calculated as the difference between the average error signal and the average correct signal) is essentially similar to the average

error signal because the average correct signal is nearly flat. For this reason, we chose not to include the error-related potential in the figure. The average correct and error signals of each subject are shown in dashed lines. The gray areas represent the time periods in which correct and error signals are significantly different (Wilcoxon signed-rank tests, Bonferroni corrected, with  $p < 0.05$ ). Figure 2 also shows the scalp distributions of the grand average error signal at  $t = 196$  ms,  $t = 404$  ms and  $t = 616$  ms.

**3.1.2. Masked and unmasked error signals.** Figure 3 shows the grand average masked and unmasked error signals at channel FCz (in pink and dark red color, respectively) as well as the average signals of each subject (in dashed lines). The grand average unmasked error signal presents a first negative peak at 192 ms, followed by a positive peak at 388 ms and a later negative peak at 592 ms. The grand average masked error signal presents a first negative peak at 212 ms, followed by a positive peak at 420 ms and a later negative peak at 652 ms.

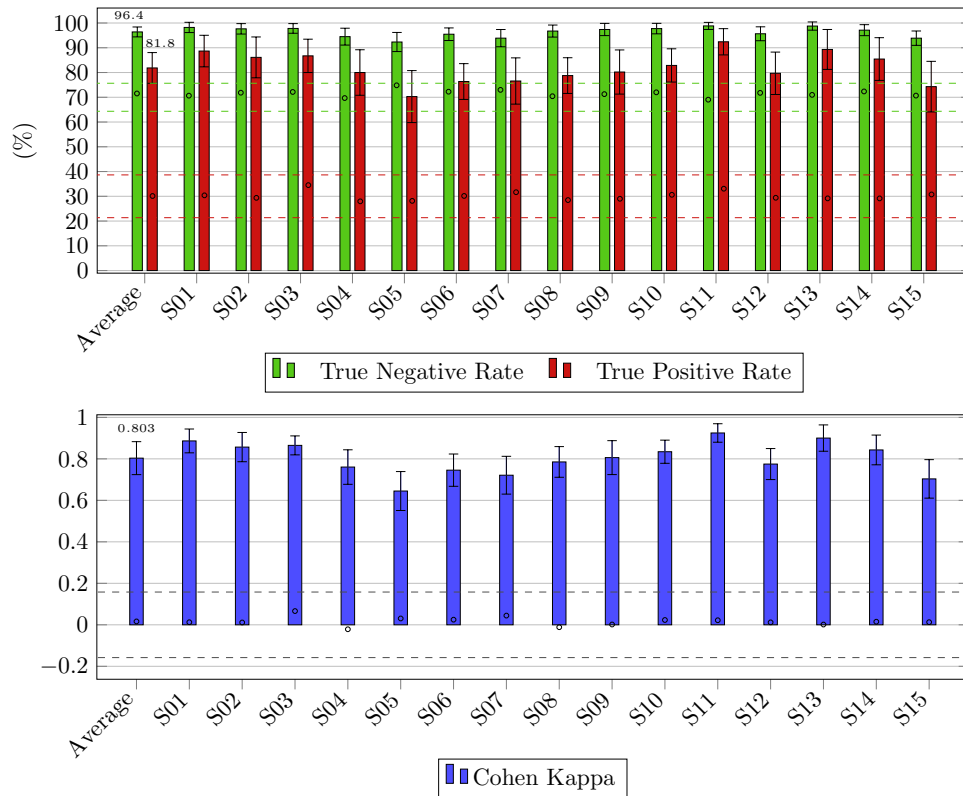


**Figure 4.** Time-locked classification of correct trials against error trials. The small circles indicate the chance level at a subject level. Top: Percentage (mean and standard deviation) of successfully classified correct and error trials (TNR (green bars) and TPR (red bars), respectively) for each subject and their average. The 95% confidence intervals for the TPR and TNR of a theoretical chance level classifier are displayed with red and green dashed lines, respectively. Bottom: Cohen- $\kappa$  coefficient (mean and standard deviation) of each subject and their average. The 95% confidence interval for Cohen- $\kappa$  coefficient of a theoretical chance level classifier is displayed with dashed lines.

The gray areas indicate the regions in which masked and unmasked error signals were significantly different (Wilcoxon signed-rank tests, Bonferroni corrected, with  $p < 0.05$ ). Figure 3 shows also the scalp distributions of the grand average masked and unmasked error signals at  $t = 180$  ms and  $t = 292$  ms (in the region where the signals were significantly different). Unmasked errors displayed significantly larger (positive and negative) peak amplitudes than masked errors (Wilcoxon signed-rank tests, one-sided,  $p = 0.027$  in both cases). Unmasked errors also displayed significantly earlier positive and negative peaks than masked errors (Wilcoxon signed-rank tests, one-sided,  $p = 0.0015$  for the positive peak and  $p = 0.0065$  for the negative peak). The time-shift that maximized the cross-correlation between the grand average masked and unmasked error signals was 28 ms.

### 3.2. Time-locked classification

The results of the time-locked classification of error trials against correct trials are displayed in figure 4. On average,  $96.4 \pm 2.0\%$  (mean  $\pm$  SD) of the correct trials were successfully classified (true negative rate (TNR)) and  $81.8 \pm 6.3\%$  (mean  $\pm$  SD) of the error trials were successfully classified (true positive rate (TPR)). The 95% confidence interval for the TNR of a theoretical chance level classifier was  $[64.3, 75.7]$  and is depicted with dashed green lines. The 95% confidence interval for the TPR of theoretical a chance level classifier was

$[21.3, 38.7]$  and is depicted with dashed red lines. The average Cohen- $\kappa$  coefficient was  $0.803 \pm 0.079$  (mean  $\pm$  SD). The 95% confidence interval for the Cohen- $\kappa$  coefficient of a chance level classifier was  $[-0.158, 0.158]$  and is depicted with dashed lines. The chance level results of each participant, for all the measures, are represented with small circles.

The results of the time-locked classification of masked error trials against unmasked error trials are displayed in figure 5. On average,  $60.6 \pm 9.7\%$  (mean  $\pm$  SD) of the masked error trials were successfully classified (true negative rate (TNR)) and  $58.3 \pm 6.8\%$  (mean  $\pm$  SD) of the unmasked error trials were successfully classified (true positive rate (TPR)). The 95% confidence interval for the TNR and TPR of a theoretical chance level classifier was  $[36.7, 63.7]$  and is depicted with dashed lines. The average Cohen- $\kappa$  coefficient was  $0.189 \pm 0.144$  (mean  $\pm$  SD). The 95% confidence interval for the Cohen- $\kappa$  coefficient of a theoretical chance level classifier was  $[-0.189, 0.189]$  and is depicted with dashed lines. The chance level results of each participant, for all the measures, are represented with small circles.

### 3.3. Asynchronous classification

In order to detect errors in an asynchronous manner, we considered a classifier with two classes: correct and error. We decided to use both masked and unmasked trials to train these classes due to the chance level outcome of the time-locked classification

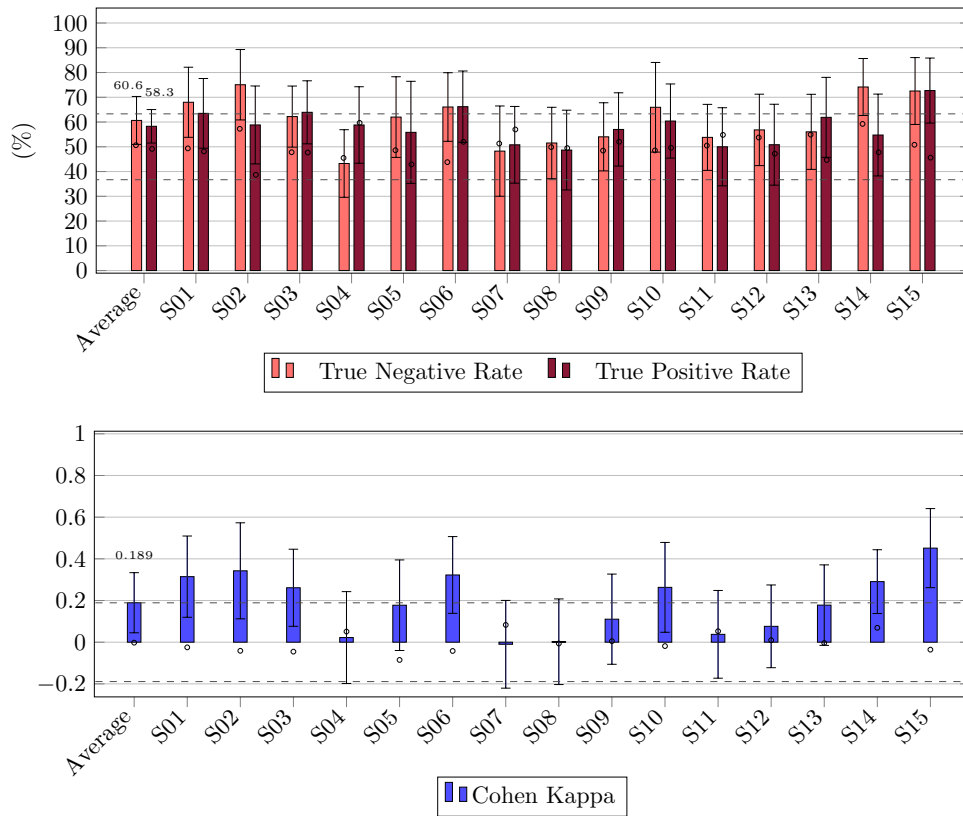


**Figure 5.** Time-locked classification of masked errors against unmasked errors. The small circles indicate the chance level at a subject level. Top: Percentage (mean and standard deviation) of successfully classified masked and unmasked error trials (TNR (pink bars) and TPR (dark red bars), respectively) for each subject and their average. The 95% confidence interval for the TPR and TNR of a theoretical chance level classifier is displayed with dashed lines. Bottom: Cohen- $\kappa$  coefficient (mean and standard deviation) of each subject and their average. The 95% confidence interval for the Cohen- $\kappa$  coefficient of a theoretical chance level classifier is displayed with dashed lines.

of masked errors against unmasked errors. We used a ten times five-fold asynchronous cross-validation in the first 80% of the data. Figure 6 (top) shows the average percentage of correct and error trials successfully classified (TNR and TPR, left and right images, respectively) in function of the considered thresholds ( $\tau$ ), for each subject (dashed colored lines). Figure 6 (bottom) shows the average TNR and TPR (green and red lines, respectively) for each of the considered thresholds, and the 95% confidence interval for the averages (shaded areas). The average chance level of TNR and TPR are displayed in green and red dashed lines, respectively. The threshold that maximized the average TPR was  $\tau = 0.575$ . Using this threshold, we obtained an average TPR of 68.0% and an average TNR of 76.0%. Figure 7 displays the average detection delay (period between the error onset and the detection of an error event by the classifier) in the masked and unmasked error trials successfully classified (TP trials) as well as the corresponding 95% confidence interval, in function of  $\tau$ . The gray shaded areas indicate the regions in which the average delay in masked and unmasked trials was significantly different (Wilcoxon signed-rank tests, Bonferroni corrected, with  $p < 0.05$ ).

In order to simulate an online scenario, we considered a chronological split (80%–20%) of the data, using the first 80% of the data to train the classifier and the last 20% to test it asynchronously. The average TNR and TPR obtained (black

solid lines) in function of  $\tau$  as well as the individual results of each participant (colored dashed lines) are shown in figure 8. Figure 9, left image, shows the TNR and TPR of each participant and their average, for  $\tau = 0.575$ . With this threshold, we obtained an average TNR of 80.9% and an average TPR of 64.9%. The chance level results of each participant are represented with small circles.

Next, in order to try to improve the classification results in the simulated online scenario, we decided to use individualized classifiers. Therefore, we considered, for each subject, the threshold  $\tau$  that maximized the individual average TPR in the asynchronous cross-validation in the first 80% of the data (see figure 6, top right). This threshold was then used in the asynchronous classification of the data in the chronological split (80%–20%). Figure 9, right image, shows the TNR and TPR obtained for each subject, using individualized thresholds, and their average. The average TNR obtained was 84.0% and the average TPR was 64.9%. The chance level results of each participant are represented with small circles. The blue numbers near the barplots of each subject indicate the threshold used for that subject. The use of individualized thresholds did not significantly change the TPR nor the TNR, in comparison with the use of  $\tau = 0.575$  (Wilcoxon signed-rank tests, with  $p = 0.828$  for the TPR comparison and  $p = 0.361$  for the TNR comparison).

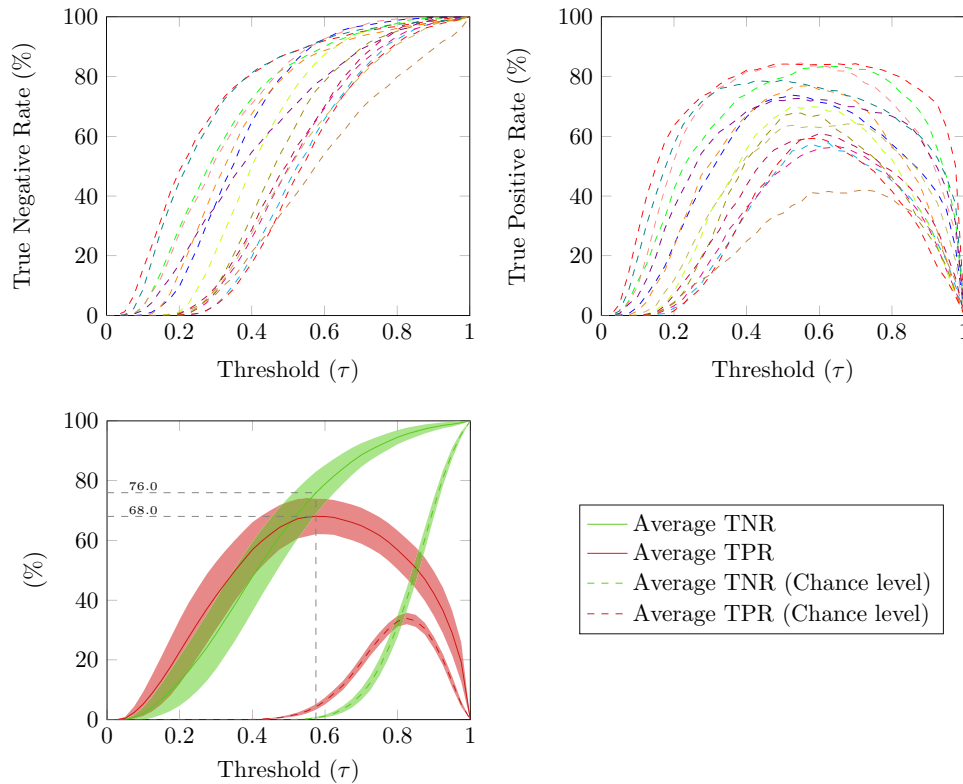


**Figure 6.** Asynchronous cross-validation in the first 80% of the data: Top: Average percentage of correct and error trials successfully classified (TNR and TPR, left and right images, respectively) in function of the thresholds ( $\tau$ ) for each subject (dashed colored lines). Bottom: Average TNR and TPR (green and red solid lines, respectively) in function of  $\tau$ . The average chance level of the TNR and TPR are represented in green and red dashed lines, respectively. The shaded areas represent the 95% confidence interval for the averages. The gray dashed lines indicate the threshold that maximizes the average TPR ( $\tau = 0.575$ ) as well as the average TNR and TPR associated with it.

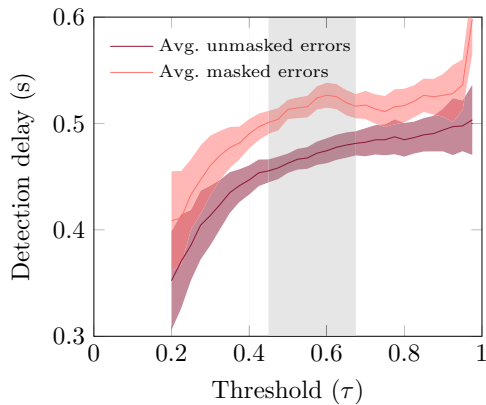


**Figure 7.** Asynchronous cross-validation in the first 80% of the data: Average delay in the detection of an error event (period between the error onset and the detection of an error event by the classifier) on masked and unmasked error trials successfully classified (TP trials) (pink and dark red lines respectively) and the corresponding 95% confidence intervals (shaded areas), in function of  $\tau$ . We considered only the thresholds in which all subjects had at least one error trial successfully classified. The shaded gray areas indicate the regions in which the average delay in masked and unmasked trials was significantly different (Wilcoxon signed-rank tests, Bonferroni corrected, with  $p < 0.05$ ).

#### 4. Discussion

We developed this study to investigate if the instability of the feedback, during a task with continuous control and

continuous feedback, would affect the error signal at a neurophysiological level. We also intended to study if different feedback modalities could make the error signals discernible in terms of classification. Finally, we aimed to asynchronously decode errors during a task with continuous control and continuous feedback. With these aims in mind, we developed a task in which participants continuously controlled a cursor on a screen using a joystick. The feedback of the cursor position was either normal (unmasked trials) or jittered (masked trials). The error trials correspond to a loss of control over the cursor's trajectory. The correct trials correspond to the period in which the cursor is moving on the screen and are not associated with any specific event. Thus, our protocol differs from standard protocols on error-related potentials in discrete BCIs, in which correct trials are associated with a correct event, but is similar to protocols described in literature regarding error-related potentials during continuous feedback [4, 28, 30].

In the electrophysiological analysis, the correct signals were mainly flat. Error and correct signals were significantly different in the time periods corresponding to the first negativity and positivity of the error trials.

When comparing the error signals under the two types of feedback (masked and unmasked errors), we obtained two small intervals in which the signals were significantly different. The masked error signal was delayed in comparison to the unmasked error signal: the peaks of the masked error signals occurred significantly later than the corresponding



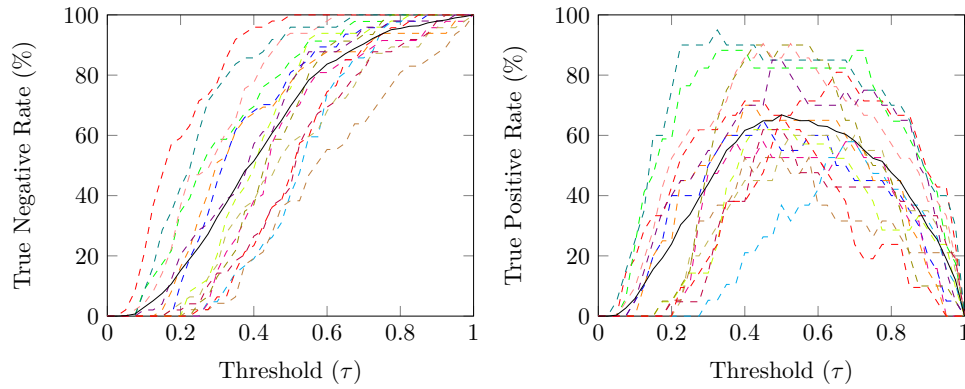


**Figure 8.** Chronological split (80%–20%): Average percentage of correct trials successfully classified (TNR) and error trials successfully classified (TPR) (black lines, left and right images respectively) in function of the threshold ( $\tau$ ). The dashed colored lines represent the TNR and TPR of each participant.

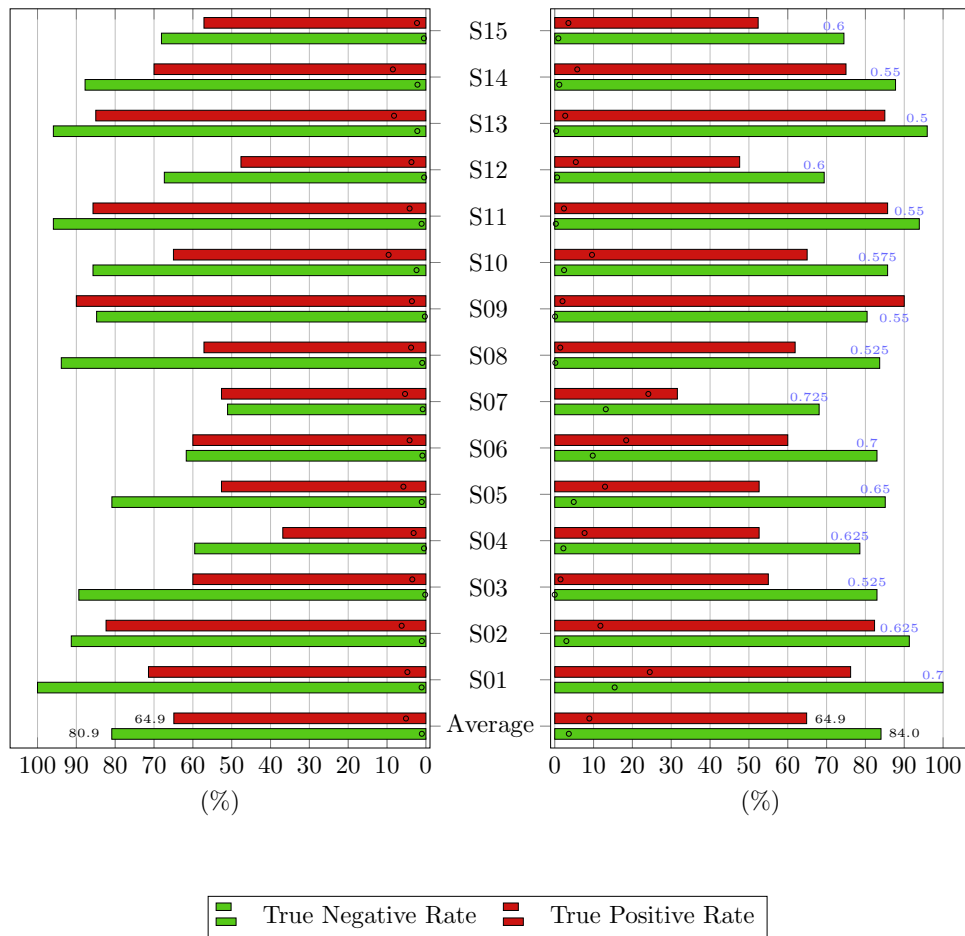


**Figure 9.** Chronological split (80%–20%): The percentage of correct trials successfully classified (TNR) are depicted with green bars and the percentage of error trials successfully classified (TPR) are depicted with red bars. The chance level results of each participant are represented with small circles. Left: Asynchronous classification using the threshold  $\tau = 0.575$ . Right: Asynchronous classification using individual thresholds. The blue numbers near the bars indicate the threshold used for each subject.

peaks of the unmasked error signals. The time shift that maximized the cross-correlation between the two grand average signals was 28 ms. Additionally, peak amplitudes in masked error signals were significantly less pronounced than the peak amplitudes in unmasked error signals. We hypothesize that this occurs due to a smearing effect in the averaged masked error signal, caused by a trial-to-trial variability in the moment

in which participants realized the occurrence of an error [36]. Alternatively, these results could be seen as evidence for conceptualizing error awareness as a decision process, involving evidence accumulation [37, 38]. Steinhäuser and Yeung suggested that the amplitude of the Pe component of ErrPs reflects the evidence strength that an error has occurred [39, 40]. Following this line of reasoning, the lower Pe

amplitude observed in the masked errors of our experiment could reflect a weaker evidence for the occurrence of an error, caused by the jittered feedback.

The time-locked classification of correct against error trials allowed a good discrimination between the type of trials. On average, 96.4% of the correct trials were successfully classified and 81.8% of the error trials were successfully classified. The obtained average Cohen- $\kappa$  was 0.803. Differently, the time-locked classification of masked errors against unmasked errors did not allow a satisfactory discrimination between the classes. On average, 60.6% of the masked errors trials were successfully classified and 58.3% of the unmasked error trials were successfully classified. The obtained average Cohen- $\kappa$  was 0.189. These value lie within the 95% confidence intervals for a chance level classifier. This indicates that the type of feedback used (normal or jittered) did not make the errors distinguishable in terms of classification. The time-locked classification results are similar to the ones obtained in [41] and comparable with state-of-the-art literature on time-locked classification of error-related potentials [15, 26, 27, 30].

Given that masked and unmasked errors were indistinguishable in terms of time-locked classification, we decided to perform asynchronous classification only for the detection of errors (correct versus error), using both masked and unmasked trials to train the classifier. First, we performed an asynchronous cross-validation in the first 80% of the data, what allowed the calculation of average results for each subject, taking into account the data variability. In this scenario, masked errors were detected significantly later than unmasked errors, for the thresholds ( $\tau$ ) that lead to better performances. Then, in order to simulate an online scenario, we considered the first 80% of the data to train the classifier and the last 20% to test it. We used two approaches to evaluate results in this simulated online scenario. The first approach consisted in a non-individualized classifier for all subjects: we chose the threshold that maximized the average TPR in the asynchronous cross-validation in the first 80% of the data ( $\tau = 0.575$ ), resulting in an average TPR of 64.9% and in an average TNR of 80.9%. The second approach consisted in individualized classifiers: we chose the threshold that maximized the individual average TPR in the asynchronous cross-validation in the first 80% of the data. The use of individualized classifiers slightly improved the classification results: the average TNR increased from 80.9% to 84.0% and the average TPR remained the same. The difference between the classifiers regarding the TPR and TNR was not significant. We were expecting fatigue to influence the results in the simulated online scenario [42] but the performances obtained in this case lied within the 95% confidence interval calculated for the cross-validated data, indicating no decrease in performance.

Other studies also performed asynchronous decoding of ErrPs. Omedes *et al* asynchronously classified sudden and gradual observation errors [28]. Their sudden errors are comparable to the unmasked errors in this study. Their gradual errors appeared to be much less time-locked to the onset than the masked errors presented here. Spüler and Niethammer

asynchronously classified outcome and execution errors during continuous control and continuous feedback [30]. According to their categorization, the errors in our protocol would be both outcome and execution errors. Both Spüler and Omedes considered frequency domain features in their classification but we obtained comparable results using only time domain features. Alternatively, one could approach the detection of error-related potentials from a more generic perspective, by taking into account frequency ranges that are not commonly considered [43, 44].

The direct transfer of our simulated online results to an online scenario would not be realistic because it would require a long training period (it took us around 50 min to record 80% of the trials). The need for big amounts of data to train the classifiers is a general problem in the BCI field and it is of extreme importance to investigate possible approaches to overcome it. Several studies used different approaches to reduce calibration time. Kim and Kirchner showed the feasibility of using a classifier trained with observation errors to classify interaction errors within the same task [45]. Iturrate and colleagues showed the feasibility of transferring a classifier between different observation tasks, using delay-corrected potentials [46]. Spinnato and colleagues showed that a wavelet domain Gaussian linear mixed model (LMM) was superior to other classifying methods, particularly when using few training trials [47]. Kim and Kirchner also showed that it was possible to use a classifier trained with errors of several participants to classify the errors of another participant, at the cost of a decrease in performance [45]. Pinegger and Müller-Putz developed a similar classifier but for the detection of P300, without loss of performance [48]. These strategies (as well as the use of adaptive classifiers) are alternatives to reduce calibration times that should be considered when developing online BCIs [17–21].


In our study, correct and error trials were successfully classifiable. Masked and unmasked errors were different in terms of electrophysiology but indistinguishable in terms of classification. The asynchronous detection of errors was reliable and not influenced by the feedback modality during the continuous control of a cursor using a joystick. Hence, we envision that we could use EEG to detect error signals during the continuous control of a robotic arm.

## Acknowledgments

The authors would like to acknowledge the help of M K Höller during the preparation of the experiments described in the article. This work was supported by ERC Consolidator Grant 681231 ‘Feel Your Reach’.

## ORCID iDs

Catarina Lopes Dias  <https://orcid.org/0000-0001-9775-3743>

Andreea I Sburlea  <https://orcid.org/0000-0001-6766-3464>

Gernot R Müller-Putz  <https://orcid.org/0000-0002-0087-3720>




## References

- [1] Millán J d R et al 2010 Combining brain–computer interfaces and assistive technologies: state-of-the-art and challenges *Frontiers Neurosci.* **4** 161
- [2] Müller-Putz G R, Leeb R, Tangermann M, Höhne J, Kübler A, Cincotti F, Mattia D, Rupp R, Müller K-R and Millán J d R 2015 Towards noninvasive hybrid brain–computer interfaces: framework, practice, clinical application, and beyond *Proc. IEEE* **103** 926–43
- [3] Évain A, Argelaguet F, Strock A, Roussel N, Casiez G and Lécuyer A 2016 Influence of error rate on frustration of BCI users *Proc. of the Int. Working Conf. on Advanced Visual Interfaces (New York, NY, USA, 2016)* pp 248–51
- [4] Chavarriaga R, Sobolewski A and Millán J d R 2014 Errore machinale est: the use of error-related potentials in brain-machine interfaces *Frontiers Neurosci.* **8** 208
- [5] Hajcak G, Moser J S, Holroyd C B and Simons R F 2006 The feedback-related negativity reflects the binary evaluation of good versus bad outcomes *Biol. Psychol.* **71** 148–54
- [6] Gehring W J, Goss B, Coles M G, Meyer D E and Donchin E 1993 A neural system for error detection and compensation *Psychol. Sci.* **4** 385–90
- [7] Falkenstein M, Hoormann J, Christ S and Hohnsbein J 2000 ERP components on reaction errors and their functional significance: a tutorial *Biol. Psychol.* **51** 87–107
- [8] Blankertz B, Dornhege G, Schäfer C, Krepki R, Kohlmorgen J, Müller K-R, Kunzmann V, Losch F and Curio G 2003 Boosting bit rates and error detection for the classification of fast-paced motor commands based on single-trial EEG analysis *IEEE Trans. Neural Syst. Rehabil. Eng.* **11** 127–31
- [9] Parra L C, Spence C D, Gerson A D and Sajda P 2003 Response error correction – a demonstration of improved human-machine performance using real-time EEG monitoring *IEEE Trans. Neural Syst. Rehabil. Eng.* **11** 173–7
- [10] van Schie H T, Mars R B, Coles M G H and Bekkering H 2004 Modulation of activity in medial frontal and motor cortices during error observation *Nat. Neurosci.* **7** 549–54
- [11] Yeung N, Holroyd C B and Cohen J D 2005 ERP correlates of feedback and reward processing in the presence and absence of response choice *Cerebral Cortex* **15** 535–44
- [12] Chavarriaga R and Millán J d R 2010 Learning from EEG error-related potentials in noninvasive brain–computer interfaces *IEEE Trans. Neural Syst. Rehabil. Eng.* **18** 381–8
- [13] Holroyd C B and Coles M 2002 The neural basis of human error processing: reinforcement learning, dopamine, and the error-related negativity *Psychol. Rev.* **109** 679–709
- [14] Schalk G, Wolpaw J R, McFarland D J and Pfurtscheller G 2000 EEG-based communication: presence of an error potential *Clin. Neurophysiol.* **111** 2138–44
- [15] Ferrez P W and Millán J d R 2005 You are wrong!: automatic detection of interaction errors from brain waves *Proc. of the 19th Int. Joint Conf. on Artificial Intelligence* pp 1413–8
- [16] Ferrez P W and Millán J d R 2008 Simultaneous real-time detection of motor imagery and error-related potentials for improved BCI accuracy *Proc. of the 4th Int. Brain–Computer Interface Workshop and Training Course* pp 197–202
- [17] Llera A, van Gerven M A, Gómez V, Jensen O and Kappen H J 2011 On the use of interaction error potentials for adaptive brain computer interfaces *Neural Netw.* **24** 1120–7
- [18] Llera A, Gómez V and Kappen H J 2012 Adaptive classification on brain–computer interfaces using reinforcement signals *Neural Comput.* **24** 2900–23
- [19] Iturrate I, Chavarriaga R, Montesano L, Minguez J and Millán J d R 2015 Teaching brain-machine interfaces as an alternative paradigm to neuroprosthetics control *Sci. Rep.* **5** 13893
- [20] Zander T, Krol L, Birbaumer N and Gramann K 2016 Neuroadaptive technology enables implicit cursor control based on medial prefrontal cortex activity *Proc. Natl Acad. Sci. USA* **113** 14898–903
- [21] Salazar-Gomez A F, DelPreto J, Gil S, Guenther F H and Rus D 2017 Correcting robot mistakes in real time using EEG signals *IEEE Int. Conf. on Robotics and Automation* pp 6570–7
- [22] Kreilinger A, Neuper C and Müller-Putz G R 2012 Error potential detection during continuous movement of an artificial arm controlled by brain–computer interface *Med. Biol. Eng. Comput.* **50** 223–30
- [23] Galán F, Nuttin M, Lew E, Ferrez P W, Vanacker G, Philips J and Millán J d R 2008 A brain-actuated wheelchair: asynchronous and non-invasive brain–computer interfaces for continuous control of robots *Clin. Neurophysiol.* **119** 2159–69
- [24] Doud A J, Lucas J P, Pisansky M T and He B 2011 Continuous three-dimensional control of a virtual helicopter using a motor imagery based brain–computer interface *PLOS One* **6** 1–10
- [25] Kreilinger A, Hiebel H and Müller-Putz G R 2016 Single versus multiple events error potential detection in a BCI-controlled car game with continuous and discrete feedback *IEEE Trans. Biomed. Eng.* **63** 519–29
- [26] Iturrate I, Montesano L and Minguez J 2010 Single trial recognition of error-related potentials during observation of robot operation *Annual Int. Conf. of the IEEE Engineering in Medicine and Biology Society* pp 4181–4
- [27] Omedes J, Iturrate I, Chavarriaga R and Montesano L 2015 Asynchronous decoding of error potentials during the monitoring of a reaching task *IEEE Int. Conf. on Systems, Man, and Cybernetics* pp 3116–21
- [28] Omedes J, Iturrate I, Minguez J and Montesano L 2015 Analysis and asynchronous detection of gradually unfolding errors during monitoring tasks *J. Neural Eng.* **12** 056001
- [29] Milekovic T, Ball T, Schulze-Bonhage A, Aertsen A and Mehring C 2012 Error-related electrocorticographic activity in humans during continuous movements *J. Neural Eng.* **9** 026007
- [30] Spüler M and Niethammer C 2015 Error-related potentials during continuous feedback: using EEG to detect errors of different type and severity *Frontiers Hum. Neurosci.* **9** 155
- [31] Ofner P and Müller-Putz G R 2012 Decoding of velocities and positions of 3D arm movement from EEG *Annual Int. Conf. of the IEEE Engineering in Medicine and Biology Society* pp 6406–9
- [32] Robinson N, Guan C and Vinod A P 2015 Adaptive estimation of hand movement trajectory in an EEG based brain–computer interface system *J. Neural Eng.* **12** 066019
- [33] Tukey J W 1977 *Exploratory Data Analysis (Addison-Wesley Series in Behavioral Science)* (Reading, MA: Addison-Wesley)
- [34] Blankertz B, Lemm S, Treder M, Haufe S and Müller K-R 2011 Single-trial analysis and classification of ERP components a tutorial *NeuroImage* **56** 814–25
- [35] McHugh M L 2012 Interrater reliability: the kappa statistic *Biochem. Med.* **22** 276–82
- [36] Ouyang G, Sommer W and Zhou C 2016 Reconstructing ERP amplitude effects after compensating for trial-to-trial latency jitter: a solution based on a novel application of residue iteration decomposition *Int. J. Psychophysiol.* **109** 9–20
- [37] O’Connell R, Dockree P and Kelly S 2012 A supramodal accumulation-to-bound signal that determines perceptual decisions in humans *Nat. Neurosci.* **15** 1729–35

- [38] PISAURO M A, FOURAGNAN E, RETZLER C and PHILIASTIDES M G 2017 Neural correlates of evidence accumulation during value-based decisions revealed via simultaneous EEG-fMRI *Nat. Commun.* **8** 15808
- [39] STEINHAUSER M and YEUNG N 2010 Decision processes in human performance monitoring *J. Neurosci.* **30** 15643–53
- [40] STEINHAUSER M and YEUNG N 2012 Error awareness as evidence accumulation: effects of speed-accuracy trade-off on error signaling *Frontiers Hum. Neurosci.* **6** 240
- [41] LOPES DIAS C, SBURLEA A I and MÜLLER-PUTZ G R 2017 Error-related potentials with masked and unmasked onset during continuous control and feedback *7th Graz Brain–Computer Interface Conf.* pp 320–32
- [42] KATO Y, ENDO H and KIZUKA T 2009 Mental fatigue and impaired response processes: event-related brain potentials in a Go/NoGo task *Int. J. Psychophysiol.* **72** 204–11
- [43] BUTTFIELD A, FERREZ P W and MILLÁN J d R 2006 Towards a robust BCI: error potentials and online learning *IEEE Trans. Neural Syst. Rehabil. Eng.* **14** 164–8
- [44] MOUSAVI M, KOERNER A S, ZHANG Q, NOH E and DE SA V R 2017 Improving motor imagery BCI with user response to feedback *Brain–Computer Interfaces* **4** 74–86
- [45] KIM S K and KIRCHNER E A 2016 Handling few training data: classifier transfer between different types of error-related potentials *IEEE Trans. Neural Syst. Rehabil. Eng.* **24** 320–32
- [46] ITURRATE I, CHAVARRIAGA R, MONTESANO L, MINGUEZ J and MILLÁN J d R 2012 Latency correction of error potentials between different experiments reduces calibration time for single-trial classification *Annual Int. Conf. of the IEEE Engineering in Medicine and Biology Society* pp 3288–91
- [47] SPINNATO J, ROUBAUD M-C, BURLE B and TORRÉSANI B 2015 Detecting single-trial EEG evoked potential using a wavelet domain linear mixed model: application to error potentials classification *J. Neural Eng.* **12** 036013
- [48] PINEGGER A and MÜLLER-PUTZ GERNOT R 2017 No training, same performance!? A generic P300 classifier approach *7th Graz Brain–Computer Interface Conf.* pp 420–4

OPEN

# Online asynchronous decoding of error-related potentials during the continuous control of a robot

Catarina Lopes-Dias , Andreea I. Sburlea  & Gernot R. Müller-Putz \*

Error-related potentials (ErrPs) are the neural signature of error processing. Therefore, the detection of ErrPs is an intuitive approach to improve the performance of brain-computer interfaces (BCIs). The incorporation of ErrPs in discrete BCIs is well established but the study of asynchronous detection of ErrPs is still in its early stages. Here we show the feasibility of asynchronously decoding ErrPs in an online scenario. For that, we measured EEG in 15 participants while they controlled a robotic arm towards a target using their right hand. In 30% of the trials, the control of the robotic arm was halted at an unexpected moment (error onset) in order to trigger error-related potentials. When an ErrP was detected after the error onset, participants regained the control of the robot and could finish the trial. Regarding the asynchronous classification in the online scenario, we obtained an average true positive rate (TPR) of 70% and an average true negative rate (TNR) of 86.8%. These results indicate that the online asynchronous decoding of ErrPs was, on average, reliable, showing the feasibility of the asynchronous decoding of ErrPs in an online scenario.

Brain-computer interfaces (BCIs) are systems that measure brain activity, often using electroencephalography (EEG), and convert it into actions of an external device<sup>1</sup>. As BCIs enable communication without movement, they are a valuable tool to provide more independence to people with severe motor disabilities<sup>2–4</sup>.

The main obstacle to the widespread use of BCIs is their non-optimal performance, which sometimes leads to a misinterpretation of the user's intention and a consequent execution of a wrong action. The user's experience with the BCI can be spoiled by occurrence of many mistakes or by the effort to correct them.

The user's awareness of the committed mistake is associated with a neural pattern named error-related potential (ErrP). ErrPs occur both in humans and in monkeys and can be measured using several imaging techniques<sup>5–12</sup>. Additionally, ErrPs morphology is comparable in humans with and without spinal cord injury<sup>13</sup>. ErrPs are related with conflict monitoring<sup>14</sup> and have been reported in association with the awareness of self-committed mistakes, observed mistakes of another person or agent, and BCI's mistakes<sup>14–17</sup>.

The use of ErrPs is an intuitive approach to improve BCIs' performance, either in a corrective manner, by allowing the BCI to take a corrective action, or in an adaptive manner, by reducing the possibility of future errors<sup>18–20</sup>.

The detection of ErrPs in a time-locked manner is well established<sup>21–23</sup>, and it has been extensively applied in discrete BCIs, whose actions occur in a discrete manner, allowing users to interact with a computer or with a robot<sup>24–31</sup>.

Recently, an effort has been made to develop BCIs that provide a more intuitive control to the user, by e.g., providing continuous control to the user<sup>32–34</sup>. In this situation, the user can perceive, at any moment, that an error occurred. This possibility triggered the research on the asynchronous detection of ErrPs<sup>35–39</sup>.

In the current study, we investigate the feasibility of the online asynchronous ErrPs' detection, while participants continuously controlled a robotic arm towards a target, using their right hand. In 30% of the trials, the user's control of the robot was halted at random point. Participants could regain the robot's control if an ErrP was detected after the error onset. To our knowledge, this is the first report of online asynchronous detection of ErrPs.

## Materials and Methods

**Participants.** 15 right-handed volunteers (5 women) participated in the experiment. All participants had normal or corrected-to-normal vision and had no history of brain disorders. The participants were, on average, 23.5 ± 2.5 years old (mean ± std). Participants were paid 7.50 euros per hour, were explained the experimental

Institute of Neural Engineering, Graz University of Technology, Graz, Austria. \*email: [gernot.mueller@tugraz.at](mailto:gernot.mueller@tugraz.at)





**Figure 1.** Experimental setup. In this figure, the robot is at its home position. The squares on the screen represent the physical targets (violet cuboids) on the wooden structure. The rectangle on the bottom part of the screen represents the participant's hand home position and the text above it states 'Bring your hand to the home position.' Inside the wooden structure, there is a Leap Motion device (not visible here) used to track the participants' right hand movement.

protocol and signed an informed consent form that had been previously approved by the local ethics committee of the Medical University of Graz (Ethical approval number 30-275 17/18). The experiment was performed in accordance with the Declaration of Helsinki.

**Hardware and measuring layout.** We recorded EEG and EOG data at a sampling rate of 500 Hz using BrainAmp amplifiers and an ActiCap cap (Brain Products, Munich, Germany). We used 61 EEG electrodes and 3 EOG electrodes. The EOG electrodes were placed above the nasion and below the outer canthi of the eyes. The ground electrode was placed at position AFz and the reference electrode was placed on the right mastoid. The layout of the EEG electrodes is described in Fig. 1 of the Supplementary Material.

**Experiment layout.** Figure 1 depicts the physical layout of the experiment. Participants sat on a chair in front of a table. On the table was a wooden structure: 4-sided box, with open sides towards the participants and the tabletop. On the ceiling of the structure was a Leap Motion device (Leap Motion, San Francisco, United States), used to track the participants' right hand (not visible in Fig. 1). The participants kept their right hand lying on the table, inside the wooden structure. This setup occluded the participants' hand from their field of view. On the right side of the participants, we placed a robotic arm (Jaco Assistive robotic arm - Kinova Robotics, Bonn, Germany). On the wooden structure, were placed two physical targets: violet cuboids with a square base of 14 cm side. The centres of the targets were 35 cm apart and their mid-point was located 30 cm in front of the home position of the robot's hand, as shown in Fig. 1. Behind the structure, within the participant's line of sight to the targets, was a monitor that displayed information regarding the experiment. The participant shown in Fig. 1 gave her informed consent for the photo to be made available in an open-access publication.

**Controlling the robot.** During the *trials*, participants could control the position of the robot's hand on a horizontal plane, by moving their hand on the table, which was tracked with the Leap Motion. To reduce the range of the participants' movements, we considered the robot's hand displacement to be three times larger than the participants' hand displacement.

**Experiment overview.** Before the experiment, two blocks in which participants performed eye movements were recorded. The experiment then consisted of 12 blocks of 30 trials each. 70% of the trials of each block were *correct trials* (21 trials) and the remaining 30% were *error trials* (9 trials).

The sequence of correct and error trials within each block was randomly generated using a uniform distribution to place the error trials. We defined a maximum of 2 consecutive error trials in each block and repeated the randomization procedure until the sequence of trials satisfied this condition.

Half of the trials in each block were associated with the left target and the remaining trials with the right target. The sequence of targets within each block was randomly assigned using a uniform distribution. We defined a maximum of 3 consecutive trials with the same target in each block and repeated the randomization procedure until the targets' sequence satisfied this requirement.

**Pre-trial.** During the pre-trial period, the monitor displayed information regarding the coming trial. As depicted in Figs. 1 and 2, on the top part of the screen were displayed two squares representing the targets lying on the wooden structure. One of the squares was filled in white and the other had no fill. The filled square indicated the selected target for the coming trial. On the bottom part of the screen was a rectangle, representing the home

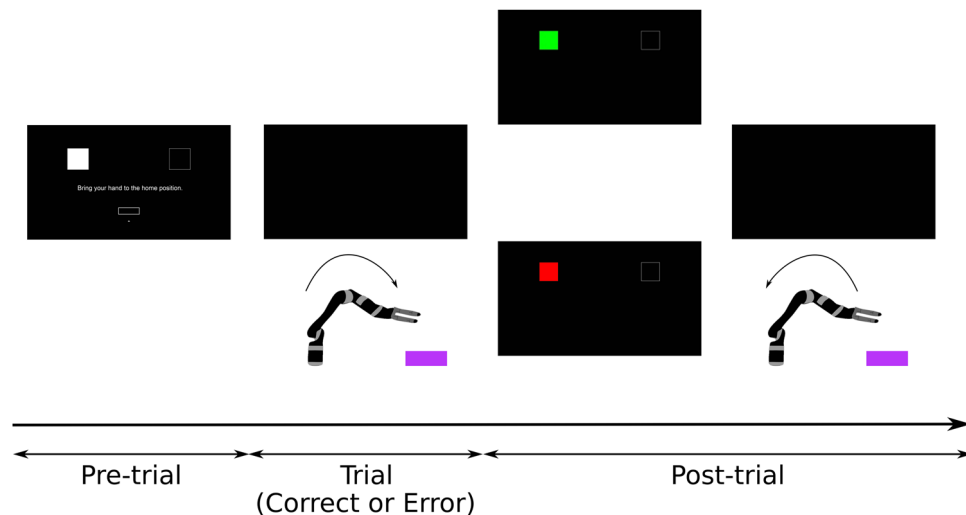


**Figure 2.** Experimental protocol. During the pre-trial period, participants could rest for as long as they wished. The pre-trial period ended and a new trial started when the participants moved their hand to its home position. During the trials, the screen was black. Participants were instructed to bring the robot's hand to the selected target. A trial finished either when the robot reached the target or after 6 seconds, in case target was not reached. Afterwards (post-trial period), the squares reappeared on the screen for 1.2 seconds and gave feedback regarding hitting the target: a green square indicated that the target was hit and a red square indicated that the target was not hit. Then, the screen turned black, the robot automatically returned to its home position and a new pre-trial period started.

position of the participant's hand. The position of the participant's hand was depicted by a dot on the screen. The trial would start when the dot entered the rectangle. This ensured that the participant's hand was at a comparable position at the beginning of each trial (within a  $1 \times 3$  cm rectangle).

Participants could use the pre-trial period to rest for as long as they needed. When participants felt ready to start the trial, they had to bring their hand below the home position, fixate their gaze on the physical target and finally enter the rectangle from below. This final step ensured a forward movement of the robot. Participants were also instructed to keep their gaze fixed at the target during the entire trial duration, in order to prevent eye movements.

**Trials.** The aim of each trial was to bring the robot's hand from its home position to the selected target. During the trials, the screen was black. A trial ended when the robot's hand was above the intended target (hit) or after 6 seconds (no hit). Afterwards (post-trial period), as shown in Fig. 2, the two squares from the pre-trial period reappeared on the screen for 1.2 seconds and the filled square was now coloured in either green (hit) or red (no hit). This feedback was always in line with the behaviour of the robot. Then, the screen would turn black, the robot would automatically return to its home position and a new pre-trial period would start.

**Error Trials.** During these trials, the paradigm triggered an *error*. The error consisted in interrupting the participants' control of the robot and adding a 5 cm upwards displacement to the robot's hand. Participants perceived the error by noticing the robot stopping and lifting. The errors occurred randomly, when the robot's hand was within 6 to 15 cm in the forward direction from its home position. This represents approximately 25 to 65% of the minimal forward displacement necessary for the robot to hit the target. For every error trial, we drew a value  $d_e$  from a uniform distribution  $U([6, 15])$ . The error was triggered when the robot's hand reached the distance  $d_e$  cm, in the forward direction, from its home position.

**Correct Trials.** In these trials, the paradigm did not trigger any error. Participants reached the selected target in  $99.75 \pm 0.14\%$  of the correct trials (mean  $\pm$  std). Correct trials lasted on average  $2.02 \pm 0.14$  s (mean  $\pm$  std). Correct trials were comparable in the *calibration and online parts of the experiment*.

**Calibration and online parts of the experiment.** The *calibration part* of the experiment comprised the first 8 blocks and the *online part* comprised the last 4 blocks. The calibration part was used to collect data to *train an ErrP classifier* and to find a *threshold* for the classifier. In the online part of the experiment, we tested the ErrP classifier, tuned with the calculated threshold, for the asynchronous detection of ErrPs.

For a matter of fluidity of the experiment, we decided not to give participants feedback of the false positive detections, i.e., of the *ErrP detections* when no error had occurred. Thus, from the participants' perspective, the online ErrP classifier had no effect on the correct trials and affected only the error trials. However, false positive detections were taken into account when evaluating the classifier.

**Calibration error trials.** In the error trials during calibration, when the error happened, the participants lost control of the robot, which remained still for the rest of the trial. The total trial duration was 6 seconds. Participants were instructed not to move until the trial ended.

**Online error trials.** In the error trials during the online part of the experiment, the participants had the possibility of correcting the robot's errors. If, after the error onset, an ErrP was detected by the ErrP classifier (true positive detection), the robot's hand lowered 5 cm and the participants regained control of the robot. The downward movement informed the participants of the ErrP detection. Participants were instructed to move the robot's hand to the selected target when regaining control of the robot. To accommodate the extra movement, we added 6 seconds to the maximal trial duration when the first true positive detection occurred. When no true positive detection occurred, the robot remained still, as in the error trials during calibration.

**Correct trials.** For the participants, correct trials were identical in both the calibration and the online parts of the experiment, due to our decision of not giving feedback of the false positive detections in the online part of the experiment.

**Data preprocessing.** Eye movements and blinks were removed from the EEG data, using the data recorded right before the beginning of the experiment and using the subspace subtraction algorithm<sup>40</sup>. The EEG signal was then filtered between [1, 10] Hz using a causal Butterworth filter of order 4.

**Defining events.** For the calibration error trials, we defined the error onset as the moment in which the robot started its upwards displacement. The error onset was individually calculated for every error trial, based on the robot's position. The average delay between the error marker and the error onset was  $0.210 \pm 0.004$  s (mean  $\pm$  std).

For the online error trials, we considered an average error onset, by adding the average delay of the robot, calculated from the calibration data (0.210 s), to the time of the error marker in every error trial. This aimed to compensate the less reliable error onset estimation in case an ErrP occurred between the error marker and the start of the robot's upwards displacement (false positive detection).

Correct trials were not associated with any intrinsic event. Therefore, we defined a virtual onset, occurring one second after the start of every correct trial. The virtual onset was chosen at a time-point in which errors could already occur in the error trials, in order to assure a comparable expectation in the participants.

**Electrophysiological analysis.** For the electrophysiological analysis, we considered an EEG epoch of 1.5 s from every trial. For the correct trials, we considered the interval  $[-0.5, 1.0]$  s, time-locked to the virtual onset (0 s). For the calibration error trials, we considered the interval  $[-0.5, 1.0]$  s, time-locked to the error onset (0 s). For the online error trials, we considered the interval  $[-0.5, 1.0]$  s, time-locked to the average error onset (0 s).

**Detection of error-related potentials.** We used the data from the calibration part of the experiment to build an ErrP classifier that was tested asynchronously in the online part of the experiment.

**Train an ErrP classifier.** For every participant, we considered all trials from the calibration part of the experiment. We took, as features, the amplitudes of all 61 EEG channels at every time-point within a 450 ms window of every trial. The window started 300 ms after the error onset of error trials and 300 ms after the virtual onset of correct trials.

Next, in order to reduce the number of features, we performed principal component analysis (PCA) on the features, keeping the components that explained 99% of the data's variability. These components were then used as features to train a shrinkage-LDA classifier with two classes: error and correct. After PCA we kept, on average,  $139.5 \pm 13.5$  features per participant (mean  $\pm$  std). Figure 2 of the Supplementary Material depicts the grand-average original feature space in the time-spatial domain as well as the grand-average projection into the time-spatial domain of the features kept after PCA.

**ErrP detection.** The classifier was constructed to be evaluated in an asynchronous manner, using a sliding window, with a leap of 18 ms. The classifier's evaluation of each window resulted in the probability of the analysed window to belong to either class (correct or error). We defined an *ErrP detection* when two consecutive windows had a probability of belonging to the error class above a certain threshold  $\tau$ .

**Threshold  $\tau$  for the ErrP classifier.** The threshold  $\tau$  was obtained using the calibration data and used in the online part of the experiment to tune the ErrP classifier.

In order to find the threshold that best suited each participant, we performed a  $2 \times 5$ -fold asynchronous cross-validation in the participant's calibration data, where we tested 41 thresholds: from 0 to 1 in steps of 0.025. We used a low number of repetitions in the cross-validation to promote a shorter duration of the experiment.

As evaluation metric for the asynchronous ErrP detection in the cross-validated data, we defined the true negative trials (TN trials) as the correct trials in which no ErrP was detected during the entire trial duration. We defined the true positive trials (TP trials) as the error trials in which no ErrP was detected before the error onset and at least one ErrP was detected within 1.5 s of the error onset.

Then, we calculated the average true negative rate (TNR) and the average true positive rate (TPR) for all the tested thresholds, based on the 10 iterations. The average TNR and average TPR were further smoothed using a moving average with 7 samples. The smoothed curves were named moving average TPR and moving average TNR.



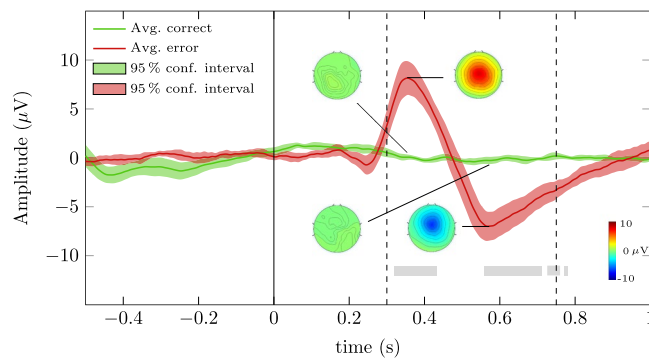


**Figure 3.** Grand average correct and error signals of the calibration part of the experiment at channel FCz (green and red solid lines, respectively). The green and red shaded areas represent the 95% confidence intervals of the grand average signals. The regions in which correct and error signals were significantly different are marked with a grey rectangle (Wilcoxon rank-sum tests, Bonferroni corrected,  $p < 0.01$ ). The vertical line at  $t = 0$  s represents the error onset of error trials and the virtual onset of correct trials. The dashed vertical lines at  $t = 0.30$  s and  $t = 0.75$  s delimit the window used to train the ErrP classifier.

For every participant, we considered the threshold that maximized performance to be the one that maximized the product of the moving average TPR and the moving average TNR. This threshold was then used in the online part of the experiment.

**Online ErrP detection.** The ErrP classifier was tested online in the last 4 blocks of the experiment. We decided to relax the evaluation metrics when testing the classifier online (in comparison with the metrics described for the cross-validated data) in order to consider the possible occurrence of secondary error-related potentials<sup>28</sup>.

In the online evaluation, we defined the true negative trials (TN trials) as the correct trials in which no ErrP was detected (keeping the same definition used in the evaluation of the cross-validated data). Additionally we now defined the true positive trials (TP trials) as the error trials in which no ErrP was detected before the average error onset and at least one ErrP was detected after the average error onset.

A video of the online experiment can be seen in the Supplementary Material. The participant in the video gave her informed consent for it to be made available in an open-access publication.

## Results

**Electrophysiology. Calibration.** Figure 3 depicts the grand average correct and error signals of the calibration part of the experiment at channel FCz (green and red solid lines, respectively). The green and red shaded areas represent the 95% confidence intervals of the grand average signals. The time-intervals in which correct and error signals were significantly different ( $t = [0.320, 0.432]$  s,  $t = [0.558, 0.710]$  s,  $t = [0.726, 0.760]$  s and  $t = [0.770, 0.780]$  s) are represented by grey rectangles (Wilcoxon rank-sum tests, Bonferroni corrected,  $p < 0.01$ ). The vertical line at  $t = 0$  s represents the error onset for the error trials and the virtual onset for the correct trials. The error signal presents a small negativity with peak amplitude  $-0.71 \mu\text{V}$  at 0.246 s, followed by a positivity with peak amplitude of  $8.46 \mu\text{V}$  at 0.354 s, which is followed by a broader negativity with peak amplitude  $-6.98 \mu\text{V}$  at 0.568 s. Figure 3 also depicts the topoplots of correct and error trials at the time-points  $t = 0.354$  s and  $t = 0.568$  s.

**Online part.** Figure 4 depicts the grand average correct and error signals of the online part of the experiment at channel FCz (green and red solid lines, respectively). The green and red shaded areas represent the 95% confidence intervals of the grand average signals. The time-intervals in which correct and error signals were significantly different ( $t = [0.316, 0.390]$  s,  $t = [0.504, 0.606]$  s and  $t = [0.698, 0.710]$  s) are represented by grey shaded areas (Wilcoxon rank-sum tests, Bonferroni corrected,  $p < 0.01$ ). The error signal presents a small negativity with peak amplitude  $-1.29 \mu\text{V}$  at 0.246 s, followed by a positivity with peak amplitude  $10.7 \mu\text{V}$  at 0.342 s and by a broader negativity with peak amplitude  $-8.63 \mu\text{V}$  at 0.532 s. Figure 4 also depicts the topoplots of correct and error trials at the time-points  $t = 0.342$  s and  $t = 0.532$  s.

**Asynchronous ErrP detection. Offline asynchronous ErrP detection in the calibration data.** During the experiment, we performed asynchronous ErrP detection in the calibration data to find the threshold  $\tau$  that was used online (using a  $2 \times 5$ -fold cross-validation to reduce the experiment duration, as described in section *Threshold  $\tau$  for the ErrP classifier*).

For visualization purposes, here we present the asynchronous ErrP detection results, obtained using a  $10 \times 5$ -fold cross-validation in the calibration data, in which we tested 41 thresholds  $\tau$  from 0 to 1, with steps of 0.025. The evaluation metric used to assess the results was the same as described in section *Threshold  $\tau$  for the ErrP classifier*. Figure 5 displays the grand average TPR and TNR of the asynchronous classification performed using a  $10 \times 5$ -fold cross-validation in the calibration data (red and green solid lines, respectively), in function of the threshold  $\tau$ . The chance-level TPR and TNR (red and green dashed lines, respectively) were obtained by performing the same classification procedure with randomly permuted training labels. The shaded green and red

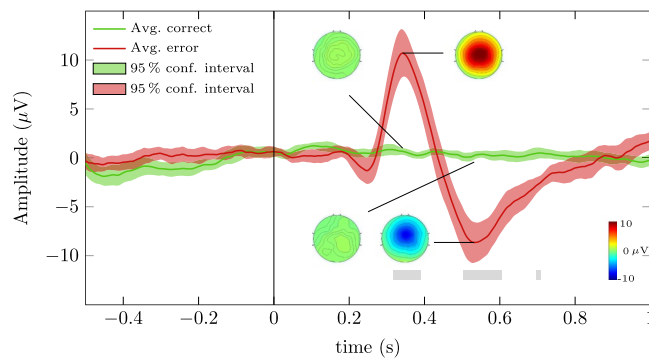


**Figure 4.** Grand average correct and error signals of the online part of the experiment at channel FCz (green and red solid lines, respectively). The green and red shaded areas represent the 95% confidence interval for the grand average signals. The grey rectangles represent the time-intervals in which correct and error signals were significantly different (Wilcoxon rank-sum tests, Bonferroni corrected,  $p < 0.01$ ). The vertical line represents the average error onset of the error trials and the virtual onset of the correct trials.

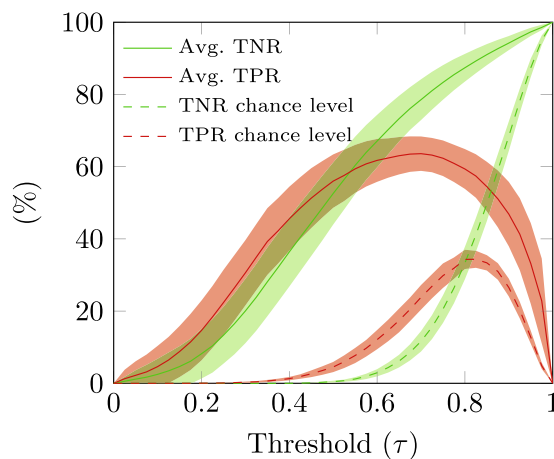


**Figure 5.** Asynchronous ErrP detection in the calibration data. Grand average TNR and TPR (solid green and red lines, respectively) in function of the threshold  $\tau$ , calculated from the  $10 \times 5$ -fold cross-validation in the calibration data. The chance-level TPR and TNR are represented with red and green dashed lines. The shaded areas represent the 95% confidence intervals for the grand average curves.

areas represent the 95% confidence intervals of the grand average curves. The obtained TPR results were significantly higher than chance levels TPR results for thresholds  $\tau \in [0.100, 0.975]$  (Wilcoxon rank-sum tests, one sided, Bonferroni corrected,  $p < 0.01$ ). The obtained TNR results were significantly higher than chance level TNR results for thresholds  $\tau \in [0.150, 0.975]$  (Wilcoxon rank-sum tests, one sided, Bonferroni corrected,  $p < 0.01$ ).

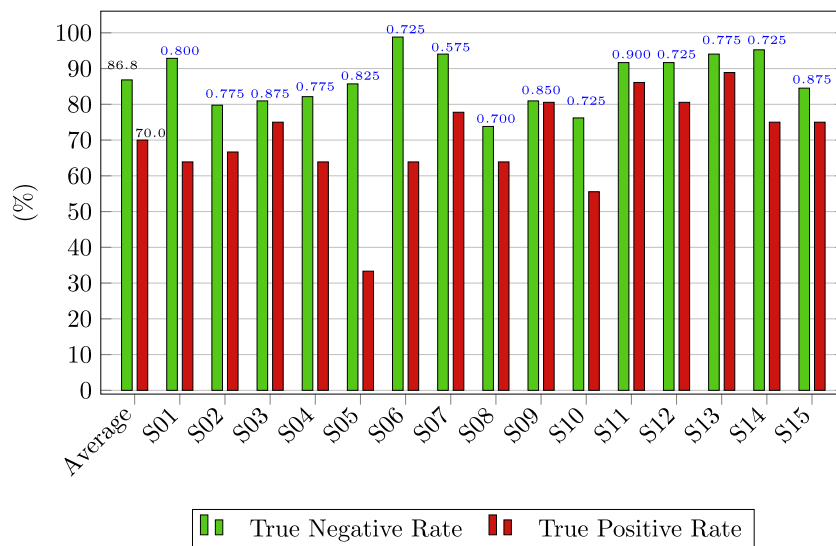
**Online asynchronous ErrP detection.** In the online part of the experiment, we used for the asynchronous ErrP detection, a subject specific-threshold  $\tau$ , calculated as described in section *Threshold  $\tau$  for the ErrP classifier*. The evaluation metric used to assess the results was described in section *Online ErrP detection*. Figure 6 depicts the TPR and TNR of the online asynchronous ErrP classification for every participant as well as the average results. We obtained an average TPR of 70.0% and average TNR of 86.8%. The blue numbers on top of the bars indicate the used threshold  $\tau$  used for every participant.

Figure 7 depicts, for every participant, a violin plot of the time-points of all the ErrP detections in the error trials of the online part of the experiment, in relation to the average error onset ( $t = 0$  s).

## Discussion

In the described experiment, we asynchronously decoded ErrPs in an online scenario. Here, we showed the ErrPs' electrophysiology during the calibration and the online parts of the experiment. In both conditions, ErrP displayed similar shapes but the grand average ErrP in the online condition exhibited stronger peak amplitudes.

We chose to display, in both conditions, the ErrPs' electrophysiology using EEG signals filtered with a causal filter in order to match the ErrPs' appearance in the online scenario. The displayed results differ from standard



**Figure 6.** Online asynchronous ErrP detection. The green bars represent the TNR of every participant and their average. The red bars represent the TPR of every participant and their average. The average TPR was 70.0% and the average TNR was 86.8%. The blue numbers indicate the threshold  $\tau$ , used for each participant.

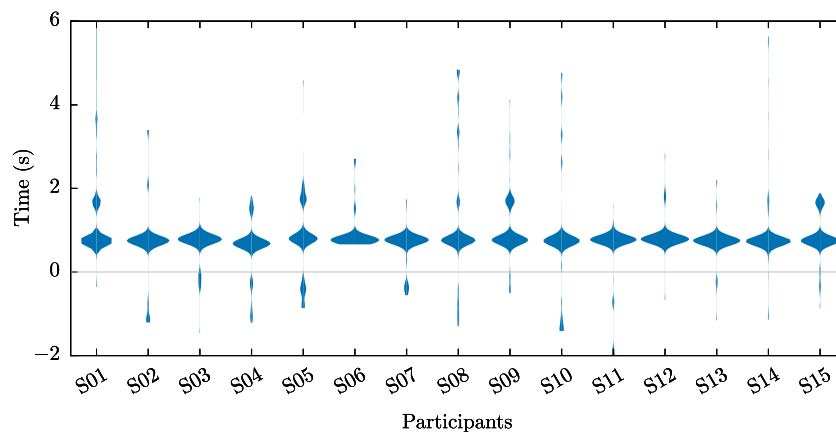


**Figure 7.** Time-points of all ErrP detections in the online scenario. Violin plots, for every participant, of the time-points of all ErrPs detections in the error trials of the online part of the experiment, in relation to the average error onset ( $t = 0$ s).

state-of-the-art literature, in which it is commonly used a zero-phase filter. In our situation, the typical N200 component of ErrPs is shifted to after the ErrPs' P300 component. The difference is a direct consequence of using a causal filter and does not reflect any particularity of the neural activity.

We also showed results regarding the asynchronous ErrP detection in the calibration data using cross-validation, where different thresholds for the ErrP classifier, ranging from 0 to 1, could be tested.

Finally, we displayed the results of the asynchronous ErrP detection for the online part of the experiment, in which we obtained an average TNR of 86.8% of and an average TPR of 70%. In the online part of the experiment, all participants displayed a major cluster of ErrP detections within one second of the error onset, as shown in Fig. 7. Some participants displayed a secondary cluster of ErrP detections, which can possibly be associated with secondary ErrPs, as described by Salazar-Gomez and colleagues<sup>28</sup>. Alternatively, these later detections could also be possibly linked to an event-related potential associated with the robot resuming its movement (that the classifier erroneously classified as an ErrP).

We decided not to give participants feedback regarding false positive detections, neither in correct nor in error trials, to maintain the flow of the experiment and avoid interruptions. Still, from Figs. 6 and 7, we can infer that the majority of ErrP detections were not associated with false positive detections.

Literature supports that, in general, feedback improves BCIs performance and several feedback modalities have been tested<sup>41–45</sup>. But, to the best of our knowledge, the effect of ErrPs' feedback has not been studied yet. Nevertheless, we believe it can help participants to be more engaged and could possibly be associated with the increase in the peak amplitudes of the ErrP verified in the online scenario. Moreover, we believe that providing

feedback of the false positive detections could help participants to understand if they have any control over these detections and, if so, adapt their behaviour accordingly.

Therefore, we conclude that the asynchronous decoding of ErrPs in an online scenario is possible and reliable and we suggest that giving participants full feedback of the ErrP detections would not decrease and would possibly increase participants' performance.

### Data availability

The datasets generated during and/or analysed during the current study are available from the corresponding author on reasonable request.

Received: 24 May 2019; Accepted: 8 November 2019;

Published online: 26 November 2019

### References

- Brunner, C. *et al.* BNCI Horizon 2020: towards a roadmap for the BCI community. *Brain-Computer Interfaces* **2**, 1–10, <https://doi.org/10.1080/2326263X.2015.1008956> (2015).
- Wolpaw, J. R., Birbaumer, N., McFarland, D. J., Pfurtscheller, G. & Vaughan, T. M. Brain-computer interfaces for communication and control. *Clinical Neurophysiology* **113**, 767–791, <http://www.sciencedirect.com/science/article/pii/S1388245702000573> (2002).
- Millán, J. D. R. *et al.* Combining brain-computer interfaces and assistive technologies: State-of-the-art and challenges. *Frontiers in Neuroscience* **4**, 161, <https://doi.org/10.3389/fnins.2010.00161> (2010).
- Müller-Putz, G. R. *et al.* Towards noninvasive hybrid brain-computer interfaces: Framework, practice, clinical application, and beyond. *Proceedings of the IEEE* **103**, 926–943 (2015).
- Gehring, W. J., Goss, B., Coles, M. G., Meyer, D. E. & Donchin, E. A neural system for error detection and compensation. *Psychological Science* **4**, 385–390 (1993).
- Falkenstein, M., Hohnsbein, J., Hoormann, J. & Blanke, L. Effects of errors in choice reaction tasks on the ERP under focused and divided attention. *Psychophysiological Brain Research* 192–195 (1990).
- Falkenstein, M., Hohnsbein, J., Hoormann, J. & Blanke, L. Effects of crossmodal divided attention on late ERP components. 2. error processing in choice reaction tasks. *Electroencephalography and Clinical Neuro-physiology* **78**, 447–455 (1991).
- Mathalon, D. H., Whitfield, S. L. & Ford, J. M. Anatomy of an error: ERP and fMRI. *Biological Psychology* **64**, 119–141, <http://www.sciencedirect.com/science/article/pii/S0301051103001054>, Information Processing and Error Analysis: Retrospectives on a Career (2003).
- Godlove, D. C. *et al.* Event-related potentials elicited by errors during the stop-signal task. i. macaque monkeys. *Journal of Neuroscience* **31**, 15640–15649, <http://www.jneurosci.org/content/31/44/15640> (2011).
- Milekovic, T., Ball, T., Schulze-Bonhage, A., Aertsen, A. & Mehring, C. Error-related electrocorticographic activity in humans during continuous movements. *Journal of Neural Engineering* **9**, 026007, <http://stacks.iop.org/1741-2552/9/i=2/a=026007> (2012).
- Milekovic, T., Ball, T., Schulze-Bonhage, A., Aertsen, A. & Mehring, C. Detection of error related neuronal responses recorded by electrocorticography in humans during continuous movements. *PLoS One* **8**, 1–20, <https://doi.org/10.1371/journal.pone.0055235> (2013).
- Völker, M. *et al.* Intracranial error detection via deep learning. In *2018 IEEE International Conference on Systems, Man, and Cybernetics (SMC)*, 568–575 (2018).
- Keyl, P. *et al.* Differences in characteristics of error-related potentials between individuals with spinal cord injury and age- and sex-matched able-bodied controls. *Frontiers in Neurology* **9**, 1192, <https://doi.org/10.3389/fneur.2018.01192> (2019).
- Yeung, N., Botvinick, M. & Cohen, J. The neural basis of error detection: Conflict monitoring and the error-related negativity. *Psychological review* **111**, 931–959 (2004).
- Schalk, G., Wolpaw, J. R., McFarland, D. J. & Pfurtscheller, G. EEG-based communication: presence of an error potential. *Clinical Neurophysiology* **111**, 2138–2144, <http://www.sciencedirect.com/science/article/pii/S1388245700004570> (2000).
- Ferrez, P. W. & Millán, J. d. R. You are wrong!: Automatic detection of interaction errors from brain waves. In *Proceedings of the 19th International Joint Conference on Artificial Intelligence, IJCAI'05*, 1413–1418, <http://dl.acm.org/citation.cfm?id=1642293.1642517> (2005).
- van Schie, H. T., Mars, R. B., Coles, M. G. H. & Bekkering, H. Modulation of activity in medial frontal and motor cortices during error observation. *Nature Neuroscience* **7**, 549–554 (2004).
- Artusi, X., Niazi, I. K., Lucas, M.-F. & Farina, D. Accuracy of a BCI based on movement-related and error potentials. In *2011 Annual International Conference of the IEEE Engineering in Medicine and Biology Society*, 3688–3691 (2011).
- Llera, A., van Gerven, M. A., Gómez, V., Jensen, O. & Kappen, H. J. On the use of interaction error potentials for adaptive brain computer interfaces. *Neural Networks* **24**, 1120–1127 (2011).
- Chavarriaga, R., Sobolewski, A. & Millán, J. D. R. Errare machinale est: the use of error-related potentials in brain-machine interfaces. *Frontiers in Neuroscience* **8**, 208, <https://doi.org/10.3389/fnins.2014.00208> (2014).
- Kim, S.-K. & Kirchner, E. A. Handling few training data: classifier transfer between different types of error-related potentials. *IEEE Transactions on Neural Systems and Rehabilitation Engineering* **24**, 320–332 (2016).
- Iturrate, I., Montesano, L. & Minguez, J. Single trial recognition of error-related potentials during observation of robot operation. In *2010 Annual International Conference of the IEEE Engineering in Medicine and Biology Society*, 4181–4184 (2010).
- Zhang, H. *et al.* EEG-based decoding of error-related brain activity in a real-world driving task. *Journal of Neural Engineering* **12**, 066028 (2015).
- Ferrez, P. W. & Millán, J. D. R. Simultaneous real-time detection of motor imagery and error-related potentials for improved BCI accuracy. In *Proceedings of the 4th International Brain-Computer Interface Workshop and Training Course*, 197–202 (2008).
- Chavarriaga, R. & Millán, J. D. R. Learning from EEG error-related potentials in noninvasive brain-computer interfaces. *IEEE Transactions on Neural Systems and Rehabilitation Engineering* **18**, 381–388 (2010).
- Kreiling, A., Neuper, C. & Müller-Putz, G. R. Error potential detection during continuous movement of an artificial arm controlled by brain-computer interface. *Medical & Biological Engineering & Computing* **50**, 223–230 (2012).
- Kreiling, A., Hiebel, H. & Müller-Putz, G. R. Single versus multiple events error potential detection in a BCI-controlled car game with continuous and discrete feedback. *IEEE Transactions on Biomedical Engineering* **63**, 519–529 (2016).
- Salazar-Gomez, A. F., DelPreto, J., Gil, S., Guenther, F. H. & Rus, D. Correcting robot mistakes in real time using EEG signals. *2017 IEEE International Conference on Robotics and Automation (ICRA)* 6570–6577 (2017).
- Kim, S.-K., Kirchner, E. A., Stefes, A. & Kirchner, F. Intrinsic interactive reinforcement learning - using error-related potentials for real world human-robot interaction. *Scientific Reports (Sci Rep)* **7**, 17562 (2017).
- Ehrlich, S. K. & Cheng, G. Human-agent co-adaptation using error-related potentials. *Journal of Neural Engineering* **15**, 066014, [10.1088/1741-2552/15/2/F066014](https://doi.org/10.1088/1741-2552/15/2/F066014) (2018).
- Ehrlich, S. K. & Cheng, G. A feasibility study for validating robot actions using eeg-based error-related potentials. *International Journal of Social Robotics*, <https://doi.org/10.1007/s12369-018-0501-8> (2018).

32. Millán, J. R. & Mourinho, J. Asynchronous BCI and local neural classifiers: an overview of the adaptive brain interface project. *IEEE Transactions on Neural Systems and Rehabilitation Engineering* **11**, 159–161 (2003).
33. Townsend, G., Graimann, B. & Pfurtscheller, G. Continuous EEG classification during motor imagery—simulation of an asynchronous BCI. *IEEE Transactions on Neural Systems and Rehabilitation Engineering* **12**, 258–265 (2004).
34. Nooh, A. A., Yunus, J. & Daud, S. M. A review of asynchronous electroencephalogram-based brain computer interface systems. In *International Conference on Biomedical Engineering and Technology* (2011).
35. Spüler, M. & Niethammer, C. Error-related potentials during continuous feedback: using EEG to detect errors of different type and severity. *Frontiers in human neuroscience* **9** (2015).
36. Omedes, J., Iturrate, I., Minguez, J. & Montesano, L. Analysis and asynchronous detection of gradually unfolding errors during monitoring tasks. *Journal of Neural Engineering* **12**, 056001 (2015).
37. Omedes, J., Iturrate, I., Chavarriaga, R. & Montesano, L. Asynchronous decoding of error potentials during the monitoring of a reaching task. In *2015 IEEE International Conference on Systems, Man, and Cybernetics*, 3116–3121 (2015).
38. Lopes-Dias, C., Sburlea, A. I. & Müller-Putz, G. R. Error-related potentials with masked and unmasked onset during continuous control and feedback. In *7th Graz Brain-Computer Interface Conference 2017*, 320–332 (2017).
39. Lopes-Dias, C., Sburlea, A. I. & Müller-Putz, G. R. Masked and unmasked error-related potentials during continuous control and feedback. *Journal of Neural Engineering* **15**, 036031, [10.1088/1741-2552/15/3/036031](https://doi.org/10.1088/1741-2552/15/3/036031) (2018).
40. Kobler, R. J., Sburlea, A. I. & Müller-Putz, G. R. A comparison of ocular artifact removal methods for block design based electroencephalography experiments. In *Proceedings of the 7th Graz Brain-Computer Interface Conference 2017* (2017).
41. Darvishi, S., Ridding, M. C., Abbott, D. & Baumert, M. Does feedback modality affect performance of brain computer interfaces? In *2015 7th International IEEE/EMBS Conference on Neural Engineering (NER)*, 232–235 (2015).
42. Kauhanen, L. *et al.* Haptic feedback compared with visual feedback for BCI. In *Proceedings of the 3rd International Brain-Computer Interface Workshop and Training Course* (2006).
43. Ramos, A., Halder, S. & Birbaumer, N. Proprioceptive feedback in BCI. In *2009 4th International IEEE/EMBS Conference on Neural Engineering*, 279–282 (2009).
44. Alimardani, M., Nishio, S. & Ishiguro, H. Effect of biased feedback on motor imagery learning in BCI-teleoperation system. *Frontiers in Systems Neuroscience* **8**, 52, <https://doi.org/10.3389/fnsys.2014.00052> (2014).
45. Barbero, A. & Grosse-Wentrup, M. Biased feedback in brain-computer interfaces. *Journal of NeuroEngineering and Rehabilitation* **7**, 34, <https://doi.org/10.1186/1743-0003-7-34> (2010).

### Acknowledgements

The authors would like to acknowledge Reinmar J. Kobler and Valeria Mondini for the fruitful discussions during the preparation of the experiment and to Lea Hehenberger and Marcel Zube for the help during the measurements. This work was supported by Horizon 2020 ERC Consolidator Grant 681231 ‘Feel Your Reach’.

### Author contributions

C.L.D., A.I.S. and G.R.M.P. conceived the study. C.L.D. implemented the paradigm and performed the acquisition. C.L.D. conducted the analysis. C.L.D., A.I.S. and G.R.M.P. interpreted the data. C.L.D. created the figures and the video. C.L.D. wrote the draft of the manuscript. C.L.D., A.I.S. and G.R.M.P. edited the manuscript.

### Competing interests

The authors declare no competing interests.

### Additional information

**Supplementary information** is available for this paper at <https://doi.org/10.1038/s41598-019-54109-x>.

**Correspondence** and requests for materials should be addressed to G.R.M.-P.

**Reprints and permissions information** is available at [www.nature.com/reprints](http://www.nature.com/reprints).

**Publisher’s note** Springer Nature remains neutral with regard to jurisdictional claims in published maps and institutional affiliations.



**Open Access** This article is licensed under a Creative Commons Attribution 4.0 International License, which permits use, sharing, adaptation, distribution and reproduction in any medium or format, as long as you give appropriate credit to the original author(s) and the source, provide a link to the Creative Commons license, and indicate if changes were made. The images or other third party material in this article are included in the article’s Creative Commons license, unless indicated otherwise in a credit line to the material. If material is not included in the article’s Creative Commons license and your intended use is not permitted by statutory regulation or exceeds the permitted use, you will need to obtain permission directly from the copyright holder. To view a copy of this license, visit <http://creativecommons.org/licenses/by/4.0/>.

© The Author(s) 2019

# ONLINE ASYNCHRONOUS DECODING OF ERROR-RELATED POTENTIALS DURING THE CONTINUOUS CONTROL OF A ROBOT

CATARINA LOPES-DIAS, ANDREEA I SBURLEA AND GERNOT R  
MÜLLER-PUTZ

Figure 1 shows the location of the 61 EEG electrodes used in the experiment.

Figure 2 shows that, in the classification procedure, the principal components retained after PCA preserve the activity of the original feature space.

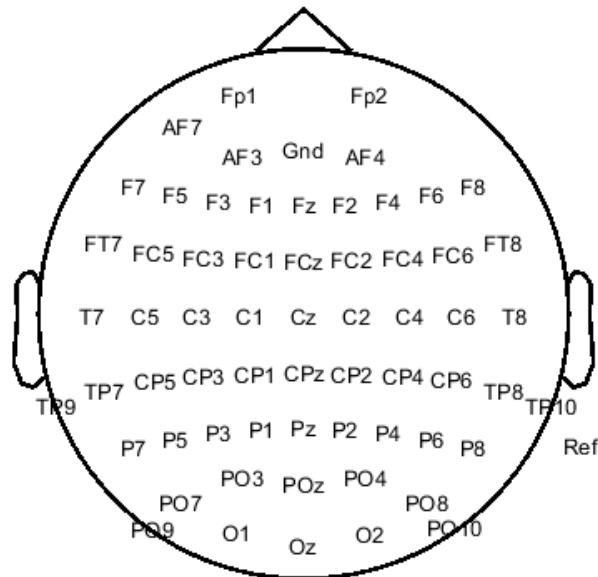


FIGURE 1. Layout of the EEG electrodes. The ground electrode was placed at position AFz and the reference electrode was placed on the right mastoid.

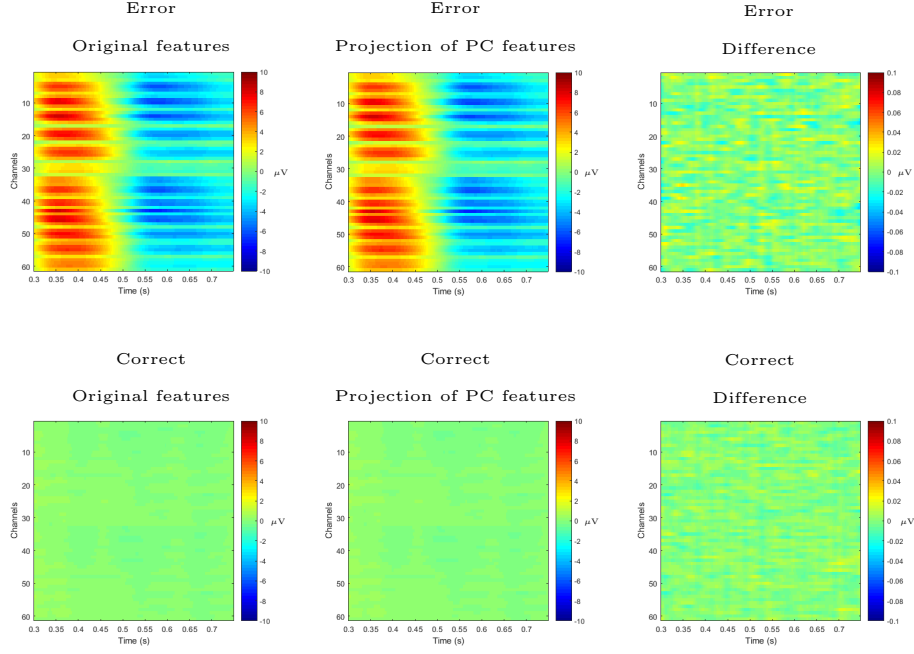


FIGURE 2. Grand average classifier features: Left: Grand-average original feature space. Middle: Grand-average projection into the temporal-spatial domain of the principal component (PC) features retained after PCA. Right: Difference between the grand-average original feature space and the grand-average projection of the features retained after PCA. The channel order is the following: 1-Fp1, 2-Fp2, 3-F7, 4-F3, 5-Fz, 6-F4, 7-F8, 8-FC5, 9-FC1, 10-FC2, 11-FC6, 12-T7, 13-C3, 14-Cz, 15-C4, 16-T8, 17-TP9, 18-CP5, 19-CP1, 20-CP2, 21-CP6, 22-TP10, 23-P7, 24-P3, 25-Pz, 26-P4, 27-P8, 28-P09, 29-O1, 30-Oz, 31-O2, 32-PO10, 33-AF3, 34-AF4, 35-F5, 36-F1, 37-F2, 38-F6, 39-FT7, 40-FC3, 41-FC4, 42-FT8, 43-FCz, 44-C5, 45-C1, 46-C2, 47-C6, 48-TP7, 49-CP3, 50-CPz, 51-CP4, 52-TP8, 53-P5, 54-P1, 55-P2, 56-P6, 57-PO7, 58-PO3, 59-POz, 60-PO4, 61-PO8.



# ASYNCHRONOUS DETECTION OF ERROR-RELATED POTENTIALS USING A GENERIC CLASSIFIER

C Lopes-Dias<sup>1</sup>, A I Sburlea<sup>1</sup>, G R Müller-Putz<sup>1</sup>

<sup>1</sup>Institute of Neural Engineering, Graz University of Technology, Graz, Austria

E-mail: gernot.mueller@tugraz.at

**ABSTRACT:** Error-related potentials (ErrPs) can be used to improve BCIs' performance but its use is often withheld by long calibration periods. We recorded EEG data of 15 participants while controlling a robotic arm towards a target. In 30 % of the trials, the protocol prompted an error during the trial in order to trigger ErrPs in the participants. For each participant, we trained an ErrP classifier using the data of the remaining 14 participants. Each of these classifiers was tested asynchronously on the data of the selected participant. The threshold that maximized the product of the average true positive rate (TPR) and the average true negative rate (TNR) was  $\tau = 0.7$ . For this threshold, the average TPR was 53.6 % and the average TNR was 82.0 %. These results hint at the feasibility of transferring ErrPs between participants as a reliable strategy to reduce or even remove the calibration period when training ErrP classifiers to be used in an asynchronous manner.

## INTRODUCTION

Brain-computer interfaces (BCIs) are a suitable tool to help restoring some autonomy to people with severe motor disabilities [1,2,3]. Most BCIs rely on converting modulated brain activity of a user (often measured using electroencephalography (EEG)) into commands of an external device, such as a robot. Nevertheless, the performance of most BCIs is not optimal and, occasionally, the interface misinterprets the intention of its user and thus a wrong command is executed. The user's awareness of the committed mistake is associated with a neural pattern named error-related (ErrP), which is also measurable by EEG [4].

Incorporating ErrPs' detection in a BCI can help to improve its performance [5, 6]. A main barrier to its widespread use is the calibration time necessary to train ErrP classifiers: many trials are needed to train a classifier and errors should not occur too often to still be perceived as so. Two main approaches have been proposed to reduce the training duration of ErrP classifiers, based on either transferring information between different tasks or transferring information between different participants. Iturrate and colleagues studied the use of classifiers trained with ErrPs from one observation task and tested in ErrPs from another observation task, using latency correction [7,8]. Kim and colleagues studied the

use of an ErrP classifier trained with ErrPs from an observation task and tested with ErrPs from an interaction task (and vice-versa) [9,10]. Nevertheless, Ehrlich and colleagues, did not recommend re-using ErrP classifiers across different experimental tasks [11]. Kim and colleagues also studied the use of an ErrP classifier trained with ErrPs from several subjects and tested in ErrPs from another subject [9]. These studies suggest that transferability of ErrPs is viable in the context of discrete BCIs (in which all events occur in a discrete way).

Recently, an effort has been made to develop BCI paradigms that promote a smoother and more intuitive interaction with their users, by relying on continuous control or actions - continuous BCIs [12,13,14]. In this context, the user's error awareness can occur at any moment and is not, necessarily, time-locked to specific events, requiring an asynchronous detection of ErrPs. The existence of ErrPs in continuous contexts as well as its asynchronous detection has been established [15, 16, 17,18]. Another approach to improve BCIs consists in developing BCIs that closer resemble end-user applications, in which users interact with or observe robots [10,19,20,21,22].

In this work, we developed a paradigm in which the user has continuous control over a robotic arm in a task in which errors are triggered by the paradigm. We studied the electrophysiological signature of the ErrPs in this task and, additionally, investigated the feasibility of using a generic ErrP classifier trained on the ErrPs of 14 participants by testing it asynchronously with data of another participant.

## MATERIALS AND METHODS

*EEG recording:* We recorded EEG and EOG data at a sampling frequency of 500 Hz, using BrainAmp amplifiers (Brain Products, Munich, Germany). We used 61 EEG electrodes and 3 EOG electrodes. The EEG electrodes were placed at positions Fp1, Fp2, AF3, AF4, F7, F5, F3, F1, Fz, F2, F4, F6, F8, FT7, FC5, FC3, FC1, FCz, FC4, FC6, FT8, T7, C5, C3, C1, Cz, C2, C4, C6, T8, TP9, TP7, CP5, CP3, CP1, CPz, CP2, CP4, CP6, TP8, TP10, P7, P5, P3, P1, Pz, P2, P4, P6, P8, PO9, PO7, PO3, POz, PO4, PO8, PO10, O1, Oz, and O2. The ground electrode was placed at position AFz and the reference electrode was placed on the right mastoid. The electrodes were placed above the nasion and below the



outer canthi of the eyes.

**Participants:** We recorded 15 right-handed healthy volunteers (5 female). The participants were, on average,  $23.4 \pm 2.5$  years old (mean  $\pm$  std). Participants were paid 7.50 € per hour and, before the experiment, read and signed an informed consent form that was previously accepted by the local ethical committee.

**Experiment layout:** Figure 1 depicts the layout of the experiment. Participants sat in front of a table, with their right hand lying flat on the table, covered by a wooden structure. On the ceiling of this structure was a Leap Motion device that tracked their right hand movements (Leap Motion, San Francisco, USA). On the right of the participants was a robotic arm (Jaco Assistive robotic arm - Kinova Robotics, Bonn, Germany). On top of the wooden structure were two violet boxes representing the physical targets, centred in relation to the home position of the robot's hand. Behind the wooden structure was a monitor that displayed information regarding the experiment. During the trials, the participants could control the position of the robot's hand on an approximately horizontal plan, by moving their right hand on the table. We considered robot's hand displacement to be three times bigger than the participants' hand displacement, to reduce the range of the participants' movements.

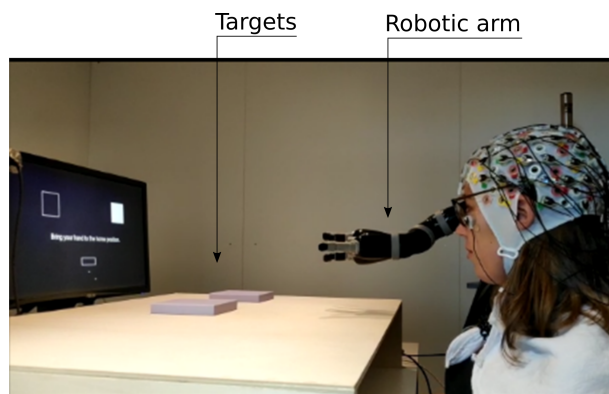


Figure 1: Experimental setup during the pre-trial period. In this image, the robot is at its home position. The squares on the screen indicate that, in the next trial, the participant should move the robot's hand towards the right target (purple box) on the wooden structure. The screen also shows the home position for the participant's hand (rectangle on the bottom part of the screen). The text on the screen (not readable in the picture) states 'Bring your hand to the home position'.

**Experiment overview:** The experiment consisted of 8 blocks of 30 trials each. Each block contained 21 correct trials and 9 error trials (70% and 30%, respectively). The position of the error trials within the block was randomly generated, using a uniform distribution.

**Pre-trial period:** During this period, on the upper part of the screen were displayed two squares, representing the two targets on the wooden structure. One of the squares was filled in white, representing the selected target for the next trial, and the other had no fill. On the bottom part of the screen was a rectangle representing

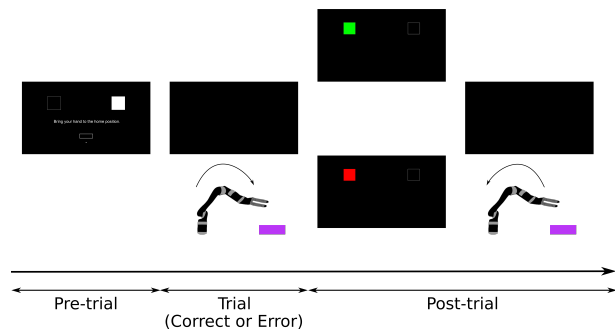


Figure 2: Experimental protocol. During the pre-trial period, the participants can rest for as long as they wish. The pre-trial period ends and a trial starts, when the participant brings his/her right hand to its home position (the bottom rectangle). During the trials, the screen is black. The participants were instructed to bring the robot's hand to the selected target (indicated by the white square). A trial finishes either when the robot reaches the target or after 6 seconds (if the target was not reached). Afterwards (post-trial), the squares reappear on the screen for 1.5 seconds and give feedback regarding hitting the target (a green square indicates that the target was hit and a red square indicates that the target was not hit). Then the screen turns black and the robot automatically returns to its home position and a new pre-trial period starts.

the home position for the participants' hand. The participants' hand was represented by a dot on the screen. A new trial started when the participants' hand entered its home position. The participants could use the pre-trial period to rest for as long as they needed. Participants were instructed to bring their hand to below the home position, to fixate their gaze on the selected physical target and to enter the home position when they felt ready to start a new trial. Participants were also instructed not to move their gaze during the entire trial duration, in order to minimize eye movements.

**Trials:** The aim of each trial was to move the robot's hand to the selected target. During the trials, the screen was black. A trial finished when the robot's hand was above the target (hit) or after 6 seconds (no hit). Afterwards, as shown in Figure 2, the two squares from the pre-trial period reappeared on the screen for 1.5 seconds and the previously filled square was now filled in either green (hit) or red (no hit). Then, the screen would turn black, the robot's hand would automatically move to its home position and a new pre-trial period would start.

**Error trials:** In these trials, the paradigm triggered an error during the trial. The error consisted on halting the participant's control of the robot and adding a 5 cm upwards displacement to the robot's hand. The errors occurred randomly when the robot's hand was within 25% to 65% of the minimal forward displacement necessary for the robot to hit the target. Participants perceived the error by noticing the robot stopping and lifting. After the error happened, the participants could not control the robot until the trial ended. Participants were instructed to remain still. The error trials lasted 6 seconds.

**Correct trials:** In these trials, no error was triggered by the paradigm. The participants reached the selected target

in  $99.7 \pm 0.5\%$  (mean  $\pm$  std) of the correct trials. Correct trials lasted, on average,  $2.06 \pm 0.17$  seconds (mean  $\pm$  std).

*Preprocessing the data:* The eye movements and blinks were removed from the EEG data, using the artefact subspace subtraction algorithm [23]. The EEG data was then filtered between 1 and 10 Hz with a Butterworth causal filter of order 4.

*Electrophysiological analysis:* For the electrophysiological analysis, we cut the EEG data in 1.5 s epochs. For the error trials, we considered the interval  $[-0.5, 1]$  s time-locked to the error onset (0 s). Since correct trials have no intrinsic onset, we defined a virtual onset, occurring one second after the start of the trial (at a time-point in which errors could already occur). For the correct trials we considered the interval  $[-0.5, 1]$  s, time-locked to the virtual onset (0 s).

*Asynchronous ErrP classification with a generic classifier:* For every participant we trained an ErrP classifier with two classes (correct and error) using the data from the remaining 14 participants. In order to train each of these classifiers, we considered as features for the error class the amplitudes of all EEG channels at all time points within the window  $[0.30, 0.75]$  s after the error onset. Similarly, we considered as features for the correct class the amplitudes of all EEG channels at all time points within the window  $[0.30, 0.75]$  s after the virtual onset. Afterwards, in order to reduce the number of features, we applied principal component analysis (PCA) to the feature matrix and kept the components that preserved 99 % of the data variance. These components were used to train a shrinkage LDA classifier [24]. Each of these classifiers was tested asynchronously in the data of the participant not used for training. For that, we slid a 450 ms window through the trials, obtaining an output from the classifier every 18 ms.

For every fixed threshold  $\tau$  ( $\tau$  from 0 to 1 in steps of 0.025), we considered an *error detection* when the classifier's probability for the error class ( $p_e$ ) was greater or equal to the threshold  $\tau$  for two consecutive windows ( $p_e \geq \tau$ ). As an evaluation metric for the asynchronous classification, we defined as true negative trials (TN trials) the correct trials in which no error detection occurred. We defined as true positive trials (TP trials), the error trials in which no error detection occurred before the error onset and at least one error detection occurred within 1.5 seconds after the error onset. We considered the group performance to be optimal for the threshold that maximized the product of the average TPR and the average TNR.

## RESULTS

Figure 3 displays the grand average correct and error signals at channel FCz (green and red solid lines respectively). The 95 % confidence interval for the average curves are represented by the shaded green and red areas. The time-regions in which correct and error signals were

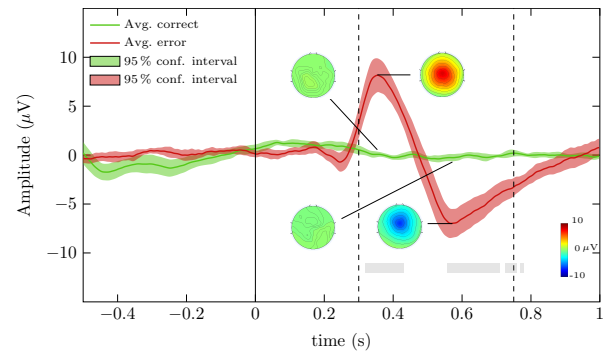


Figure 3: Grand average correct and error signal at channel FCz (green and red solid lines, respectively). The shaded areas represent the 95 % confidence interval for the average signals. The grey regions represent the time-regions in which correct and error signals were significantly different (Wilcoxon signed-rank tests,  $p < 0.01$ , Bonferroni corrected). The topoplots for the correct and error grand average signals are displayed for  $t = 0.354$  s and  $t = 0.568$  s. The time point  $t = 0$  represents the error onset of error trials and the virtual onset of correct trials

significantly different are represented by grey shaded areas (Wilcoxon signed-rank tests,  $p < 0.01$ , Bonferroni corrected). Figure 3 displays also the topoplots for the correct and error grand average signals at the peaks of the grand average error signal ( $t = 0.354$  s and  $t = 0.568$  s). Figure 4 shows the average true negative rate (TNR) and the average true positive rate (TPR) (represented with green and red solid lines, respectively), for all the tested thresholds in the asynchronous ErrP classification with a generic classifier. The chance-level TNR and TPR were calculated by performing the same classification procedure with shuffled training labels. The 95 % confidence intervals for the average curves are represented by shaded areas. The threshold that maximized the group performance was  $\tau = 0.700$ . For this threshold, the average TNR was 82.0 % and the average TPR was 53.6 %. Figure 5 depicts the individual TNR and TPR of each participant. It depicts also the threshold that maximizes group performance ( $\tau = 0.700$ , grey dashed lines) and the thresholds that maximizes the individual performance (blue dashed lines).

## DISCUSSION

We developed an experimental task relying on continuous control of a robot towards a target. In 30 % of the trials (error trials), an error was triggered by the paradigm, causing the participants to loose control over the robot during the trial. We then studied the electrophysiological features associated with the error trials. The peaks of the error signal occurred at  $t = 0.354$  s and  $t = 0.568$  s. Our results are not directly comparable with state-of-the-art literature because we processed the EEG signal with a causal filter, causing the N200 component of the ErrP to shift to around 600 ms. We decided to keep the causal filter because it depicts the ErrP's shape in the scenario of an online ErrP decoder, bringing awareness to the fact that ERP shapes can be influenced by the filter used to

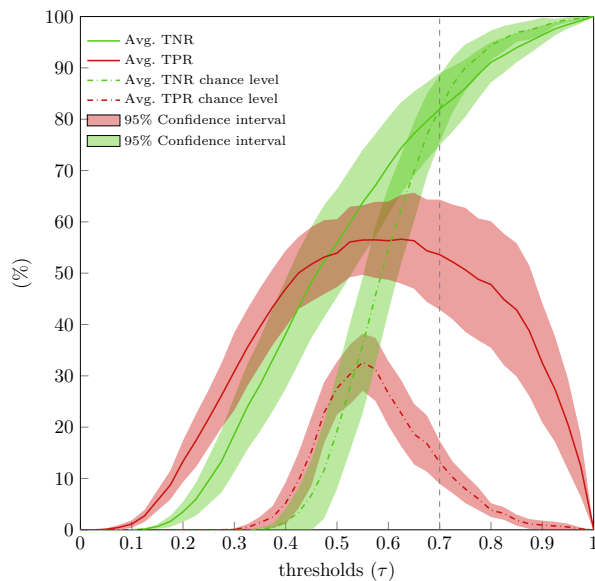


Figure 4: Average TNR and average TPR (green and red solid lines, respectively) for the different thresholds tested in the asynchronous ErrP classification with a generic classifier. The chance-level TNR and TPR are depicted with green and red dashed lines. The shadowed areas represent the 95 % confidence intervals for the average curves. The threshold that maximizes the group performance is represented with a grey vertical dashed line.

process the signal.

Afterwards, we evaluated the feasibility of transferring ErrP information across participants, by training a classifier with the data from 14 participants and testing it with the data of the remaining participant in an asynchronous manner (generic classifier). From Figure 4, we observe that the average TPR is above chance-level for all the thresholds and that the average TNR is increasing with the threshold. This points to the feasibility of using such classifiers as a starting point for an adaptive BCI. In Figure 5, it is possible to compare the individual performance of every participant with the generic classifier. We observe that participants with higher individual threshold present minor or negligible drops in performance with the use of a generic classifier tuned to the group performance (e.g. participants 1, 2 and 3). On the other hand, participants with lower individual threshold can present major performance drops (e.g. participants 5 and 8). This indicates that the performance of such classifier is still determined by individual characteristics of the participants. Nevertheless it seemed a suitable option for the majority of the participants.

## CONCLUSION

In this work we showed the feasibility of transferring ErrP information across participants, by training a classifier with the data from 14 participants and testing it with the data of the remaining participant in an asynchronous manner. We then showed that, although the performance of such classifiers is still dependent on indi-

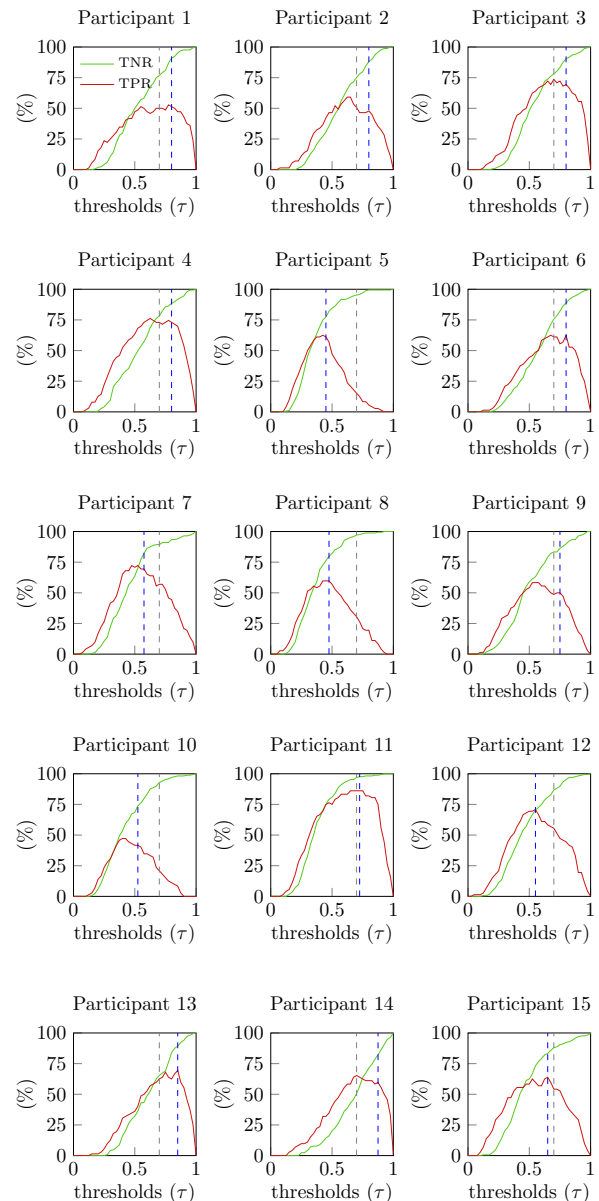


Figure 5: Individual TNR and TPR (green and red solid lines, respectively) for the different thresholds tested in the asynchronous ErrP classification with a generic classifier. The threshold that maximizes the group performance is represented with a grey dashed line ( $\tau = 0.7$ ). The threshold that maximizes the individual performance is represented with a blue dashed line.

vidual characteristics of the participants, the majority of them would benefit from such generic approach. Therefore, we believe that transferring ErrP information across participants is a viable alternative to reduce the calibration period in a scenario of asynchronous ErrP classification, as a starting point for an adaptive BCI.

## ACKNOWLEDGEMENTS

The authors would like to acknowledge the fruitful discussions with the members of 'Feel Your Reach'. This work was supported by Horizon 2020 ERC Consolidator

Grant 681231 'Feel Your Reach'.

## REFERENCES

- [1] Millán JdR et al. Combining Brain-Computer Interfaces and Assistive Technologies: State-of-the-Art and Challenges. *Frontiers in Neuroscience* 2010; 4:161.
- [2] Müller-Putz G et al. Towards Noninvasive Hybrid Brain-Computer Interfaces: Framework, Practice, Clinical Application, and Beyond, in *Proc. of the IEEE*, 2015, 103(6), 926-943.
- [3] Müller-Putz GR et al. Towards non-invasive brain-computer interface for hand/arm control in users with spinal cord injury, in *Proc. 5th International Winter Conference on Brain-Computer Interface (BCI)*, Sabuk, 2017, 63-65.
- [4] Chavarriaga R, Sobolewski A, Millán JdR. Errare machinale est: the use of error-related potentials in brain-machine interfaces. *Frontiers in Neuroscience* 2014; 8:208.
- [5] Schmidt NM, Blankertz B, Treder MS. Online detection of error-related potentials boosts the performance of mental typewriters. *BMC Neuroscience*. 2012; 13(1):13-19.
- [6] Spüler M, Bensch M, Kleih S, Rosenstiel W, Bogdan M, Kübler A. Online use of error-related potentials in healthy users and people with severe motor impairment increases performance of a P300-BCI. *Clinical Neurophysiology*. 2012; 123(7):1388-1337.
- [7] Iturrate, I, Chavarriaga R, Montesano L, Minguez J, Millán JdR. Latency correction of error-related potentials reduces BCI calibration time, in *Proc. of the 6th International Brain-Computer Interface Conference*, Graz, Austria, 2014.
- [8] Iturrate I, Chavarriaga R, Montesano L, Minguez J, Millán JdR. Latency correction of event-related potentials between different experimental protocols. *Journal of Neural Engineering* 2014; 11(3):036005.
- [9] Kim SK, Kirchner EA. Handling few training data: classifier transfer between different types of error-related potentials. *IEEE Transactions on Neural Systems and Rehabilitation Engineering*. 2016, 24(3):320-332.
- [10] Kim SK, Kirchner EA, Stefes A, Kirchner F. Intrinsic interactive reinforcement learning – Using error-related potentials for real world human-robot interaction. *Scientific Reports*. 2017, 7:17562.
- [11] Ehrlich S, Cheng G. A Feasibility Study for Validating Robot Actions Using EEG-Based Error-Related Potentials *International Journal of Social Robotics*. 2018.
- [12] Doud AJ, Lucas JP, Pisansky MT, He B. Continuous three-dimensional control of a virtual helicopter using a motor imagery based brain-computer interface. *PLOS ONE*. 2011; 6(10):e26322.
- [13] Coyle D, Garcia J, Satti A, McGinnity TM. EEG-based continuous control of a game using a 3 channel motor imagery BCI: BCI game. in *2011 IEEE Symposium on Computational Intelligence, Cognitive Algorithms, Mind, and Brain (CCMB)*, Paris, France, 2011, 1-7.
- [14] Galán F et al. A brain-actuated wheelchair: Asynchronous and non-invasive Brain-computer interfaces for continuous control of robots. *Clinical Neurophysiology*. 2008; 119(9):2159 - 2169.
- [15] Omedes J, Iturrate I, Minguez J, Montesano L. Analysis and asynchronous detection of gradually unfolding errors during monitoring tasks. *Journal of Neural Engineering* 2015; 12(5):056001.
- [16] Omedes J, Iturrate I, Chavarriaga R, Montesano L. Asynchronous Decoding of Error Potentials during the Monitoring of a Reaching Task 2015 *IEEE International Conference on Systems, Man, and Cybernetics*, Kowloon, 2015, 3116-3121.
- [17] Spüler M, Niethammer C. Error-related potentials during continuous feedback: using EEG to detect errors of different type and severity. *Frontiers in Human Neuroscience*. 2015; 9:155.
- [18] Lopes-Dias C, Sburlea AI, Müller-Putz GR. Masked and unmasked error-related potentials during continuous control and feedback. *Journal of Neural Engineering*. 2018; 15(3):036031.
- [19] Kreiling A, Neuper C, Müller-Putz G. Error potential detection during continuous movement of an artificial arm controlled by brain-computer interface. *Med Biol Eng Comput*. 2012; 60:223.
- [20] Iturrate I, Chavarriaga R, Montesano L, Minguez J, Millán JdR. Latency correction of error potentials between different experiments reduces calibration time for single-trial classification, in *2012 Annual International Conference of the IEEE Engineering in Medicine and Biology Society*, San Diego, CA, 2012, 3288-3291.
- [21] Salazar-Gomez AF, DelPreto J, Gil S, Guenther FH, Rus D. Correcting robot mistakes in real time using EEG signals, in *2017 IEEE International Conference on Robotics and Automation (ICRA)*, Singapore, 2017, 6570-6577.
- [22] Ehrlich SK, and Cheng G. Human-agent co-adaptation using error-related potentials. *Journal of Neural Engineering*. 2018; 15(6):066014.
- [23] Kobler RJ, Sburlea AI, Müller-Putz GR. A comparison of ocular artifact removal methods for block design based electroencephalography experiments, in *Proc. of the 7th International Brain-Computer Interface Conference*, Graz, 2017, 236-241.
- [24] Blankertz B, Lemm S, Trede M, Haufe S, and Müller KR. Single-trial analysis and classification of ERP components — A tutorial. *NeuroImage*; 2011 56(2):814 - 825.

# A Generic Error-related Potential Classifier Offers a Comparable Performance to a Personalized Classifier

Catarina Lopes-Dias<sup>1</sup>, Andreea I. Sburlea<sup>1</sup> and Gernot R. Müller-Putz<sup>1</sup>

**Abstract**—Brain-computer interfaces (BCIs) provide more independence to people with severe motor disabilities but current BCIs' performance is still not optimal and often the user's intentions are misinterpreted. Error-related potentials (ErrPs) are the neurophysiological signature of error processing and their detection can help improving a BCI's performance.

A major inconvenience of BCIs is that they commonly require a long calibration period, before the user can receive feedback of their own brain signals. Here, we use the data of 15 participants and compare the performance of a personalized ErrP classifier with a generic ErrP classifier. We concluded that there was no significant difference in classification performance between the generic and the personalized classifiers (Wilcoxon signed rank tests, two-sided and one-sided left and right). This results indicate that the use of a generic ErrP classifier is a good strategy to remove the calibration period of a ErrP classifier, allowing participants to receive immediate feedback of the ErrP detections.

## I. INTRODUCTION

Brain-computer interfaces (BCIs) allow to restore some autonomy to people with severe motor disabilities by converting thoughts into the control of an external device (e.g. a robotic arm or a cursor). BCIs' performance is still not optimal and sometimes they misinterpret the user's intentions giving rise to errors.

The cortical signature of error processing is named error-related potential (ErrP). The detection of ErrPs can be used to improve a BCI's performance [1]–[3]

The majority of state-of-the-art BCIs are personalized BCIs – they rely on the brain signals of each individual user. Such BCIs need a long calibration time, during which the brain signals of the user are recorded and processed in order to train a classifier, before the user can receive feedback of their own brain signals. Alternatively, generic BCIs – which rely on the brain signals of other individuals rather than of the final user - allow the user to receive immediate feedback. Nevertheless, generic BCIs are believed to offer a worse performance than personalized BCIs.

ErrP classifiers are often meant to be used in combination with other classifiers (that classify e.g. motor imagery tasks or movement-related cortical potentials) [4]–[6]. In a personalized approach, combining several decoders leads to an even longer calibration time. Therefore, using a generic ErrP classifier is an appealing possibility, if performance is not severely compromised.

This work has been supported by the ERC consolidator grant 681231 Feel Your Reach

<sup>1</sup> Institute of Neural Engineering, Graz University of Technology, Graz, Austria gernot.mueller@tugraz.at

Some works already explored the development of generic classifiers for error-related potentials and other event-related potentials in the context of discrete tasks [7]–[11]. But BCIs are developing in the direction of providing the user continuous control of an external device [12]. In such a situation, the user can perceive at any moment that an error occurred and therefore it requires a continuous (asynchronous) ErrP detection. Continuous decoding of ErrPs using personalized classifiers has been explored in offline and online situations [13]–[17] but the continuous decoding of ErrPs using generic classifiers remains largely unexplored [18].

In this work, we analyse the data from an asynchronous online ErrP decoding experiment [15] and compare the performance of a personalized classifier with a generic classifier in an asynchronous context.

## II. MATERIALS AND METHODS

### A. Dataset description

We used a dataset previously recorded [15] containing the data of 15 right-handed healthy volunteers (5 female). The participants were, on average,  $23.5 \pm 2.5$  years old (mean  $\pm$  std).

EEG and EOG data was recorded at a sampling frequency of 500 Hz, using BrainAmp amplifiers (Brain Products, Munich, Germany). We used 61 EEG electrodes and 3 EOG electrodes. The EEG electrodes were placed in a 10-10 layout. The ground electrode was placed at position AFz and the reference electrode was placed on the right mastoid. The EOG electrodes were placed above the nasion and below the outer canthi of the eyes.

### B. Experimental layout

In the experiment analysed, participants could control a robotic arm (Jaco assistive robotic arm - Kinova Robotics, Bonn, Germany) towards two physical targets, depicted in Figure 1. The control was done using the participants' right hand, which was tracked with a Leap Motion device. The details regarding the control of the robot and the experimental layout are described in [15].

### C. Experiment overview

The experiment consisted of 12 blocks. Each block contained 30 trials: 21 *correct trials* and 9 *error trials*. The aim of every trial was to bring the robot's hand from its home position to above the selected physical target. A trial ended when the robot reached the target or after 6 seconds, in case the target was not reached. As depicted in Figure 2, each trial was preceded by a pre-trial period, when



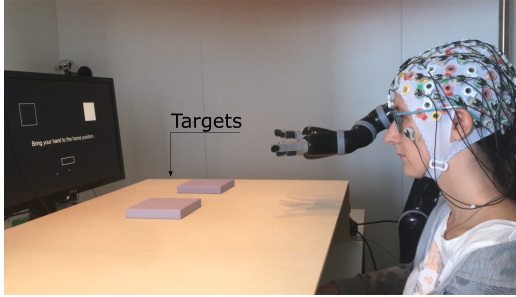


Fig. 1. Experimental setup: The violet cuboids on the wooden structure represent the physical targets. During the trials, the participants can steer the robotic arm towards the targets, using their right hand movement on the tabletop. In this figure, the robotic arm is at its home position. The participant on this image gave her informed consent for the photo to be made available in this publication. This figure was adapted from [15].

the monitor indicated the target of the coming trial (white square). Each trial was followed by a post-trial period, when the participants received feedback of the robot reaching or not the desired target (green or red square) and then the robot returned to its home position.

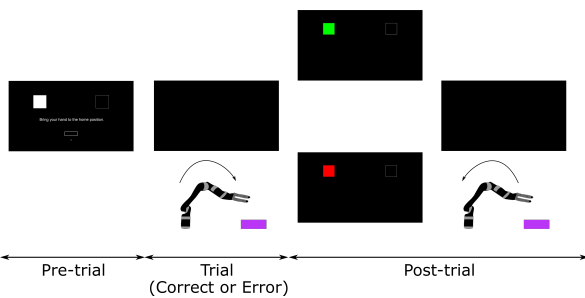


Fig. 2. Trial description. Each trial was preceded by a pre-trial period and followed by a post-trial period. During the pre-trial period participants received information regarding the target of the coming trial. During the trial, participants controlled the robot towards the selected target. In the post-trial period, participants received information of the behaviour of the robot (green or red square) and then the robot returned to its home position. This figure was adapted from [15].

1) *Correct trials*: In these trials no error was triggered by the paradigm. Participants could steer the robot towards the selected target.

2) *Error trials*: In these trials, the paradigm triggered an error during the motion of the robot. The error consisted in halting the participant's control of the robot. Participants would perceive the error by noticing the robot stopping and realizing that they were no longer in control.

#### D. Calibration and online blocks

The first 8 blocks of the experiment were calibration blocks and the last 4 blocks were online blocks, as depicted in Figure 3.

From the participants' perspective, only the error trials were different in the offline and online blocks. In the error trials of the calibration blocks, the participants had no possibility of correcting the robot's errors: when an error occurred, the robot remained still for the rest of the trial. In

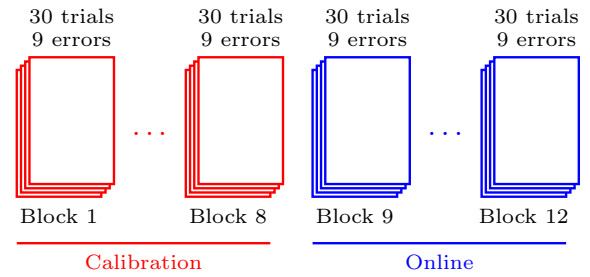


Fig. 3. Experiment overview: The experiment consisted of 12 blocks. Each block contained 30 trials, of which 9 were error trials and 21 correct trials. The first 8 blocks were calibration blocks and the last 4 blocks were online blocks.

the error trials of the online blocks, the participants had the possibility of correcting the robot's errors: if an ErrP was detected by the classifier after the error onset, participants regained control of the robot and could steer it towards the desired target. The correct trials during calibration and online blocks were indistinguishable for the participants.

#### E. Data preprocessing

Eye movements and blinks were removed from the EEG data using the subspace subtraction algorithm [19], relying on 2 blocks of eye movements recorded right before the experiment. The EEG signal was then filtered between 1 and 10 Hz using a causal Butterworth filter of order 4.

#### F. Personalized classifier

The personalized classifier used here is the same as the one described in detail in [15]. For every participant, we used the data of their calibration blocks to train a shrinkage-LDA classifier based on time-domain features. We also used the calibration blocks to determine a personalized threshold, as described in [15].

#### G. Generic classifier

The generic classifier used here is the same as the one described in [18]. For each participant, we used the calibration blocks from the 14 other participants to train a shrinkage-LDA classifier based on time-domain features. Additionally, as suggested in [18], we tailored the generic classifier for each participant by using a personalized threshold.

To determine the threshold for every participant, we performed an asynchronous classification with the generic classifier on the participant's own calibration data where we tested the performance of thresholds from 0 to 1 in steps of 0.025, similarly to the procedure described in [15].

#### H. Metrics to evaluate the classifiers

As an evaluation metric for the asynchronous classification, we defined as true negative trials (TN trials) the correct trials in which no error detection occurred. We defined as true positive trials (TP trials), the error trials in which no error detection occurred before the error onset and at least one error detection occurred after the error onset. The classification performance of the classifiers will be described

in terms of the true positive rate (TPR) - percentage of error trials successfully classified - and true negative rate (TNR) - percentage of correct trials successfully classified.

### I. Comparing the personalized and generic classifiers

Both personalized and generic classifiers were evaluated asynchronously using the same metrics (TNR and TPR) and both classifiers were tested in the same data set: the 4 online blocks of each of the 15 participants.

## III. RESULTS

### A. Personalized classifier

Figure 4 depicts the TPR and TNR obtained using the personalized classifier (in light green and pink respectively), for every participant as well as their average. On average, we obtained a TPR of 70.0 % and a TNR of 86.8 %.

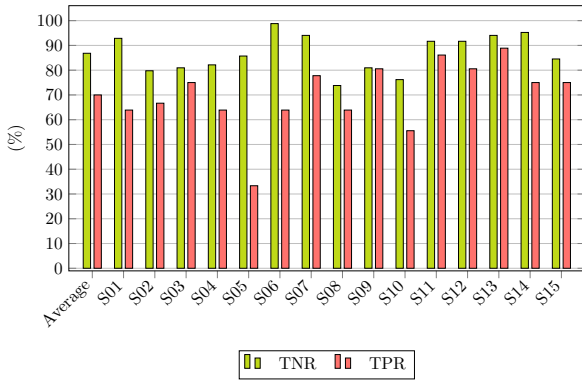


Fig. 4. Classification results of the personalized classifier: TNR (in light green) and TPR (in pink) for every participant and their average. This figure was adapted from [15]

### B. Generic classifier

The TPR and TNR obtained using a generic classifier for every participant and their average are depicted in Figure 5. On average, we obtained a TPR of 72.6 % and a TNR of 87.9 %.

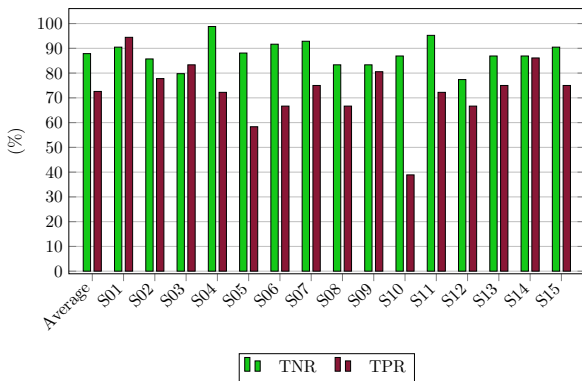


Fig. 5. Classification results of the generic classifier: TNR (in dark green) and TPR (in dark red) for every participant and their average.

### C. Comparison of classifiers

Figure 6 depicts the TNR results using both a personalized and a generic classifier while Figure 7 summarizes the TPR results using both a personalized and a generic classifier.

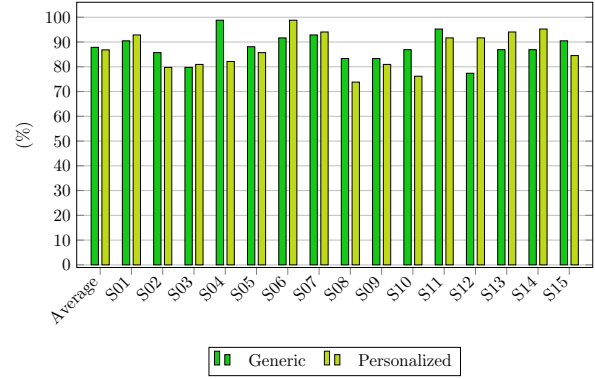


Fig. 6. Comparison of the TNR performance using the generic and the personalized classifiers (dark green and light green, respectively).

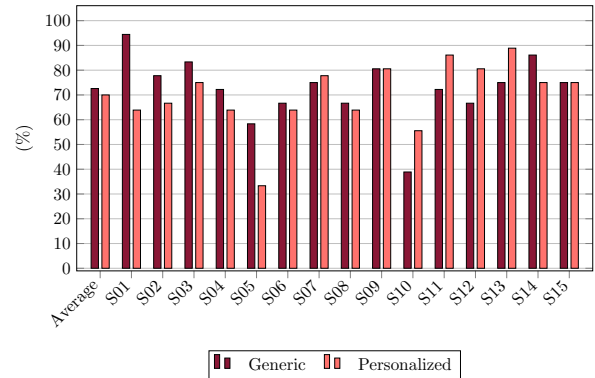


Fig. 7. Comparison of the TPR performance using the generic and the personalized classifiers (dark red and pink, respectively).

To test if the results obtained with the two classifiers were significantly different, we performed a two-sided Wilcoxon signed rank test for the TPR results and also for the TNR results. The significance test for the TPR resulted in  $p = 0.7219$ . The significance test for the TNR resulted in  $p = 0.6275$ . This indicates that the performance of both classifiers is not significantly different. Moreover, we performed also one-sided significance tests. When testing if the generic classifier performance was better than the personalized classifier we obtained  $p = 0.3610$  for the TPR and  $p = 0.3138$  for the TNR. When testing if the generic classifier performance was worse than the personalized classifier we obtained:  $p = 0.6488$  for the TPR and  $p = 0.6963$  for the TNR.

## IV. DISCUSSION

In this work, we compared the classification results obtained using a generic and a personalized classifiers. Both classifiers were tested asynchronously on the same dataset and evaluated with the same metrics. We found no significant

difference in the classification results of the generic and of the personalized classifiers.

It is commonly believed that personalized classifiers offer a superior performance than generic classifiers. Surprisingly, in our dataset, the performance of both classifiers was comparable. We verified that some participants with an above-average performance when using the personalized classifier (e.g. participants S11 and S13) had a drop in performance when using the generic classifier. Nevertheless, some participants with a below-average performance when using the personalized classifier (e.g. participant S05) had an increase in performance when using the generic classifier.

The main drawback of using personalized classifiers is the need of a long calibration period before the participants can receive feedback of their own performance. This is particularly critical in a real-life BCI scenario, where ErrP classification is usually used in combination with other classifiers (e.g. motor imagery or movement attempt). Such scenario requires a long calibration period to collect enough data to train the different classifiers.

Given that the ErrP generic classifier revealed no drop in performance, it is a good alternative to reduce, or even eliminate, the calibration period of a BCI, leading to shorter experimental time and possibly to reduced fatigue in the participants.

In a real-life BCI scenario such dichotomy between a personalized and a generic ErrP classifier could even be accessed on-site during the experiment. Constructing a BCI with a generic ErrP classifier would allow immediate feedback to the participants while still collecting data to train a personalized ErrP classifier. A regular on-site comparison of both classifiers would allow switching from the generic ErrP classifier to the personalized ErrP classifier when the latter reliably produced better results.

## V. CONCLUSIONS

The generic and personalized classifiers analysed in this work held a comparable performance. This indicates that the use of a generic ErrP classifier is a good strategy to eliminate the calibration period and give immediate feedback to the participants regarding error detection while preserving, on average, the classification performance.

## ACKNOWLEDGMENT

The authors would like to thank Reinmar Kobler for the fruitful discussions and to Marcel Zube and Lea Hehenberger for their help during the experiment preparation.

## REFERENCES

- [1] R. Chavarriaga, A. Sobolewski, and J. d. R. Millán, "Errare machinale est: the use of error-related potentials in brain-machine interfaces," *Frontiers in Neuroscience*, vol. 8, p. 208, 2014.
- [2] M. Spüler, M. Bensch, S. Kleih, W. Rosenstiel, M. Bogdan, and A. Kübler, "Online use of error-related potentials in healthy users and people with severe motor impairment increases performance of a p300-bci," *Clinical Neurophysiology*, vol. 123, no. 7, pp. 1328 – 1337, 2012.
- [3] A. Llera, M. A. van Gerven, V. Gómez, O. Jensen, and H. J. Kappen, "On the use of interaction error potentials for adaptive brain computer interfaces," *Neural Networks*, vol. 24, no. 10, pp. 1120–1127, 2011.

- [4] A. Kreiling, C. Neuper, and G. R. Müller-Putz, "Error potential detection during continuous movement of an artificial arm controlled by brain-computer interface," *Medical & Biological Engineering & Computing*, vol. 50, no. 3, pp. 223–230, 2012.
- [5] R. Yousefi, A. R. Sereshkeh, and T. Chau, "Online detection of error-related potentials in multi-class cognitive task-based bcis," *Brain-Computer Interfaces*, vol. 6, no. 1-2, pp. 1–12, 2019.
- [6] J. Omedes, A. Schwarz, G. R. Müller-Putz, and L. Montesano, "Factors that affect error potentials during a grasping task: toward a hybrid natural movement decoding BCI," *Journal of Neural Engineering*, vol. 15, p. 046023, jun 2018.
- [7] S. Bhattacharyya, A. Konar, D. N. Tibarewala, and M. Hayashibe, "A generic transferable eeg decoder for online detection of error potential in target selection," *Frontiers in Neuroscience*, vol. 11, p. 226, 2017.
- [8] S. K. Kim and E. A. Kirchner, "Handling few training data: Classifier transfer between different types of error-related potentials," *IEEE Transactions on Neural Systems and Rehabilitation Engineering*, vol. 24, pp. 320–332, March 2016.
- [9] A. Pinegger and G. R. Müller-Putz, "No training, same performance!? – A generic P300 classifier approach," in *7th Graz Brain-Computer Interface Conference 2017*, September 2017.
- [10] S. Lu, C. Guan, and H. Zhang, "Unsupervised brain computer interface based on intersubject information and online adaptation," *IEEE Transactions on Neural Systems and Rehabilitation Engineering*, vol. 17, pp. 135–145, April 2009.
- [11] P.-J. Kindermans, M. Schreuder, B. Schrauwen, K.-R. Müller, and M. Tangermann, "True zero-training brain-computer interfacing – an online study," *PLOS ONE*, vol. 9, pp. 1–13, 07 2014.
- [12] R. J. Kobler, A. I. Sburlea, and G. R. Müller-Putz, "Tuning characteristics of low-frequency eeg to positions and velocities in visuomotor and oculomotor tracking tasks," *Scientific Reports*, vol. 8, no. 1, p. 17713, 2018.
- [13] M. Spüler and C. Niethammer, "Error-related potentials during continuous feedback: using EEG to detect errors of different type and severity," *Frontiers in Human Neuroscience*, vol. 9, p. 155, 2015.
- [14] C. Lopes-Dias, A. I. Sburlea, and G. R. Müller-Putz, "Masked and unmasked error-related potentials during continuous control and feedback," *Journal of Neural Engineering*, vol. 15, p. 036031, apr 2018.
- [15] C. Lopes-Dias, A. I. Sburlea, and G. R. Müller-Putz, "Online asynchronous decoding of error-related potentials during the continuous control of a robot," *Scientific Reports*, vol. 9, no. 1, p. 17596, 2019.
- [16] J. Omedes, I. Iturrate, R. Chavarriaga, and L. Montesano, "Asynchronous decoding of error potentials during the monitoring of a reaching task," in *2015 IEEE International Conference on Systems, Man, and Cybernetics*, pp. 3116–3121, Oct 2015.
- [17] J. Omedes, I. Iturrate, J. Minguez, and L. Montesano, "Analysis and asynchronous detection of gradually unfolding errors during monitoring tasks," *Journal of Neural Engineering*, vol. 12, no. 5, p. 056001, 2015.
- [18] C. Lopes-Dias, A. I. Sburlea, and G. R. Müller-Putz, "Asynchronous detection of error-related potentials using a generic classifier," in *8th International Brain Computer Interface Conference 2019*, Sep 2019.
- [19] R. J. Kobler, A. I. Sburlea, and G. R. Müller-Putz, "A comparison of ocular artifact removal methods for block design based electroencephalography experiments," in *Proceedings of the 7th Graz Brain-Computer Interface Conference 2017*, Sep 2017.



# Online asynchronous detection of error-related potentials in participants with spinal cord injury by adapting a pre-trained generic classifier

Catarina Lopes-Dias<sup>1</sup>, Andreea I. Sburlea<sup>1</sup>, Katharina Breitegger<sup>2</sup>, Daniela Wyss<sup>2</sup>, Harald Drescher<sup>2</sup>, Renate Wildburger<sup>2</sup> and Gernot R. Müller-Putz<sup>1,3</sup>

<sup>1</sup> Institute of Neural Engineering, Graz University of Technology, Graz, Austria

<sup>2</sup> AUVA-Rehabilitationsklinik Tobelbad, Tobelbad, Austria

<sup>3</sup> BioTechMed, Graz, Austria

E-mail: [gernot.mueller@tugraz.at](mailto:gernot.mueller@tugraz.at)

**Abstract.** A brain-computer interface (BCI) user awareness of an error is associated with a cortical signature named error-related potential (ErrP). The incorporation of ErrPs' detection in BCIs can improve BCIs' performance.

**Objective:** This work is three-folded. First, we investigate if an ErrP classifier is transferable from able-bodied participants to participants with spinal cord injury (SCI). Second, we test this generic ErrP classifier with SCI and control participants, in an online experiment without offline calibration. Third, we investigate the morphology of ErrPs in both groups of participants.

**Approach:** We used previously recorded electroencephalographic (EEG) data from able-bodied participants to train an ErrP classifier. We tested the classifier asynchronously, in an online experiment with 16 new participants: 8 participants with SCI and 8 able-bodied control participants. The experiment had no offline calibration and participants received feedback regarding the ErrPs' detection from its start. For a matter of fluidity of the experiment, the feedback regarding false positive ErrP detections was not presented to the participants but these detections were taken into account in the evaluation of the classifier. The generic classifier was not trained with the user's brain signals. Still, its performance was optimized during the online experiment with the use of personalized decision thresholds. The classifier's performance was evaluated using trial-based metrics, which consider the asynchronous detection of ErrPs during the entire trials' duration.

**Main results:** Participants with SCI presented a non-homogenous ErrP morphology, and four of them did not present clear ErrP signals. The generic classifier performed above chance level in participants with clear ErrP signals, independently of the SCI (11 out of 16 participants). Three out of the five participants that obtained chance level results with the generic classifier would have not benefited from the use of a personalized classifier.

**Significance:** This work shows the feasibility of transferring an ErrP classifier from able-bodied participants to participants with SCI, for asynchronous detection of ErrPs in an online experiment without offline calibration, which provided immediate feedback to the users.

*Keywords:* error-related potential, asynchronous classification, generic classifier, online experiment, spinal cord injury, end-users, brain-computer interface

## 1. Introduction

Brain-computer interfaces (BCIs) can assist people with severe motor impairments to operate external devices by converting their modulated brain activity into the control of these devices [1–3]. Although being a promising technology, most BCIs are still error-prone, and the frequent occurrence of errors can spoil the experience of the BCI user. The user’s awareness of an unintended response from the device that he/she is controlling is associated with a neural signature known as error-related potential (ErrP) [4, 5].

ErrPs are associated with conflict monitoring and error processing [6] and can be measured using non-invasive techniques, such as electroencephalography (EEG), that are often used for BCIs’ control. Therefore, ErrPs can be used to improve BCIs’ performance either in a corrective manner, by allowing corrective actions, or in an adaptive manner, by reducing the possibility of future errors [7–11]. The real-time detection of ErrPs is pertinent in BCIs used by persons with motor impairments and also in applications targeting healthy users [12–15]. The incorporation of ErrPs’ detection in a BCI promotes a smoother interaction with its user. Nevertheless, this incorporation is not widely investigated.

The use of ErrPs in discrete BCIs, which are controlled in discrete steps, is well established in healthy participants [4, 10, 16–22] and has also been marginally tested in potential end-users of BCIs [23]. Still, BCIs are developing in the direction of offering users continuous control of an external device - continuous BCIs [24–28]. The incorporation of ErrPs in such BCIs requires an asynchronous detection of ErrPs, since the user can realise at any moment, during the control of the device, that an error has occurred. The asynchronous detection of ErrPs has been studied in healthy participants, both in offline scenarios [13, 29–34] and more recently in online scenarios [35].

A possible explanation for the limited use of ErrPs in BCIs can be linked with most BCIs relying on personalised classifiers, which are constructed with the user’s brain signals. Since a considerable amount of data is necessary to reliably train the classifier, personalised classifiers commonly require a long calibration period before the user can receive feedback of its own brain signals. In this manner, combining ErrPs with other controlling signals would imply collecting calibration data for all the different signals, increasing even more the calibration period. Alternatively, using an ErrP classifier that would not require calibration with the user could encourage the integration of ErrPs with other control signals when constructing BCIs. This could be achieved by either transferring an ErrP classifier across different tasks or across different participants. Both options have been tested in discrete tasks, in offline conditions [23, 36–43] and in online conditions [20]. Recently, the asynchronous detection of ErrPs with a generic classifier has been studied in the context of a continuous task, in offline conditions [44] and in pseudo-online conditions [45].

Very few works addressed the study of ErrPs in potential BCI end-users and the existing studies are mainly conducted offline. Keyl and colleagues characterized the morphology of ErrPs of spinal cord injured participants and compared it with

able-bodied control participants [46]. The ErrP morphology was comparable in the two groups but the ErrPs of the participants in the SCI group showed smaller peak amplitudes. Kumar and colleagues studied ErrPs during post-stroke rehabilitation movements [47]. In this work, individual participants did not display very clear ErrP patterns. Spüler and colleagues studied ErrPs in six participants with amyotrophic lateral sclerosis (ALS) in an online experiment, and showed that the incorporation of ErrPs improves the BCI performance [23]. This work also analysed, offline, the transfer of an ErrP classifier from ALS participants to able-bodied control participants.

Our study has three main aims. First, we test the feasibility of transferring an ErrP classifier for asynchronous classification from able-bodied participants to potential end-users of BCIs, in particular participants with a high spinal cord injury (SCI). Second, we test the feasibility of using a generic ErrP classifier asynchronously in an online experiment in which both participants with SCI and control participants took part. Third, we investigate the morphology of ErrPs both in participants with SCI and in control participants.

In the work presented here, we recorded EEG from both participants with SCI and control participants while testing asynchronously a generic ErrP classifier in a closed-loop online experiment. The generic classifier has been trained with the EEG data of 15 able-bodied participants from a previous study of ours and was not retrained during the experiment [35]. This allowed us to create an online experiment with no offline calibration period, in which participants received immediate feedback of their brain signals from the very beginning of the experiment onwards.

## 2. Methods

### 2.1. Participants

Sixteen volunteers participated in the experiment, eight of which had a spinal cord injury. The age of the participants with SCI was  $37.5 \pm 9.7$  years (mean  $\pm$  std). The remaining participants were able-bodied control participants. Each participant with SCI was matched with a control participant of the same sex and a maximum age difference of 5 years. The control participants were  $35.9 \pm 10.8$  years old (mean  $\pm$  std).

All participants with SCI had a spinal cord injury between levels C4 and Th2. Table 1 summarizes the demographical and clinical data of the participants with SCI: age, sex, neurological level of injury (NLI) and ASIA impairment score (AIS).

*2.1.1. Inclusion and exclusion criteria* All participants had to be of age between 18 and 65 years. Given that the experimental paradigm required a preserved arm function, all participants with SCI had to have the injury at level C4 or lower. Participants with SCI were excluded if they were artificially ventilated or had major spasms due to possible interference with the EEG measurement. Control participants were required to be able-bodied and with no history of neurological diseases.

Participant	Age	Sex	NLI	AIS	Time since injury
P1	24	F	C5	B	> 10 years
P2	29	M	C7	C	> 10 years
P3	33	M	Th2	D	> 9 years
P4	36	F	C7	B	> 10 years
P5	37	M	C4	B	>10 years
P6	39	M	C6	B	> 10 years
P7	48	M	C4	B	6 - 12 months
P8	54	M	C4	B	> 1 year

**Table 1:** Summary of the demographical and clinical data of the participants with SCI.

### 2.2. Ethical approval and measurements

This study was approved by the local ethics committee of the Medical University of Graz (ethical approval number 31-501 ex 18/19) and by the Allgemeine Unfallversicherungsanstalt (AUVA) ethical committee. All participants read and signed an informed consent form before the start of the experiment and were paid for their participation. The EEG measurements of the participants with SCI took place at AUVA Rehabilitation Clinic Tobelbad and the EEG measurements of the control participants took place at Graz University of Technology.

### 2.3. Hardware and electrodes' layout

We recorded EEG data with a sampling rate of 500 Hz using BrainAmp amplifiers and ActiCap caps (Brain Products, Munich, Germany) with 61 active electrodes positioned in a 10-10 layout, as detailed in Figure 1 of the supplementary material. The ground electrode was placed on AFz and the reference electrode was placed on the right mastoid. Additionally, we used 3 EOG electrodes that were placed above the nasion and below the outer canthi of the eyes.

### 2.4. Experimental setup

Similarly to the experimental setup described in [35], participants sat in front of a table, on top of which was a wooden 4-sided box, with open sides towards the participant and the tabletop, as depicted in Figure 1 (top). On the ceiling of the box was a Leap Motion device (Leap Motion, San Francisco, United States) that tracked the participants' right or left hand, according to their preferred hand. The position of the Leap Motion on the ceiling of the box was adjusted to the handedness of each participant. The participants kept their hand inside the wooden box. On the right side of the participants, attached to the table, we placed a robotic arm (Jaco Assistive robotic arm - Kinova Robotics, Bonn, Germany). Differently from [35], a screen monitor was lying on the wooden box, centred in relation to the robotic arm. The monitor was slightly inclined, with a 15-degree angle,

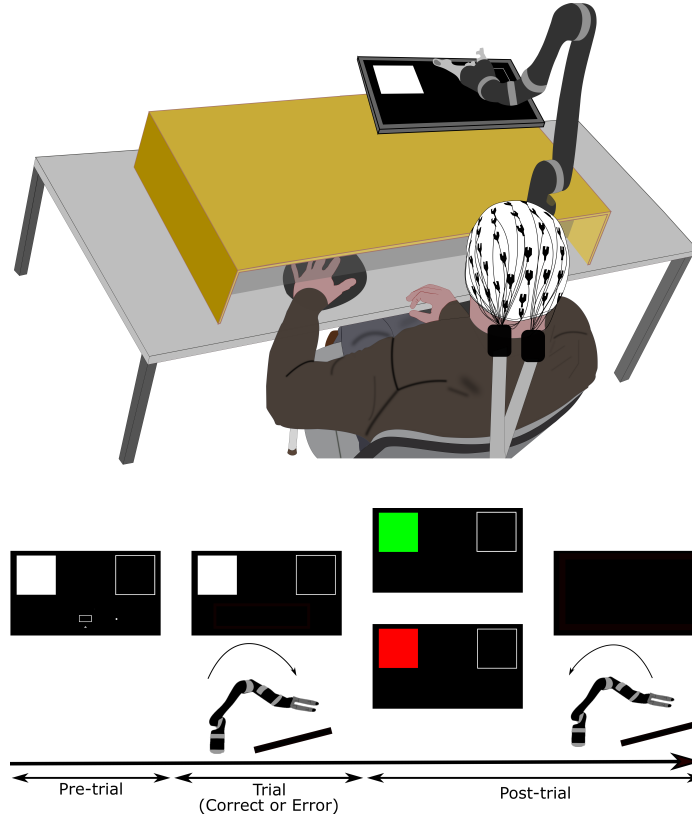


**Figure 1: Top:** Experimental setup. Participants sat in front of a table, attached which was a robotic arm. The participants controlled the robotic arm during the trials using their hand. **Bottom:** The experimental protocol displayed on the monitor. During the pre-trial period, the white square represented the target of the coming trial. The small rectangle located centrally, on the bottom part of the screen, represented the home position of the participant’s hand. A trial started when the participants moved their hand to its home position. The participants were instructed to move the robot to the target square during the trials. After the trial (post-trial period), the target changed colour, indicating whether or not it was reached, and the robot automatically returned to its home position.

to offer the participants a better view of the screen. This change in relation to [35] was introduced to minimize head and eye movements during the experiment.

### 2.5. Controlling the robotic arm

During the trials, participants could control the robotic arm on a horizontal plane by moving their preferred hand on the tabletop. To reduce the range of the participants’ movements, we considered the robot’s hand displacement to be three times larger than the participants’ hand displacement.

Many participants with SCI had a very closed fist, due to hand spasticity caused by their injury, and this impaired their hand’s recognition by the Leap Motion. When

this occurred, we inserted a small object in the participants' hand in order to sustain the hand in a more open position and facilitate its tracking.

### 2.6. Experiment overview

Before the experiment, we recorded one block in which the participant performed eye movements [48, 49]. The experiment then consisted of 8 blocks of 30 trials each. 30% of the trials of each block were *error trials* (9 trials). The remaining 70% of the trials were *correct trials* (21 trials). The sequence of correct and error trials within each block was randomly generated using a uniform distribution. We defined a maximum of 2 consecutive error trials in each block and repeated the randomization procedure until the sequence of trials satisfied this condition. Similarly, the trials of each block were equally split between the right and the left targets. The sequence of targets within each block were randomly assigned using a uniform distribution. We defined a maximum of 3 consecutive trials with the same target in each block and repeated the randomization procedure until the targets' sequence satisfied this requirement.

All the 8 blocks were online blocks: we used a *generic ErrP classifier* in an asynchronous manner to give participants real-time feedback of the *ErrP detections* during the experiment. For a matter of fluidity of the experiment, we decided not to give participants feedback of false positive ErrP detections, i.e., of the *ErrP detections* that happened when no error had occurred. This decision assured that all participants experienced the same number of errors, which aimed to create a comparable expectation regarding the occurrence of errors across participants. False ErrP detections can occur both in correct and error trials and were considered when evaluating the classifier. The details regarding the generic classifier are described in the section *Generic ErrP classifier*.

### 2.7. Experimental protocol

During the pre-trial period, the monitor displayed two squares, on the top part of the screen, each with a 14 cm side. As depicted in Figure 1, one of the squares was filled in white and the other square had no fill. The filled square represented the target of the coming trial. The centres of the squares were 35 cm apart and their midpoint was located 30 cm in front of the home position of the robot's hand. On the bottom part of the screen was a rectangle, representing the home position of the participant's hand. The position of the participant's hand in relation to its home position was depicted by a dot on the screen.

Participants could decide when to start a new trial and could rest for as long as they needed in between trials. A trial started when the dot entered the rectangle. This ensured that the participant's hand was at a similar position at the beginning of each trial. Participants were instructed to, when they felt ready to start a new trial, position the dot representing their hand below the home position's rectangle, fixate their gaze

on the target and finally enter the rectangle from the bottom. This last step ensured a forward movement of the robot. Participants were also asked to keep their gaze fixed at the target during the entire trial in order to prevent eye movements.

The aim of each trial was to move the robot's hand from its home position to the target square. During the trials, only the two squares were displayed on the screen: the white square representing the target and the square with no fill. A trial ended when the robot's hand was above the target or after 6 seconds (time out), in case the target has not been reached. After the end of the trial (post-trial period), the target's colour changed from white to either green or red, for 1.2 s, indicating whether or not the target was reached, respectively. This feedback was always in line with the robot's behaviour. Then, the screen turned black, the robot automatically returned to its home position and a new pre-trial period would start.

*2.7.1. Error trials* In these trials, the paradigm triggered an error, during the movement of the robot towards the target. The error consisted in interrupting the participant's control of the robot and adding a 5 cm upwards displacement to the robot's hand. The participants perceived the error by noticing the robot stopping and lifting and by realizing that the control of the robot was lost. The errors occurred randomly, when the robot's hand was within 6 to 15 cm from its home position, in the forward direction. For every error trial, this distance was drawn from a continuous uniform distribution. In participants with SCI, the error onset occurred, on average,  $1.36 \pm 0.14$  s after the start of the error trial (mean  $\pm$  std). In control participants, the error onset occurred, on average,  $1.30 \pm 0.07$  s after the start of the error trial (mean  $\pm$  std).

We used the generic ErrP classifier in an asynchronous manner to give participants feedback of the *ErrP detections* occurring after the error onset. Figure 2 illustrates all the possible interactions between the participants and the robot during error trials, taking into account the generic ErrP classifier feedback. If no ErrP was detected after the error onset, the robot remained still for the rest of the trial. In this situation, the total duration of the trial was 6 seconds and afterwards the target square turned red. Differently, if an ErrP was detected by the classifier after the error onset, the robot's hand lowered 5 cm and the participants regained its control. The downward movement informed the participants of the ErrP detection and consequent regain of control. Since participants instinctively stopped their hand movement when noticing the error, they were instructed to reinitiate the movement and move the robot's hand to the selected target when regaining control of the robot. To accommodate the extra movement, we added 6 seconds to the maximal trial duration, once the first ErrP detection after the error onset occurred. If the robot reached the target, after the error onset, the target square turned green. Participants did not receive feedback of the false positive detections occurring during the error trials, i.e., of the *ErrP detections* occurring before the error onset. Prior to the experiment, participants were informed that errors would occur and were shown the characteristic robot movement associated with error occurrence, i.e., the robot stopping and lifting.



*2.7.2. Correct trials* In these trials, the paradigm did not trigger any error. Participants did not receive feedback of the false positive ErrP detections occurring during the correct trials. Figure 2 illustrates all the possible interactions between a participant and the robot during correct trials. Correct trials lasted, on average,  $2.11 \pm 0.17$ s for participants with SCI and  $2.05 \pm 0.13$ s for the control participants (mean  $\pm$  std). All participants reached the target in more than 99.4% of the correct trials.

## *2.8. Data processing*

Eye movements and blinks were removed online from the EEG data, using the subspace subtraction algorithm [48,49] and the eye movement data recorded right before the start of the experiment. For the online detection of ErrPs with the generic classifier, the EEG data were bandpass filtered between 1 and 10 Hz with a causal Butterworth filter of order 4. For the offline electrophysiological analysis presented here, the EEG data were bandpass filtered between 1 and 10 Hz with a noncausal Butterworth filter of order 4.

## *2.9. Defining events*

In the error trials, we defined the error onset as the moment in which the robot started its upwards displacement once the participant's lost its control. Prior to the experiment, we calculated the robot's delay on 100 uncorrected errors, i.e., the time difference between the error marker and the robot upwards displacement. This resulted in an average delay of  $0.225 \pm 0.005$ s (mean  $\pm$  std). Since the robot's delay was rather stable, we added the average delay to each recorded error marker in order to obtain the error onset.

Correct trials had no clear onset. Therefore, to obtain comparable onsets in correct and error trials for the electrophysiological analysis, we defined a virtual onset for the correct trials at a time point in which errors could occur in the error trials. For every participant, we defined the virtual onset for his/her correct trials as the average time difference between the error onsets and the start of the corresponding trials. For the participants with SCI, the correct onset occurred, on average,  $1.36 \pm 0.14$ s after the start of the correct trials (mean  $\pm$  std). For the control participants, the correct onset occurred, on average,  $1.30 \pm 0.07$ s after the start of the correct trials (mean  $\pm$  std).

## *2.10. Generic ErrP classifier*

We built a generic error-related potential classifier using the EEG data from 15 able-bodied participants of a previous study for ours [35]. None of these previous participants took part in the experiment described here. The EEG data from those participants were filtered between 1 and 10 Hz using a causal Butterworth filter of order 4. Eye movements were removed from the data using the subspace subtraction algorithm [48].

For each participant from [35], we used the 8 calibration runs of the dataset and extracted an epoch with 450 ms from every trial. In the error trials, the selected epoch

started 300 ms after the error onset. In the correct trials, the selected epoch started 300 ms after the virtual onset. Hence, our initial features were the amplitudes of the 61 EEG electrodes at all the time points of the 450 ms of each epoch.

In order to remove outlier epochs, we first applied principal component analysis (PCA) on the initial features and kept the PCA components that explained 99 % of the data variability. Then, we removed 1 % of the correct epochs and 1 % of the error epochs as outliers. The rejection criterion was based on a large Mahalanobis distance of the rejected epochs within each class type (error or correct) in the PCA space. After this step, 2475 correct epochs and 1059 error epochs were kept.

Finally, we repeated the PCA step on the initial feature space, after discarding the outlier epochs, and kept as features the PCA components that preserved 99 % of the data variability. This step resulted in 412 PCA components. These components were then used as features to train a shrinkage-LDA classifier with two classes: error and correct [50]. The linear scores of the classifier were transformed into probabilities using a softmax function. The PCA components preserved most of the activity of the original space, as depicted in Figure 2 of the supplementary material. Figure 3 of the supplementary material depicts the classifier pattern, obtained by applying the discriminant feature analysis (DFA) method to the training matrix with 3534 epochs and 412 features [51]. The generic classifier remained unchanged during the entire experiment. In [45], we showed that the generic ErrP classifier offers a comparable performance to a personalized ErrP classifier for the asynchronous detection of ErrPs. Therefore, we chose not to retrain the classifier with the participants' own data.

### 2.11. ErrP detection

Similarly to the classifier developed in [35], the generic classifier developed here was constructed to be used and evaluated in an asynchronous manner. In the online experiment, the incoming EEG signals were analysed in real-time by the ErrP classifier, which received as input an EEG window of 450 ms. Consecutive analyzed windows had a leap of 18 ms. The classifier's evaluation of each window resulted in the probability of the analysed window belonging to either class (correct or error). Hence, the classifier produced a probability output every 18 ms, during the entire duration of each block. We defined an *ErrP detection* when two consecutive windows had a probability of belonging to the error class above a certain threshold  $\tau$ . In [44], we evaluated offline the asynchronous ErrP detection with the generic classifier and tested the effect of varying the decision threshold. From [44] we concluded that the combination of the generic ErrP classifier with a personalized decision threshold leads to the achievement of better performances. Hence, in this online experiment, we decided to apply this strategy. The procedure to determine the personalized thresholds is described in the section *Tailoring the decision threshold of the generic classifier to each participant*.

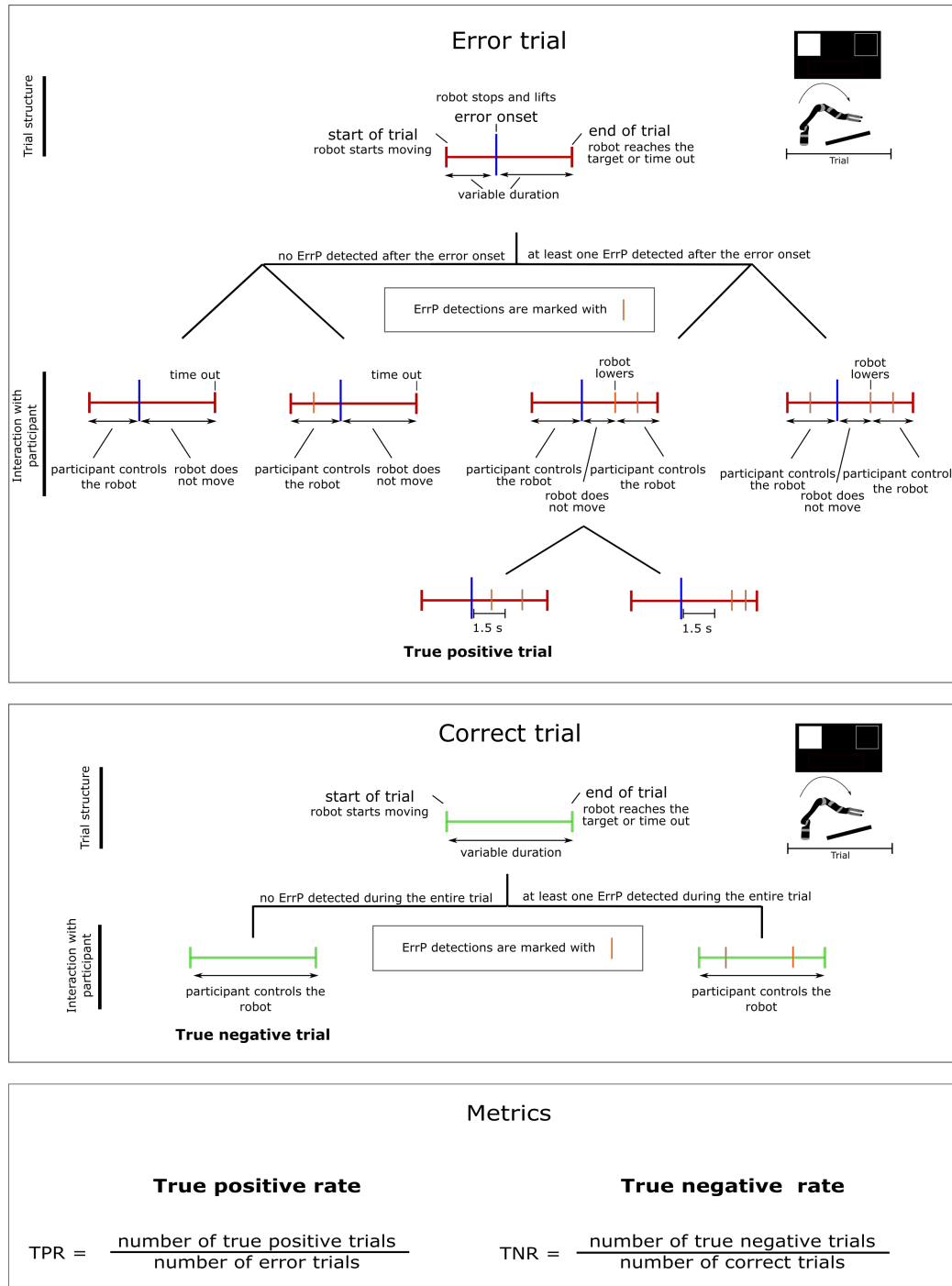


**Figure 2:** Experimental protocol and metrics. Graphical representation of the trial structure, of the interaction between the participant and the robot during the trials, and of the trial-based metrics used for the evaluation of the classifier. All the occurrences that are not labelled nor detailed, inherit the corresponding description from the preceding node.

### 2.12. Metrics to evaluate the ErrP classifier

To evaluate the performance of the generic classifier, we considered the trial structure of the experiment and the asynchronous nature of the decoding. The proposed metrics assess a trial as successful or unsuccessful, based on the asynchronous detection of ErrPs over the entire trial’s duration. This strategy has been applied to the study of asynchronous detection of ErrPs and other event-related potentials, in several other works [29–35, 44, 45, 52–54]. Figure 2 presents a graphical representation of the metrics proposed here. Correct trials were labelled negative and error trials were labelled positive.

*2.12.1. True negative trials* We defined the true negative trials (TN trials) as the correct trials in which no *ErrP detection* occurred during the entire trial duration. For the classifier’s evaluation we considered the true negative rate (TNR): the fraction of correct trials that are TN trials, i.e., that have no *ErrP detections* ‡.

*2.12.2. True positive trials* We defined the true positive trials (TP trials) as the error trials in which no ErrP detection occurred before the error onset and at least one ErrP detection occurred within the 1.5 s after the error onset. For the classifier’s evaluation we considered the true positive rate (TPR): the fraction of error trials that were TP trials. An additional metric, *ErrP detection rate* (EDR), considering only the ErrP detections within the 1.5 s after the error onset, is defined in Figure 5 of the supplementary material, where its relation with the TPR is detailed ‡.

*2.12.3. Chance level* To calculate the chance level for TNR and TPR we performed several classifications with a classifier in which the training labels were randomly permuted (500 times for the evaluation of the online detection with the generic classifier and 50 times for the evaluation of the offline cross-validation with a personalized classifier). Furthermore, we used permutation based *p*-values to present the significance of the classification results obtained with the generic ErrP classifier [55, 56].

### 2.13. False activation rate

The false activation rate (FAR) is the percentage of 1-second long intervals that are contaminated with at least one false positive ErrP detection [57]. For this evaluation, we considered the entire duration of correct trials and the period before the error onset in error trials. These periods were divided into 1-second long intervals and these intervals were evaluated for the presence of false positive ErrP detections.

‡ The metrics TNR and TPR used here address the asynchronous detection of ErrPs in a trial-based scenario and are not directly comparable with the TNR and TPR definitions commonly used in time-locked classification.

#### 2.14. Tailoring the decision threshold of the generic classifier to each participant

In [44] we evaluated offline the asynchronous detection of ErrPs with a generic classifier similar to the one described here. There, we observed that the decision threshold  $\tau$  that maximized the group performance was  $\tau = 0.7$ . Moreover, we also concluded that in order to optimize the individual performance with the generic classifier, participants benefit from the use of a personalized threshold. Therefore, in this experiment, we decided to initiate the generic classifier with  $\tau = 0.7$  in the first block. This enabled us to skip the offline calibration and allowed us to give participants immediate feedback of their ErrP detections. Afterwards, we tailored  $\tau$  to each participant. After each of the first 3 blocks, we performed offline an asynchronous classification with the generic ErrP classifier on all the available data and tested thresholds between 0 and 1 in steps of 0.025. For each of the 41 thresholds analysed, we calculated the corresponding TPR and TNR. The TNR and TPR curves were further smoothed using a moving average with 7 samples. The smoothed curves were named smooth TPR and smooth TNR. For every participant, we chose the threshold that maximized the product of the smooth TPR and the smooth TNR. This was considered the threshold that maximized performance and it was used in the next block. From block 4 onwards, the generic ErrP classifier was combined with the threshold  $\tau$  obtained after the third block. The generic ErrP classifier was not retrained with the participants' data and only the decision threshold was updated based on the data.

#### 2.15. Evaluation of the generic ErrP classifier

We stopped tailoring  $\tau$  to each participant after the third block because we wanted to collect a substantial amount of data in unchanged conditions. From blocks 4 to 8, all participants used the generic classifier with a fixed but personalized threshold. Therefore, we only use the data from blocks 4 to 8 to evaluate the performance of the generic classifier, ensuring comparable conditions across the participants.

#### 2.16. Personalized ErrP classifier

In order to evaluate, offline, the performance of a personalized classifier, we performed 10 times a 5-fold cross-validation in the entire dataset of each participant, where a personalized classifier was tested in an asynchronous manner in each fold. There, we also tested all thresholds from 0 to 1 in steps of 0.025. For every participant, we obtained, in each fold, a TPR and a TNR for every threshold tested. For every participant, we averaged the TPR and TNR of the 50 iterations in the cross-validation, obtaining an average TPR and an average TNR per participant. Finally, we selected the threshold that maximized the product of the average TPR and the average TNR, for every participant. The evaluation of the personalized classifier followed the metrics defined in the section *Metrics to evaluate the ErrP classifier*.

### 3. Results

#### 3.1. Neurophysiology

The electrophysiological results presented here comprise the entire recorded dataset. Figure 3 shows the grand average correct and error signals at channel FCz (green and red lines, respectively) for participants with SCI and control participants. The green and red shaded areas depict the 95% confidence interval for the grand average signals. The vertical line at  $t = 0$  s depicts the error onset of the error trials and the virtual onset of the correct trials. For the participants with SCI, the grand average error signal displays a negativity, with peak amplitude of  $-2.4 \mu\text{V}$  at time  $t = 0.154$  s after the error onset, followed by a positivity, with peak amplitude of  $3.8 \mu\text{V}$  at time  $t = 0.332$  s. For the control participants, the grand average error signal displays a negativity, with peak amplitude of  $-5.5 \mu\text{V}$  at time  $t = 0.176$  s after the error onset, followed by a positivity, with peak amplitude of  $5.8 \mu\text{V}$  at time  $t = 0.334$  s. The grand average correct signal displays no particular peaks, both in participants with SCI and control participants. Figure 3 displays also the topographic plots of the grand average correct and error signals at the time points of the peaks of the grand average error signal.

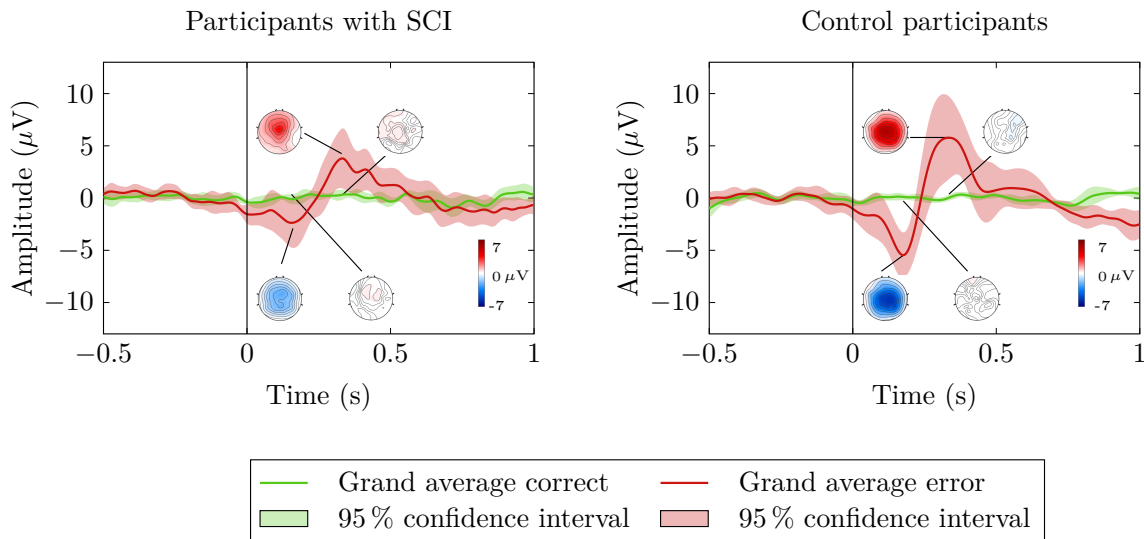


**Figure 3:** Grand average correct and error signals at channel FCz (green and red solid lines, respectively) for participants with SCI and control participants. The shaded areas represent the 95% confidence interval of the grand average curves. The vertical black line at  $t = 0$  s represents the error onset of the error trials and the virtual onset of the correct trials. The figure displays also the topographic plots of the grand-average correct and error signals at the time points of the peaks in the grand average error signal.

As the morphology of the error signals was not homogeneous across participants, we found it relevant to also present the electrophysiological results of the individual participants. Figure 4 displays the average correct and error signals at channel FCz

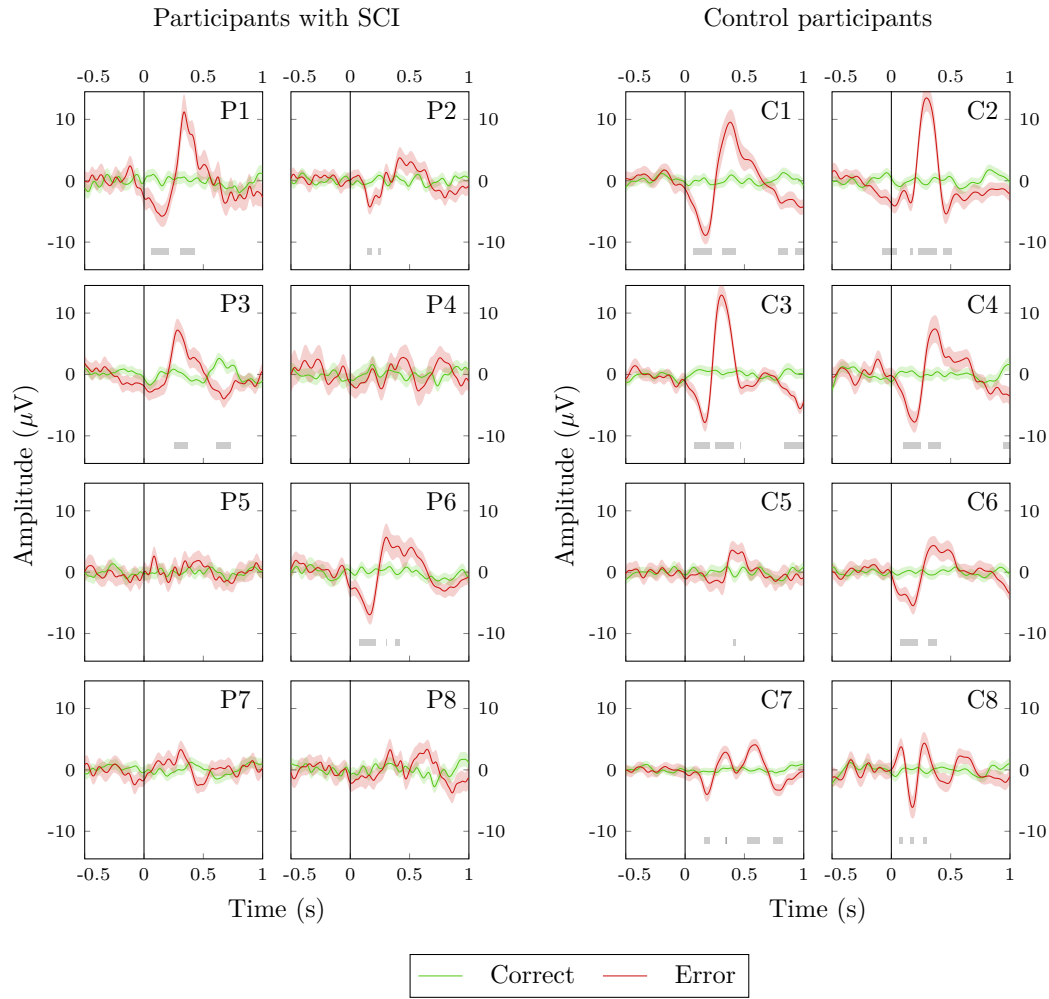


**Figure 4:** Average correct and error signals at channel FCz of every participant (green and red lines, respectively). The shaded areas represent the 95% confidence interval of the average signals. The black line at  $t = 0$  s represents the error onset of the error trials and the virtual onset of the correct trials. The grey regions indicate the time points in which correct and error signals were statistically different (Wilcoxon ranksum tests, Bonferroni corrected, with  $\alpha = 0.01$ ).

(green and red lines, respectively) of every participant. The green and red shaded areas depict the 95% confidence interval for the average signals. The grey areas indicate the time points in which correct and error signals were statistically different (Wilcoxon ranksum tests, Bonferroni corrected, with  $\alpha = 0.01$ ). Figures 6 and 7 of the supplementary material depict the topographic plots of the average correct and error signals of every participant at different time points.

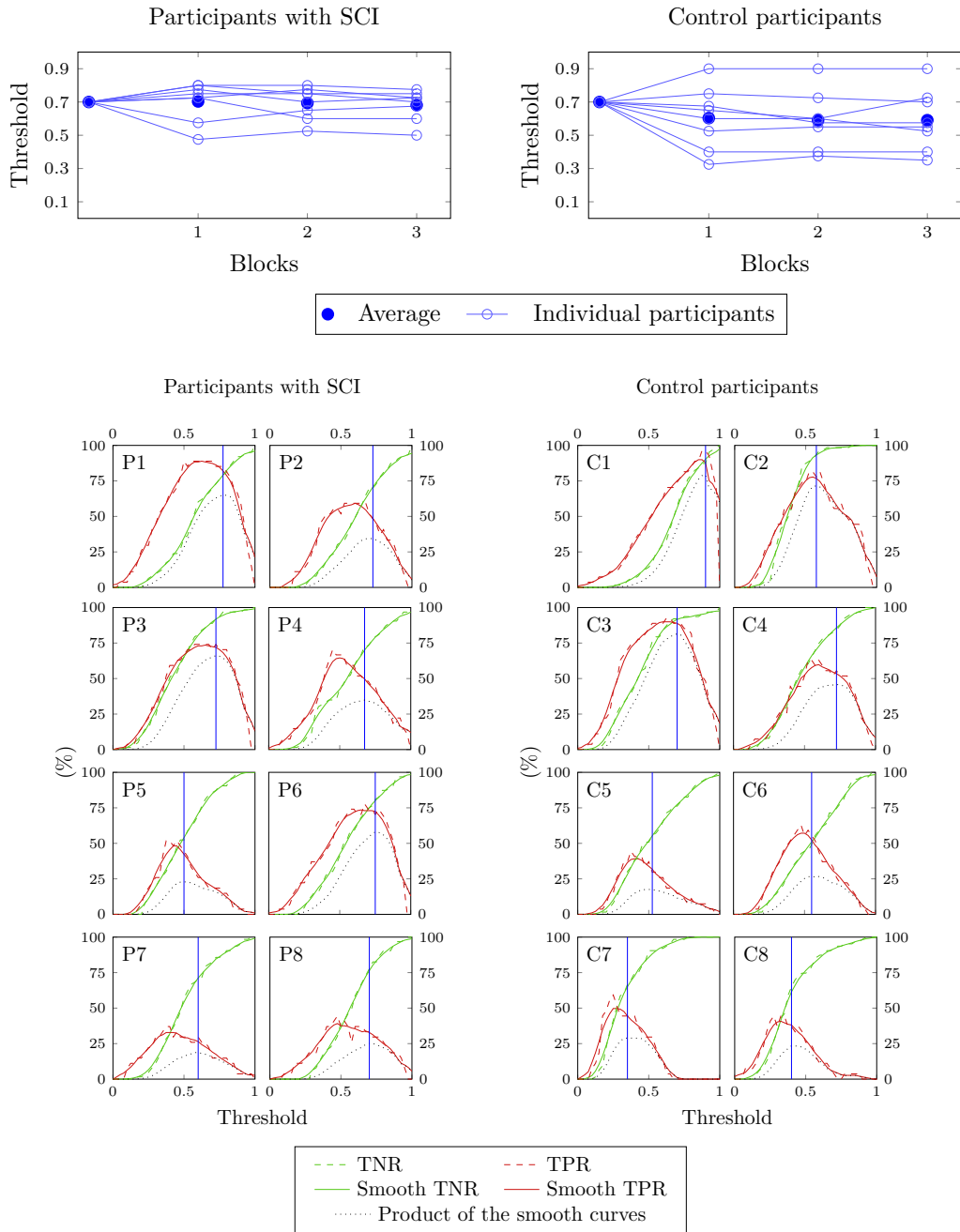


**Figure 5:** Optimization of the decision threshold used with the generic ErrP classifier. **Top:** Evolution of the decision threshold: Initial threshold ( $\tau = 0.7$ ) and the calculated thresholds after each of the first 3 blocks, for every participant. **Bottom:** TNR and TPR obtained offline, after the third block (dashed green and red lines, respectively) and the corresponding smooth curves (green and red solid lines). The blue line represents the threshold that maximizes the product of the smooth curves, which is represented with a black dotted line.



### 3.2. Adaptation of the classifier’s threshold in the first three experimental blocks

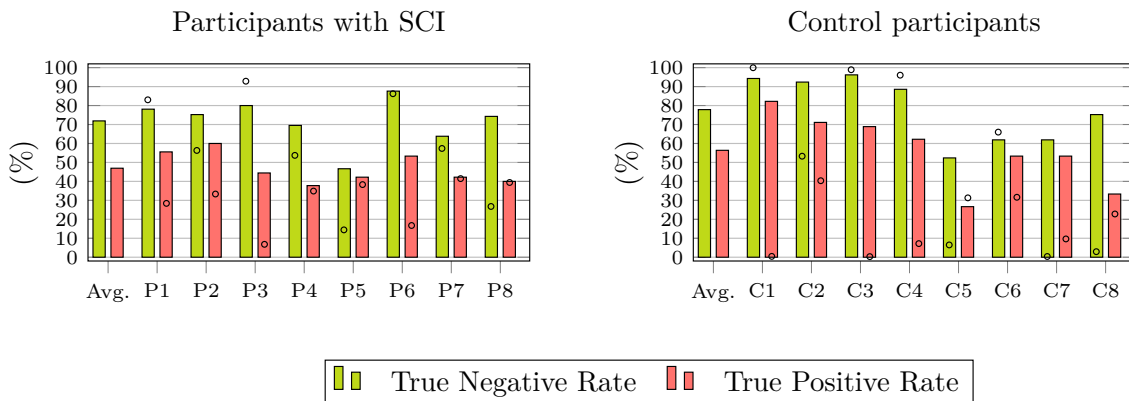
This experiment required no offline calibration and the participants received feedback regarding their ErrP detections from its very beginning. This was possible by combining the generic ErrP classifier with a generic decision threshold ( $\tau = 0.7$ ) for the first experimental block. Still, we used the first three experimental blocks to reach a fixed personalized decision threshold. After each of the first three blocks, we updated the decision threshold  $\tau$  in order to maximize the participant’s performance. Hence, participants used a generic classifier combined with a personalized decision threshold from block 2 onwards. Figure 5 (top) depicts the initial threshold ( $\tau = 0.7$ ) and the calculated thresholds after each of the first 3 blocks, for every participant. At the end of block 3, the average threshold was  $\tau = 0.68$  for the participants with SCI and  $\tau = 0.59$  for the control participants. Figure 5 (bottom) shows the TNR and TPR obtained offline after block 3, for all the tested thresholds (green and red dashed lines, respectively). It also shows the smooth TNR and smooth TPR, obtained with a moving average (green and red solid lines). The black dotted line depicts the product of these smooth curves and the blue vertical line indicates the threshold that maximizes it. This is the decision threshold used for every participant from blocks 4 to 8.

### 3.3. Evaluation of the online asynchronous classification with a generic ErrP classifier

To evaluate the asynchronous classification results obtained with the generic ErrP classifier during the experiment, we only considered the data of the last five blocks of the experiment, i.e., from blocks 4 to 8, since no parameters were changed during these blocks.

Figure 6 (top) depicts the classification results obtained with the generic classifier in terms of true positive rate (TPR) and true negative rate (TNR). For participants with SCI, we obtained an average TPR of 46.9% and an average TNR of 71.9%. For control participants, we obtained an average TPR of 56.4% and an average TNR of 77.9%. The circles on the individual bars represent the chance level of the corresponding metrics. The chance level results for each participant were obtained by averaging the classification results of 500 classifiers in which the training labels were randomly permuted and by considering the final participant-specific threshold, as depicted in Figure 4 of the supplementary material. Figure 6 (bottom) presents the permutation based  $p$ -values regarding the significance of the classification results [55, 56]. Figure 5 of the supplementary material depicts the comparison between the metrics TPR and EDR. Table 1 of the supplementary material presents the false activation rate (FAR) in correct and error trials.

Figure 7 illustrates the online asynchronous detection of ErrPs and the trials’ offline evaluation for participant C1. The dark grey areas represent the trials and the white marks within them represent the ErrP detections. The narrow rectangles colour code the trials’ offline evaluation. In these rectangles, trials successfully classified (true positive trials and true negative trials) are coded in white and trials with false positive ErrP



Participants with SCI				Control Participants					
Participants	p-value	TPR	p-value	TNR	Participants	p-value	TPR	p-value	TNR
P1		0.004		0.796	C1		0.002		1
P2		0.004		0.198	C2		0.002		0.002
P3		0.002		0.998	C3		0.002		1
P4		0.325		0.058	C4		0.002		0.968
P5		0.273		0.002	C5		0.719		0.002
P6		0.002		0.413	C6		0.014		0.653
P7		0.369		0.369	C7		0.002		0.002
P8		0.433		0.002	C8		0.098		0.002

**Figure 6:** Evaluation of the generic ErrP classifier. **Top:** Classification results in terms of true positive rate (TPR) and true negative rate (TNR). The circles on the individual bars represent the chance-level of the corresponding metrics. **Bottom:** Permutation based  $p$ -value regarding the significance of the results obtained with the classifier.

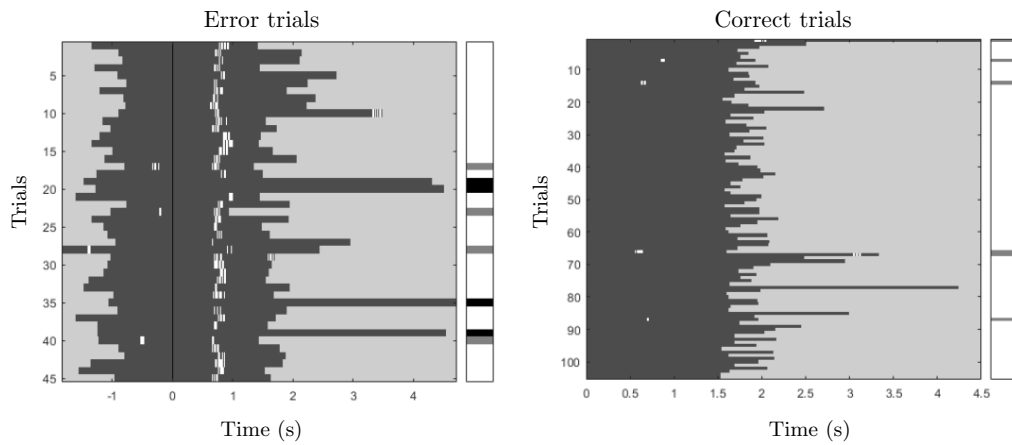
detections are coded in grey. The error trials with no ErrP detection are coded in black.

### 3.4. Offline evaluation of the asynchronous ErrP classification with a personalized classifier

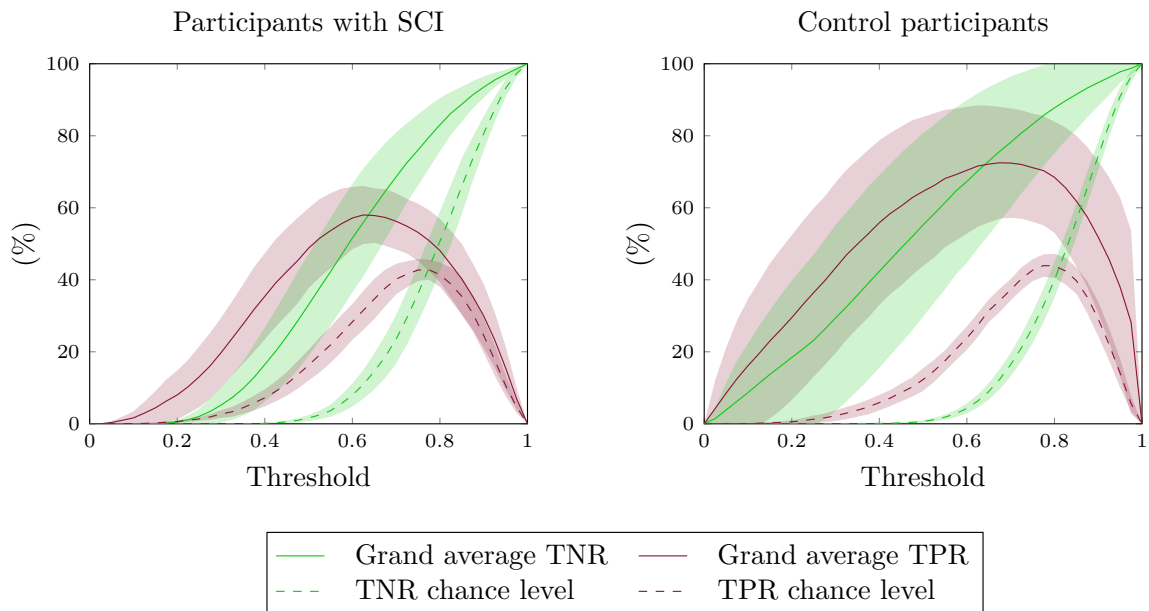
To evaluate offline the asynchronous classification results with a personalized classifier, we considered the 8 experimental blocks and performed 10 times a 5-fold cross-validation. As this evaluation was done offline, we tested thresholds from 0 to 1 with a leap of 0.025 and the results obtained are shown in function of the threshold  $\tau$ .

Figure 8 depicts the grand average TNR and TPR (green and red solid lines, respectively) as well as the grand average chance level for TNR and TPR (green and red dashed lines, respectively) in function of the threshold. The shaded areas represent the 95% confidence intervals of the grand average curves. The chance level curves were obtained by performing 10 times a 5-fold cross-validation with 50 classifiers in which the labels of the training trials were randomly permuted.

Figure 9 depicts, for every participant, the average TNR and TPR (green and red solid lines, respectively) and the chance level TNR and TPR (green and red dashed lines, respectively). The blue vertical line indicates the threshold that maximizes the individual performance with the personalized ErrP classifier.



**Figure 7:** Online detection of ErrPs and trials' offline evaluation for participant C1. Left: Error trials, aligned to the error onset (black vertical line). Right: Correct trials, aligned to the start of the trial. The dark grey areas represent the trials and the white marks within them represent the ErrP detections. The narrow rectangles colour code the trials' offline evaluation. In these rectangles, trials successfully classified (true positive trials and true negative trials) are coded in white and trials with false positive ErrP detections are coded in light grey. Error trials with no ErrP detections are coded in black.



**Figure 8:** Evaluation of the personalized ErrP classifier. Grand average TNR and TPR (green and red solid lines, respectively) and grand average chance level TNR and TPR (green and red dashed lines, respectively) in function of the threshold. The shaded areas indicate the 95% confidence interval for the grand average curves.

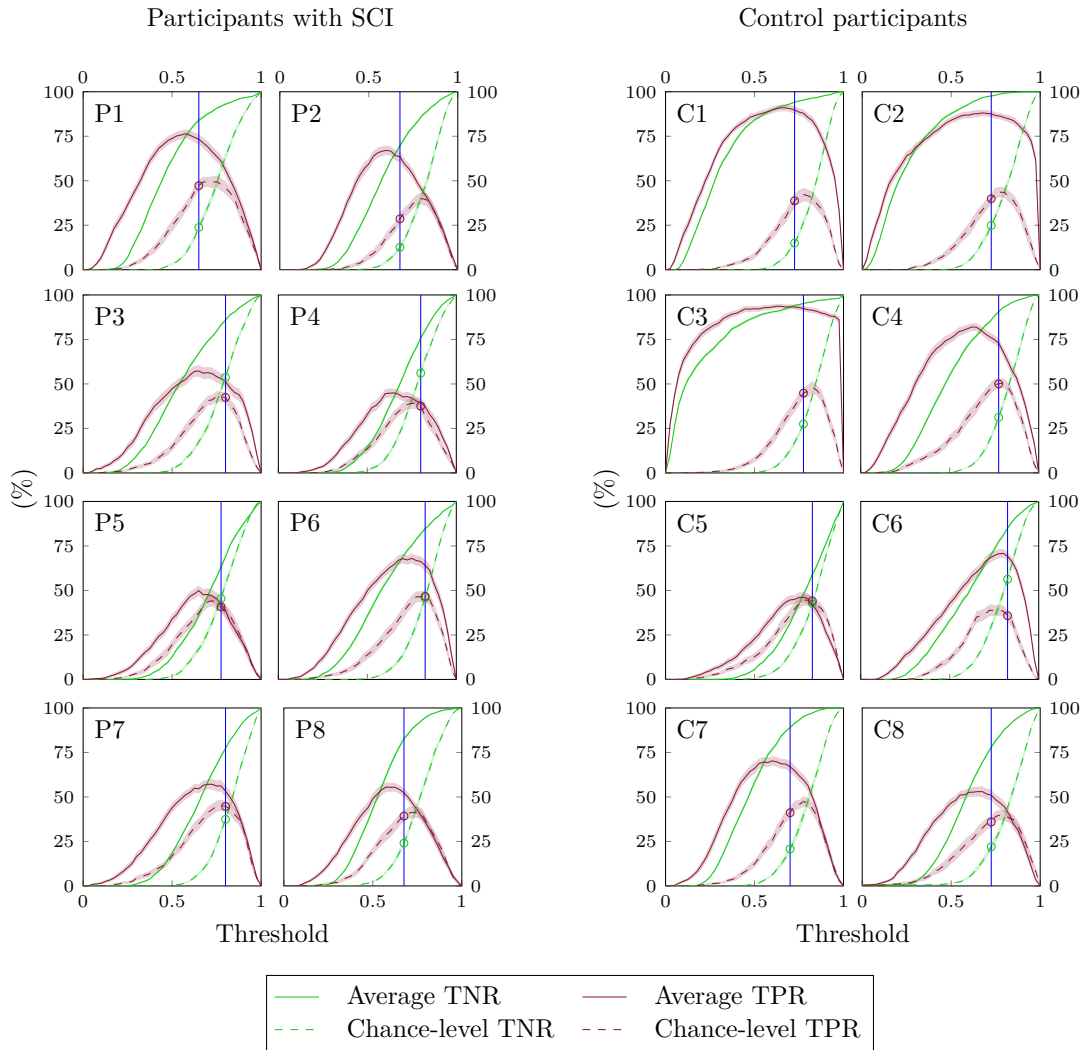


**Figure 9:** Evaluation of the personalized ErrP classifier. Single subject average TNR and TPR (green and red solid lines, respectively) and chance level TNR and TPR in function of the threshold (green and red dashed lines, respectively). The shaded areas indicate the 95 % confidence interval for the average curves. The blue vertical line indicates the threshold that maximizes the individual performance.

Figure 10 depicts the average TNR and TPR obtained in the cross-validation, when using the optimal personalized decision threshold for every participant (green and red bars, respectively). The small circles on the bars indicate the chance level obtained for every participant with the considered threshold. For participants with SCI, the grand average TNR was 77.9% and the grand average TPR was 55.0%. For control participants, the grand average TNR was 86.1 % and the grand average TPR was 71.5 %.

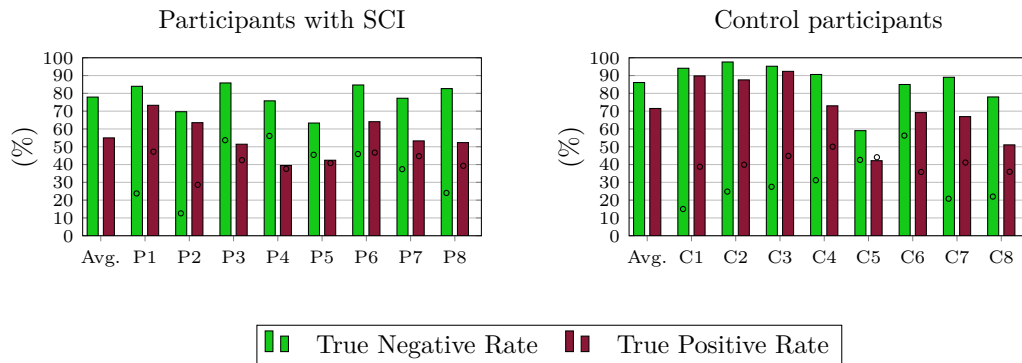


**Figure 10:** Evaluation of the personalized ErrP classifier. Average TNR and TPR calculated from the cross-validation procedure, with the optimal personalized threshold, for every participant and their average. The small dots on each bar indicate the chance level with the considered threshold, for every participant.

#### 4. Discussion

In this work we investigated the transfer of a generic ErrP classifier from able-bodied participants to participants with SCI. The classifier was developed using the data from able-bodied participants from a previous experiment of ours [35] and was tested asynchronously in a closed-loop online experiment in which participants with SCI and able-bodied control participants took part. Using the classifier asynchronously, the entire trials were evaluated and not only a time-locked window. The online experiment required no offline calibration period and the participants received feedback of the ErrP detections immediately from the start of the experiment onwards. Additionally, we also analysed the morphology of error-related potentials in participants with SCI and in able-bodied control participants.

The grand average correct signal displayed, as expected, no particular potential both in participants with SCI and in control participants. The correct epochs correspond to the period in which the participants were continuously controlling the robot and were not associated with any specific event. The grand average error signal was associated with a fronto-central activity both in participants with SCI and control participants. The peaks of the grand average error signal were less pronounced in participants with SCI than in control participants, as visible in Figure 3. This matches the results described in [46]. Nevertheless, the electrophysiological patterns of participants with SCI were rather heterogeneous and half of the participants with SCI did not display the characteristic error-related activity (participants P4, P5, P7 and P8). The remaining participants with SCI revealed patterns comparable to control participants. Therefore, we believe that in our study the decrease in peak amplitudes observed in the grand average error signal of participants with SCI is not directly related with the injury, but rather a consequence of heterogeneity of the signals in the population with SCI. Several studies reported the effect of psychological factors, such as depression and anxiety, on

error-related potentials [58, 59]. The population with SCI is particularly vulnerable to emotional disorders and higher levels of distress [60–62]. Nevertheless, individual differences are large [62]. To consider a psychiatric evaluation and medication of the participants would have been valuable for the current work and should be considered in future studies involving a population with SCI [63]. Interestingly, the error signals of control participants were also less homogeneous than in our previous studies with a similar experimental protocol [34, 35]. Several studies showed that ageing affects error processing and consequently the error-related potentials, hence we hypothesise that the higher variability observed in the signals of control participants of this study is related to the wider age range of the participants in comparison with previous studies [64–66].

In order to interpret the classification results we focus on the TPR. This metric considers an interval after the error onset and the period before the error onset. Hence, it translates not only the classifier’s ability to decode ErrPs after the occurrence of an error but also its ability to not detect ErrPs when no error occurs. The TNR only captures the classifier’s ability to not detect ErrPs when no error occurs. It is still a meaningful metric but the TNR’s outcome can be artificially increased by the use of a high decision threshold, as depicted in Figure 4 of the supplementary material. The classification results of the generic classifier were, on average, lower in participants with SCI than in control participants. Only half of the participants with SCI obtained a TPR above chance level. These participants were the ones that displayed clear error patterns. In the control participants, seven out of eight participants obtained a TPR above chance level. The remaining participant (participant C5) did not obtain a TPR above chance level and did not display a very clear error signal. Summarizing, all participants that displayed clear ErrP patterns in the electrophysiological analysis obtained above chance level results with the generic classifier, independently of the group (SCI or control). It would be rather interesting to further investigate the factors that affect the error patterns, independently of the spinal cord injury. These results support that using a generic ErrP classifier is a valuable option to give immediate feedback to the participants. Moreover, it indicates that ErrPs are transferable across participants, and that the transfer can be applied to distinct populations, such as participants with SCI.

With the generic classifier developed, participants received real-time feedback of the ErrP detections from the beginning of the experiment. Still, the first three blocks of the experiment were used to update the threshold applied to the generic classifier. We made this choice because we had previously shown that some participants strongly benefit from combining the generic ErrP classifier with a personalized decision threshold [44]. For most participants, the threshold was relatively stable after the first block. This supports the use of a personalized threshold with the generic classifier, as suggested in [44]. In a real-world online application, the occurrence of errors can not be easily assessed, since it is determined by a subjective perception of the BCI user. Such a constraint hinders an objective evaluation of any ErrP classifier, unless the participants can use a motor-based strategy to report the occurrence of errors. Still, our approach could be applied to a real-world asynchronous situation in which the occurrence of errors

is unknown. Nevertheless, in order to establish a personalized decision threshold, our approach would need, beforehand, a short online application in which the occurrence of errors is known. Such application could be the equivalent of one of our experimental blocks, which contained 9 errors and lasted less than 5 minutes.

In our experiment, we only gave participants feedback of the ErrPs detected after the error onset. This aimed to assure that participants experienced the same number of errors and had comparable expectations regarding the occurrence of errors. Providing participants with feedback of the false positive ErrP detections would have brought our experiment closer to a real-world application at the cost of putting participants in dissimilar circumstances, given that false positive ErrP detections could affect their behaviour and the generation of ErrPs. For instance, participants with many false positive ErrP detections would certainly be affected by the feedback in a negative manner. Either by losing engagement or by disregarding the feedback. Such participants would no longer perceive the errors as meaningful and relevant and this could alter their ErrPs.

When testing offline, the asynchronous classification with a personalized classifier, two participants with SCI (participants P4 and P5) and one control participant (participant C5) obtained chance level TPR results. This indicates that the signals of these participants were not sufficiently different to build a personalized classifier and these participants obtained chance level results with both generic and personalized classifiers.

The classification results obtained with the personalized classifier are not directly comparable with the results obtained with the generic classifier because the classifiers were evaluated on different datasets. In a real-world scenario, we could provide participants immediate feedback of their brain signals using a generic classifier, while collecting data to train a personalized classifier. Simultaneously, we could compare, at regular intervals, the performance of the personalized and generic classifiers and swap the generic classifier for a personalized classifier, once the latter would grant significantly better performance.

## 5. Conclusion

Our work shows that a generic ErrP classifier can be used, asynchronously and online, by participants with SCI and able-bodied participants. Moreover, the generic ErrP classifier is transferable from an able-bodied population to a population with SCI. The developed classifier required no previous calibration with the participant and granted immediate feedback of the ErrP detections. Therefore, our findings can help to widespread the incorporation of ErrPs in BCIs for different types of users.

### 5.1. Acknowledgements

This work was supported by Horizon 2020 ERC Consolidator Grant 681231 ‘Feel Your Reach’. The authors would like to thank Reinmar J. Kobler, Lea Hehenberger and Joana Pereira for the fruitful discussions. The authors would also like to thank the staff and patients of the AUVA-Rehabilitationsklinik Tobelbad for the warm welcome.

## 6. References

- [1] C. Brunner, N. Birbaumer, B. Blankertz, C. Guger, A. Kübler, D. Mattia, J. del R Millán, F. Miralles, A. Nijholt, E. Opisso, N. Ramsey, P. Salomon, and G. R. Müller-Putz, “BNCI Horizon 2020: towards a roadmap for the BCI community,” *Brain-Computer Interfaces*, vol. 2, no. 1, pp. 1–10, 2015.
- [2] J. d. R. Millán, R. Rupp, G. Müller-Putz, R. Murray-Smith, C. Giugliemma, M. Tangermann, C. Vidaurre, F. Cincotti, A. Kübler, R. Leeb, C. Neuper, K. Müller, and D. Mattia, “Combining brain–computer interfaces and assistive technologies: State-of-the-art and challenges,” *Frontiers in Neuroscience*, vol. 4, p. 161, 2010.
- [3] J. R. Wolpaw, N. Birbaumer, D. J. McFarland, G. Pfurtscheller, and T. M. Vaughan, “Brain–computer interfaces for communication and control,” *Clinical Neurophysiology*, vol. 113, no. 6, pp. 767 – 791, 2002.
- [4] G. Schalk, J. R. Wolpaw, D. J. McFarland, and G. Pfurtscheller, “EEG-based communication: presence of an error potential,” *Clinical Neurophysiology*, vol. 111, no. 12, pp. 2138 – 2144, 2000.
- [5] P. W. Ferrez and J. d. R. Millán, “You are wrong!: Automatic detection of interaction errors from brain waves,” in *Proceedings of the 19th International Joint Conference on Artificial Intelligence, IJCAI’05*, pp. 1413–1418, 2005.
- [6] N. Yeung, M. Botvinick, and J. D Cohen, “The neural basis of error detection: Conflict monitoring and the error-related negativity,” *Psychological review*, vol. 111, pp. 931–59, 11 2004.
- [7] R. Chavarriaga, A. Sobolewski, and J. d. R. Millán, “Errare machinale est: the use of error-related potentials in brain-machine interfaces,” *Frontiers in Neuroscience*, vol. 8, p. 208, 2014.
- [8] A. Llera, M. A. van Gerven, V. Gómez, O. Jensen, and H. J. Kappen, “On the use of interaction error potentials for adaptive brain computer interfaces,” *Neural Networks*, vol. 24, no. 10, pp. 1120–1127, 2011.
- [9] A. Llera, V. Gómez, and H. J. Kappen, “Adaptive classification on brain-computer interfaces using reinforcement signals,” *Neural Computation*, vol. 24, no. 11, pp. 2900–2923, 2012.
- [10] R. Yousefi, A. R. Sereshkeh, and T. Chau, “Online detection of error-related potentials in multi-class cognitive task-based bcis,” *Brain-Computer Interfaces*, vol. 6, no. 1-2, pp. 1–12, 2019.
- [11] X. Artusi, I. K. Niazi, M.-F. Lucas, and D. Farina, “Accuracy of a BCI based on movement-related and error potentials,” in *2011 Annual International Conference of the IEEE Engineering in Medicine and Biology Society*, pp. 3688–3691, Aug 2011.
- [12] H. Zhang, R. Chavarriaga, Z. Khaliliardali, L. Gheorghe, I. Iturrate, and J. d. R. M. , “EEG-based decoding of error-related brain activity in a real-world driving task,” *Journal of Neural Engineering*, vol. 12, p. 066028, nov 2015.
- [13] M. Spüler and C. Niethammer, “Error-related potentials during continuous feedback: using EEG to detect errors of different type and severity,” *Frontiers in Human Neuroscience*, vol. 9, p. 155, 2015.
- [14] A. Kreiling, H. Hiebel, and G. R. Müller-Putz, “Single versus multiple events error potential detection in a BCI-controlled car game with continuous and discrete feedback,” *IEEE Transactions on Biomedical Engineering*, vol. 63, no. 3, pp. 519–529, 2016.
- [15] H. Si-Mohammed, C. Lopes-Dias, M. Duarte, F. Argelaguet, C. Jeunet, G. Casiez, G. R. Müller-Putz, A. Lécuyer, and R. Scherer, “Detecting system errors in virtual reality using eeg through



- error-related potentials,” in *2020 IEEE Conference on Virtual Reality and 3D User Interfaces (VR)*, pp. 653–661, 2020.
- [16] L. C. Parra, C. D. Spence, A. D. Gerson, and P. Sajda, “Response error correction - a demonstration of improved human-machine performance using real-time EEG monitoring,” *IEEE Transactions on Neural Systems and Rehabilitation Engineering*, vol. 11, pp. 173–177, June 2003.
- [17] A. Kreiling, C. Neuper, and G. R. Müller-Putz, “Error potential detection during continuous movement of an artificial arm controlled by brain–computer interface,” *Medical & Biological Engineering & Computing*, vol. 50, no. 3, pp. 223–230, 2012.
- [18] T. Zander, L. Krol, N. Birbaumer, and K. Gramann, “Neuroadaptive technology enables implicit cursor control based on medial prefrontal cortex activity,” in *Proceedings of the National Academy of Sciences of the United States of America*, vol. 113(12), pp. 14898–14903, Dez 2016.
- [19] A. F. Salazar-Gomez, J. DelPreto, S. Gil, F. H. Guenther, and D. Rus, “Correcting robot mistakes in real time using EEG signals,” *2017 IEEE International Conference on Robotics and Automation (ICRA)*, pp. 6570–6577, May 2017.
- [20] S.-K. Kim, E. A. Kirchner, A. Stefes, and F. Kirchner, “Intrinsic interactive reinforcement learning - using error-related potentials for real world human-robot interaction,” *Scientific Reports (Sci Rep)*, vol. 7: 17562, 12 2017.
- [21] M. Mousavi, A. S. Koerner, Q. Zhang, E. Noh, and V. R. de Sa, “Improving motor imagery BCI with user response to feedback,” *Brain-Computer Interfaces*, vol. 4, no. 1-2, pp. 74–86, 2017.
- [22] S. K. Ehrlich and G. Cheng, “Human-agent co-adaptation using error-related potentials,” *Journal of Neural Engineering*, vol. 15, p. 066014, sep 2018.
- [23] M. Spüler, M. Bensch, S. Kleih, W. Rosenstiel, M. Bogdan, and A. Kübler, “Online use of error-related potentials in healthy users and people with severe motor impairment increases performance of a P300-BCI,” *Clinical Neurophysiology*, vol. 123, no. 7, pp. 1328 – 1337, 2012.
- [24] R. J. Kobler, A. I. Sburlea, and G. R. Müller-Putz, “Tuning characteristics of low-frequency eeg to positions and velocities in visuomotor and oculomotor tracking tasks,” *Scientific Reports*, vol. 8, no. 1, p. 17713, 2018.
- [25] P. Ofner and G. R. Müller-Putz, “Decoding of velocities and positions of 3D arm movement from EEG,” in *2012 Annual International Conference of the IEEE Engineering in Medicine and Biology Society*, pp. 6406–6409, Aug 2012.
- [26] Y. Inoue, H. Mao, S. B. Suway, J. Orellana, and A. B. Schwartz, “Decoding arm speed during reaching,” *Nature Communications*, vol. 9, no. 1, p. 5243, 2018.
- [27] A. A. Nooh, J. Yunus, and S. M. Daud, “A review of asynchronous electroencephalogram-based brain computer interface systems,” in *International Conference on Biomedical Engineering and Technology*, 2011.
- [28] B. Z. Allison, C. Brunner, C. Altstätter, I. C. Wagner, S. Grissmann, and C. Neuper, “A hybrid ERD/SSVEP BCI for continuous simultaneous two dimensional cursor control,” *Journal of Neuroscience Methods*, vol. 209, no. 2, pp. 299 – 307, 2012.
- [29] J. Omedes, I. Iturrate, and L. Montesano, “Detection of event-less error related potentials,” in *Proceedings of IROS 2013 Workshop on Neuroscience and Robotics ”Towards a robot-enabled, neuroscience-guided healthy society”*, 2013.
- [30] J. Omedes, I. Iturrate, and L. Montesano, “Asynchronous detection of error potentials,” in *Proceedings of the 6th Brain-Computer Interface Conference 2014*, 2014.
- [31] J. Omedes, I. Iturrate, J. Minguez, and L. Montesano, “Analysis and asynchronous detection of gradually unfolding errors during monitoring tasks,” *Journal of Neural Engineering*, vol. 12, no. 5, p. 056001, 2015.
- [32] J. Omedes, I. Iturrate, R. Chavarriaga, and L. Montesano, “Asynchronous decoding of error potentials during the monitoring of a reaching task,” in *2015 IEEE International Conference on Systems, Man, and Cybernetics (SMC2015)*, pp. 3116–3121, Oct 2015.
- [33] C. Lopes-Dias, A. I. Sburlea, and G. R. Müller-Putz, “Error-related potentials with masked and

- unmasked onset during continuous control and feedback,” in *7th Graz Brain-Computer Interface Conference 2017*, pp. 320–332, September 2017.
- [34] C. Lopes-Dias, A. I. Sburlea, and G. R. Müller-Putz, “Masked and unmasked error-related potentials during continuous control and feedback,” *Journal of Neural Engineering*, vol. 15, p. 036031, apr 2018.
- [35] C. Lopes-Dias, A. I. Sburlea, and G. R. Müller-Putz, “Online asynchronous decoding of error-related potentials during the continuous control of a robot,” *Scientific Reports*, vol. 9, no. 1, p. 17596, 2019.
- [36] I. Iturrate, L. Montesano, R. Chavarriaga, J. del R. Millán, and J. Minguez, “Minimizing calibration time using inter-subject information of single-trial recognition of error potentials in brain-computer interfaces,” in *2011 Annual International Conference of the IEEE Engineering in Medicine and Biology Society*, pp. 6369–6372, 2011.
- [37] I. Iturrate, R. Chavarriaga, L. Montesano, J. Minguez, and J. d. R. Millán, “Latency correction of error potentials between different experiments reduces calibration time for single-trial classification,” in *2012 Annual International Conference of the IEEE Engineering in Medicine and Biology Society*, pp. 3288–3291, Aug 2012.
- [38] I. Iturrate, R. Chavarriaga, L. Montesano, J. Minguez, and J. Millán, “Latency correction of event-related potentials between different experimental protocols,” *Journal of Neural Engineering*, vol. 11, p. 036005, apr 2014.
- [39] S. K. Kim and E. A. Kirchner, “Handling few training data: Classifier transfer between different types of error-related potentials,” *IEEE Transactions on Neural Systems and Rehabilitation Engineering*, vol. 24, pp. 320–332, March 2016.
- [40] S. K. Kim and E. A. Kirchner, “Classifier transferability in the detection of error related potentials from observation to interaction,” in *2013 IEEE International Conference on Systems, Man, and Cybernetics*, pp. 3360–3365, Oct 2013.
- [41] S. Bhattacharyya, A. Konar, D. N. Tibarewala, and M. Hayashibe, “A generic transferable EEG decoder for online detection of error potential in target selection,” *Frontiers in Neuroscience*, vol. 11, p. 226, 2017.
- [42] S. K. Ehrlich and G. Cheng, “A feasibility study for validating robot actions using EEG-based error-related potentials,” *International Journal of Social Robotics*, Nov 2018.
- [43] F. M. Schönleitner, L. Otter, S. K. Ehrlich, and G. Cheng, “Calibration-free error-related potential decoding with adaptive subject-independent models: A comparative study,” *IEEE Transactions on Medical Robotics and Bionics*, vol. 2, no. 3, pp. 399–409, 2020.
- [44] C. Lopes-Dias, A. I. Sburlea, and G. R. Müller-Putz, “Asynchronous detection of error-related potentials using a generic classifier,” in *8th International Brain Computer Interface Conference 2019*, Sep 2019.
- [45] C. Lopes-Dias, A. I. Sburlea, and G. R. Müller-Putz, “Generic error-related potential classifier offers a comparable performance to a personalized classifier,” in *EMBC*, 2020.
- [46] P. Keyl, M. Schneiders, C. Schuld, S. Franz, M. Hommelsen, N. Weidner, and R. Rupp, “Differences in characteristics of error-related potentials between individuals with spinal cord injury and age- and sex-matched able-bodied controls,” *Frontiers in Neurology*, vol. 9, p. 1192, 2019.
- [47] A. Kumar, Q. Fang, J. Fu, E. Pirogova, and X. Gu, “Error-related neural responses recorded by electroencephalography during post-stroke rehabilitation movements,” *Frontiers in Neurorobotics*, vol. 13, p. 107, 2019.
- [48] R. J. Kobler, A. I. Sburlea, and G. R. Müller-Putz, “A comparison of ocular artifact removal methods for block design based electroencephalography experiments,” in *Proceedings of the 7th Graz Brain-Computer Interface Conference 2017*, Sep 2017.
- [49] R. J. Kobler, “Corneo-retinal-dipole and eyelid-related eye artifacts can be corrected offline and online in electroencephalographic and magneticencephalographic signals,” *NeuroImage*, 2020.
- [50] B. Blankertz, S. Lemm, M. Treder, S. Haufe, and K.-R. Müller, “Single-trial analysis and classification of ERP components — a tutorial,” *NeuroImage*, vol. 56, no. 2, pp. 814 – 825,

2011. Multivariate Decoding and Brain Reading.
- [51] G. A. Giraldi, P. S. Rodrigues, E. C. Kitani, J. R. Sato, and C. E. Thomaz, “Statistical learning approaches for discriminant features selection,” *Journal of the Brazilian Computer Society*, vol. 14, pp. 7–22, Jun 2008.
- [52] E. López-Larraz, L. Montesano, Á. Gil-Agudo, and J. Minguez, “Continuous decoding of movement intention of upper limb self-initiated analytic movements from pre-movement eeg correlates,” *Journal of NeuroEngineering and Rehabilitation*, vol. 11, p. 153, Nov 2014.
- [53] A. I. Sburlea, L. Montesano, and J. Minguez, “Continuous detection of the self-initiated walking pre-movement state from EEG correlates without session-to-session recalibration,” *Journal of Neural Engineering*, vol. 12, p. 036007, apr 2015.
- [54] J. Pereira, A. I. Sburlea, and G. R. Müller-Putz, “Eeg patterns of self-paced movement imaginations towards externally-cued and internally-selected targets,” *Scientific Reports*, vol. 8, p. 13394, Sep 2018.
- [55] P. Good and P. Good, *Permutation Tests: A Practical Guide to Resampling Methods for Testing Hypotheses*. Springer series in statistics, Springer, 2000.
- [56] M. Ojala and G. C. Garriga, “Permutation tests for studying classifier performance,” *J. Mach. Learn. Res.*, vol. 11, p. 1833–1863, Aug. 2010.
- [57] M. Fatourech, R. Ward, and G. Birch, “Evaluating the performance of a self-paced bci with a new movement and using a more engaging environment,” *Conference proceedings: Annual International Conference of the IEEE Engineering in Medicine and Biology Society. IEEE Engineering in Medicine and Biology Society. Conference*, vol. 2008, pp. 650–3, 02 2008.
- [58] M. Ruchow, B. Herrnberger, P. Beschoner, G. Grön, M. Spitzer, and M. Kiefer, “Error processing in major depressive disorder: Evidence from event-related potentials,” *Journal of Psychiatric Research*, vol. 40, no. 1, pp. 37 – 46, 2006.
- [59] D. M. Olvet, D. N. Klein, and G. Hajcak, “Depression symptom severity and error-related brain activity,” *Psychiatry Research*, vol. 179, no. 1, pp. 30 – 37, 2010.
- [60] Z. Khazaepour, S.-M. Taheri-Otaghsara, and M. Naghdi, “Depression following spinal cord injury: Its relationship to demographic and socioeconomic indicators,” *Topics in spinal cord injury rehabilitation*, vol. 21, no. 2, pp. 149–155, 2015. 26364284[pmid].
- [61] C. Migliorini, B. Tonge, and G. Taleporos, “Spinal cord injury and mental health,” *Australian & New Zealand Journal of Psychiatry*, vol. 42, no. 4, pp. 309–314, 2008. PMID: 18330773.
- [62] M. W. M. Post and C. M. C. van Leeuwen, “Psychosocial issues in spinal cord injury: a review,” *Spinal Cord*, vol. 50, no. 5, pp. 382–389, 2012.
- [63] C. M. C. van Leeuwen, L. H. V. van der Woude, and M. W. M. Post, “Validity of the mental health subscale of the sf-36 in persons with spinal cord injury,” *Spinal Cord*, vol. 50, no. 9, pp. 707–710, 2012.
- [64] M. Falkenstein, J. Hoormann, and J. Hohnsbein, “Changes of error-related ERPs with age,” *Experimental Brain Research*, vol. 138, no. 2, pp. 258–262, 2001.
- [65] S. Hoffmann and M. Falkenstein, “Aging and error processing: age related increase in the variability of the error-negativity is not accompanied by increase in response variability,” *PloS one*, vol. 6, pp. e17482–e17482, Feb 2011.
- [66] S. Nieuwenhuis, K. R. Ridderinkhof, D. Talsma, M. G. H. Coles, C. B. Holroyd, A. Kok, and M. W. van der Molen, “A computational account of altered error processing in older age: Dopamine and the error-related negativity,” *Cognitive, Affective, & Behavioral Neuroscience*, vol. 2, no. 1, pp. 19–36, 2002.

# Online asynchronous detection of error-related potentials in participants with spinal cord injury by adapting a pre-trained generic classifier

Catarina Lopes-Dias<sup>1</sup>, Andreea I. Sburlea<sup>1</sup>, Katharina Breitegger<sup>2</sup>, Daniela Wyss<sup>2</sup>, Harald Drescher<sup>2</sup>, Renate Wildburger<sup>2</sup> and Gernot R. Müller-Putz<sup>1</sup>

Figure 1 shows the location of the 61 EEG electrodes used in the experiment. Figure 2 displays the grand average of the features used to train the generic ErrP classifier. Figure 3 depicts the pattern of the generic ErrP classifier. Figure 4 displays the average TPR and TNR obtained from 500 generic classifiers in which the training labels were randomly permuted. Figure 5 defines the metric 'ErrP detection rate' and depicts it together with the true positive rate, for all participants. Table 1 presents the false activation rate of every participant for correct and error trials. Figures 6 and 7 display the topographic plots for correct and error signals at different time points for participants with SCI and control participants.

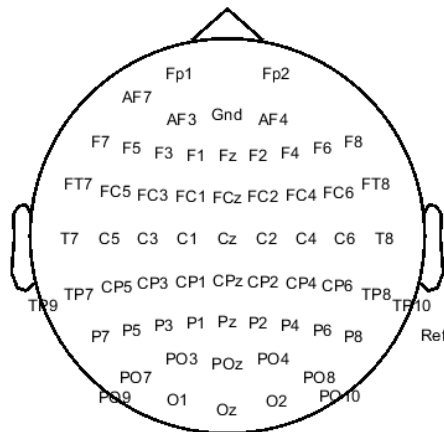


**Figure 1: Layout of the EEG electrodes:** Location of the 61 EEG electrodes used in the experiment. The ground electrode was placed at position AFz and the reference electrode was placed on the right mastoid.

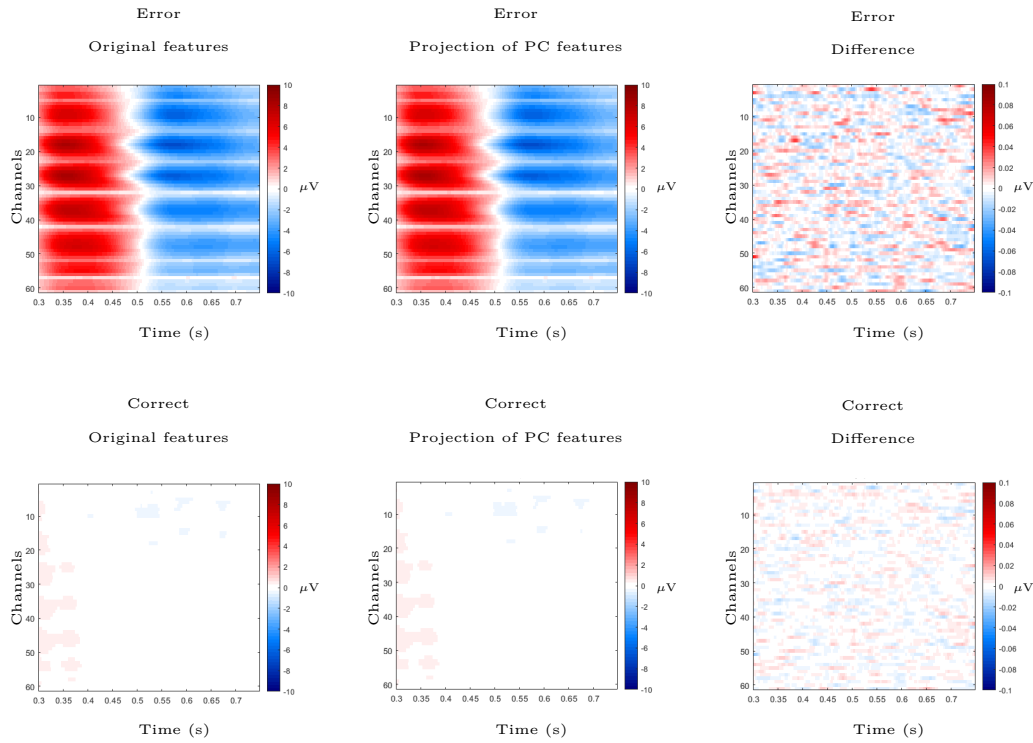


**Figure 2:** Grand average features of the generic classifier. **Left:** Grand average of the 1059 error epochs and of the 2475 correct epochs of the original feature space. **Middle:** Grand average of the projection into the temporal-spatial domain of the training matrix with 412 features, for error and correct epochs. The 412 features correspond to the principal components (PC) retained after PCA. **Right:** Difference between the grand average of the original feature space and the grand average of the projection of PCA features. The channels are ordered from left to right and from front to back.

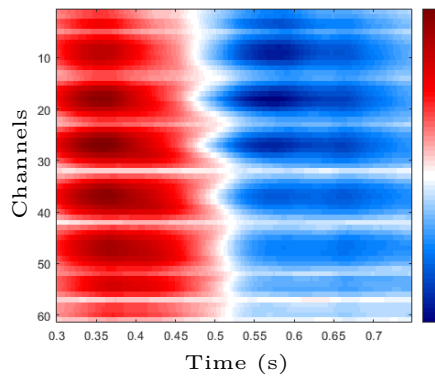


**Figure 3:** Generic classifier pattern: Pattern obtained by applying the discriminative feature analysis (DFA) method to the training matrix with 3534 trials and 412 features, used to train the shrinkage LDA classifier. The channels are ordered from left to right and from front to back.

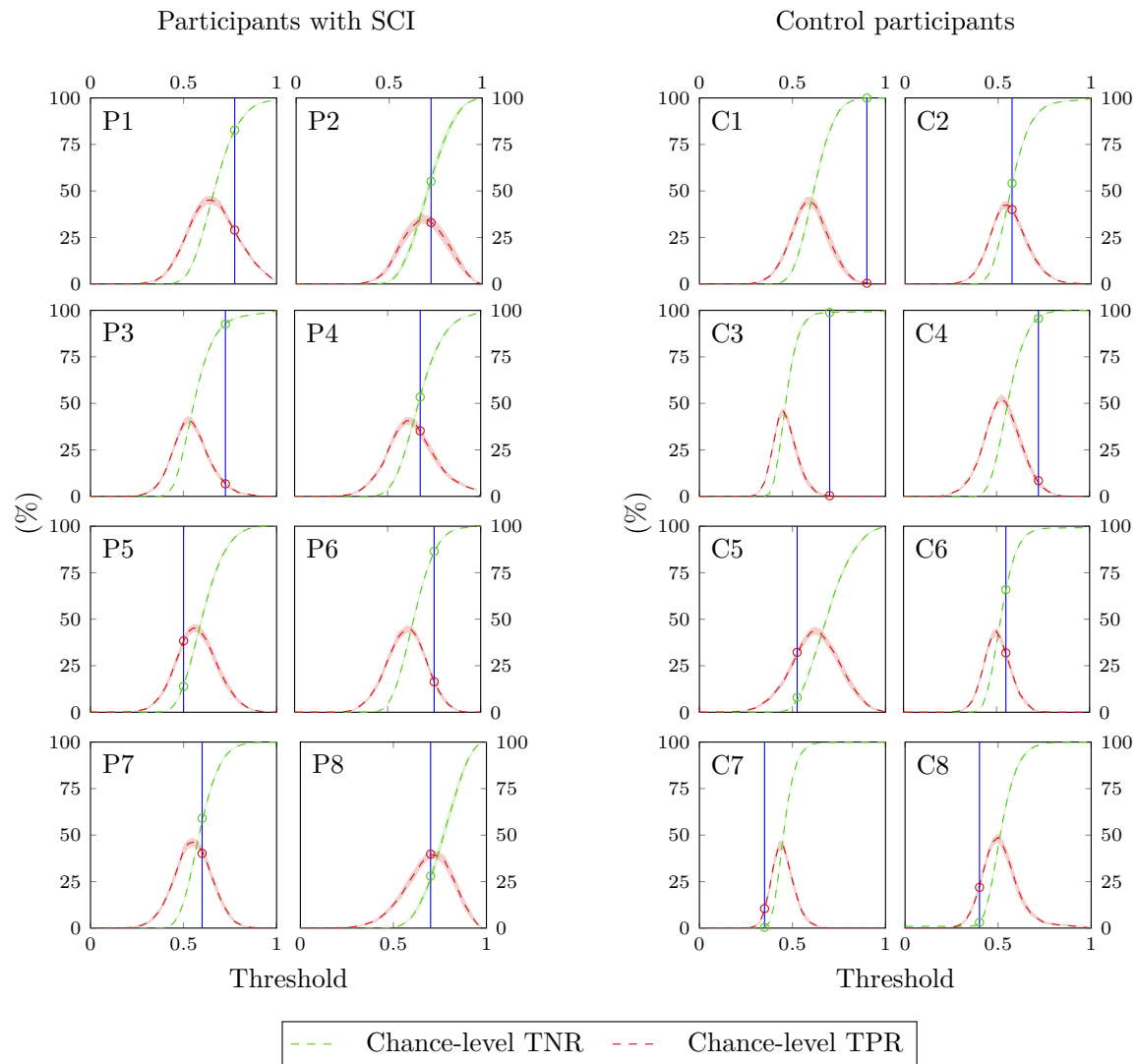


**Figure 4:** Chance level of the generic ErrP classifier: Average TPR and TNR obtained from 500 generic classifiers in which the training labels were randomly permuted (dashed red and green lines, respectively). These classifiers were evaluated on blocks 4 to 8 of every participant. The shaded areas indicate the 95% confidence interval of the average curves. The vertical blue line indicates the threshold used for every participant during blocks 4 to 8 of the online experiment, obtained as described in Figure 5 of the manuscript. The chance levels depicted in Figure 6 of the manuscript, result from the intersection of the vertical threshold line with the average curves of TNR and TPR.

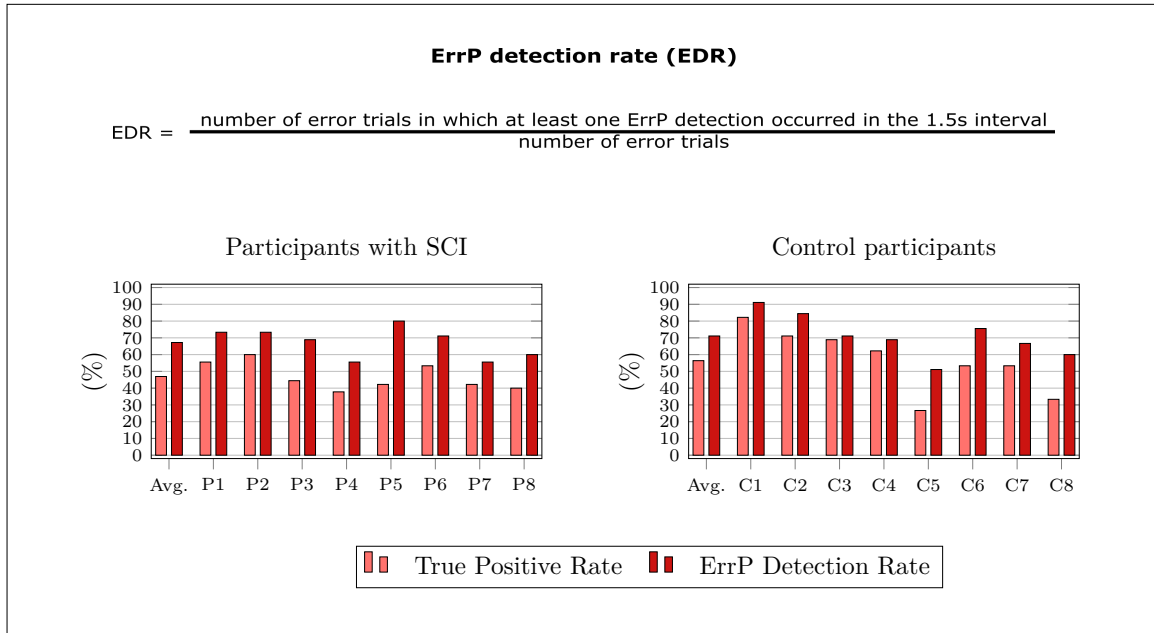


**Figure 5:** ErrP detection rate with the generic classifier: Definition of the metric ErrP detection rate (EDR) and its comparison with the metric true positive rate. The ErrP detection rate captures the portion of error trials in which at least one ErrP was successfully detected in the 1.5s after the error onset, independently of the classifier output before the error onset. The ErrP detection rate is less restrictive than the true positive rate. The difference between ErrP detection rate and true positive rate captures the portion of error trials in which a false ErrP detection occurred before the error onset despite at least one successful ErrP detection also occurred in the assigned 1.5s. In participants with SCI, the average ErrP detection rate was 67.2%. In control participants, the average ErrP detection rate was 71.1%.

Participants with SCI					Control Participants				
	FAR (%)		Total nr of sec			FAR (%)		Total nr of sec	
	Correct	Error	Correct	Error		Correct	Error	Correct	Error
P1	13.9	23.9	172	46	C1	3.5	9.1	173	44
P2	12.1	14.0	215	50	C2	6.3	14.3	113	42
P3	14.2	27.9	141	43	C3	2.3	4.7	174	43
P4	20.4	25.0	167	40	C4	11.1	9.7	117	31
P5	36.6	17.9	142	39	C5	27.9	33.3	147	39
P6	11.0	23.7	118	38	C6	23.8	30.4	168	46
P7	22.1	21.6	131	37	C7	25.2	20.9	147	43
P8	16.8	32.5	154	40	C8	20.0	35.0	153	40

**Table 1:** False activation rate (FAR). The false activation rate in correct and error trials is denoted by FAR. The total number of 1-second long intervals evaluated in correct and error trials is denoted by Total nr of sec.



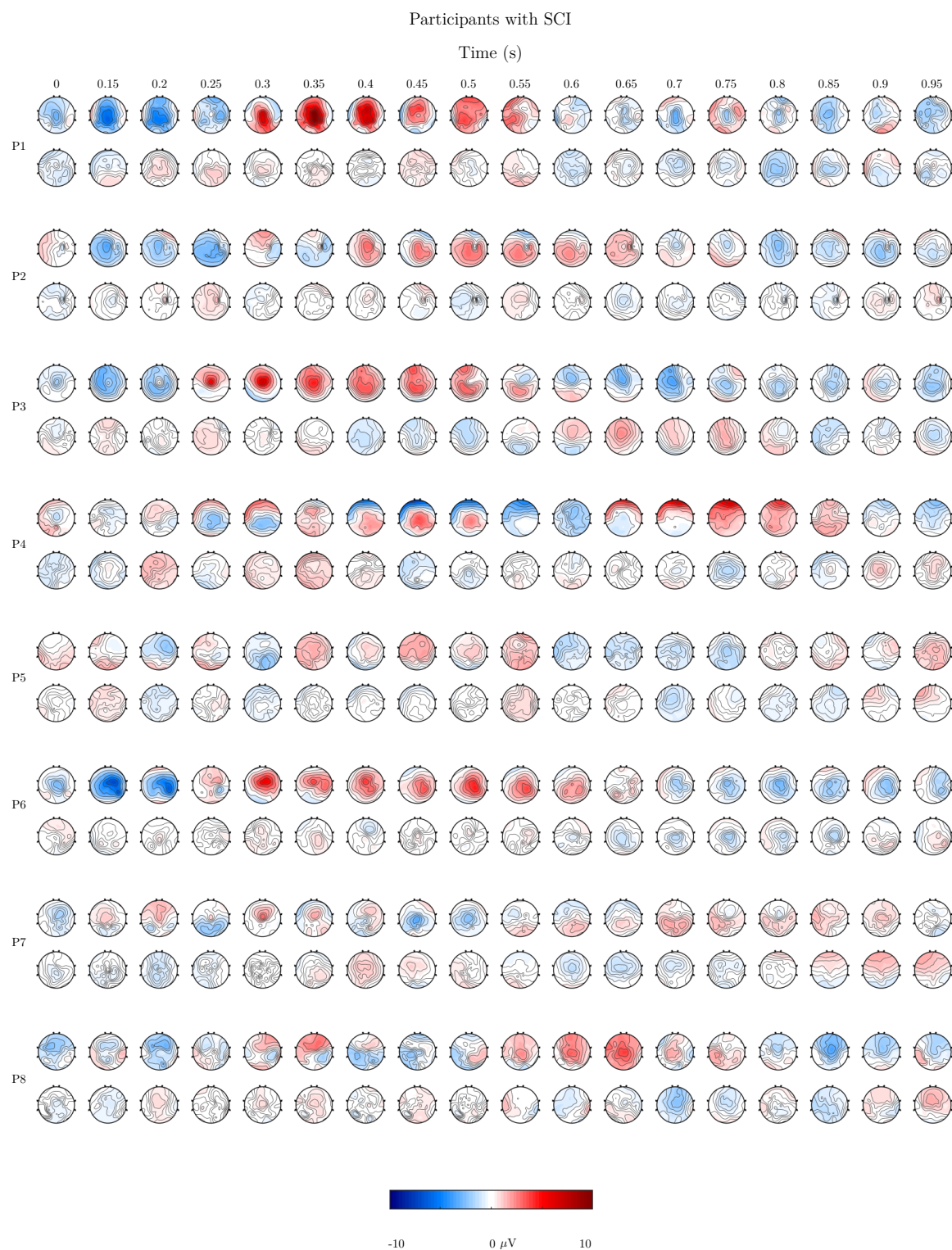


**Figure 6:** Participants with SCI: Topographic plots at different time points for error and correct signals (top and bottom row, respectively) for participants with SCI.

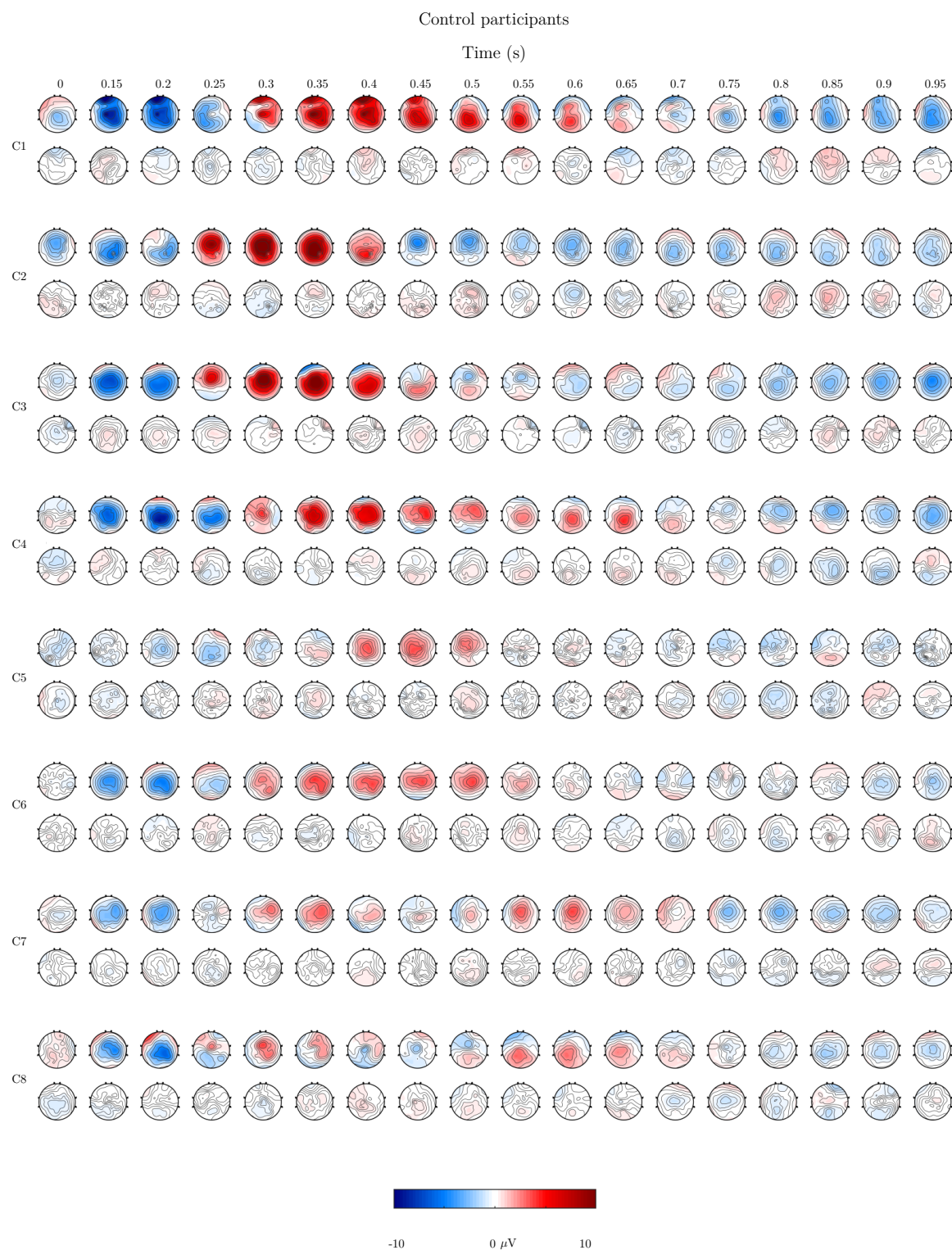


**Figure 7:** Control participants: Topographic plots at different time points for error and correct signals (top and bottom row, respectively) for control participants.